Winter 1975

WAVE PROPAGATION IN VISCOELASTIC MEDIA

GARY KENNETH STEWART

WAVE PROPAGATION IN VISCOELASTIC MEDIA

by

GARRY KENNETH STEWART

B.S., University of New Hampshire, 1970

M.S., University of New Hampshire, 1972

A THESIS

Submitted to the University of New Hampshire

In Partial Fulfillment of

The Requirements for the Degree of

Doctor of Philosophy

Graduate School

Engineering Ph.D. Program

Theoretical and Applied Mechanics

December, 1975

This thesis has been examined and approved.

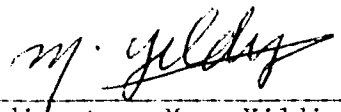

Thesis director, Musa Yildiz, Visiting
Professor of Engineering Physics

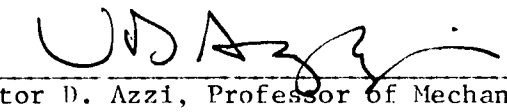

Victor D. Azzi, Professor of Mechanics

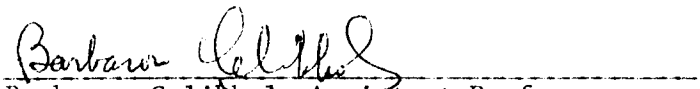

Barbaros Celikkol, Assistant Professor
of Mechanical Engineering

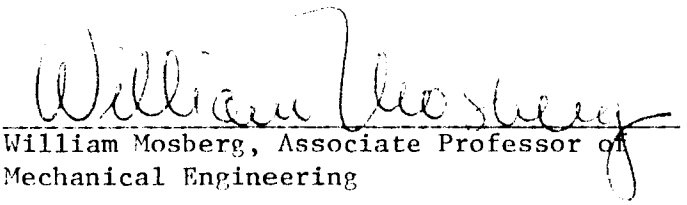

William Mosberg, Associate Professor of
Mechanical Engineering

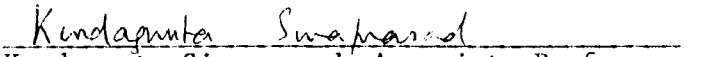

Kondagunta Sivaprasad, Associate Professor
of Electrical Engineering

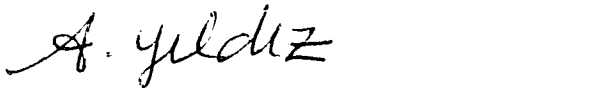

Asim Yildiz, Professor of Mechanics

August 25, 1975
Date

ACKNOWLEDGEMENTS

The author would like to thank his advisor, Professor Musa Yildiz, for the guidance and encouragement he provided during the performance of this research. His keen insight into the physical nature of the field problems considered within this thesis and his suggestions regarding the methods of approach to be followed for their solution have proved to be invaluable. The author also gratefully acknowledges Professor Asim Yildiz, who was inspirational throughout his program of study and research. His notes from courses, publications, and relevant discussions have been a source of information that has contributed significantly to the theoretical development of these thesis subjects. The author would also like to thank Professor Victor Azzi for his continued support and encouragement while the author was a graduate student. Professor Azzi's courses have provided the fundamentals necessary to pursue the study of the advanced topics of solid mechanics treated in this thesis. Appreciation is extended to Professor Barbaros Celikkol, whose courses and discussions were helpful in the preparation leading to the undertaking of this research.

Helpful discussions with Dr. M. R. Swift are gratefully acknowledged. Appreciation is also expressed to Dr. Robert Carrier for his contribution of the computer programming necessary to perform the numerical analyses contained within this thesis.

This thesis is a result of research supported financially by the National Science Foundation and the National Sea Grant Program of the National Oceanic and Atmospheric Administration.

PART I

THE EFFECTS OF COUPLE-STRESSES ON THE PROPAGATION OF WAVES IN AN UNBOUNDED VISCOELASTIC MEDIUM

TABLE OF CONTENTS

LIST OF TABLES

LIST OF ILLUSTRATIONS

NOMENCLATURE

PART I

BW	Bandwidth
c_i	Body-couple vector (couple per unit mass)
C	Velocity of wave propagation
d	Transverse-wave damping factor for viscoelastic medium with couple-stresses
D	Attenuation factor
f_i	Body-force vector (force per unit mass)
g	Transverse wave-damping factor for viscoelastic medium
G_{ij}	Tensorial Green's function
G_L	Longitudinal component of Green's function
G_T	Transverse component of Green's function
G'	Real part of complex Green's function
G"	Imaginary part of complex Green's function
h	Longitudinal-wave damping factor for viscoelastic medium
i	Imaginary unit ($i^2 = -1$)
Im{ }	Denotes imaginary part of complex quantity
k	Magnitude of vector wavenumber; spherical coordinate measuring radial distance from the origin
$k_i, \vec{k}$	Vector wavenumber
ℓ	Elastic material parameter for couple-stresses
L_{ij}	Linear tensorial operator for displacement-equation of motion
$M_i^{(h)}$	Couple-stress vector (couple per unit area)
$\hat{n}_i$	Unit normal vector outward from a surface S

P	Denotes principal value integral
P^{L}_{jm}	Longitudinal tensorial projection operator
P^{T}_{jm}	Transverse tensorial projection operator
Q	Quality factor
$Re\{\ \}$	Denotes real part of complex quantity
S	Closed surface bounding a portion of a material volume
t	Time coordinate
t'	Time at which impulsive point-source excitation is applied
$T^{(n)}_{i}$	Force-stress vector (force per unit area)
u	Unit step function
u_i	Displacement vector
U	Internal energy per unit mass
v_i	Velocity vector
V	Portion of a material volume
x	Cartesian coordinate
$x_i, \vec{x}$	Spatial position vector from a fixed origin
$\vec{x}'$	Spatial position vector from a fixed origin to an impulsive point-source excitation
y	Cartesian coordinate
z	Cartesian coordinate; complex variable
β'	Elastic bending-twisting modulus
β''	Viscous bending-twisting modulus
γ	Attenuation factor
δ	Dirac delta function
δ_{ij}	Kronecker delta
Δ	Dilatation

ε_{ij}	Strain tensor
ε_{ijk}	Permutation symbol
ζ	Damping factor
η'	Elastic bending-twisting modulus
η''	Viscous bending-twisting modulus
θ	Spherical coordinate measuring angle from the positive z-axis (colatitude)
κ_{ij}	Curvature-twist tensor
λ	Wavelength
λ'	Elastic Lamé parameter
λ''	Viscous Lamé parameter
μ'	Elastic Lamé parameter
μ''	Viscous Lamé parameter
μ_{ij}	Couple-stress tensor
μ^{D}_{ij}	Deviatoric part of couple-stress tensor
ρ	Mass density
ρ_x, ρ_y	Radü of curvature
σ_x, σ_y	Normal components of the stress tensor
τ	Period
τ_{ij}	Stress tensor
τ^{A}_{ij}	Antisymmetric part of the stress tensor
τ^{S}_{ij}	Symmetric part of the stress tensor
ϕ	Spherical coordinate measuring angle from the positive x-side of the xz-plane (longitude)
ω	Angular frequency
ω_d	Damped frequency

ω_i	Rotation vector
ω_n	Natural frequency
$\partial/\partial x_i \equiv \nabla$	Spatial gradient operator
$\partial^2/\partial x_i^2 \equiv \nabla^2$	Laplacian operator
$\partial/\partial t$	Local time-derivative operator
d/dt	Material time-derivative operator
$\lvert\ \rvert$	Denotes absolute value of quantity
$\cdot$	Denotes scalar multiplication of two vectors; local time-derivative operator

Subscripts

cT	Denotes quantities appropriate to the transverse mode of wave propagation with couple-stresses
L	Denotes quantities appropriate to the longitudinal mode of wave propagation
T	Denotes quantities appropriate to the transverse mode of wave propagation
i,j,k,ℓ,m,n	Indices

Superscripts

e	Denotes quantities appropriate to an elastic medium
ec	Denotes quantities appropriate to an elastic medium with couple-stresses
v	Denotes quantities appropriate to a viscoelastic medium

PART II

a	z-component of the wavenumber
$\vec{A}$	Vector displacement potential for transverse(shear) field
A,B,C,D	Potential coefficients
b	Damping coefficient
BD	Bounce distance
c	Velocity of wave propagation
d	Distance in z-direction to a solid-solid interface
$\hat{e}$	Unit vector
f	Frequency
f_i	Body-force vector (force per unit mass)
g	Green's function in time domain
G	Green's function in frequency domain
G_b	Green's function expressive of boundary effect
G_f	Green's function for unbounded space
h	Thickness of layer
$H(\omega)$	Spectrum of pulse
$H_m^{(1)}$	Hankel function of the first kind of order m
$H_m^{(2)}$	Hankel function of the second kind of order m
i	Imaginary unit ($i^2 = -1$)
J_m	Bessel function of order m
k	Wavenumber
m_{ij}	Element of [M] matrix
[M]	(4×4) matrix in recurrence relation
p	Pressure

R	Distance between source and receiver
R_I	Distance between image source and receiver
t	Time coordinate
t'	Time at which impulsive point-source excitation is applied
$\vec{u}, u_i$	Displacement vector
U	Eigenfunction for region in liquid layer above point source
V	Eigenfunction for region in liquid layer below point source
W	Denotes Wronskian determinant
x	Cartesian coordinate
$\vec{x}, x_i$	Spatial position vector from a fixed origin
$\vec{x}'$	Spatial position vector from a fixed origin to an impulsive point-source excitation
y	Cartesian coordinate
z	Cartesian coordinate; cylindrical coordinate
Z	Acoustic impedance
γ	Nondimensional parameter
Γ	Plane-wave reflection coefficient
δ	Dirac delta function
δ_{ij}	Kronecker delta
ε_{ij}	Strain tensor
ζ	Bulk viscosity
η	Variable in Fourier integral representation in Cartesian coordinates; coefficient of viscosity(shear viscosity); porosity
θ	Angle of incidence
κ	Bulk modulus
κ_j	Propagation constant of mode propagating in the z-direction

λ	Lamé operator representing Voigt viscoelasticity; coefficient of viscosity; wavelength
λ'	Elastic Lamé parameter
λ''	Viscous Lamé parameter
μ	Lamé operator representing Voigt viscoelasticity; coefficient of viscosity(shear viscosity)
μ'	Elastic Lamé parameter
μ''	Viscous Lamé parameter
ξ	Variable in Fourier-Bessel integral representation in cylindrical coordinates; variable in Fourier integral representation in Cartesian coordinates
Π	Denotes repeated multiplication
ρ	Mass density; cylindrical coordinate measuring radial distance in plane transverse to z-direction
σ_{ij}	Stress tensor
ϕ	Cylindrical coordinate measuring angle from the positive x-side of the xz-plane; scalar displacement potential in time domain
Φ	Scalar displacement potential in frequency domain
$\Phi_j(\vec{\rho})$	Two-dimensional set of mode functions
χ	Scalar displacement potential for longitudinal(compressional) field
ψ	Scalar displacement potential for transverse(shear)field
ω	Angular frequency
$\nabla \equiv \partial/\partial x_i$	Spatial gradient operator
$\nabla^2 \equiv \partial^2/\partial x_i^2$	Laplacian operator

$\partial/\partial t$	Local time-derivative operator
$\lvert\ \rvert$	Denotes absolute value of quantity
[ ]	Denotes a matrix quantity
$\cdot$	Denotes scalar multiplication of two vectors; local time-derivative operator
$\times$	Denotes cross product of two vectors
$\sum$	Summation symbol

Subscripts

e	Denotes quantities appropriate to an elastic medium
L	Denotes quantities appropriate to the longitudinal(compressional) mode of wave propagation
T	Denotes quantities appropriate to the transverse(shear) mode of wave propagation
ρ,ϕ,z	Denotes components in cylindrical coordinates
i,j	Indices
$0,1,2,\cdots,j,\cdots,n$	Denotes layer
<	Denotes lesser of a quantity
>	Denotes greater of a quantity
$\_$	Denotes Fourier-Bessel transformed quantity

Superscript

$\_$	Denotes quantities appropriate to a fluid

ABSTRACT

WAVE PROPAGATION IN VISCOELASTIC MEDIA

by

GARY KENNETH STEWART

In a linear viscoelastic medium with the couple stresses, the Green's function for an infinitely extended medium is examined and the wave propagation properties of the field are discussed by studying the analytical structure of the Green's function. It is observed that the longitudinal wave propagation is unaltered, and that the transverse mode undergoes a change (due to couple-stresses) with an appropriate wave number; and an overdamped propagation mode is further modified due to viscoelastic effects. The consistency of the results is checked for various special cases.

The second part of the investigation deals with the problem of acoustic subbottom sediment identification and classification. The purpose of this study is to develop expressions for the acoustic response in a liquid halfspace overlying a multilayered halfspace consisting of viscoelastic soil and viscous fluid layers. The multilayered problem is solved using the Green's function formalism, integral transforms and by matching boundary conditions at each interface between layers. A recurrence relation is developed for the potentials in adjoining viscoelastic layers. This recurrence relation is applied successively to eliminate the potentials between the first and last viscoelastic layers.

Special cases of the multilayer problem are developed. Two viscoelastic layer halfspace cases are analyzed in detail for both finite and infinite depth of the overlying liquid. The integral form is evaluated by using digital computer and saddle-point approximation.

CHAPTER I

INTRODUCTION

This report consists of two parts: 1) Effects of Couple-Stresses in Linear Viscoelasticity, and the second part examines 2) Reflection of Acoustic Waves in a Liquid Halfspace Overlying a Multilayered Halfspace Consisting of Viscoelastic and Viscous Fluid Layers.

In theory of deformation of continua, originated by Voigt and amplified by E. & F. Cosserat [8], the couple per unit area, acting across a surface within a material volume or on its boundary, was taken into account in addition to the usual force per unit area. Some typical effects of such "couple-stresses" are exhibited, in this report, by means of solutions of problems of wave-propagation, vibration, stress-concentration and nuclei of strain--all within the framework of a linearized form of the couple-stress theory for perfectly elastic, centrosymmetric-isotropic materials.

A modern derivation of the Cosserat equations has been given by Truesdell & Toupin [9]. More recently, Toupin has derived the associated constitutive equations for finite deformation of perfectly elastic materials. Upon linearization, Toupin's equation becomes identical with those which are obtained, for example, by Aero & Kuvshinskii, without first establishing constitutive equations for finite deformation. On the other hand, Grioli has also obtained constitutive equations for finite deformation--equally correct, though of different form; but, upon linearization, he obtains results at variance with Toupin's.

In the linear theory that takes into account couple-stresses in a centrosymmetric-isotropic, elastic material, there is an additional modulus of elasticity (the ratio of couple-stress to curvature or twist, i.e., a modulus of bending and twisting) with the dimensions of force. The square root of the ratio of the bending-twisting modulus to the usual shear modulus has the dimension of length. This length, ℓ, is a material property which carries with it all of the difference between analogous equations or solutions with and without couple-stresses. The larger ℓ may be, the greater is the difference. Presumably ℓ is small, in comparison with bodily dimensions and wave-lengths normally encountered, as there appears to be no conclusive experimental evidence of its existence. However, even though small, its influence might become important as dimensions of a body or wave-lengths diminish to the order of the length ℓ. The assumption of positive-definiteness of the internal energy-density requires the bending-twisting modulus to be positive. In the contrary case, ℓ^2 would be replaced by its negative, in the equations; and the forms of solutions would be drastically different.

Recently, in a linear elastic field with couple stresses, the tensor Green's function is obtained by A. Yildiz [7].

It is observed that the longitudinal wave propagation is unaltered, and that the transverse mode (VS-type) undergoes a change (due to couple-stresses) with a modified wave number, and a new overdamped propagation mode is generated.

The purpose of the present work is (to consider within the frame-work of the theory of asymmetric elasticity) to take into account of the viscous effects.

Recently, viscoelastic as well as thermo-viscoelastic field with the couple stresses has been discussed by M. Yildiz [1 & 2].

The second part of the thesis is related to the identification. The problem of remote acoustic classification and identification of sediments on the continental shelf has become increasingly important due to increased interest in the coastal zone. Presently, most acoustic sounding for sediments is done using seismic profiling where the intensity of the return is indicated as a function of pulse return time. This technique is valuable in obtaining a qualitative understanding of the subbottom; however, more detailed, quantitative information is usually required for underwater construction and commercial dredging for sand and gravel. In addition, it is difficult to interpret multiple return signals which imply sublayering in the sediment.

Recent sounding and coring data taken as part of the joining UNH-Raytheon Sea Grant project in Narragansett Bay and in Massachusetts Bay shows that commercially important sand and gravel deposits lie on a first layer 10 to 15 feet deep, below which lies finer clay sediment. Therefore, knowledge of the thickness of the first layer is important from a commercial standpoint.

In this investigation, we take into account the multiple layering of the subbottom using a realistic three-dimensional model for the coupled acoustic-viscoelastic field. Earlier investigators, notably Thomson and Haskell considered only the two-dimensional case for dissipationless solids. Hamilton in [25] concludes that unconsolidated underwater sediments can be modeled as elastic solids. Recently, Hamilton has presented data indicating that the sediments behave as a lightly damped

elastic solid. Subsequently, Hamilton's measurements were verified by Celikkol and Vogel.

The Green's function integral, containing the complete description of the acoustic return signal as a function of all the water and sediment parameters involved, is too complex to be integrated in closed-form.

Therefore, IBM 360-50 digital computer subroutines were prepared in FORTRAN IV (G-level) to compute the value of the integral as various parameters were varied, to obtain the information and insight needed for the optimum system design for remote acoustic sensing of the ocean sediments.

Numerical integration on the computer presents many difficulties due to the behavior of the integrand. The integrand, when plotted versus integration variable ζ, displays large rapid fluctuations that result in large computation times, serving to make the exact integration procedure rather expensive.

However, several excellent approximations for this integral have been obtained analytically. One of these, known as a "saddle-point" approximation, where contributions from branch cut singularities are dominant and this represents reflected soundwaves from the layered thermo-viscoelastic subbottom.

So far, we have studied the sound responses in deterministic, as well as, in statistical form in $(\vec{k},t)$ or $(\vec{k},\omega)$ (see references [1],[2],[7],[36]) and at present in $(\vec{r},\omega)$ domains with the following purpose in mind: to classify the characteristics of the sea floor soil according to their thermo-elastic and thermo-viscoelastic transport coefficients. To interpret remotely obtained data (which are in the form of analogue and digitized

forms) and correlate them correctly with the coring experiments we had to construct the appropriate analytically realistic engineering models.

We have two types of data which are available to us: digitized data (through which we interpret Q of the thermo-viscoelastic soil), and analogue data (through which we interpret the reflection coefficient of the thermo-viscoelastic soil).

Keeping in mind that we have to design analytical models which corresponds oblique incident reflectivity measurement since the normal incident reflectivity measurement prescribes only the compressional elastic parameters of the thermo-viscoelastic soil (it is also necessary to describe elastic-shear parameters).

In this investigation, therefore, we obtained the numerical solutions of the multilayer Green's function via the spectral representation which reduces the oblique incident results to an integration which corresponds to an evaluation Fourier-Hankel transform in the transformed wave-number domain. The integrations involving the oblique incidence are performed first with the computer, and then by the method of saddle-point of the integration.

CHAPTER II

FIELD DESCRIPTION OF A COSSERAT CONTINUUM

It is appropriate to begin an investigation into wave propagation phenomena in a linear viscoelastic medium with couple-stresses by reviewing linear Cosserat field theory. Therefore, the fundamental equations of the linear couple-stress theory of elasticity, given in the detailed derivation of Mindlin and Tiersten (1962), are reviewed here. An approach similar to the one taken by Graff and Pao (1967b) in their brief account of the basic elements of couple-stress theory is followed, whereby only those equations pertinent to the propagation of waves in a homogeneous, isotropic linear elastic medium are included.

Consider the motion of a portion V, of a material volume, which is bounded by a closed surface S, whose outward unit normal vector at each point is specified by $\hat{n}_i$. Cosserat field theory is formulated on the assumption that the remainder of the material volume exerts loads on V, which consist, at each point along S, of a force per unit area, $T_i^{(n)}$, and a couple per unit area, $M_i^{(n)}$; also, at each point within V, there exist an extrinsic force per unit mass, f_i, and an extrinsic couple per unit mass, c_i. The force-stress vector $T_i^{(n)}$ and the body-force vector f_i are polar vectors, whereas the couple-stress vector $M_i^{(n)}$ and the body-couple vector c_i are axial vectors. The fundamental laws, namely the principles of conservation of mass, balance of momentum and moment of momentum, and conservation of mechanical energy, which govern the behavior of physical phenomena in a Cosserat continuum, are summarized, respectively, in the following system of field equations:

$$\frac{d}{dt}\int_V \rho \, dV = 0 \, , \tag{2.1}$$

$$\frac{d}{dt}\int_V v_i \rho \, dV = \int_S T_i^{(n)} dS + \int_V f_i \rho \, dV \, , \tag{2.2}$$

$$\frac{d}{dt}\int_V \varepsilon_{ijk} x_j v_k \rho \, dV = \int_S (\varepsilon_{ijk} x_j T_k^{(n)} + M_i^{(n)}) dS + \int_V (\varepsilon_{ijk} x_j f_k + c_i) \rho \, dV \, , \tag{2.3}$$

$$\frac{d}{dt}\int_V (\frac{1}{2} v_i v_i + U) \rho \, dV = \int_S (T_i^{(n)} v_i + \frac{1}{2} M_i^{(n)} \varepsilon_{ijk} \frac{\partial v_k}{\partial x_j}) dS$$

$$+ \int_V (f_i v_i + \frac{1}{2} c_i \varepsilon_{ijk} \frac{\partial v_k}{\partial x_j}) \rho \, dV \, , \tag{2.4}$$

where d/dt is the material time-derivative operator, ρ is the mass density, x_i is the spatial position vector from a fixed origin, u_i is the material displacement, v_i is the material velocity du_i/dt, U is the internal energy per unit mass, $\partial/\partial x_i$ is the spatial gradient operator, and ε_{ijk} is the usual permutation symbol. Thus, in addition to the usual surface force per unit area, the derivation of the Cosserat field equations takes into account the effects of a surface couple per unit area (see Figure 1), which have generally been neglected in the development of the classical theory of elasticity (Love, 1927). Such a consideration seems appropriate for materials with granular or crystalline structure, where the interaction between adjacent elements may introduce internal couples.

In order to specify the action at a point within a material volume or on its surface, nine components of couple-stress are required in addition to the usual nine components of stress. As the stress tensor τ_{ji} is

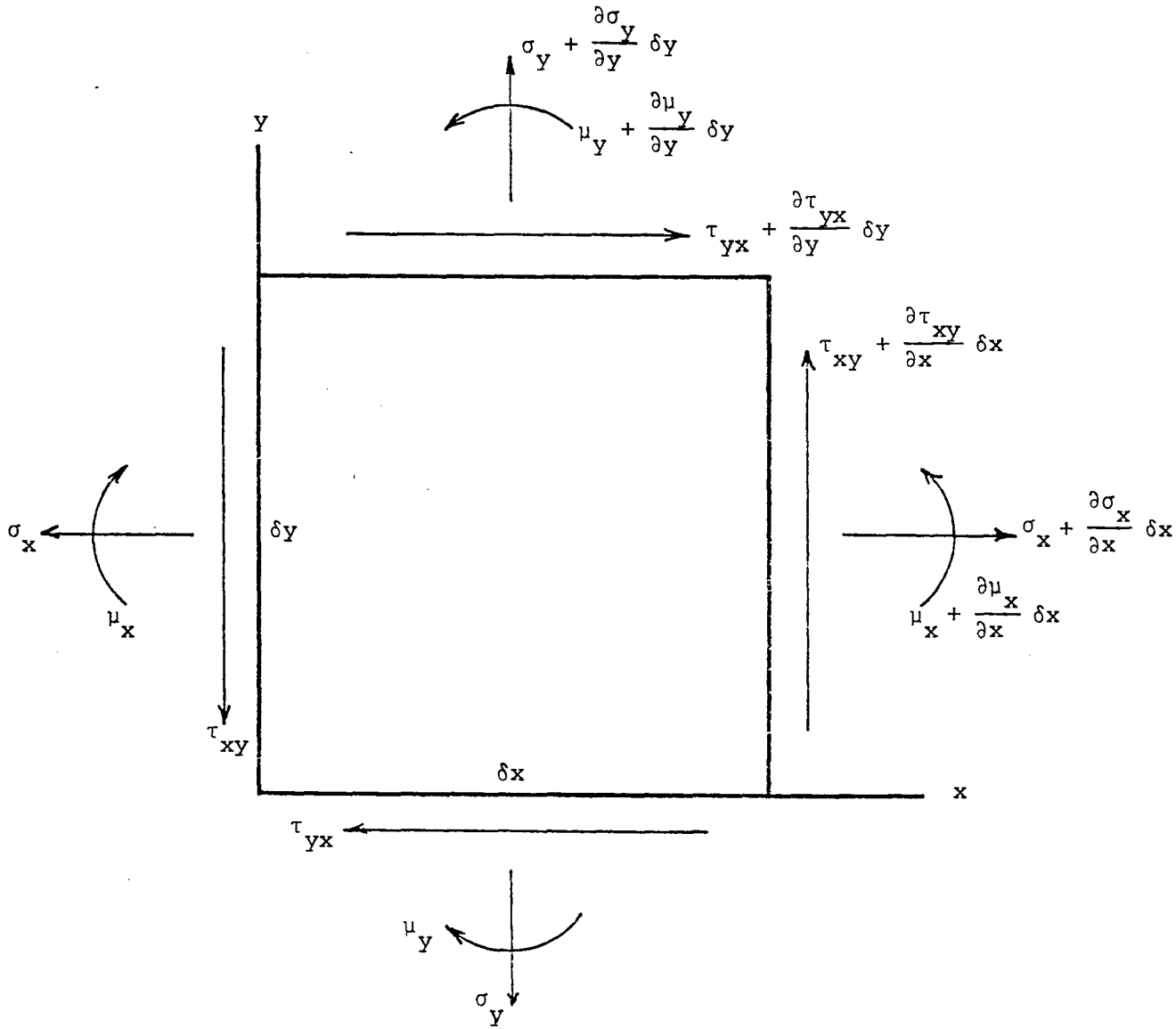

Figure 1. Components of stress and couple-stress in a varying two-dimensional field.

related to the stress vector $T_i^{(n)}$ over a surface with unit normal vector $\hat{n}_j$ by

$$T_i^{(n)} = \tau_{ji}\hat{n}_j \ , \tag{2.5}$$

the couple-stress tensor μ_{ji} is related to the surface couple-stress vector $M_i^{(n)}$ by

$$M_i^{(n)} = \mu_{ji}\hat{n}_j \ . \tag{2.6}$$

Employing the relations in equations (2.1), (2.5), and (2.6) and the divergence theorem, the principles of conservation of linear and angular momentum, expressed in equations (2.2) and (2.3), yield the stress and couple-stress equations of motion, respectively,

$$\frac{\partial \tau_{ji}}{\partial x_j} + \rho f_i = \rho \frac{dv_i}{dt} \tag{2.7}$$

and

$$\frac{\partial \mu_{ji}}{\partial x_j} + \rho c_i + \varepsilon_{ijk}\tau_{jk} = 0 \ . \tag{2.8}$$

It is observed in equation (2.8) that when spatially varying couple-stresses or body-couples are considered, the stress tensor is not necessarily symmetric. Conversely, if the stress tensor is symmetric, or even zero, the couple-stresses and body-couples need not vanish: only the sum of the first two terms in equation (2.8) must then be zero. If both the couple-stress tensor μ_{ij} and the body-couple vector c_i are absent, the antisymmetric part of the stress tensor vanishes, and consequently, the stress tensor τ_{ij} must be symmetric.

The stress tensor may be expressed in terms of its symmetric part τ^S_{ij} and antisymmetric part τ^A_{ij} as

$$\tau_{ij} = \tau^S_{ij} + \tau^A_{ij} , \tag{2.9}$$

where

$$\tau^S_{ij} = \frac{1}{2} (\tau_{ij}+\tau_{ji}) \tag{2.9a}$$

and

$$\tau^A_{ij} = \frac{1}{2} (\tau_{ij}-\tau_{ji}) = - \frac{1}{2} \varepsilon_{ijk}\varepsilon_{kmn}\tau_{nm} . \tag{2.9b}$$

Additionally, the couple-stress tensor may be expressed in terms of its deviatoric part μ^D_{ij} and scalar part $\mu_{\ell\ell}$ by the relation

$$\mu_{ij} = \mu^D_{ij} + \frac{1}{3} \mu_{\ell\ell}\delta_{ij} , \tag{2.10}$$

where δ_{ij} is the Kronecker delta. Then, by substituting equation (2.9b) into equation (2.9) and using the latter with equation (2.10), equations (2.7) and (2.8) may be combined to give an alternative form of the equation of motion:

$$\frac{\partial \tau^S_{ji}}{\partial x_j} + \frac{1}{2} \varepsilon_{ijk} \frac{\partial^2 \mu^D_{\ell k}}{\partial x_j \partial x_\ell} + \rho f_i + \frac{1}{2} \varepsilon_{ijk} \frac{\partial \rho c_k}{\partial x_j} = \rho \frac{dv_i}{dt} . \tag{2.11}$$

It should be noted that the antisymmetric part of the stress tensor and the scalar of the couple-stress tensor are not present in this form of the equation of motion. Characteristically, the antisymmetric part of the stress and the scalar of the couple-stress are left indeterminate in the treatment of Cosserat field equation (2.11).

Equation (2.11) can be expressed in still another form upon development of the constitutive relations. In formulating the constitutive equations, the procedure followed here is based on consideration of the

functional form of the expression for internal energy. Employing equations (2.1), (2.5 - 2.8) and the divergence theorem, the principle of conservation of mechanical energy may be expressed as

$$\rho \frac{dU}{dt} = \tau^{S}_{ji} \frac{\partial v_i}{\partial x_j} + \frac{1}{2} \varepsilon_{ijk} \mu_{\ell i} \frac{\partial^2 v_k}{\partial x_\ell \partial x_j} . \tag{2.12}$$

Then substituting equation (2.10) into equation (2.12), the latter gives

$$\rho \frac{dU}{dt} = \tau^{S}_{ji} \frac{\partial v_i}{\partial x_j} + \frac{1}{2} \varepsilon_{ijk} \mu^{D}_{\ell i} \frac{\partial^2 v_k}{\partial x_\ell \partial x_j} . \tag{2.13}$$

It is observed in equation (2.13) that the antisymmetric part of the stress and the scalar of the couple-stress do not contribute to the internal energy.

At this point in the development, the theory, which so far has remained general, is specialized to apply to linear Cosserat fields. Therefore, the expression for internal energy in equation (2.13) must undergo linearization. Performing this operation, equation (2.13) becomes

$$\rho \dot{U} = \tau^{S}_{ij} \frac{\partial \dot{u}_i}{\partial x_j} + \frac{1}{2} \varepsilon_{ijk} \mu^{D}_{\ell i} \frac{\partial^2 \dot{u}_k}{\partial x_\ell \partial x_j} , \tag{2.14}$$

where the material-time derivative reduces to a local-time derivative after linearization, or $d(\ )/dt = \partial(\ )/\partial t$, and the local-time derivative is denoted as $\partial(\ )/\partial t = \dot{(\ )}$. It is convenient to introduce the small-strain tensor ε_{ij} , which is related to the displacements by

$$\varepsilon_{ij} = \frac{1}{2} \left(\frac{\partial u_i}{\partial x_j} + \frac{\partial u_j}{\partial x_i} \right) , \tag{2.15}$$

and the curvature-twist tensor κ_{ij}, which is defined in terms of the gradient of a small-rotation vector $\omega_j = \frac{1}{2}\varepsilon_{jmn}\partial u_n/\partial x_m$ as

$$\kappa_{ij} = \frac{\partial \omega_j}{\partial x_i} = \frac{1}{2}\varepsilon_{jmn}\frac{\partial^2 u_n}{\partial x_i \partial x_m} . \tag{2.16}$$

Using relations (2.15) and (2.16) in equation (2.14), the internal energy may be expressed alternatively as

$$\rho\dot{U} = \tau^S_{ij}\dot{\varepsilon}_{ij} + \mu^D_{ij}\dot{\kappa}_{ij} . \tag{2.17}$$

It is of interest to account for the deformations produced by the stresses and couple-stresses. From equation (2.9b), it may be seen that, with $i = j$, $\tau^A_{ij} = 0$. In this instance, the normal components of the strain are related to the normal components of the stress by the usual stress-strain relations of classical linear elasticity. When $i \neq j$, however, $\tau^A_{ij} \neq 0$, and it is found that the symmetric part of the shear stress produces the usual shear strains, while the antisymmetric part of the shear stress tends to produce local rigid rotations as indicated in Figure 2. The rotations are balanced by the couple-stresses and body-couples in accordance with equation (2.8). With regard to the deformations attributable to couple-stresses, the couple-stresses produce curvatures, as shown in Figure 3, which are related to the local rigid rotations according to equation (2.16). It can be shown from equation (2.16) that the components of the gradient of the rotation, that is, the components of the curvature-twist tensor, are expressible as eight independent linear combinations of the eighteen components of the strain gradient. Thus, the components of the curvature-twist tensor represent

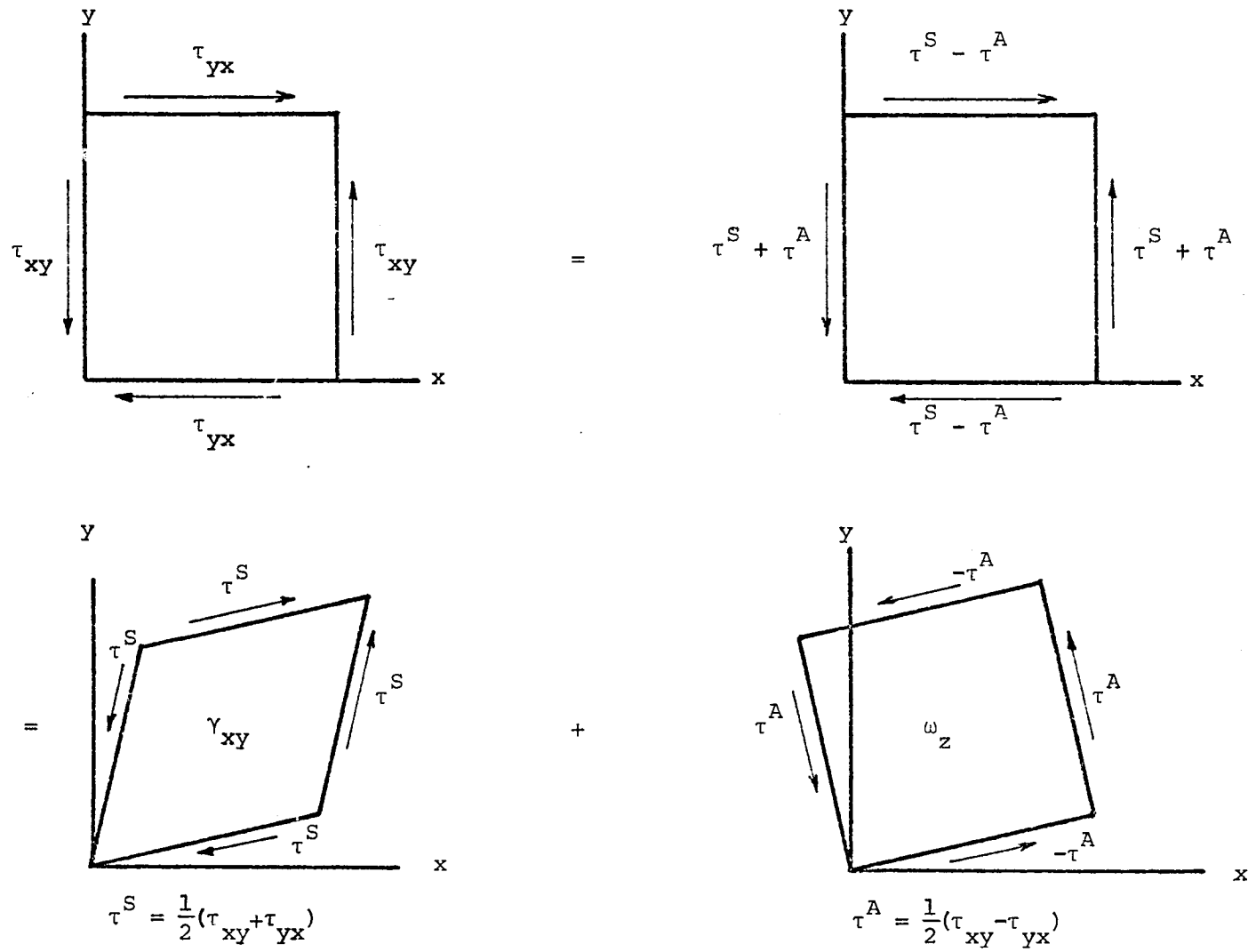

Figure 2. Strain and unbalanced rotation produced by symmetric and antisymmetric parts of the shear stress (two-dimensional).

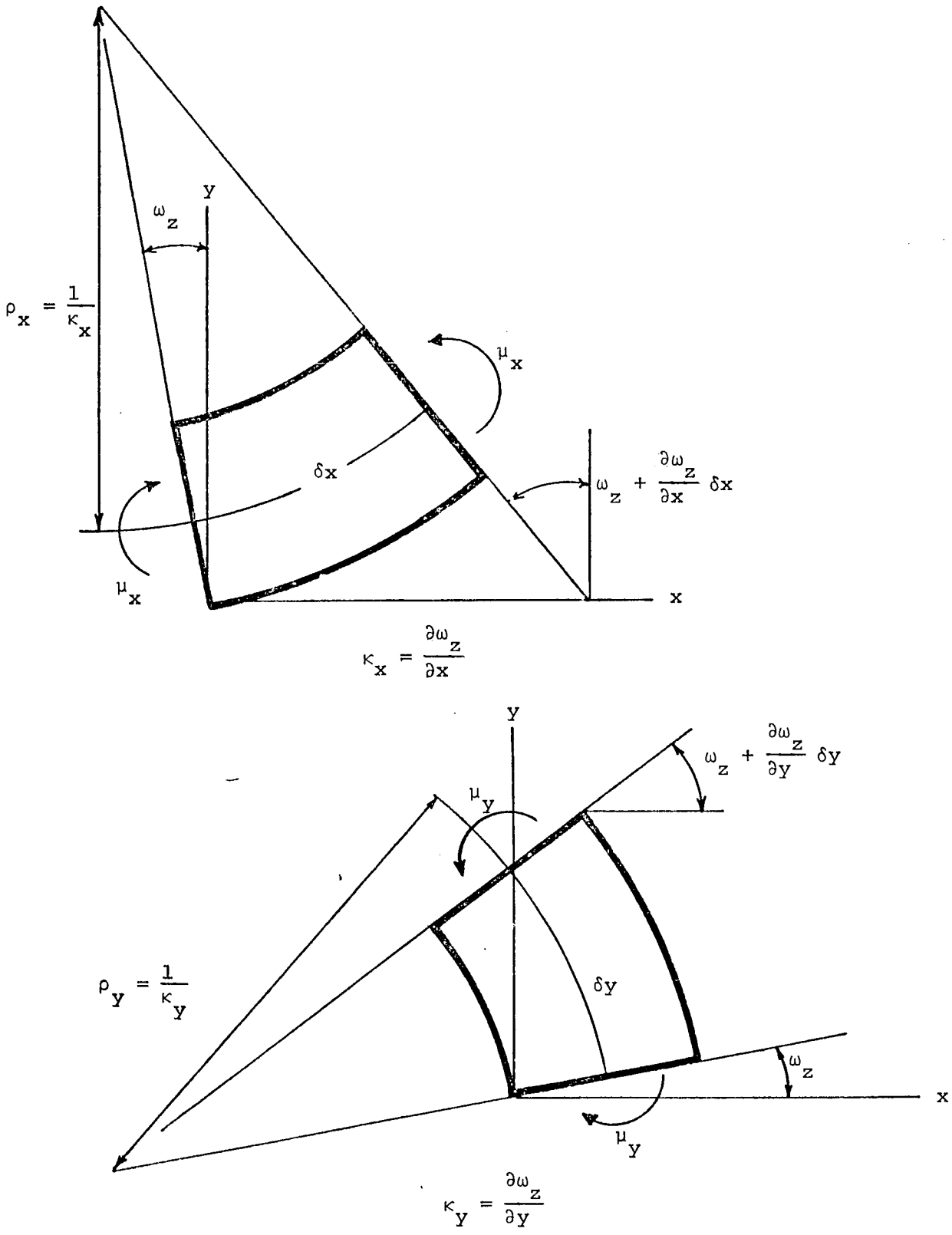

Figure 3. Curvatures produced by couple-stresses (two-dimensional).

the additional deformations that the continuum may undergo due to the effects of couple-stresses. When couple-stresses are not taken into account, the specific energy of an elastic medium may be expressed solely as a function of the strain tensor.

If the internal energy is assumed to be a positive quadratic function of ε_{ij} and κ_{ij}, a pair of constitutive relations can be derived from equation (2.17). For a homogeneous, isotropic, linear elastic medium, these relations are

$$\tau^{S}_{ij} = \lambda'\varepsilon_{\ell\ell}\delta_{ij} + 2\mu'\varepsilon_{ij} \tag{2.18}$$

and

$$\mu^{D}_{ij} = 4\eta'\kappa_{ij} + 4\beta'\kappa_{ji} , \tag{2.19}$$

where λ' and μ' are the usual Lamé parameters, while η' and β' are newly introduced bending-twisting parameters. It is observed that the couple-stresses are proportional to the curvatures. Couple-stress has the dimensions of couple per unit area or force per unit length, while curvature is the reciprocal of length. Therefore, η' and β' have the dimensions of force. When relations (2.15) and (2.16) are substituted into (2.18) and (2.19), and the latter are inserted into the linearized version of equation of motion (2.11),

$$\frac{\partial \tau^{S}_{ji}}{\partial x_j} + \frac{1}{2}\varepsilon_{ijk}\frac{\partial^2 \mu^{D}_{\ell k}}{\partial x_j \partial x_\ell} + \rho f_i + \frac{1}{2}\rho\varepsilon_{ijk}\frac{\partial c_k}{\partial x_j} = \rho\frac{\partial^2 u_i}{\partial t^2} \tag{2.20}$$

one obtains Mindlin and Tiersten's (1962) displacement-equation of motion

for a homogeneous, isotropic, linear elastic field with couple-stresses:

$$\mu' \frac{\partial^2 u_i}{\partial x_j^2} + (\lambda'+\mu') \frac{\partial^2 u_j}{\partial x_i \partial x_j} + \eta' \frac{\partial^2}{\partial x_\ell^2} (\epsilon_{ijk} \epsilon_{kmn} \frac{\partial^2 u_n}{\partial x_j \partial x_m}) + \rho f_i + \frac{1}{2} \rho \epsilon_{ijk} \frac{\partial c_k}{\partial x_j} = \rho \frac{\partial^2 u_i}{\partial t^2} . \tag{2.21}$$

The mass density ρ in equations (2.20) and (2.21) is a constant as a result of the linearization.

CHAPTER III

FORMULATION OF THE PROBLEM

In the development of the previous chapter, a perfectly elastic medium was considered. For studies where small deformations occur, many elastic materials do not deviate grossly from perfectly elastic behavior, as is corroborated by experimental investigations with elastic materials, where the observed results agree quite well with the predictions of the elastic theory. It is well-known, however, that when materials are set in vibration, the vibrations are accompanied by dissipation, due to the conversions of elastic energy to internal energy. The various mechanisms by which this phenomenon occurs are collectively termed internal friction.

According to the work of Kolsky (1953) and others, dissipative behavior in solid media is found to be quite complex and to vary considerably with the nature of the medium. In general, it may be stated that the effect of internal friction is to produce attenuation and dispersion in the propagation of elastic waves. Several mathematically convenient mechanisms, which occasionally fit experimental data over a limited range of frequencies, have been proposed in order to describe energy dissipation in vibrating solid media. Yet, at present there is no satisfactory theory of internal friction in solid media, and more experimental data needs to be collected for further studies in this area.

One class of mechanisms that has been utilized to describe the dissipative behavior of elastic media is dependent on the assumption that in addition to the elastic restoring force, which is proportional to the displacement, a viscous dissipative force, which is proportional to the

velocity, exists in the medium. Hence, a medium characterized by mechanisms of this type is called a "viscoelastic" medium. Within this class of internal friction mechanisms, the behavior of the viscoelastic medium may be represented by models consisting of elastic and viscous elements joined in either parallel, series, or slightly more complicated arrangements which combine the features of both of these models, depending on the relaxation properties of the medium. The more complicated models have been shown to give results more in accordance with the behavior of real solid media.

A viscoelastic model which features a parallel type of coupling between elastic and viscous elements was originally considered by Meyer (1874) and later extended by Voigt (1892). Another model for viscoelasticity, which consists of an elastic element connected in series with a viscous element, was suggested by Maxwell (1890). When the application of a load results in an irrecoverable deformation, the material is described best by the Maxwell model. On the other hand, the Voigt model applies favorably to a material whose deformation upon loading approaches a constant value asymptotically with time and recovers slowly when the load is removed. It should be emphasized that very few solid media behave, even approximately, like either the Maxwell or Voigt model. To allow for the fact that a number of different relaxation phenomena may occur simultaneously in a solid medium, more complicated models have been considered. Thus, it is only when the solid medium is considered as having a number of different relaxation times, that is, a relaxation time spectrum, that the dynamic behavior can be defined adequately. The only reason for using simpler models with single relaxation times is that the more complex models require extremely involved mathematics. However, when the dynamic

mechanical behavior of a viscoelastic medium is required for only a limited range of frequencies, the Voigt or Maxwell model frequently provides a convenient method of describing its mechanical properties under the prescribed conditions. The Voigt model is employed exclusively in this work.

The theory advanced by Voigt assumed that the stress components in a viscoelastic medium could be expressed as the sum of two sets of terms: one set being proportional to the strains, and the other set proportional to the rate of change of the strains. This assumption implies that if displacement equation of motion (2.21), which governs the dynamic behavior of an elastic medium with couple-stresses, is modified to include the effects of Voigt viscoelasticity, constitutive relations (2.18) and (2.19) must be reformulated in order to account for the additional viscous contributions discussed here. It is well-known, however, that in the case of a homogeneous, isotropic, linear elastic medium, the modification of the stress-strain relation of elasticity to include the effects of Voigt viscoelasticity leads to a relation similar to the one obtained for the elastic case, except that the operators $\lambda' + \lambda''(\partial/\partial t)$ and $\mu' + \mu''(\partial/\partial t)$ replace λ' and μ', respectively. According to this scheme, relation (2.18) may be expressed as

$$\tau^{S}_{ij} = (\lambda' + \lambda'' \frac{\partial}{\partial t})\varepsilon_{\ell\ell}\delta_{ij} + 2(\mu' + \mu'' \frac{\partial}{\partial t})\varepsilon_{ij} \tag{3.1}$$

for a homogeneous, isotropic, linear viscoelastic medium, where λ'' and μ'' denote the viscous parameters which correspond to Lamé's parameters. If the Voigt approach to viscoelasticity is generalized to the case in which couple-stresses are present, then the couple-stress parameters, η' and β' in equation (2.19), change form in a manner analogous to the Lamé

parameters, so that the couple-stress-curvature-twist relation becomes

$$\mu_{ij}^{D} = 4(\eta'+\eta'' \frac{\partial}{\partial t})\kappa_{ij} + 4(\beta'+\beta'' \frac{\partial}{\partial t})\kappa_{ji} , \tag{3.2}$$

where the viscous parameters which correspond to the elastic bending-twisting parameters are denoted as η'' and β'' .

By introducing the modified constitutive relations (3.1) and (3.2) into the linearized equation of motion (2.20), the linear couple-stress theory of elasticity is extended to consider the effects of Voigt viscoelasticity in a homogeneous, isotropic medium:

$$(\mu'+\mu'' \frac{\partial}{\partial t}) \frac{\partial^2 u_i}{\partial x_j^2} + [\lambda'+\mu'+(\lambda''+\mu'')\frac{\partial}{\partial t}] \frac{\partial^2 u_j}{\partial x_i \partial x_j} + (\eta'+\eta'' \frac{\partial}{\partial t}) \frac{\partial^2}{\partial x_\ell^2}(\varepsilon_{ijk}\varepsilon_{kmn} \frac{\partial^2 u_n}{\partial x_j \partial x_m})$$

$$+ \rho f_i + \frac{1}{2} \rho \varepsilon_{ijk} \frac{\partial c_k}{\partial x_j} = \rho \frac{\partial^2 u_i}{\partial t^2} . \tag{3.3}$$

Expanding the permutation symbols, one obtains the identity

$$\varepsilon_{ijk}\varepsilon_{kmn} \frac{\partial^2 u_n}{\partial x_j \partial x_m} = \frac{\partial^2 u_j}{\partial x_i \partial x_j} - \frac{\partial^2 u_i}{\partial x_j^2} . \tag{3.4}$$

Upon substituting this identity into equation (3.3) and rearranging terms, the displacement-equation of motion becomes

$$L_{ij}u_j = f_i , \tag{3.5}$$

where the operator L_{ij} is given by

$$L_{ij} = \left[\left(\frac{\eta'+\eta''\frac{\partial}{\partial t}}{\rho}\right)\frac{\partial^2}{\partial x_\ell^2}\frac{\partial^2}{\partial x_j^2} - \left(\frac{\mu'+\mu''\frac{\partial}{\partial t}}{\rho}\right)\frac{\partial^2}{\partial x_j^2} + \frac{\partial^2}{\partial t^2}\right]\delta_{ij}$$

$$- \left[\left(\frac{\eta'+\eta''\frac{\partial}{\partial t}}{\rho}\right)\frac{\partial^2}{\partial x_\ell^2} + \frac{\lambda'+\mu'+(\lambda''+\mu'')\frac{\partial}{\partial t}}{\rho}\right]\frac{\partial^2}{\partial x_i \partial x_j} . \qquad (3.5a)$$

The effects of a body-couple loading are disregarded here.

CHAPTER IV

METHOD OF APPROACH

In this chapter, a method of approach is prescribed for the study of wave propagation phenomena in the unbounded, homogeneous, isotropic, linear viscoelastic medium with couple-stresses, whose dynamic behavior is governed by field equation (3.5). As was mentioned earlier, many of the studies regarding couple-stresses, for example, investigations of stress concentration problems, have been concerned with the effects of static loadings on the medium. Recent studies have revealed however, that the dynamic stress concentrations are also influenced by the frequency of the applied force. In view of these developments and the stated objective of this study, it seems appropriate that one employ a general approach, applicable to problems wherein the medium may be acted upon dynamically by the body forces in question. Such an approach is provided within the framework of linear field theory.

Linear field theory is one of the classical field theories dealing with the space-time dependent behavior of physical variables which describe field phenomena that are excited by prescribed sources. In the linear regime, the methodology of description is to a large extent independent of the nature of the field and generally applicable to different fields. Within a specified space-time domain, the general linear field requires a description of the field variables and prescribed sources, usually in terms of partial differential equations, subject to the statement of initial and boundary conditions. Solution of the so specified field problem can be effected by formal field representations

in the appropriate space-time domains.

It is observed that knowledge of the symmetry properties of a field often facilitates the determination of explicit field solutions to the field problems. Therefore, if field symmetries exist, it is advantageous to infer such properties from the general form of the field equations prior to their explicit solution. Accordingly, linear field theory suggests that one consider certain auxiliary or adjoint problems, related to the original field problem in such a manner as to reveal the space-time symmetry of the original field. If a technique is employed whereby field problems are formulated in terms of Green's functions which describe the field response to a "point-source excitation", the desired properties appear as symmetries in these Green's functions.

The Green's function technique for the solution of field problems utilizes analytical procedures which have the advantages of (a) displaying in simple terms the field dependence on the excitation, and (b) permitting the use of a mathematical format common to all linear field problems. Since studying the analytical structure of the Green's function for continuous systems provides an effective method for the investigation of the dynamical properties of such systems, the use of a Green's function formalism appears to be consistent with the statement of the problem. It should be emphasized that the Green's function formalism to be applied herein has features common to the description of any linear field.

Consider the unbounded medium whose displacement field is governed by linear partial differential equation (3.5). The linearity of the field implies a corresponding linear dependence of the displacement field u_j on the excitation f_m. Thus, the displacement at any space-time

point, $\vec{x},t$, can be expressed as

$$u_j(\vec{x};t) = \int_{-\infty}^{\infty}\int\int\int\int G_{jm}(\vec{x},\vec{x}';t,t')f_m(\vec{x}';t')d^3\vec{x}'dt' \ , \qquad (4.1)$$

where the integrals are extended over four-dimensional space-time volume elements $d^3\vec{x}'dt'$, wherein the excitation is nonvanishing. $G_{jm}(\vec{x},\vec{x}';t,t')$ is identifiable as a tensorial Green's function representing the displacement at $\vec{x},t$ arising from a unit vector force density acting in the direction e'_m at $\vec{x} = \vec{x}'$, $t = t'$. Thus, a general expression for the solution of the displacement field is written in terms of a newly introduced tensorial Green's function, which is independent of the form of the source distribution.

As noted previously, a peculiarity of the Cosserat field equations is that the antisymmetric part of the stress tensor and the scalar of the couple-stress tensor are left indeterminate. It is observed that the system of Cosserat field equations consists of thirty-seven equation in thirty-eight dependent variables. From a solution, u_j , of equation (3.5), given by equation (4.1), six components of ε_{ij} , three of ω_i , eight of κ_{ij} , nine of τ^A_{ij} and nine of μ^D_{ij} can be computed, leaving only the remaining parts of the stress, namely the three components of the antisymmetric part of the stress and the scalar of the couple-stress, unknown. Although the method of approach employed here allows one to calculate the space- and time-dependent response $u_j(\vec{x};t)$ of the linear field described by equation (3.5) to a known excitation $f_m(\vec{x};t)$, the scope of this investigation does not include the explicit determination of the displacement $u_j(\vec{x};t)$. The central theme of this investigation revolves essentially about the evaluation of Green's function representations for the

displacement field.

The field representation in equation (4.1) reduces the problem of solving field equation (3.5) to the determination of the Green's function G_{jm}. The benefit of this reduction is that, in the solution of the field problem for the Green's function, complexities associated with the functional form of the excitation $f_m(\vec{x};t)$ are eliminated. To develop the defining equation for the Green's function, one substitutes the representation (4.1) into equation (3.5). In view of the arbitrariness of the excitation, one obtains

$$L_{ij}G_{jm}(\vec{x},\vec{x}';t,t') = \delta_{im}\delta(\vec{x}-\vec{x}')\delta(t-t') \quad , \tag{4.2}$$

where L_{ij} is the linear operator in relation (3.5a). It is seen from equation (4.2) that the explicit determination of the Green's function G_{jm} is essentially concerned with the inversion of the tensorial operator L_{ij}. In free space, the inversion is simple and may be accomplished by means of an operator method or an equivalent analytical method.

If field symmetries exist, it is of interest to explore properties of the Green's function that can be inferred prior to the explicit solution of equation (4.2). For example, in the case of an unbounded, homogeneous medium, one readily infers from the invariance of the form of equation (4.2) to arbitrary displacements in space and time that the solution of equation (4.2) is a function of the differences $\vec{x} - \vec{x}'$ and $t - t'$, that is,

$$G_{jm}(\vec{x},\vec{x}';t,t') = G_{jm}(\vec{x}-\vec{x}';t-t') \quad . \tag{4.3}$$

The term "invariant" suggests that the method and result are independent of the choice of coordinate system for the medium. Additional symmetry properties of the Green's function can be inferred by relating the solution of field equation (3.5) to the one obtained from an adjoint problem.

Although a number of formal solutions have been obtained via operator or equivalent techniques for problems where space- and time-dependent fields are excited by arbitrary, space-time source distributions, it is not generally possible to obtain closed-form solutions for such problems. Frequently, their explicit evaluation requires a complicated integration process, depending on the form of the space-time source distributions. When free-space sources of harmonic plane-wave form are considered, however, the determination of field solutions is much simpler to effect because the operator analysis becomes essentially algebraic. Thus, in suitable media, if the source distributions can be analyzed in terms of their plane-wave constituents, the corresponding field response can generally be obtained by algebraic techniques. Then the desired space-time fields can be evaluated by synthesis of the constituent plane-wave responses. When they are applied to appropriate linear fields, analysis and synthesis procedures provide an effective methodology for studying the dynamical properties of a medium as was illustrated by A. Yildiz (1972) when he considered an unbounded medium and examined the wave propagation properties of a linear elastic field with couple-stresses. The remainder of this work concentrates on the development of modal analysis and synthesis procedures in application to the present field problem.

Now, reconsider the unbounded, homogeneous, isotropic, linear

viscoelastic medium whose displacement-equation of motion is given by partial differential equation (3.5). As discussed previously, the displacement field which is describable by linear field equation (3.5) leads to the Green's function $G_{jm}(\vec{x}-\vec{x}';t-t')$ defined by

$$L_{ij}G_{jm}(\vec{x}-\vec{x}';t-t') = \delta_{im}\delta(\vec{x}-\vec{x}')\delta(t-t') \quad , \tag{4.4}$$

where equation (4.3) is substituted into equation (4.2). Since L_{ij} is representable by a square matrix whose elements are tensorial operators, the Green's function G_{jm} is likewise represented as a square matrix whose elements are subsidiary Green's functions.

The invariance of the unbounded, homogeneous, linear medium of equation (4.4) under arbitrary space-time displacements, evident in the independence of L_{ij} on the coordinates $\vec{x}$, t, implies the existence of a plane-wave representation for the Green's function G_{jm}. The Green's function may be represented in various ways as the superposition of wave functions that display the field symmetries. The plane-wave functions $\exp\{-i[\vec{k}\cdot(\vec{x}-\vec{x}')-\omega(t-t')]\}$ constitute a convenient set capable of representing completely the space-time dependent field. The vector wave number $\vec{k}$ and the angular frequency ω characterize the wave periodicities along the spatial and temporal coordinates, $\vec{x}$ and t, respectively. The mathematical basis for such a representation is provided by the four-dimensional Fourier-integral theorem. An integrable space-time function $G_{jm}(\vec{x}-\vec{x}';t-t')$ is accordingly representable as

$$G_{jm}(\vec{x}-\vec{x}';t-t') = \int_{-\infty}^{\infty}\int\int\int\int G_{jm}(\vec{k};\omega)e^{-i[\vec{k}\cdot(\vec{x}-\vec{x}')-\omega(t-t')]}\frac{d^3\vec{k}d\omega}{(2\pi)^4} \quad , \tag{4.5a}$$

where the transform amplitude $G_{jm}(\vec{k};\omega)$ is given by

$$G_{jm}(\vec{k};\omega) = \int_{-\infty}^{\infty}\int\int\int\int G_{jm}(\vec{x}-\vec{x}';t-t')e^{i[\vec{k}\cdot(\vec{x}-\vec{x}')-\omega(t-t')]}d^3(\vec{x}-\vec{x}')d(t-t') \tag{4.5b}$$

with $d^3\vec{k}$ and $d^3(\vec{x}-\vec{x}')$ denoting volume elements in $\vec{k}$ and $\vec{x}$ space, respectively.

The Fourier transforms (4.5a) and (4.5b) can be combined into the more compact form of a "completeness relation", which establishes a plane-wave representation for the four-dimensional space-time delta function:

$$\delta(\vec{x}-\vec{x}')\delta(t-t') = \int_{-\infty}^{\infty}\int\int\int\int e^{-i[\vec{k}\cdot(\vec{x}-\vec{x}')-\omega(t-t')]}\frac{d^3\vec{k}d\omega}{(2\pi)^4} . \tag{4.6a}$$

The transform relations (4.5) are recoverable from equation (4.6a), as is evident on the replacement of $\vec{x}'$ by $\vec{x}' + \vec{x}"$ in the latter, followed by multiplication with $G_{jm}(\vec{x}";t")$ and integration over all space-time volume elements $d^3\vec{x}"dt"$. The transform relations (4.5) also imply an "orthogonality" property,

$$(2\pi)^4\delta(\vec{k}-\vec{k}')\delta(\omega-\omega') = \int_{-\infty}^{\infty}\int\int\int\int e^{i[(\vec{k}-\vec{k}')\cdot(\vec{x}-\vec{x}')-(\omega-\omega')(t-t')]}d^3(\vec{x}-\vec{x}')d(t-t') . \tag{4.6b}$$

With the knowledge of a proper set of modes or waves as a base, modal representation of the solution to the field problem requires a twofold procedure: (a) an analysis or transform process to determine the dependence of the modal amplitude $G_{jm}(\vec{k};\omega)$ on the source, and (b) a modal synthesis or inverse transform process for the evaluation of the space-time Green's function $G_{jm}(\vec{x}-\vec{x}';t-t')$. In field equations that

are invariant to space-time translations, a characteristic feature of the plane-wave representation is that it algebraizes the spatial and temporal derivative operators $\partial/\partial x_j$ and $\partial/\partial t$. According to the basis defined in equations (4.5) and (4.6),

$$\frac{\partial}{\partial x_j} \equiv -ik_j \quad \text{and} \quad \frac{\partial}{\partial t} \equiv i\omega \quad . \tag{4.7}$$

Substitution of equations (4.5a) and (4.6a) into defining equation (4.4) leads via property (4.7) to the transformed equation

$$L_{ij}(\vec{k};\omega)G_{jm}(\vec{k};\omega) = \delta_{im} \tag{4.8}$$

in $\vec{k}$, ω space, where the operator L_{ij} in relation (3.5a) becomes

$$L_{ij}(\vec{k};\omega) = [(\frac{\eta'+i\omega\eta"}{\rho})k^4 + (\frac{\mu'+i\omega\mu"}{\rho})k^2-\omega^2]\delta_{ij}$$

$$- [(\frac{\eta'+i\omega\eta"}{\rho})k^2 - \frac{\lambda'+\mu'+i\omega(\lambda"+\mu")}{\rho}]k_ik_j \quad . \tag{4.8a}$$

The singularity properties of $G_{jm}(\vec{k};\omega)$ in the complex $\vec{k}$, ω planes determine the dispersion properties of plane waves characteristic of the source-free field within the medium. Dispersion implies that the various harmonic wave constituents required to synthesize the field travel at different speeds. Explicit knowledge of the transformed Green's function $G_{jm}(\vec{k};\omega)$ via inversion of equation (4.8) permits by equation (4.5a) the determination of the space- and time-dependent Green's function in equation (4.4). The generality of the analytical procedures employed herein suggests their applicability to any linear field that is invariant under spatial

and temporal displacements.

The inversion of equation (4.8) to solve for the transformed Green's function $G_{jm}(\vec{k};\omega)$ cannot be readily effected due to the contraction of "j" indices between the linear operator L_{ij} and the Green's function G_{jm}. However, by taking the divergence of equation (4.8), the following auxiliary relation, which facilitates the inversion, is found:

$$k_j G_{jm}(\vec{k};\omega) = \frac{k_m}{[\frac{\lambda'+2\mu'+i\omega(\lambda''+2\mu'')}{\rho}]k^2-\omega^2} \quad . \tag{4.9}$$

Substituting equation (4.9) into equation (4.8) and solving for $G_{jm}(\vec{k};\omega)$ yields

$$G_{jm}(\vec{k};\omega) = (\delta_{jm} - \frac{k_j k_m}{k^2})\, G_T(k;\omega) + \frac{k_j k_m}{k^2} G_L(k;\omega) \quad , \tag{4.10}$$

where $G_T(k;\omega)$ and $G_L(k;\omega)$, which depend only on the magnitude of $\vec{k}$, are given by

$$G_T(k;\omega) = \frac{-1}{\omega^2 - i(\frac{\eta''k^2+\mu''}{\rho})k^2\omega - (\frac{\eta'k^2+\mu'}{\rho})k^2} \tag{4.10a}$$

and

$$G_L(k;\omega) = \frac{-1}{\omega^2 - i(\frac{\lambda''+2\mu''}{\rho})k^2\omega - (\frac{\lambda'+2\mu'}{\rho})k^2} \tag{4.10b}$$

Here the subscripts T and L denote, respectively, the transverse and longitudinal components of the Green's function. It is observed that

the longitudinal component $G_L(k;\omega)$ is not influenced by the presence of couple-stresses, whereas the transverse component $G_T(k;\omega)$ is modified by this effect. It should be noted that the tensorial Green's function in equation (4.10) is symmetric with respect to an interchange of "j" and "m" indices.

The components of the Green's function are classified as transverse and longitudinal since they are descriptive of these modes of wave propagation in the medium. In accordance with usual procedure the transverse mode of wave propagation describes waves which propagate through the medium with no dilatation, that is, elements within the medium do not experience a fractional change in volume, while the longitudinal mode of wave propagation corresponds to waves which propagate with no rotation, that is, elements within the medium do not undergo rotation as a rigid body. The conditions for these two types of waves are expressed as $\Delta = \partial u_i/\partial x_i = 0$ and $\omega_i = \frac{1}{2}\varepsilon_{ijk}\partial u_k/\partial x_j = 0$, where Δ is the dilatation and ω_i is the rotation vector which was defined earlier. Transverse waves are also referred to as equivoluminal, distortional, or rotational waves, while the terms irrotational waves and dilatational waves are often used to describe longitudinal waves.

The properties of these two types of waves are reflected in the Green's function by the analytical form of the projection operators which accompany each of the components. An illustration of these properties may be effected by first substituting equation (4.10) into the transformed version of equation (4.1) for $u_j(k;\omega)$, and then operating upon both sides of the resultant equation, in one instance taking the divergence and in another the curl. In the former case the longitudinal component $G_L(k;\omega)$ should be disregarded, whereas in the latter case the transverse

component $G_T(k;\omega)$ should be disregarded. After performing each of these operations, inspection of the altered forms of the equation reveals that the action of the divergence and curl operators eliminate, respectively, the transverse and longitudinal contributions to the expression for the Green's function, according to the definitions prescribed earlier for these quantities. Thus, the Green's function satisfies the conditions stated earlier for the propagation of these two types of waves. The Green's function gives a complete description of wave propagation in the medium, since it is well-known that any displacement field vector can be expressed as the sum of an equivoluminal and an irrotational component, the propagation characteristics of which are given separately by the components $G_T(k;\omega)$ and $G_L(k;\omega)$. It is to be noted that the projection operators not only preserve the transverse and longitudinal properties of the displacement field vector $u_j(\vec{x};t)$, but also indicate its directions as shown in equation (4.1).

One readily infers that the components $G_T(k;\omega)$ and $G_L(k;\omega)$ may be expressed in terms of the tensorial Green's function $G_{jm}(\vec{k};\omega)$ as

$$G_T(k;\omega) = \frac{1}{2}(\delta_{jm} - \frac{k_j k_m}{k^2})G_{jm}(\vec{k};\omega), \quad G_L(k;\omega) = \frac{k_j k_m}{k^2} G_{jm}(\vec{k};\omega) \ . \qquad (4.10c)$$

Having related the propagation of transverse and longitudinal waves in the medium to the components of the Green's function, it is observed, in agreement with previous investigations, that the longitudinal mode of wave propagation is not influenced by the presence of couple-stresses, while the transverse mode of wave propagation is modified by this effect.

According to the twofold analytical procedure outlined for the modal representation of the solution to the field problem, following the

analysis or transform process whereby the dependence of the modal amplitude $G_{jm}(\vec{k};\omega)$ on the source is determined, the space-time Green's function $G_{jm}(\vec{x}-\vec{x}';t-t')$ can be evaluated by performing a modal synthesis or inverse transform process. Recalling that the transformed Green's function $G_{jm}(\vec{k};\omega)$ is explicitly determined in equation (4.10), the corresponding space-time Green's function $G_{jm}(\vec{x}-\vec{x}';t-t')$ is derivable therefrom via inverse Fourier transform relation (4.5a). The subsequent chapters are devoted to the evaluation of the space-time Green's function representation by successive application of the temporal and spatial parts of the inverse Fourier transform to the transformed Green's function. Intermediate Green's function representations in k,ω, $\vec{k},t$, and $\vec{x},\omega$ space are elaborated upon as they constitute an essential part of the synthesis process. Each of these representations for the Green's function by virtue of its different mathematical perspective on the behavior of physical phenomena in the medium provides an alternative point of view from which to examine the dynamical properties of the medium.

In addition to determining the properties characteristic of wave propagation in the infinitely extended, homogeneous, isotropic, linear viscoelastic medium with couple-stresses, it is desirable to compare these properties, both analytically and numerically, with those of other media. It is particularly useful, as a basis for comparison, if media wherein basic wave phenomena are well-known are reexamined from the viewpoint of the method of approach proposed here. In the investigation that follows, the additional media selected for this purpose include a viscoelastic medium without couple-stresses, an elastic medium with couple-stresses, and an elastic medium without couple-stresses: each medium being unbounded, homogeneous, isotropic and linear. It is convenient to

refer to the viscoelastic medium with couple-stresses as the general case, and these additional media as special cases, as each is structurally less complicated, that is, each requires the use of fewer material parameters for its characterization. It appears that a transition from the general case to each special case may be effected via reduction of the formulation. Thus, when one considers the special cases, usually it is not necessary to rederive expressions previously derived for the general case. In most instances, expressions for the special cases may be obtained directly from the corresponding expressions for the general case by disregarding the contribution of specific effects as required by the particular specialization. Expressions obtained for the special cases via these limiting techniques also serve as a check on the consistency of the more complex expressions developed for the general case.

Viscoelastic Medium

The first special case examined is that for a viscoelastic medium without couple-stresses. The absence of couple-stresses in the medium is equivalent to the assumption that the medium offers no resistance to local curvature. The absence of both couple-stresses and body-couples in the medium implies that the properties of stress in the medium are symmetric, that is, $\tau_{ij} = \tau_{ji}$.

It is worthwhile to briefly summarize the fundamental equations applicable to this special case, beginning with the displacement-equation of motion. Once the displacement-equation of motion for the general case is specialized for a viscoelastic medium, duplicating the analytical procedures which are employed in the formal development of the general

case yields the remaining equations. When the terms that account for the effects of couple-stresses on the behavior of dynamical phenomena in the viscoelastic medium with couple-stresses are eliminated by setting the material parameters η' and η'' to zero, displacement-equation of motion (3.3) reduces to the form appropriate for a viscoelastic medium:

$$(\mu'+\mu''\frac{\partial}{\partial t})\frac{\partial^2 u_i}{\partial x_j^2} + [\lambda'+\mu'+(\lambda''+\mu'')\frac{\partial}{\partial t}]\frac{\partial^2 u_j}{\partial x_i \partial x_j} + \rho f_i + \frac{1}{2}\rho\varepsilon_{ijk}\frac{\partial c_k}{\partial x_j} = \rho\frac{\partial^2 u_i}{\partial t^2} . \tag{4.11}$$

Rearranging terms and disregarding the body-couple vector, the displacement equation of motion becomes

$$L^v_{ij} u_j = f_i , \tag{4.12}$$

where the operator L^v_{ij} is given by

$$L^v_{ij} = [-(\frac{\mu'+\mu''\frac{\partial}{\partial t}}{\rho})\frac{\partial^2}{\partial x_j^2} + \frac{\partial^2}{\partial t^2}]\delta_{ij} - [\frac{\lambda'+\mu'+(\lambda''+\mu'')\frac{\partial}{\partial t}}{\rho}]\frac{\partial^2}{\partial x_i \partial x_j} . \tag{4.12a}$$

The superscript v is employed to distinguish quantities appropriate to a viscoelastic medium.

The tensorial Green's function for field equation (4.12) may be expressed as

$$L^v_{ij} G^v_{jm}(\vec{x}-\vec{x}';t-t') = \delta_{im}(\vec{x}-\vec{x}')\delta(t-t') . \tag{4.13}$$

Employing Fourier analysis technique, equation (4.13) is transformed in space and time according to the basis defined in equations (4.5) and (4.6) to yield

$$L^v_{ij}(\vec{k};\omega) G^v_{jm}(\vec{k};\omega) = \delta_{im} , \tag{4.14}$$

where

$$L^{v}_{ij}(\vec{k};\omega) = [(\frac{\mu'+i\omega\mu''}{\rho})k^2-\omega^2]\delta_{ij} + [\frac{\lambda'+\mu'+i\omega(\lambda''+\mu'')}{\rho}]k_i k_j \quad . \quad (4.14a)$$

The inversion of equation (4.14) to solve for the transformed Green's function $G^{v}_{jm}(\vec{k};\omega)$ gives

$$G^{v}_{jm}(\vec{k};\omega) = (\delta_{jm}-\frac{k_j k_m}{k^2})G^{v}_{T}(k;\omega) + \frac{k_j k_m}{k^2} G^{v}_{L}(k;\omega) \quad , \quad (4.15)$$

where

$$G^{v}_{T}(k;\omega) = \frac{-1}{\omega^2-i(\frac{\mu''}{\rho})k^2\omega-(\frac{\mu'}{\rho})k^2} \quad , \quad G^{v}_{L}(k;\omega) = \frac{-1}{\omega^2-i(\frac{\lambda''+2\mu''}{\rho})k^2\omega-(\frac{\lambda'+2\mu'}{\rho})k^2} \quad . \quad (4.15a)$$

It is observed, as expected, that characteristics of the longitudinal mode of wave propagation in the viscoelastic medium with couple-stresses do not undergo change in the transition to the viscoelastic medium, since couple-stresses affect only the transverse mode of wave propagation.

Elastic Medium with Couple-Stresses

The next special case studied is that for an elastic medium with couple-stresses. This case, which earlier was the subject of a brief review, is the one most frequently encountered in literature regarding couple-stresses. It should be recalled from previous discussion that the properties of stress in a medium supporting spatially varying couple-stresses are not necessarily symmetric.

It is worthwhile to briefly summarize the fundamental equations that apply to this special case. If the terms that account for the effects of viscoelasticity on the behavior of dynamical phenomena in the viscoelastic medium with couple-stresses are eliminated by setting the material parameters η'', λ'' and μ'' to zero, displacement-equation of motion (3.3) assumes the form in equation (2.21), which is appropriate for an elastic medium with couple-stresses. After rearranging terms and disregarding the body-couple vector, displacement-equation of motion (2.21) becomes

$$L_{ij}^{ec} u_j = f_i \ , \tag{4.16}$$

where the operator L_{ij}^{ec} is given by

$$L_{ij}^{ec} = \left[\left(\frac{\eta'}{\rho}\right) \frac{\partial^2}{\partial x_\ell^2} \frac{\partial^2}{\partial x_j^2} - \left(\frac{\mu'}{\rho}\right) \frac{\partial^2}{\partial x_j^2} + \frac{\partial^2}{\partial t^2}\right]\delta_{ij} - \left[\left(\frac{\eta'}{\rho}\right) \frac{\partial^2}{\partial x_\ell^2} + \frac{\lambda'+\mu'}{\rho}\right] \frac{\partial^2}{\partial x_i \partial x_j} \ . \tag{4.16a}$$

The superscript ec denotes quantities appropriate to an elastic medium with couple-stresses.

The tensorial Green's function for field equation (4.16) may be expressed as

$$L_{ij}^{ec} G_{jm}^{ec}(\vec{x}-\vec{x}';t-t') = \delta_{im}(\vec{x}-\vec{x}')\delta(t-t') \ . \tag{4.17}$$

Employing Fourier analysis technique, equation (4.17) is transformed in space and time in accordance with the basis defined by relations (4.5) and (4.6) to read as follows:

$$L_{ij}^{ec}(\vec{k};\omega) G_{jm}^{ec}(\vec{k};\omega) = \delta_{im} \ , \tag{4.18}$$

where

$$L_{ij}^{ec}(\vec{k};\omega) = [(\frac{\eta'}{\rho})k^4+(\frac{\mu'}{\rho})k^2-\omega^2]\delta_{ij} -[(\frac{\eta'}{\rho})k^2 - \frac{\lambda'+\mu'}{\rho}]k_i k_j \quad .(4.18a)$$

Solving for $G_{jm}^{ec}(\vec{k};\omega)$ via inversion of equation (4.18) gives

$$G_{jm}^{ec}(\vec{k};\omega) = (\delta_{jm} - \frac{k_j k_m}{k^2})G_T^{ec}(k;\omega) + \frac{k_j k_m}{k^2} G_L^{ec}(k;\omega) \ , \qquad (4.19)$$

where

$$G_T^{ec}(k;\omega) = \frac{-1}{\omega^2-(\frac{\eta'k^2+\mu'}{\rho})k^2} \ , \quad G_L^{ec}(k;\omega) = \frac{-1}{\omega^2-(\frac{\lambda'+2\mu'}{\rho})k^2} \ . \quad (4.19a)$$

Elastic Medium

The last special case considered is that for an elastic medium without couple-stresses. As stated in the discussion regarding the first special case, the absence of couple-stresses in the medium implies that the medium has no resistance to local curvature. If both the couple-stresses and body-couples are absent, the properties of stress in the medium are symmetric, that is, $\tau_{ij} = \tau_{ji}$.

It is worthwhile to briefly summarize the fundamental equations that apply to this special case, beginning with the displacement-equation of motion. When the terms that account for the effects of couple-stresses and viscoelasticity on the behavior of dynamical phenomena in the visco-elastic medium with couple-stresses are eliminated by setting the material parameters η', η'', λ'' and μ'' to zero, displacement-equation of motion

(3.3) reduces to the form appropriate for an elastic medium:

$$\mu' \frac{\partial^2 u_i}{\partial x_j^2} + (\lambda'+\mu') \frac{\partial^2 u_j}{\partial x_i \partial x_j} + \rho f_i + \frac{1}{2} \rho \varepsilon_{ijk} \frac{\partial c_k}{\partial x_j} = \rho \frac{\partial^2 u_i}{\partial t^2} \quad . \tag{4.20}$$

Disregarding the body-couple vector and rearranging terms, displacement-equation of motion (4.20) becomes

$$L^e_{ij} u_j = f_i \ , \tag{4.21}$$

where the operator L^e_{ij} is given by

$$L^e_{ij} = [-(\frac{\mu'}{\rho}) \frac{\partial^2}{\partial x_j^2} + \frac{\partial^2}{\partial t^2}] \delta_{ij} - [\frac{\lambda'+2\mu'}{\rho}] \frac{\partial^2}{\partial x_i \partial x_j} \quad . \tag{4.21a}$$

The superscript e is employed to denote quantities appropriate to an elastic medium.

The tensorial Green's function for field equation (4.21) may be expressed as

$$L^e_{ij} G^e_{jm} (\vec{x}-\vec{x}';t-t') = \delta_{im} \delta(\vec{x}-\vec{x}') \delta(t-t') \quad . \tag{4.22}$$

Employing Fourier analysis technique, equation (4.22) is transformed in space and time according to the basis defined in equations (4.5) and (4.6) to yield

$$L^e_{ij}(\vec{k};\omega) G^e_{jm}(\vec{k};\omega) = \delta_{im} \ , \tag{4.23}$$

where

$$L^e_{ij}(\vec{k};\omega) = [(\frac{\mu'}{\rho}) k^2 - \omega^2] \delta_{ij} + [\frac{\lambda'+\mu'}{\rho}] k_i k_j \quad . \tag{4.23a}$$

The inversion of equation (4.23) to solve for $G^{e}_{jm}(\vec{k};\omega)$ gives

$$G^{e}_{jm}(\vec{k};\omega) = (\delta_{jm} - \frac{k_j k_m}{k^2}) G^{e}_{T}(k;\omega) + \frac{k_j k_m}{k^2} G^{e}_{L}(k;\omega) \ , \qquad (4.24)$$

where

$$G^{e}_{T}(k;\omega) = \frac{-1}{\omega^2 - (\frac{\mu'}{\rho})k^2} \ , \quad G^{e}_{L}(k;\omega) = \frac{-1}{\omega^2 - (\frac{\lambda'+2\mu'}{\rho})k^2} \ . \qquad (4.24a)$$

It is observed that the characteristics of the longitudinal mode of wave propagation for this special case are identical to those for the special case of an elastic medium with couple-stresses, as the longitudinal mode of wave propagation is unaltered by the presence of couple-stresses.

CHAPTER V

GREEN'S FUNCTION REPRESENTATIONS IN THE $\vec{k},\omega$ AND $\vec{k},t$ DOMAINS

The Green's function representation in the $\vec{k},t$ domain may be obtained by application of the temporal part of inverse Fourier transform relation (4.5a) to equation (4.10) for the transformed Green's function in the $\vec{k},\omega$ domain. It is convenient to adopt a more concise notation for $G_{jm}(\vec{k};\omega)$ at this time. Accordingly, the transformed Green's function in equation (4.10) is rewritten as

$$G_{jm}(\vec{k};\omega) = - \frac{P^{T}_{jm}}{\omega^2 - iD_{cT}k^2\omega - C^2_{cT}k^2} - \frac{P^{L}_{jm}}{\omega^2 - iD_{L}k^2\omega - C^2_{L}k^2} , \qquad (5.1)$$

where

$$P^{T}_{jm} = (\delta_{jm} - \frac{k_j k_m}{k^2}) , \quad D_{cT} = \frac{\eta''k^2+\mu''}{\rho} , \quad C^2_{cT} = \frac{\eta'k^2+\mu'}{\rho} = C^2_T(1+\ell^2k^2)$$

$$C^2_T = \frac{\mu'}{\rho} , \quad \ell^2 = \frac{\eta'}{\mu'} \qquad (5.1a)$$

$$P^{L}_{jm} = \frac{k_j k_m}{k^2} , \quad D_L = \frac{\lambda''+2\mu''}{\rho} , \quad C^2_L = \frac{\lambda'+2\mu'}{\rho} .$$

Thus, the material parameter ℓ, mentioned in the introduction, is equal to the square root of the ratio of the elastic bending-twisting modulus to the elastic shear modulus and has the dimension of length. This material length ℓ and the viscous parameter η'' carry with them, respectively, all the elastic and viscous effects of couple-stresses in the subsequent expressions. It can be shown that, with ℓ and η'' not zero, high stress gradients may lead to large couple-stresses. In as

much as the classical theory of elasticity has been verified experimentally in great detail, ℓ and η'' are probably very small in relation to bodily dimensions and wavelengths that are normally encountered.

Applying the temporal part of Fourier inversion integral (4.5a) to the transformed Green's function $G_{jm}(\vec{k};\omega)$ gives

$$G_{jm}(\vec{k};t-t') = \int_{-\infty}^{\infty} G_{jm}(\vec{k};\omega)\, e^{i\omega(t-t')} \frac{d\omega}{2\pi}$$

$$= -P^{T}_{jm} \int_{-\infty}^{\infty} \frac{e^{i\omega(t-t')}}{\omega^2 - iD_{cT}k^2\omega - C_{cT}^2 k^2} \frac{d\omega}{2\pi}$$

$$-P^{L}_{jm} \int_{-\infty}^{\infty} \frac{e^{i\omega(t-t')}}{\omega^2 - iD_{L}k^2\omega - C_{L}^2 k^2} \frac{d\omega}{2\pi} \quad . \tag{5.2}$$

For the purpose of evaluating the Green's function, it is convenient to rewrite equation (5.2) as

$$G_{jm}(\vec{k};t-t') = -P^{T}_{jm} I_1 - P^{L}_{jm} I_2 \, , \tag{5.3}$$

where I_1 and I_2 are the integrals in equation (5.2):

$$I_1 = \int_{-\infty}^{\infty} \frac{e^{i\omega(t-t')}}{\omega^2 - iD_{cT}k^2\omega - C_{cT}^2 k^2} \frac{d\omega}{2\pi} \tag{5.3a}$$

and

$$I_2 = \int_{-\infty}^{\infty} \frac{e^{i\omega(t-t')}}{\omega^2 - iD_{L}k^2\omega - C_{L}^2 k^2} \frac{d\omega}{2\pi} \tag{5.3b}$$

Since these integrals are structurally identical with respect to the variable of integration, they are discussed and evaluated coincidentally in what follows.

The real integrals I_1 and I_2 can be converted into complex integrals and subsequently treated as portions of these integrals by replacing ω with the complex variable z which defines the complex frequency domain. Applying the residue theorem to the closed contours C and C' in the upper and lower halves of the complex z-plane (see Figure 4) yields

$$\oint_{C,C'} \frac{e^{iz(t-t')}}{z^2-iD_{cT}k^2z-C_{cT}^2k^2} \frac{dz}{2\pi} = \pm 2\pi i \sum \text{Residues} \qquad (5.4a)$$

and

$$\oint_{C,C'} \frac{e^{iz(t-t')}}{z^2-iD_{L}k^2z-C_{L}^2k^2} \frac{dz}{2\pi} = \pm 2\pi i \sum \text{Residues} \ , \qquad (5.4b)$$

where the plus and minus signs apply, respectively, to the integrals evaluated along the contours C and C', which are traversed in the positive (counterclockwise) and negative (clockwise) senses, and $\sum$Residues denotes the sum of the residues at all singularities enclosed by the chosen contour. Each of these integrals is well defined and exponentially decreasing in the upper half of the z-plane for $t > t'$ and the lower half of the z-plane for $t < t'$. Thus, the contours C and C' must be selected, respectively, for the cases of $t > t'$ and

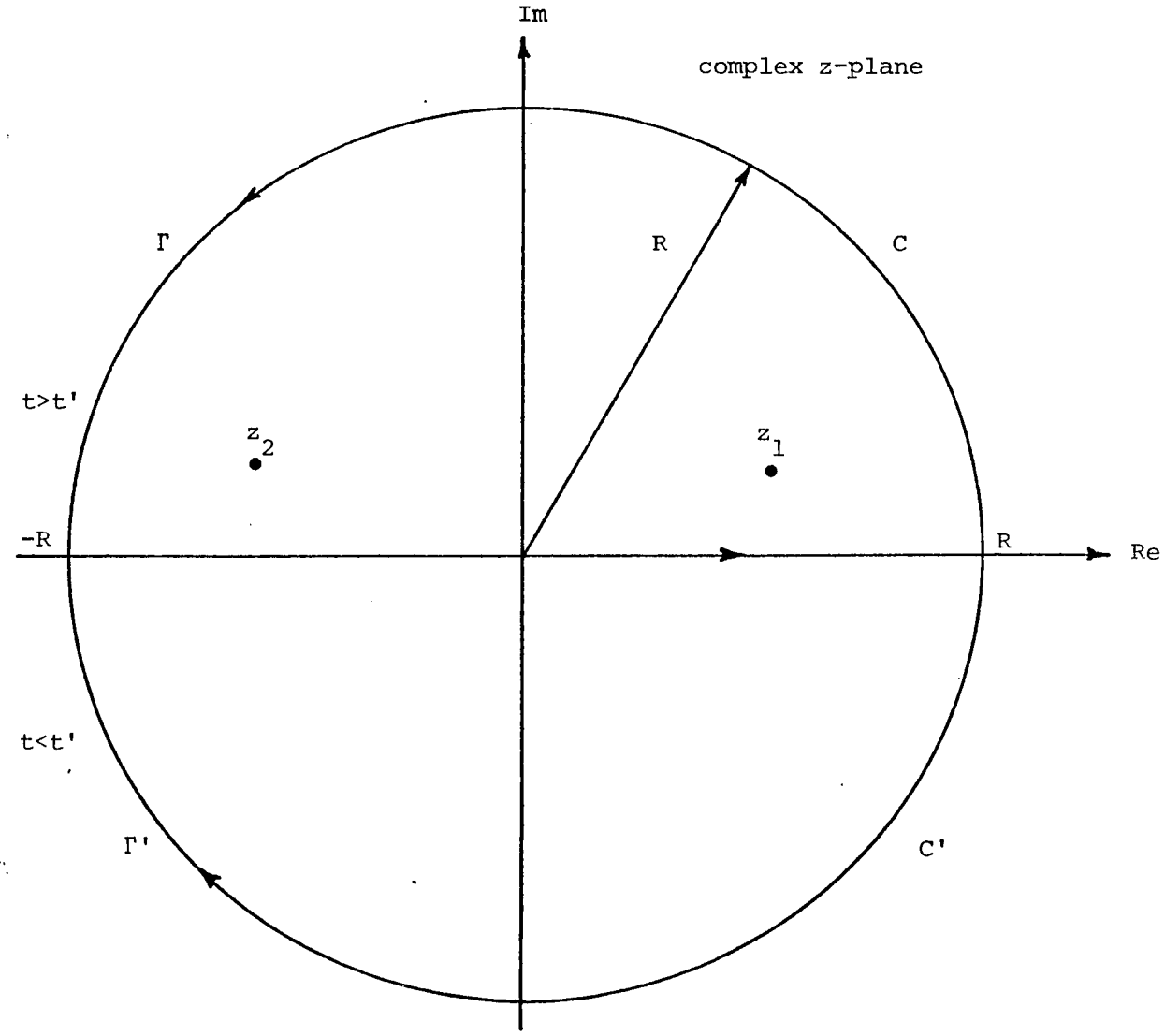

Figure 4. Contours of integration for the complex integrals in equations (5.4).

$t < t'$. The integrals in equations (5.4) may be expressed alternatively as

$$\int_{-R}^{R} \frac{e^{i\omega(t-t')}}{\omega^2 - iD_{cT}k^2\omega - C_{cT}^2k^2} \frac{d\omega}{2\pi}$$

$$+ \int_{\Gamma,\Gamma'} \frac{e^{iz(t-t')}}{z^2 - iD_{cT}k^2 z - C_{cT}^2k^2} \frac{dz}{2\pi} = \pm\, 2\pi i \sum \text{Residues} \qquad (5.5a)$$

and

$$\int_{-R}^{R} \frac{e^{i\omega(t-t')}}{\omega^2 - iD_{L}k^2\omega - C_{L}^2k^2} \frac{d\omega}{2\pi}$$

$$+ \int_{\Gamma,\Gamma'} \frac{e^{iz(t-t')}}{z^2 - iD_{L}k^2 z - C_{L}^2k^2} \frac{dz}{2\pi} = \pm\, 2\pi i \sum \text{Residues} \ , \qquad (5.5b)$$

since they are to be evaluated along the closed paths C and C' in the upper and lower halves of the complex z-plane consisting of the real axis from $-R$ to R and either the semicircle Γ or Γ' . Taking the limit as $R \to \infty$, it follows from equations (5.5) that

$$I_1 = \int_{-\infty}^{\infty} \frac{e^{i\omega(t-t')}}{\omega^2 - iD_{cT}k^2\omega - C_{cT}^2k^2} \frac{d\omega}{2\pi} = \pm\, 2\pi i \sum \text{Residues} \qquad (5.6a)$$

and

$$I_2 = \int_{-\infty}^{\infty} \frac{e^{i\omega(t-t')}}{\omega^2 - iD_{L}k^2\omega - C_{L}^2k^2} \frac{d\omega}{2\pi} = \pm\, 2\pi i \sum \text{Residues} \ . \qquad (5.6b)$$

The integrals over the semicircular arcs $\Gamma(t>t')$ and $\Gamma'(t<t')$ both

approach zero as $R \to \infty$, and thus do not contribute to their respective integrations.

The singularities contributing to the integrals in equations (5.4) consist of simple poles which occur, respectively, at

$$z_{1,2} = \pm C_{cT} k (1-d^2 k^2/\rho)^{1/2} + i \frac{1}{2} D_{cT} k^2$$

and (5.7)

$$z_{1,2} = \pm C_L k (1-h^2 k^2/\rho)^{1/2} + i \frac{1}{2} D_L k^2$$

where

$$d^2 = \frac{(\eta'' k^2+\mu'')^2}{4\mu'(1+\ell^2 k^2)}, \quad h^2 = \frac{(\lambda''+2\mu'')^2}{4(\lambda'+2\mu')} \quad . \tag{5.7a}$$

It is observed that the path of integration in the upper half of the z-plane encloses all the poles of the integrands, or equivalently, that the integrands are analytic within the region enclosed by the path of integration in the lower half of the z-plane. This arrangement of poles is physically significant, suggesting that the medium obeys the principle of causality.

After evaluating the sum of the residues from the poles enclosed within the chosen contour, one obtains the tensorial Green's function

$$G_{jm}(\vec{k};t-t') = u(t-t') \{P^T_{jm} e^{-1/2 D_{cT} k^2 (t-t')} \frac{\sin[C_{cT} k (1-d^2 k^2/\rho)^{1/2} (t-t')]}{C_{cT} k (1-d^2 k^2/\rho)^{1/2}}$$

$$+ P^L_{jm} e^{-1/2 D_L k^2 (t-t')} \frac{\sin[C_L k (1-h^2 k^2/\rho)^{1/2} (t-t')]}{C_L k (1-h^2 k^2/\rho)^{1/2}}\} \quad , \tag{5.8}$$

where $u(t-t')$ represents the unit step function which equals 1 for $t > t'$ and 0 for $t < t'$. Specifically, the Green's function in equation (5.8) gives the response of the medium to a unit vector force density acting in the direction e'_m at $\vec{x} = \vec{x}'$, $t = t'$, as represented in the $\vec{k}$, t domain. Because the response vanishes until a force is applied, $G_{jm}(\vec{k};t-t')$ is called the retarded response function and the medium is said to be causal. Clearly this property of causality follows directly from the analyticity of $G_{jm}(\vec{k};z)$ in the lower half of the complex z-plane. The conditions for the case of underdamped oscillation in the transverse and longitudinal modes are given, respectively, by $2[\mu'(1+\ell^2k^2)\rho]^{1/2} > (\eta''k^2+\mu'')k$ and $2[(\lambda'+2\mu')\rho]^{1/2} > (\lambda''+2\mu'')k$. The overdamped case, where the response decays without oscillation, occurs for these modes when
$2[\mu'(1+\ell^2k^2)\rho]^{1/2} < (\eta''k^2+\mu'')k$ and $2[(\lambda'+2\mu')\rho]^{1/2} < (\lambda''+2\mu'')k$.
It should be noted that the tensorial Green's function obtained here is symmetric under an interchange of "j" and "m" indices.

The natural frequency, ω_n, and damping, ζ, characteristic of the transverse and longitudinal modes of wave propgation in the $\vec{k}$, ω and $\vec{k}$, t domains can be ascertained directly by inspection of the analytical structure of the Green's function representations in these domains. Furthermore, using this information, it is possible to determine other properties of the medium including the attenuation, γ, damped frequency ω_d, quality factor, Q, period, τ, and bandwidth, BW, in terms of the material parameters of the medium. The properties which characterize the transverse and longitudinal modes of wave propagation in the $\vec{k}$, ω and $\vec{k}$, t domains for a viscoelastic medium with couple-

stresses are summarized as follows:

Transverse Wave Properties

$$\omega_{nT} = \left(\frac{\mu'}{\rho}\right)^{1/2}(1+\ell^2k^2)^{1/2}k, \quad \zeta_T = \frac{(\eta''k^2+\mu'')k}{2[\mu'(1+\ell^2k^2)\rho]^{1/2}}, \quad \gamma_T = \zeta_T\omega_{nT} = \frac{1}{2}\left(\frac{\eta''k^2+\mu''}{\rho}\right)k^2$$

$$\omega_{dT} = \omega_{nT}(1-\zeta_T^2)^{1/2} = \left(\frac{\mu'}{\rho}\right)^{1/2}(1+\ell^2k^2)^{1/2}\left[1 - \frac{(\eta''k^2+\mu'')^2k^2}{4\mu'(1+\ell^2k^2)\rho}\right]^{1/2} k ,$$

$$Q_T = \frac{1}{2\zeta_T} = \frac{[\mu'(1+\ell^2k^2)\rho]^{1/2}}{(\eta''k^2+\mu'')k}$$

$$\tau_T = \frac{2\pi}{\omega_{nT}(1-\zeta_T^2)^{1/2}} = \frac{2\pi}{\left(\frac{\mu'}{\rho}\right)^{1/2}(1+\ell^2k^2)^{1/2}\left[1 - \frac{(\eta''k^2+\mu'')^2k^2}{4\mu'(1+\ell^2k^2)\rho}\right]^{1/2} k} ,$$

$$BW_T = 2\zeta_T\omega_{nT} = \left(\frac{\eta''k^2+\mu''}{\rho}\right)k^2 \qquad (5.9a)$$

Longitudinal Wave Properties

$$\omega_{nL} = \left(\frac{\lambda'+2\mu'}{\rho}\right)^{1/2}k, \quad \zeta_L = \frac{(\lambda''+2\mu'')k}{2[(\lambda'+2\mu')\rho]^{1/2}}, \quad \gamma_L = \zeta_L\omega_{nL} = \frac{1}{2}\left(\frac{\lambda''+2\mu''}{\rho}\right)k^2$$

$$\omega_{dL} = \omega_{nL}(1-\zeta_L^2)^{1/2} = \left(\frac{\lambda'+2\mu'}{\rho}\right)^{1/2}\left[1 - \frac{(\lambda''+2\mu'')^2k^2}{4(\lambda'+2\mu')\rho}\right]^{1/2} k, \quad Q_L = \frac{1}{2\zeta_L} = \frac{[(\lambda'+2\mu')\rho]^{1/2}}{(\lambda''+2\mu'')k}$$

$$\tau_L = \frac{2\pi}{\omega_{nL}(1-\zeta_L^2)^{1/2}} = \frac{2\pi}{\left(\frac{\lambda'+2\mu'}{\rho}\right)^{1/2}\left[1 - \frac{(\lambda''+2\mu'')^2k^2}{4(\lambda'+2\mu')\rho}\right]^{1/2} k}, \quad BW_L = 2\zeta_L\omega_{nL} = \left(\frac{\lambda''+2\mu''}{\rho}\right)k^2 .$$

(5.9b)

It is observed that the longitudinal mode of wave propagation is not influenced by the presence of couple-stresses, whereas the transverse mode is modified by this effect.

For real ω , the response function, $G_{jm}(\vec{k};\omega)$, is usually divided into two parts: a dissipative response and a reactive response. When the medium is time-reversal invariant, these are given, respectively, by the imaginary and real parts of $G_{jm}(\vec{k};\omega)$, and denoted as $G''_{jm}(\vec{k};\omega)$ and $G'_{jm}(\vec{k};\omega)$. The dissipative response, also known as the absorptive response, is given by the real odd function of frequency

$$G''_{jm}(\vec{k};\omega) = - \frac{P^T_{jm} D_{cT} k^2 \omega}{(\omega^2 - C_{cT}^2 k^2)^2 + (D_{cT} k^2 \omega)^2} - \frac{P^L_{jm} D_L k^2 \omega}{(\omega^2 - C_L^2 k^2)^2 + (D_L k^2 \omega)^2} . \quad (5.10a)$$

The Fourier transform of $G''_{jm}(\vec{k};\omega)$ is the imaginary odd function of time

$$G''_{jm}(\vec{k};t-t') = \int_{-\infty}^{\infty} G''_{jm}(\vec{k};\omega) e^{i\omega(t-t')} \frac{d\omega}{2\pi}$$

$$= P^T_{jm} e^{-1/2 D_{cT} k^2 |t-t'|} \frac{\sin[C_{cT} k (1-d^2 k^2/\rho)^{1/2} (t-t')]}{2iC_{cT} k (1-d^2 k^2/\rho)^{1/2}}$$

$$+ P^L_{jm} e^{-1/2 D_L k^2 |t-t'|} \frac{\sin[C_L k (1-h^2 k^2/\rho)^{1/2} (t-t')]}{2iC_L k (1-h^2 k^2/\rho)^{1/2}} . \quad (5.11a)$$

The reactive response, also known as the dispersive response, is given by

the real even function of frequency

$$G'_{jm}(\vec{k};\omega) = -\frac{P^T_{jm}(\omega^2-C_{cT}^2k^2)}{(\omega^2-C_{cT}^2k^2)^2+(D_{cT}k^2\omega)^2} - \frac{P^L_{jm}(\omega^2-C_L^2k^2)}{(\omega^2-C_L^2k^2)^2+(D_Lk^2\omega)^2} \quad (5.10b)$$

The Fourier transform of $G'_{jm}(\vec{k};\omega)$ is the real even function of time

$$G'_{jm}(\vec{k};t-t') = \int_{-\infty}^{\infty} G'_{jm}(\vec{k};\omega)e^{i\omega(t-t')}\frac{d\omega}{2\pi}$$

$$= P^T_{jm}e^{-1/2D_{cT}k^2|t-t'|}\frac{\sin[C_{cT}k(1-d^2k^2/\rho)^{1/2}|t-t'|]}{2C_{cT}k(1-d^2k^2/\rho)^{1/2}}$$

$$+ P^L_{jm}e^{-1/2D_Lk^2|t-t'|}\frac{\sin[C_Lk(1-h^2k^2/\rho)^{1/2}|t-t'|]}{2C_Lk(1-h^2k^2/\rho)^{1/2}} \quad (5.11b)$$

The reactive response is symmetric with respect to an interchange of "j" with "m" and t with t' , whereas the dissipative response is antisymmetric under the same interchange.

Because the response function for the dissipative medium discussed here is causal, or equivalently, because $G_{jm}(\vec{k};z)$ which is defined in the lower half of the complex z-plane is also analytic there, it follows that a mutual relationship exists between the real and imaginary parts of $G_{jm}(\vec{k};\omega)$ for real frequencies ω . This relationship is expressed by the Kramers-Kronig relations:

$$G'_{jm}(\vec{k};\omega) = -P\int_{-\infty}^{\infty}\frac{G''_{jm}(\vec{k};\omega')}{\omega'-\omega}\frac{d\omega'}{\pi} \quad (5.12a)$$

$$G''_{jm}(\vec{k};\omega) = P \int_{-\infty}^{\infty} \frac{G'_{jm}(\vec{k};\omega')}{\omega'-\omega} \frac{d\omega'}{\pi} , \qquad (5.12b)$$

where "P" denotes the principal value integral, that is, an integral symmetrical about the singularity (see Appendix A). It is deduced that, with the use of relations (5.12), explicit knowledge of either $G''_{jm}(\vec{k};\omega)$ or $G'_{jm}(\vec{k};\omega)$ is sufficient to permit the determination of $G_{jm}(\vec{k};\omega)$. Thus, for a dissipative medium that obeys the principle of causality, it follows that the real and imaginary parts of the Green's function $G_{jm}(\vec{k};\omega)$ satisfy the Kramers-Kronig relations and the Green's function is uniquely determined by either of its components $G''_{jm}(\vec{k};\omega)$, $G'_{jm}(\vec{k};\omega)$ for real values of ω.

Since the medium discussed here is causal and the time domain response is real, the temporal part of Fourier inversion integral (4.5a) assumes a special form which leads to a relationship between $G_{jm}(\vec{k};t-t')$ and the real and imaginary parts of $G_{jm}(\vec{k};\omega)$. $G_{jm}(\vec{k};t-t')$ may be expressed in terms of either $G'_{jm}(\vec{k};\omega)$ or $G''_{jm}(\vec{k};\omega)$ alone as follows (M. Yildiz, 1974):

$$G_{jm}(\vec{k};t-t') = \begin{matrix} \frac{2}{\pi}\int_0^{\infty} G'_{jm}(\vec{k};\omega)\cos[\omega(t-t')]d\omega \\ \\ -\frac{2}{\pi}\int_0^{\infty} G''_{jm}(\vec{k};\omega)\sin[\omega(t-t')]d\omega \end{matrix} , \quad t > t' . \qquad (5.13)$$

It was remarked earlier that $G'_{jm}(\vec{k};\omega)$ and $G''_{jm}(\vec{k};\omega)$ are not independent of each other but that one of them can be uniquely determined in terms of the other.

Viscoelastic Medium

Green's function representations that appropriately describe the properties of wave propagation for the special case of a viscoelastic medium may be obtained directly from the corresponding representations for the general case of a viscoelastic medium with couple-stresses by disregarding the contribution due to couple-stresses. Since couple-stresses affect only the transverse mode of wave propagation, characteristics of the longitudinal mode of wave propagation do not undergo alteration in the transition to this special case. It should be mentioned that since a viscoelastic medium is a dissipative medium, previous discussion pertaining to the principle of causality may be applied to this special case. When the terms that account for the effects of couple-stresses in the medium are eliminated by setting the material parameters $\ell = \eta'' = 0$, the Green's function representations previously developed for the general case reduce to the following forms:

$$G^{V}_{jm}(\vec{k};\omega) = - \frac{P^{T}_{jm}}{\omega^2 - iD_T k^2 \omega - C_T^2 k^2} - \frac{P^{L}_{jm}}{\omega^2 - iD_L k^2 \omega - C_L^2 k^2} , \qquad (5.14a)$$

$$G^{V}_{jm}(\vec{k};t-t') = u(t-t') \left\{ P^{T}_{jm} e^{-1/2 D_T k^2 (t-t')} \frac{\sin[C_T k (1-g^2 k^2/\rho)^{1/2} (t-t')]}{C_T k (1-g^2 k^2/\rho)^{1/2}} \right.$$

$$\left. + P^{L}_{jm} e^{-1/2 D_L k^2 (t-t')} \frac{\sin[C_L k (1-h^2 k^2/\rho)^{1/2} (t-t')]}{C_L k (1-h^2 k^2/\rho)^{1/2}} \right\} , \qquad (5.14b)$$

$$G''^{V}_{jm}(\vec{k};\omega) = - \frac{P^{T}_{jm} D_T k^2 \omega}{(\omega^2 - C_T^2 k^2)^2 + (D_T k^2 \omega)^2} - \frac{P^{L}_{jm} D_L k^2 \omega}{(\omega^2 - C_L^2 k^2)^2 + (D_L k^2 \omega)^2} , \qquad (5.14c)$$

$$G''^{v}_{jm}(\vec{k};t-t') = P^{T}_{jm} e^{-1/2D_T k^2 |t-t'|} \frac{\sin[C_T k(1-g^2k^2/\rho)^{1/2}(t-t')]}{2iC_T k(1-g^2k^2/\rho)^{1/2}}$$

$$+ P^{L}_{jm} e^{-1/2D_L k^2 |t-t'|} \frac{\sin[C_L k(1-h^2k^2/\rho)^{1/2}(t-t')]}{2iC_L k(1-h^2k^2/\rho)^{1/2}}, \quad (5.14d)$$

$$G'^{v}_{jm}(\vec{k};\omega) = -\frac{P^{T}_{jm}(\omega^2-C_T^2k^2)}{(\omega^2-C_T^2k^2)^2+(D_T k^2\omega)^2} - \frac{P^{L}_{jm}(\omega^2-C_L^2k^2)}{(\omega^2-C_L^2k^2)^2+(D_L k^2\omega)^2}, \quad (5.14e)$$

$$G'^{v}_{jm}(\vec{k};t-t') = P^{T}_{jm} e^{-1/2D_T k^2 |t-t'|} \frac{\sin[C_T k(1-g^2k^2/\rho)^{1/2}|t-t'|]}{2C_T k(1-g^2k^2/\rho)^{1/2}}$$

$$+ P^{L}_{jm} e^{-1/2D_L k^2 |t-t'|} \frac{\sin[C_L k(1-h^2k^2/\rho)^{1/2}|t-t'|]}{2C_L k(1-h^2k^2/\rho)^{1/2}}, \quad (5.14f)$$

where it is necessary to define the new quantities $D_T = \mu''/\rho$ and $g^2 = \mu''^2/4\mu'$. The conditions for the case of underdamped oscillation in the transverse and longitudinal modes are given, respectively, by $2[\mu'\rho]^{1/2} > \mu''k$ and $2[(\lambda'+2\mu')\rho]^{1/2} > (\lambda''+2\mu'')k$. The overdamped case, where the response decays without oscillation, occurs for these modes when $2[\mu'\rho]^{1/2} < \mu''k$ and $2[(\lambda'+2\mu')\rho]^{1/2} < (\lambda''+2\mu'')k$. The properties which characterize the transverse and longitudinal modes of wave propagation in the $\vec{k}$, ω and $\vec{k}$, t domains for a viscoelastic medium are expressed in terms of the material parameters of the medium

as follows:

Transverse Wave Properties

$$\omega_{nT} = \left(\frac{\mu'}{\rho}\right)^{1/2} k, \quad \zeta_T = \frac{\mu'' k}{2(\mu'\rho)^{1/2}}, \quad \gamma_T = \zeta_T \omega_{nT} = \frac{1}{2}\frac{\mu''}{\rho} k^2$$

$$\omega_{dT} = \omega_{nT}(1-\zeta_T^2)^{1/2} = \left(\frac{\mu'}{\rho}\right)^{1/2}\left[1 - \frac{\mu''^2 k^2}{4\mu'\rho}\right]^{1/2} k, \quad Q_T = \frac{1}{2\zeta_T} = \frac{(\mu'\rho)^{1/2}}{\mu'' k}$$

$$\tau_T = \frac{2\pi}{\omega_{nT}(1-\zeta_T^2)^{1/2}} = \frac{2\pi}{\left(\frac{\mu'}{\rho}\right)^{1/2}\left[1 - \frac{\mu''^2 k^2}{4\mu'\rho}\right]^{1/2} k}, \quad BW_T = 2\zeta_T \omega_{nT} = \frac{\mu''}{\rho} k^2 \qquad (5.15a)$$

Longitudinal Wave Properties

$$\omega_{nL} = \left(\frac{\lambda'+2\mu'}{\rho}\right)^{1/2} k, \quad \zeta_L = \frac{(\lambda''+2\mu'')k}{2[(\lambda'+2\mu')\rho]^{1/2}}, \quad \gamma_L = \zeta_L \omega_{nL} = \frac{1}{2}\left(\frac{\lambda''+2\mu''}{\rho}\right)k^2$$

$$\omega_{dL} = \omega_{nL}(1-\zeta_L^2)^{1/2} = \left(\frac{\lambda'+2\mu'}{\rho}\right)^{1/2}\left[1 - \frac{(\lambda''+2\mu'')^2 k^2}{4(\lambda'+2\mu')\rho}\right]^{1/2} k, \quad Q_L = \frac{1}{2\zeta_L} = \frac{[(\lambda'+2\mu')\rho]^{1/2}}{(\lambda''+2\mu'')k}$$

$$\tau_L = \frac{2\pi}{\omega_{nL}(1-\zeta_L^2)^{1/2}} = \frac{2\pi}{\left(\frac{\lambda'+2\mu'}{\rho}\right)^{1/2}\left[1 - \frac{(\lambda''+2\mu'')^2 k^2}{4(\lambda'+2\mu')\rho}\right]^{1/2} k}, \quad BW_L = 2\zeta_L \omega_{nL} = \left(\frac{\lambda''+2\mu''}{\rho}\right)k^2.$$

(5.15b)

Elastic Medium with Couple-Stresses

Green's function representations that appropriately describe the properties of wave propagation for the special case of an elastic medium

with couple-stresses may be obtained directly from the corresponding representations for the general case of a viscoelastic medium with couple-stresses by disregarding the contribution due to viscoelasticity. Since an elastic medium is not a dissipative medium, previous discussion relating to the principle of causality is not applicable to this special case. When the terms that account for the effects of viscoelasticity in the medium are eliminated by setting the material parameters $\eta'' = \lambda'' = \mu'' = 0$, the Green's function representations previously developed for the general case reduce to the following forms:

$$G^{ec}_{jm}(\vec{k};\omega) = - \frac{P^T_{jm}}{\omega^2 - C_{cT}^2 k^2} - \frac{P^L_{jm}}{\omega^2 - C_L^2 k^2} , \qquad (5.16a)$$

$$G^{ec}_{jm}(\vec{k};t-t') = u(t-t') \left\{ P^T_{jm} \frac{\sin[C_{cT}k(t-t')]}{C_{cT}k} + P^L_{jm} \frac{\sin[C_L k(t-t')]}{C_L k} \right\} . \qquad (5.16b)$$

The properties which characterize the transverse and longitudinal modes of wave propagation in the $\vec{k}, \omega$ and $\vec{k}, t$ domains for an elastic medium with couple-stresses are expressed in terms of the material parameters of the medium as follows:

Transverse Wave Properties

$$\omega_{nT} = \left(\frac{\mu'}{\rho}\right)^{1/2} (1+\ell^2 k^2)^{1/2} k, \quad \zeta_T = 0, \quad \gamma_T = \zeta_T \omega_{nT} = 0$$

$$\omega_{dT} = \omega_{nT}(1-\zeta_T^2)^{1/2} = \left(\frac{\mu'}{\rho}\right)^{1/2} (1+\ell^2 k^2)^{1/2} k, \quad Q_T = \frac{1}{2\zeta_T} \text{(undefined)}$$

$$\tau_T = \frac{2\pi}{\omega_{nT}(1-\zeta_T^2)^{1/2}} = \frac{2\pi}{\left(\frac{\mu'}{\rho}\right)^{1/2} (1+\ell^2 k^2)^{1/2} k}, \quad BW_T = 2\zeta_T \omega_{nT} = 0 . \qquad (5.17a)$$

Longitudinal Wave Properties

$$\omega_{nL} = \left(\frac{\lambda'+2\mu'}{\rho}\right)^{1/2} k, \quad \zeta_L = 0, \quad \gamma_L = \zeta_L \omega_{nL} = 0$$

$$\omega_{dL} = \omega_{nL}(1-\zeta_L^2)^{1/2} = \left(\frac{\lambda'+2\mu'}{\rho}\right)^{1/2} k, \quad Q_L = \frac{1}{2\zeta_L}(\text{undefined})$$

$$\tau_L = \frac{2\pi}{\omega_{nL}(1-\zeta_L^2)^{1/2}} = \frac{2\pi}{\left(\frac{\lambda'+2\mu'}{\rho}\right)^{1/2} k}, \quad BW_L = 2\zeta_L \omega_{nL} = 0 \; . \qquad (5.17b)$$

Elastic Medium

Green's function representations that appropriately describe the properties of wave propagation for the special case of an elastic medium may be obtained directly from the corresponding representations for the general case of a viscoelastic medium with couple-stresses by disregarding the contributions due to viscoelasticity and couple-stresses. They may also be obtained from either the special case of a viscoelastic medium or the special case of an elastic medium with couple-stresses by disregarding, respectively, the contributions due to viscoelasticity and couple-stresses. Since couple-stresses influence only the transverse mode of wave propagation, characteristics of the longitudinal mode of wave propagation for this special case are identical to those for the previous special case of an elastic medium with couple-stresses. Because an elastic medium is not a dissipative medium, previous discussion pertaining to the principle of causality is not applicable to this special case. When the terms that account for the effects of viscoelasticity and

couple-stresses are eliminated by setting the material parameters $\ell = \eta'' = \lambda'' = \mu'' = 0$, the Green's function representations previously developed for the general case reduce to the following forms:

$$G^{e}_{jm}(\vec{k};\omega) = - \frac{P^{T}_{jm}}{\omega^2 - C_T^2 k^2} - \frac{P^{L}_{jm}}{\omega^2 - C_L^2 k^2} , \qquad (5.18a)$$

$$G^{e}_{jm}(k;t-t') = u(t-t') \left\{ P^{T}_{jm} \frac{\sin[C_T k(t-t')]}{C_T k} + P^{L}_{jm} \frac{\sin[C_L k(t-t')]}{C_L k} \right\} . \qquad (5.18b)$$

The properties which characterize the transverse and longitudinal modes of wave propagation in the $\vec{k}$, ω and $\vec{k}$, t domains for an elastic medium are expressed in terms of the material parameters of the medium as follows:

Transverse Wave Properties

$$\omega_{nT} = \left(\frac{\mu'}{\rho}\right)^{1/2} k, \quad \zeta_T = 0, \quad \gamma_T = \zeta_T \omega_{nT} = 0$$

$$\omega_{dT} = \omega_{nT}(1-\zeta_T^2)^{1/2} = \left(\frac{\mu'}{\rho}\right)^{1/2} k, \quad Q_T = \frac{1}{2\zeta_T}(\text{undefined})$$

$$\tau_T = \frac{2\pi}{\omega_{nT}(1-\zeta_T^2)^{1/2}} = \frac{2\pi}{\left(\frac{\mu'}{\rho}\right)^{1/2} k}, \quad BW_T = 2\zeta_T \omega_{nT} = 0 \qquad (5.19a)$$

Longitudinal Wave Properties

$$\omega_{nL} = \left(\frac{\lambda'+2\mu'}{\rho}\right)^{1/2} k, \quad \zeta_L = 0, \quad \gamma_L = \zeta_L \omega_{nL} = 0$$

$$\omega_{dL} = \omega_{nL}(1-\zeta_L^2)^{1/2} = \left(\frac{\lambda'+2\mu'}{\rho}\right)^{1/2} k, \quad Q_L = \frac{1}{2\zeta_L}(\text{undefined})$$

$$\tau_L = \frac{2\pi}{\omega_{nL}(1-\zeta_L^2)^{1/2}} = \frac{2\pi}{\left(\frac{\lambda'+2\mu'}{\rho}\right)^{1/2} k}, \quad BW_L = 2\zeta_L \omega_{nL} = 0 \ . \quad (5.19b)$$

CHAPTER VI

GREEN'S FUNCTION REPRESENTATION IN THE $\vec{x},\omega$ DOMAIN

The Green's function representation in the $\vec{x},\omega$ domain may be obtained by application of the spatial part of inverse Fourier transform relation (4.5a) to equation (4.10) for the transformed Green's function in the $\vec{k},\omega$ domain:

$$G_{jm}(\vec{x}-\vec{x}';\omega) = \iiint_{-\infty}^{\infty} G_{jm}(\vec{k};\omega)\, e^{-i\vec{k}\cdot(\vec{x}-\vec{x}')}\, \frac{d^3\vec{k}}{(2\pi)^3}$$

$$= \delta_{jm} \iiint_{-\infty}^{\infty} \frac{e^{-i\vec{k}\cdot(\vec{x}-\vec{x}')}}{(\frac{\eta'+i\omega\eta''}{\rho})k^4+(\frac{\mu'+i\omega\mu''}{\rho})k^2-\omega^2}\, \frac{d^3\vec{k}}{(2\pi)^3}$$

$$+ \frac{\partial^2}{\partial x_j \partial x_m} \iiint_{-\infty}^{\infty} \frac{e^{-i\vec{k}\cdot(\vec{x}-\vec{x}')}}{k^2[(\frac{\eta'+i\omega\eta''}{\rho})k^4+(\frac{\mu'+i\omega\mu''}{\rho})k^2-\omega^2]}\, \frac{d^3\vec{k}}{(2\pi)^3}$$

$$- \frac{\partial^2}{\partial x_j \partial x_m} \iiint_{-\infty}^{\infty} \frac{e^{-i\vec{k}\cdot(\vec{x}-\vec{x}')}}{k^2[[\frac{\lambda'+2\mu'+i\omega(\lambda''+2\mu'')}{\rho}]k^2-\omega^2]}\, \frac{d^3\vec{k}}{(2\pi)^3}\,, \qquad (6.1)$$

where the integrals are to be evaluated over the entire space of $\vec{k}$-vectors.

A convenient approach for the valuation of these integrals utilizes a spatial representation in spherical coordinates. In spherical coordinates an arbitrary vector $\vec{k}$ is related to the orthogonal coordinate directions k_1, k_2, k_3 by the relation

$$k = (k_1,k_2,k_3) = (k\sin\theta\cos\phi, k\sin\theta\sin\phi, k\cos\theta)\,, \qquad (6.2)$$

where $k = |\vec{k}|$. A volume element in this space is given by $d^3\vec{k}$ $= k^2 \sin\theta \, dk \, d\theta \, d\phi$, and if the polar axis is chosen along the direction of $\vec{x} - \vec{x}'$, the quantity $\vec{k}\cdot(\vec{x}-\vec{x}')$, which appears in the exponential term within each integrand, can be replaced by $k|\vec{x}-\vec{x}'|\cos\theta$. Integrating over the angles θ and ϕ first, the Green's function assumes the form

$$G_{jm}(\vec{x}-\vec{x}';\omega) = \delta_{jm}\{\frac{-i}{(2\pi)^2|\vec{x}-\vec{x}'|}\int_0^\infty \frac{k[e^{ik|\vec{x}-\vec{x}'|}-e^{-ik|\vec{x}-\vec{x}'|}]}{(\frac{\eta'+i\omega\eta''}{\rho})k^4+(\frac{\mu'+i\omega\mu''}{\rho})k^2-\omega^2}\,dk\}$$

$$+\frac{\partial^2}{\partial x_j \partial x_m}\{\frac{-i}{(2\pi)^2|\vec{x}-\vec{x}'|}\int_0^\infty \frac{e^{ik|\vec{x}-\vec{x}'|}-e^{-ik|\vec{x}-\vec{x}'|}}{k[(\frac{\eta'+i\omega\eta''}{\rho})k^4+(\frac{\mu'+i\omega\mu''}{\rho})k^2-\omega^2]}\,dk\}$$

$$-\frac{\partial^2}{\partial x_j \partial x_m}\{\frac{-i}{(2\pi)^2|\vec{x}-\vec{x}'|}\int_0^\infty \frac{e^{ik|\vec{x}-\vec{x}'|}-e^{-ik|\vec{x}-\vec{x}'|}}{k[[\frac{\lambda'+2\mu'+i\omega(\lambda''+2\mu'')}{\rho}]k^2-\omega^2]}\,dk\}, \quad (6.3)$$

where the integrations with respect to the angles yield

$$\int_0^\pi e^{-ik|\vec{x}-\vec{x}'|\cos\theta}\sin\theta d\theta \int_0^{2\pi} d\phi = \frac{-2\pi i}{k|\vec{x}-\vec{x}'|}[e^{ik|\vec{x}-\vec{x}'|}-e^{-ik|\vec{x}-\vec{x}'|}] \; . \quad (6.3a)$$

Performing the change of variables $k \to -k$ on the first exponential function in the integrand of each of the integrals permits the limits of integration to be extended from $-\infty$ to ∞ , leaving the following

integrations over k:

$$G_{jm}(\vec{x}-\vec{x}';\omega) = \delta_{jm}\{\frac{i}{(2\pi)^2|\vec{x}-\vec{x}'|}\int_{-\infty}^{\infty}\frac{ke^{-ik|\vec{x}-\vec{x}'|}}{(\frac{\eta'+i\omega\eta''}{\rho})k^4+(\frac{\mu'+i\omega\mu''}{\rho})k^2-\omega^2}\,dk\}$$

$$+\frac{\partial^2}{\partial x_j\partial x_m}\{\frac{i}{(2\pi)^2|\vec{x}-\vec{x}'|}\int_{-\infty}^{\infty}\frac{e^{-ik|\vec{x}-\vec{x}'|}}{k[(\frac{\eta'+i\omega\eta''}{\rho})k^4+(\frac{\mu'+i\omega\mu''}{\rho})k^2-\omega^2]}\,dk\}$$

$$-\frac{\partial^2}{\partial x_j\partial x_m}\{\frac{i}{(2\pi)^2|\vec{x}-\vec{x}'|}\int_{-\infty}^{\infty}\frac{e^{-ik|\vec{x}-\vec{x}'|}}{k[[\frac{\lambda'+2\mu'+i\omega(\lambda''+2\mu'')}{\rho}]k^2-\omega^2]}\,dk\}\ . \qquad (6.4)$$

For the purpose of evaluating the Green's function, it is convenient to express equation (6.4) as

$$G_{jm}(\vec{x}-\vec{x}';\omega) = \delta_{jm}\{\frac{\rho(\eta'-i\omega\eta'')}{(\eta'^2+\omega^2\eta''^2)}\frac{i}{(2\pi)^2|\vec{x}-\vec{x}'|}I_1\}$$

$$+\frac{\partial^2}{\partial x_j\partial x_m}\{\frac{\rho(\eta'-i\omega\eta'')}{(\eta'^2+\omega^2\eta''^2)}\frac{i}{(2\pi)^2|\vec{x}-\vec{x}'|}I_2\}$$

$$-\frac{\partial^2}{\partial x_j\partial x_m}\{\frac{\rho[\lambda'+2\mu'-i\omega(\lambda''+2\mu'')]}{[(\lambda'+2\mu')^2+\omega^2(\lambda''+2\mu'')^2]}\frac{i}{(2\pi)^2|\vec{x}-\vec{x}'|}I_3\}\ , \qquad (6.5)$$

where I_1, I_2, and I_3 denote the integrals

$$I_1 = \int_{-\infty}^{\infty} \frac{k e^{-ik|\vec{x}-\vec{x}'|}}{k^4 + \frac{(\mu'+i\omega\mu")(\eta'-i\omega\eta")}{\eta'^2+\omega^2\eta"^2} k^2 - \frac{\rho\omega^2(\eta'-i\omega\eta")}{\eta'^2+\omega^2\eta"^2}} dk \ , \qquad (6.5a)$$

$$I_2 = \int_{-\infty}^{\infty} \frac{e^{-ik|\vec{x}-\vec{x}'|}}{k[k^4 + \frac{(\mu'+i\omega\mu")(\eta'-i\omega\eta")}{\eta'^2+\omega^2\eta"^2} k^2 - \frac{\rho\omega^2(\eta'-i\omega\eta")}{\eta'^2+\omega^2\eta"^2}]} dk \ , \qquad (6.5b)$$

$$I_3 = \int_{-\infty}^{\infty} \frac{e^{-ik|\vec{x}-\vec{x}'|}}{k[k^2 - \frac{\rho\omega^2[\lambda'+2\mu'-i\omega(\lambda"+2\mu")]}{(\lambda'+2\mu')^2+\omega^2(\lambda"+2\mu")^2}]} dk \ . \qquad (6.5c)$$

Since the integrals I_1 and I_2, which comprise the transverse component of the Green's function, are similar in structure with respect to the variable of integration k, they are evaluated coincidently in what follows.

The real integrals I_1 and I_2 can be converted into complex integrals and subsequently treated as portions of these integrals by replacing k with the complex variable z which defines the complex wavenumber domain. Applying the residue theorem to the closed contour C in the lower half of the complex z-plane (see Figure 5), since each of these integrals is well defined and exponentially decreasing there, yields

$$\oint_C \frac{z e^{-iz|\vec{x}-\vec{x}'|}}{z^4 + \frac{(\mu'+i\omega\mu")(\eta'-i\omega\eta")}{\eta'^2+\omega^2\eta"^2} z^2 - \frac{\rho\omega^2(\eta'-i\omega\eta")}{\eta'^2+\omega^2\eta"^2}} dz = -2\pi i \sum \text{Residues} \qquad (6.6a)$$

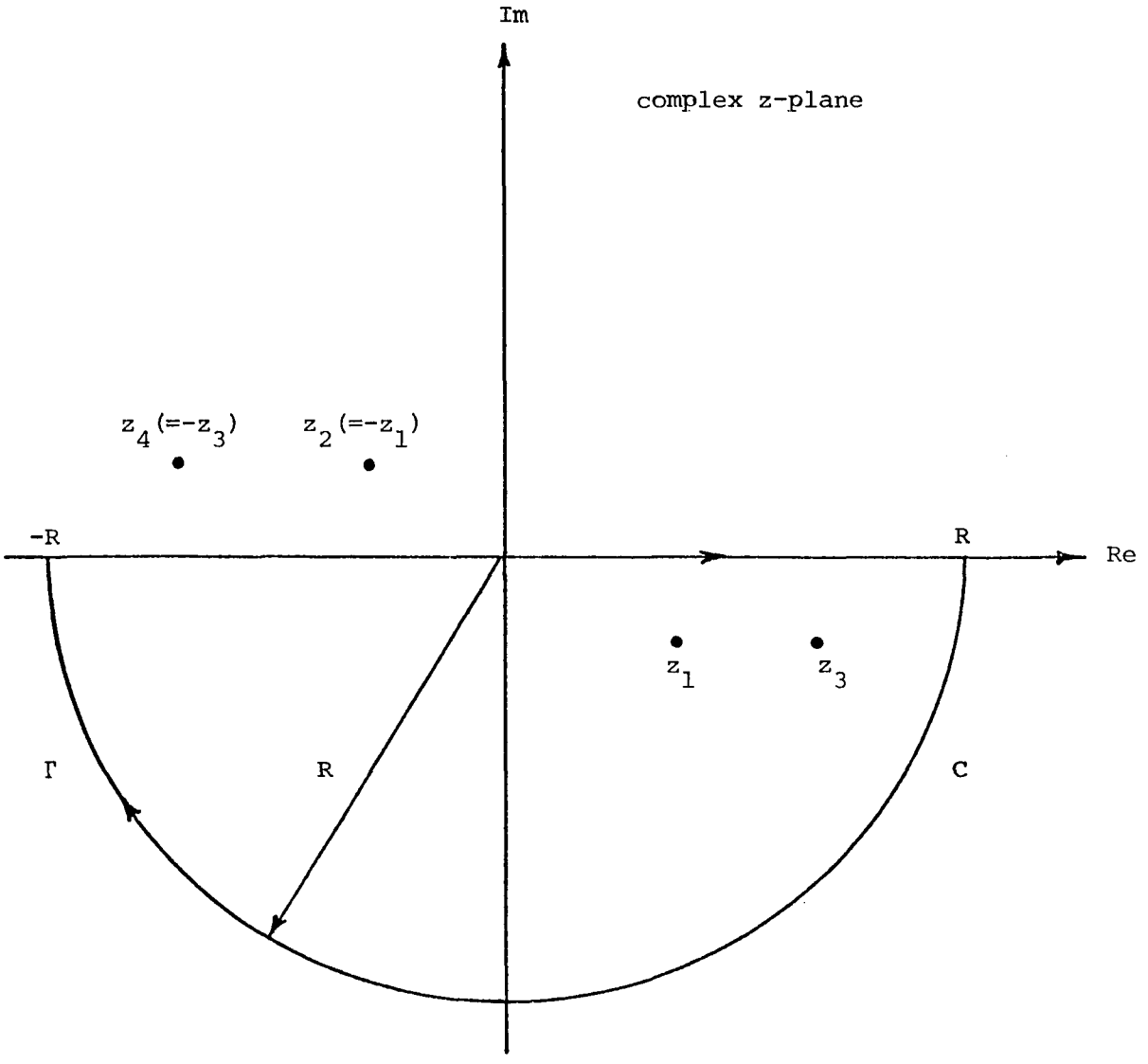

Figure 5. Contour of integration for the complex integrals in equations (6.6).

and

$$\oint_C \frac{e^{-iz|\vec{x}-\vec{x}'|}}{z\left[z^4 + \frac{(\mu'+i\omega\mu")(\eta'-i\omega\eta")}{\eta'^2+\omega^2\eta"^2} z^2 - \frac{\rho\omega^2(\eta'-i\omega\eta")}{\eta'^2+\omega^2\eta"^2}\right]} dz = -2\pi i \sum \text{Residues} , \quad (6.6b)$$

where the minus signs indicate that the contour C is traversed in the negative (clockwise) sense, and $\sum$Residues denotes the sum of the residues at all singularities enclosed by the contour. The integrals in equation (6.6) may be expressed alternatively as

$$\int_{-R}^{R} \frac{ke^{-ik|\vec{x}-\vec{x}'|}}{k^4 + \frac{(\mu'+i\omega\mu")(\eta'-i\omega\eta")}{\eta'^2+\omega^2\eta"^2} k^2 - \frac{\rho\omega^2(\eta'-i\omega\eta")}{\eta'^2+\omega^2\eta"^2}} dk$$

$$+ \int_\Gamma \frac{ze^{-iz|\vec{x}-\vec{x}'|}}{z^4 + \frac{(\mu'+i\omega\mu")(\eta'-i\omega\eta")}{\eta'^2+\omega^2\eta"^2} z^2 - \frac{\rho\omega^2(\eta'-i\omega\eta")}{\eta'^2+\omega^2\eta"^2}} dz = -2\pi i \sum \text{Residues} \quad (6.7a)$$

and

$$\int_{-R}^{R} \frac{e^{-ik|x-x'|}}{k\left[k^4 + \frac{(\mu'+i\omega\mu")(\eta'-i\omega\eta")}{\eta'^2+\omega^2\eta"^2} k^2 - \frac{\rho\omega^2(\eta'-i\omega\eta")}{\eta'^2+\omega^2\eta"^2}\right]} dk$$

$$+ \int_\Gamma \frac{e^{-iz|\vec{x}-\vec{x}'|}}{z\left[z^4 + \frac{(\mu'+i\omega\mu")(\eta'-i\omega\eta")}{\eta'^2+\omega^2\eta"^2} z^2 - \frac{\rho\omega^2(\eta'-i\omega\eta")}{\eta'^2+\omega^2\eta"^2}\right]} dz = -2\pi i \sum \text{Residues}, \quad (6.7b)$$

since they are to be evaluated along the closed path C in the lower half of the complex z-plane consisting of the real axis from $-R$ to R and

the semicircle Γ of radius R. Taking the limit as $R \to \infty$, it follows from equations (6.7) that

$$I_1 = \int_{-\infty}^{\infty} \frac{k e^{-ik|\vec{x}-\vec{x}'|}}{k^4 + \frac{(\mu'+i\omega\mu")(\eta'-i\omega\eta")}{\eta'^2+\omega^2\eta"^2} k^2 - \frac{\rho\omega^2(\eta'-i\omega\eta")}{\eta'^2+\omega^2\eta"^2}} = -2\pi i \sum \text{Residues} \tag{6.8a}$$

and

$$I_2 = \int_{-\infty}^{\infty} \frac{e^{-ik|\vec{x}-\vec{x}'|}}{k\left[k^4 + \frac{(\mu'+i\omega\mu")(\eta'-i\omega\eta")}{\eta'^2+\omega^2\eta"^2} k^2 - \frac{\rho\omega^2(\eta'-i\omega\eta")}{\eta'^2+\omega^2\eta"^2}\right]} dk = -2\pi i \sum \text{Residues} . \tag{6.8b}$$

The integrals over the semicircular arc Γ both approach zero as $R \to \infty$, and thus do not contribute to their respective integrations.

The singularities contributing to the integrals in equations (6.6) consist of simple poles which may be located by setting the denominators of the integrands to zero. The poles of I_2 differ from those of I_1 in that I_2 contains an additional pole at the origin. This pole is, however, a noncontributing factor in the evaluation of I_2, since its residue has no spatial dependence, and, after the residues of I_2 are summed, a spatial operator acts on them. The poles common to I_1 and I_2 are indicated symbolically by

$$z = \pm \left[\frac{-(\mu'+i\omega\mu")(\eta'-i\omega\eta")}{2(\eta'^2+\omega^2\eta"^2)} \pm \frac{(\eta'-i\omega\eta")}{2(\eta'^2+\omega^2\eta"^2)}\left[(\mu'+i\omega\mu")^2+4\rho\omega^2(\eta'+i\omega\eta")\right]^{1/2}\right]^{1/2} . \tag{6.9}$$

It is apparent that the introduction of complex material parameters for the medium renders the task of locating the poles rather cumbersome.

After considerable algebra the poles can be expressed as

$$z_{1,2} = \pm(k'_{T1} - ik''_{T1}) \qquad z_{3,4} = \pm(k'_{T2} - ik''_{T2}) \ , \tag{6.10}$$

where

$$k'_{T1} = \frac{1}{2(\eta'^2+\omega^2\eta''^2)^{1/2}} \times \{[(\eta' f+\mu'\eta'+\omega\eta'' g+\omega^2\mu''\eta'')^2+(\eta' g-\omega\mu'\eta''+\omega\eta'\mu''-\omega\eta'' f)^2]^{1/2}$$

$$-(\eta' f+\mu'\eta'+\omega\eta'' g+\omega^2\mu''\eta'')\}^{1/2} \ , \tag{6.10a}$$

$$k''_{T1} = \frac{1}{2(\eta'^2+\omega^2\eta''^2)^{1/2}} \times \{[(\eta' f+\mu'\eta'+\omega\eta'' g+\omega^2\mu''\eta'')^2+(\eta' g-\omega\mu'\eta''+\omega\eta'\mu''-\omega\eta'' f)^2]^{1/2}$$

$$+(\eta' f+\mu'\eta'+\omega\eta'' g+\omega^2\mu''\eta'')\}^{1/2} \ , \tag{6.10b}$$

$$k'_{T2} = \frac{1}{2(\eta'^2+\omega^2\eta''^2)^{1/2}} \times \{[(\eta' f-\mu'\eta'+\omega\eta'' g-\omega^2\mu''\eta'')^2+(-\eta' g-\omega\mu'\eta''+\omega\eta'\mu''+\omega\eta'' f)^2]^{1/2}$$

$$+(\eta' f-\mu'\eta'+\omega\eta'' g-\omega^2\mu''\eta'')\}^{1/2} \ , \tag{6.10c}$$

$$k''_{T2} = \frac{1}{2(\eta'^2+\omega^2\eta''^2)^{1/2}} \times \{[(\eta' f-\mu'\eta'+\omega\eta'' g-\omega^2\mu''\eta'')^2+(-\eta' g-\omega\mu'\eta''+\omega\eta'\mu''+\omega\eta'' f)^2]^{1/2}$$

$$-(\eta' f-\mu'\eta'+\omega\eta'' g-\omega^2\mu''\eta'')\}^{1/2} \ , \tag{6.10d}$$

$$f = \frac{1}{2^{1/2}} \{[(\mu'^2-\omega^2\mu''^2+4\rho\omega^2\eta')^2+(2\omega\mu'\mu''+4\rho\omega^3\eta'')^2]^{1/2}+(\mu'^2-\omega^2\mu''^2+4\rho\omega^2\eta')\}^{1/2} \ , \tag{6.10e}$$

and

$$g = \frac{1}{2^{1/2}} \{[(\mu'^2-\omega^2\mu''^2+4\rho\omega^2\eta')^2+(2\omega\mu'\mu''+4\rho\omega^3\eta'')^2]^{1/2}-(\mu'^2-\omega^2\mu''^2+4\rho\omega^2\eta')\}^{1/2} \ . \tag{6.10f}$$

It is observed that the path of integration in the lower half of the z-plane contains only the contributions due to z_1 and z_3 which

represent propagation modes. The noncontributing poles z_2 and z_4 which lie outside of the contour correspond to reflection modes from infinity. Thus, the contributing poles in I_1 and I_2 are effectively the same; but of course, the residues themselves are different due to the algebraic forms.

After evaluating the sum of the residues from the poles enclosed within the contour in the lower half plane, one obtains

$$I_1 = \frac{-\pi(\eta'+i\omega\eta")(f-ig)i}{f^2+g^2}\{e^{-k"_{T2}|\vec{x}-\vec{x}'|}e^{-ik'_{T2}|\vec{x}-\vec{x}'|} - e^{-k"_{T1}|\vec{x}-\vec{x}'|}e^{-ik'_{T1}|\vec{x}-\vec{x}'|}\} \tag{6.11a}$$

and

$$I_2 = \frac{-\pi(\eta'+i\omega\eta")(f-ig)i}{f^2+g^2}\{\frac{2(\eta'+i\omega\eta")}{(f+ig)-(\mu'+i\omega\mu")}e^{-k"_{T2}|\vec{x}-\vec{x}'|}e^{-ik'_{T2}|\vec{x}-\vec{x}'|}$$

$$+\frac{2(\eta'+i\omega\eta")}{(f+ig)+(\mu'+i\omega\mu")}e^{-k"_{T1}|\vec{x}-\vec{x}'|}e^{-ik'_{T1}|\vec{x}-\vec{x}'|}\}\ . \tag{6.11b}$$

Now only the integral I_3 for the longitudinal component of the Green's function must be evaluated to complete the inversion procedure.

The real integral I_3 in equation (6.5c) can be converted into a complex integral and subsequently treated as a portion of this integral by replacing k with the complex variable z which defines the complex wavenumber domain. Applying the residue theorem to the closed contour C in the lower half of the complex z-plane (see Figure 6), since this

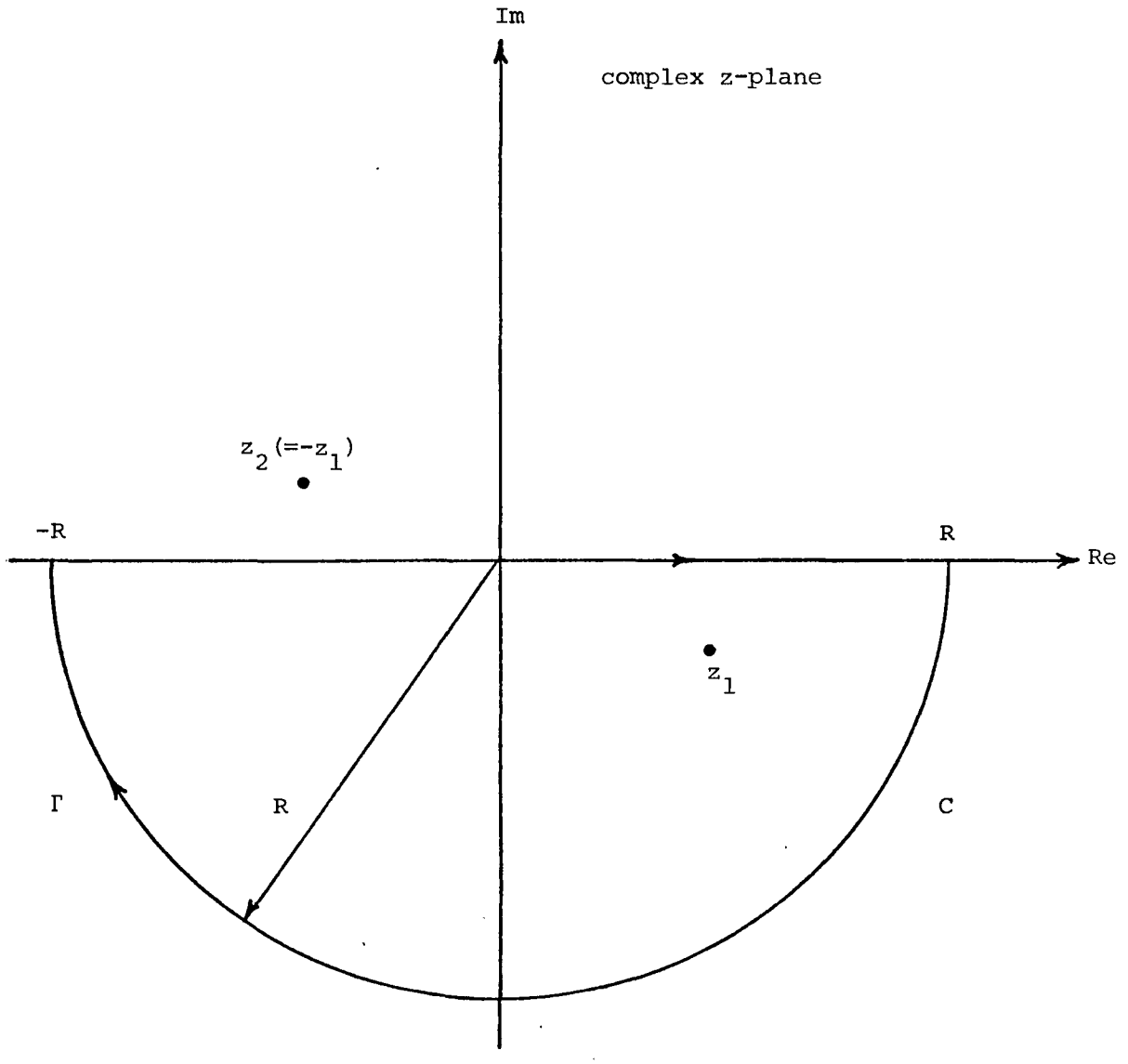

Figure 6. Contour of integration for the complex integral in equation (6.12).

integral is well defined and exponentially decreasing there, yields

$$\oint_C \frac{e^{-iz|\vec{x}-\vec{x}'|}}{z\left[z^2 - \frac{\rho\omega^2[\lambda'+2\mu'-i\omega(\lambda''+2\mu'')]}{(\lambda'+2\mu')^2+\omega^2(\lambda''+2\mu'')^2}\right]} dz = -2\pi i \sum \text{Residues} , \qquad (6.12)$$

where the minus sign denotes that the contour C is traversed in the negative (clockwise) sense, and $\sum$Residues denotes the sum of the residues at all singularities enclosed by the contour. The integral in equation (6.12) may also be expressed as

$$\int_{-R}^{R} \frac{e^{-ik|x-x'|}}{k\left[k^2 - \frac{\rho\omega^2[\lambda'+2\mu'-i\omega(\lambda''+2\mu'')]}{(\lambda'+2\mu')^2+\omega^2(\lambda''+2\mu'')^2}\right]} dk$$

$$+ \int_{\Gamma} \frac{e^{-iz|\vec{x}-\vec{x}'|}}{z\left[z^2 - \frac{\rho\omega^2[\lambda'+2\mu'-i\omega(\lambda''+2\mu'')]}{(\lambda'+2\mu')^2+\omega^2(\lambda''+2\mu'')^2}\right]} dz = -2\pi i \sum \text{Residues} \qquad (6.13)$$

since it is to be evaluated around the closed path C in the lower half of the complex z-plane consisting of the real axis from $-R$ to R and the semicircle Γ of radius R. Taking the limit as $R \to \infty$, it follows from equation (6.13) that

$$I_3 = \int_{-\infty}^{\infty} \frac{e^{-ik|\vec{x}-\vec{x}'|}}{k\left[k^2 - \frac{\rho\omega^2[\lambda'+2\mu'-i\omega(\lambda''+2\mu'')]}{(\lambda'+2\mu')^2+\omega^2(\lambda''+2\mu'')^2}\right]} dk = -2\pi i \sum \text{Residues} . \qquad (6.14)$$

The integral over the semicircular arc Γ approaches zero as $R \to \infty$, and thus does not contribute to the integration.

The singularity contributing to the integral in equation (6.12) consists of a simple pole which may be located by setting the denominator of the integrand to zero. The pole which occurs at the origin does not contribute to the result for I_3, since its residue is not spatially dependent, and, after the residues of I_3 are summed, a spatial operator acts on them. The remaining poles are expressed symbolically as

$$z = \pm\left[\frac{\rho\omega^2[\lambda'+2\mu'-i\omega(\lambda''+2\mu'')]}{(\lambda'+2\mu')^2+\omega^2(\lambda''+2\mu'')^2}\right]^{1/2} . \tag{6.15}$$

After considerable algebra the poles can be expressed as

$$z_{1,2} = (k_L'-ik_L'') , \tag{6.16}$$

where

$$k_L' = k_L\left\{\frac{[1+\omega^2(\frac{\lambda''+2\mu''}{\lambda'+2\mu'})^2]^{1/2}+1}{2[1+\omega^2(\frac{\lambda''+2\mu''}{\lambda'+2\mu'})^2]}\right\}^{1/2} , \quad k_L'' = k_L\left\{\frac{[1+\omega^2(\frac{\lambda''+2\mu''}{\lambda'+2\mu'})^2]^{1/2}-1}{2[1+\omega^2(\frac{\lambda''+2\mu''}{\lambda'+2\mu'})^2]}\right\}^{1/2} ,$$

$$k_L = \frac{\omega}{C_L} = \frac{\omega}{(\frac{\lambda'+2\mu'}{\rho})^{1/2}} . \tag{6.16a}$$

It is observed that the path of integration in the lower half of the z-plane contains only the contribution due to z_1 which represents a propagation mode. The noncontributing pole z_2 which lies outside of the contour corresponds to a reflection mode from infinity.

After evaluating the residue from the pole enclosed within the contour in the lower half plane, one obtains

$$I_3 = \frac{-\pi[\lambda'+2\mu'+i\omega(\lambda''+2\mu'')]i}{\rho\omega^2} e^{-k_L''|\vec{x}-\vec{x}'|} e^{-ik_L'|\vec{x}-\vec{x}'|} . \tag{6.17}$$

Combining the transverse and longitudinal components of the Green's function by substituting the values of I_1, I_2, and I_3 from equations (6.11) and (6.17) into equation (6.5) gives

$$G_{jm}(x-x';\omega) =$$

$$\frac{-\rho(f-ig)}{(f^2+g^2)}\left[\delta_{jm} + \frac{2(\eta'+i\omega\eta'')}{(f+ig)+(\mu'+i\omega\mu'')}\frac{\partial^2}{\partial x_j \partial x'_m}\right]\frac{e^{-k''_{T1}|\vec{x}-\vec{x}'|}\, e^{-ik'_{T1}|\vec{x}-\vec{x}'|}}{4\pi|\vec{x}-\vec{x}'|}$$

$$+\frac{\rho(f-ig)}{f^2+g^2}\left[\delta_{jm} - \frac{2(\eta'+i\omega\eta'')}{(f+ig)-(\mu'+i\omega\mu'')}\frac{\partial^2}{\partial x_j \partial x'_m}\right]\frac{e^{-k''_{T2}|\vec{x}-\vec{x}'|}\, e^{-ik'_{T2}|\vec{x}-\vec{x}'|}}{4\pi|\vec{x}-\vec{x}'|}$$

$$+\frac{1}{\omega^2}\frac{\partial^2}{\partial x_j \partial x'_m}\frac{e^{-k''_{L}|\vec{x}-\vec{x}'|}\, e^{-ik'_{L}|\vec{x}-\vec{x}'|}}{4\pi|\vec{x}-\vec{x}'|}, \qquad (6.18)$$

where $\partial/\partial x'_m = -\partial/\partial x_m$. A comparison with the special case of a visco-elastic medium, which follows, shows that the longitudinal mode of wave propagation in the viscoelastic medium is unaltered by the presence of couple-stresses; however, the transverse mode of wave propagation undergoes changes due to the effects of couple-stresses that include: (i) the introduction of a new mode of wave propagation with complex wavenumber $k'_{T1} - ik''_{T1}$; (ii) the modification of the complex wavenumber for the usual mode of wave propagation from $k'_T - ik''_T$ to $k'_{T2} - ik''_{T2}$; and (iii) the modification of the amplitude of the usual mode of wave propagation. The propagation of an additional transverse wave due to the effects of couple-stresses is in agreement with the findings of Mindlin and Tiersten (1962) in their study of the propagation of waves in an elastic medium with couple-stresses. They found that three types of waves, including an

additional transverse wave, may exist in such a medium in contrast to the two predicted by classical elasticity. It should be noted that the tensorial Green's function obtained here is symmetric under an interchange of the "j" and "m" indices and also symmetric with respect to an interchange of $\vec{x}$ and $\vec{x}'$.

The attenuation constants and velocities of propagation characteristic of the transverse and longitudinal modes of wave propagation in the $\vec{x},\omega$ domain can be determined directly by inspection of the analytical structure of the Green's function representation in this domain. The amplitudes of the transverse and longitudinal waves are attenuated with distance as they propagate through the medium in accordance with the terms $\exp(-k''_{T1}|\vec{x}-\vec{x}'|)$, $\exp(-k''_{T2}|\vec{x}-\vec{x}'|)$, and $\exp(-k''_{L}|\vec{x}-\vec{x}'|)$, where k''_{T1}, k''_{T2}, and k''_{L} are the respective attenuation constants for these waves. These attenuation constants serve as a measure of the internal friction of the medium. The velocities of propagation of these modes, known as phase velocities, are defined by means of the equations $C'_{T1} = \omega/k'_{T1}$, $C'_{T2} = \omega/k'_{T2}$, and $C'_{L} = \omega/k'_{L}$. It may be seen from equations (6.10a - f) and (6.16a) that k'_{T1}, k''_{T1}, k'_{T2}, k''_{T2}, k'_{L}, and k''_{L} all vary with frequency. The quantities k'_{T1}, k'_{T2}, and k'_{L} vary with frequency in a manner such that the phase velocities C'_{T1}, C'_{T2}, and C'_{L} are also dependent on frequency. This dependence of phase velocity on frequency indicates that the relaxation behavior of waves associated with the viscous properties of the medium not only produces attenuation in the amplitudes but also dispersion in the velocities of propagation.

Viscoelastic Medium

The Green's function representation that appropriately describes the properties of wave propagation for the special case of a viscoelastic medium may be obtained directly from the corresponding representation for the general case of a viscoelastic medium with couple-stresses by disregarding the contribution due to couple-stresses. Since couple-stresses affect only the transverse mode of wave propagation, characteristics of the longitudinal mode of wave propagation do not undergo alteration in the transition to this special case. When the terms that account for the effects of couple-stresses in the medium are eliminated by setting the material parameters $\eta' = \eta'' = 0$, the Green's function representation previously developed for the general case reduces to the form

$$G^{v}_{jm}(\vec{x}-\vec{x}';\omega) =$$

$$\left[\frac{\rho(\mu'-i\omega\mu'')}{\mu'^2+\omega^2\mu''^2}\,\delta_{jm} - \frac{1}{\omega^2}\frac{\partial^2}{\partial x_j \partial x'_m}\right]\frac{e^{-k''_T|\vec{x}-\vec{x}'|}\,e^{-ik'_T|\vec{x}-\vec{x}'|}}{4\pi|\vec{x}-\vec{x}'|}$$

$$+\frac{1}{\omega^2}\frac{\partial^2}{\partial x_j \partial x'_m}\frac{e^{-k''_L|\vec{x}-\vec{x}'|}\,e^{-ik'_L|\vec{x}-\vec{x}'|}}{4\pi|\vec{x}-\vec{x}'|}, \qquad (6.19)$$

where the quantities k'_{T1}, k''_{T1}, k'_{T2}, and k''_{T2} in the general case, upon which the attenuation constants and velocities of propagation of waves in the medium are dependent, have undergone the following changes:

$$k'_{T1} \to \infty \quad , \quad k''_{T1} \to \infty$$

$$k'_{T2} \to k'_T = k_T\left\{\frac{[1+\omega^2(\frac{\mu''}{\mu'})^2]^{1/2}+1}{2[1+\omega^2(\frac{\mu''}{\mu'})^2]}\right\}^{1/2}, \quad k''_{T2} \to k''_T = k_T\left\{\frac{[1+\omega^2(\frac{\mu''}{\mu'})^2]^{1/2}-1}{2[1+\omega^2(\frac{\mu''}{\mu'})^2]}\right\}^{1/2} \qquad (6.19a)$$

$$k_T = \frac{\omega}{C_T} = \frac{\omega}{\left(\frac{\mu'}{\rho}\right)^{1/2}} \quad .$$

It is observed that the additional transverse mode of wave propagation with wavenumber $k'_{T1} - ik''_{T1}$, introduced by the presence of couple-stresses in the medium, vanishes in the absence of couple-stresses, while the usual transverse mode is modified during the transition to this special case.

The amplitudes of the transverse and longitudinal waves are attenuated with distance as they propagate through the medium in accordance with the terms $\exp(-k''_T|\vec{x}-\vec{x}'|)$ and $\exp(-k''_L|\vec{x}-\vec{x}'|)$, where k''_T and k''_L are the respective attenuation constants for these waves. The phase velocities corresponding to these modes of wave propagation are defined by the equations $C'_T = \omega/k'_T$ and $C'_L = \omega/k'_L$. It may be seen from equation (6.16a) and (6.19a) that k'_T, k''_T, k'_L and k''_L all vary with frequency. The quantities k'_T and k'_L vary with frequency in a manner such that the phase velocities C'_T and C'_L are also dependent on frequency. This dependence of phase velocity on frequency indicates that the relaxation behavior of waves associated with the viscous properties of the medium produces dispersion in the velocities of propagation in addition to attenuation in the amplitudes.

Elastic Medium with Couple-Stresses

The Green's function representation that appropriately describes the properties of wave propagation for the special case of an elastic medium with couple-stresses may be obtained directly from the corresponding

representation for the general case of a viscoelastic medium with couple-stresses by disregarding the contribution due to viscoelasticity. When the terms that account for the effects of viscoelasticity in the medium are eliminated by setting the material parameters $\eta'' = \lambda'' = \mu'' = 0$, the Green's function representation previously developed for the general case reduces to the form

$$G^{ec}_{jm}(\vec{x}-\vec{x}';\omega) = \frac{-1}{C_T^2(1+4\ell^2k_T^2)^{1/2}}(\delta_{jm} + \frac{1}{k_{T1}^2}\frac{\partial^2}{\partial x_j \partial x'_m})\frac{e^{-k_{T1}|\vec{x}-\vec{x}'|}}{4\pi|\vec{x}-\vec{x}'|}$$

$$+ \frac{1}{C_T^2(1+4\ell^2k_T^2)^{1/2}}(\delta_{jm} - \frac{1}{k_{T2}^2}\frac{\partial^2}{\partial x_j \partial x'_m})\frac{e^{-ik_{T2}|\vec{x}-\vec{x}'|}}{4\pi|\vec{x}-\vec{x}'|} + \frac{1}{\omega^2}\frac{\partial^2}{\partial x_j \partial x'_m}\frac{e^{-ik_L|\vec{x}-\vec{x}'|}}{4\pi|\vec{x}-\vec{x}'|}\,, \tag{6.20}$$

where the quantities k'_{T1}, k''_{T1}, k'_{T2}, k''_{T2}, k'_L and k''_L in the general case, upon which the attenuation constants and velocities of propagation of waves in the medium are dependent, have undergone the following changes:

$$k'_{T1} \to 0\,, \quad k''_{T1} \to k_{T1} = \frac{1}{2^{1/2}\ell}[(1+4\ell^2k_T^2)^{1/2}+1]^{1/2}$$

$$k'_{T2} \to k_{T2} = \frac{1}{2^{1/2}\ell}[(1+4\ell^2k_T^2)^{1/2}-1]^{1/2}\,, \quad k''_{T2} \to 0$$

$$k'_L \to k_L\,, \quad k''_L \to 0\,. \tag{6.20a}$$

It is observed that both transverse modes of wave propagation and the longitudinal mode of wave propagation are modified during the transition to this special case. The additional transverse mode of wave propagation associated with the presence of couple-stresses in the medium becomes a

non-propagating, or purely attenuated mode, whereas the other transverse mode and the longitudinal mode are no longer attenuated in this special case. The expression for $G^{ec}_{jm}(\vec{x}-\vec{x}';\omega)$ in equation (6.20) agrees with the one obtained by A. Yildiz (1972) except that it contains an additional $-1/C_T^2$ factor and the time dependence employed is different. The former difference is attributable to the manner in which the Green's function is defined and does not affect the value of the displacement predicted by use of equation (4.1).

The overdamped transverse mode associated with the presence of couple-stresses in the medium is attenuated with distance in accordance with the term $\exp(-k_{T1}|\vec{x}-\vec{x}'|)$, where k_{T1} is the attenuation constant. The other transverse mode and the longitudinal mode are not attenuated as they propagate through the medium. The phase velocities corresponding to these modes of wave propagation are defined by the equations $C_{T2} = \omega/k_{T2}$ and $C_L = \omega/k_L$. It may be seen from equations (6.16a), (6.19), and (6.20a) that k_{T2} and k_L vary with frequency. The quantity k_{T2} varies with frequency in a manner such that the phase velocity C_{T2} is also dependent on frequency. This dependence of phase velocity on frequency indicates that the wave is propagated dispersively. On the other hand, k_L is directly proportional to the first power of the frequency such that the velocity of propagation C_L is independent of frequency. Thus, the longitudinal wave is propagated non-dispersively.

A comparison with the special case of an elastic medium, which follows, shows that the longitudinal mode of wave propagation in the elastic medium is unaltered by the presence of couple-stresses; however, the transverse mode of wave propagation undergoes changes due to the

effects of couple-stresses that include: (i) the introduction of a new mode of wave propagation with wavenumber k_{T1}; (ii) the modification of the wavenumber for the usual mode of wave propagation from k_T to k_{T2}; and (iii) the modification of the amplitude of the usual mode of wave propagation.

Elastic Medium

The Green's function representation that appropriately describes the properties of wave propagation for the special case of an elastic medium may be obtained directly from the corresponding representations for the special cases of either a viscoelastic medium or an elastic medium with couple-stresses by disregarding, respectively, the contributions due to viscoelasticity and couple-stresses. Since couple-stresses influence only the transverse mode of wave propagation, characteristics of the longitudinal mode of wave propagation for this special case are identical to those for the previous special case of an elastic medium with couple-stresses. When the terms that account for the effects of viscoelasticity in the special case of a viscoelastic medium are eliminated by setting the material parameters $\lambda'' = \eta'' = 0$, or the terms that account for the effects of couple-stresses in the special case of an elastic medium with couple-stresses are eliminated by setting the material parameter $\ell = 0$, the Green's function representations previously developed for these special cases reduce to the form

$$G^{e}_{jm}(\vec{x}-\vec{x}';\omega) = \frac{1}{c_T^2}\left(\delta_{jm} - \frac{1}{k_T^2}\frac{\partial^2}{\partial x_j \partial x'_m}\right)\frac{e^{-ik_T|\vec{x}-\vec{x}'|}}{4\pi|\vec{x}-\vec{x}'|} + \frac{1}{\omega^2}\frac{\partial^2}{\partial x_j \partial x'_m}\frac{e^{-ik_L|\vec{x}-\vec{x}'|}}{4\pi|\vec{x}-\vec{x}'|}. \quad (6.21)$$

The quantities k_T'', k_T', k_L'', and k_L', upon which the attenuation constants and velocities of propagation of waves in the viscoelastic medium are dependent, have undergone the changes

$$k_T'' \to 0 \ , \quad k_T' \to k_T \ , \quad k_L'' \to 0 \ , \quad k_L' \to k_L \ , \tag{6.21a}$$

while the quantities k_{T1} and k_{T2}, upon which these same wave properties in the elastic medium with couple-stresses are dependent, have undergone the changes

$$k_{T1} \to \infty \ , \quad k_{T2} \to k_T \ . \tag{6.21b}$$

It is observed that the transverse and longitudinal modes of wave propagation are modified during the transition from the viscoelastic medium to this special case, while only the transverse modes of wave propagation are altered in the transition from the elastic medium with couple-stresses to this special case, since couple-stresses influence only the transverse mode of wave propagation. The transition from the viscoelastic medium leads to an expression for $G_{jm}^{e}(\vec{x}-\vec{x}';\omega)$ wherein the transverse and longitudinal modes are no longer attenuated for this special case. The additional transverse mode of wave propagation with wavenumber k_{T1}, associated with the presence of couple-stresses in the elastic medium, vanishes in the absence of couple-stresses, while the usual transverse mode is modified during the transition from the elastic medium with couple-stresses. The expression for $G_{jm}^{e}(\vec{x}-\vec{x}';\omega)$ in equation (6.21) agrees with the one obtained by A. Yildiz (1964, 1972) except that it contains an additional $-1/C_T^2$ factor and the time dependence is different. The former difference is a direct consequence of the manner in which the

Green's function is defined and does not affect the value of the displacement predicted by use of equation (4.1). Since k_T and k_L are directly proportional to the first power of frequency, the velocities of propagation $C_T = \omega/k_T$ and $C_L = \omega/k_L$ are independent of frequency. Thus, the transverse and longitudinal waves propagating through the elastic medium do not undergo attenuation in their amplitudes or dispersion in their velocities of propagation.

CHAPTER VII

GREEN'S FUNCTION REPRESENTATION IN THE $\vec{x},t$ DOMAIN

The Green's function representation in the $\vec{x},t$ domain may be obtained by application of the spatial part of inverse Fourier transform relation (4.5a) to equation (5.8) for the transformed Green's function in the $\vec{k},t$ domain:

$$G_{jm}(\vec{x}-\vec{x}';t-t') = \iiint_{-\infty}^{\infty} G_{jm}(\vec{k};t-t')e^{-i\vec{k}\cdot(\vec{x}-\vec{x}')}\frac{d^3\vec{k}}{(2\pi)^3} = u(t-t') \times$$

$$\{\delta_{jm}\iiint_{-\infty}^{\infty} e^{-1/2D_{cT}k^2(t-t')}\frac{\sin[C_{cT}k(1-d^2k^2/\rho)^{1/2}(t-t')]}{C_{cT}k(1-d^2k^2/\rho)^{1/2}}e^{-i\vec{k}\cdot(\vec{x}-\vec{x}')}\frac{d^3\vec{k}}{(2\pi)^3}$$

$$+\frac{\partial^2}{\partial x_j\partial x_m}\iiint_{-\infty}^{\infty} e^{-1/2D_{cT}k^2(t-t')}\frac{\sin[C_{cT}k(1-d^2k^2/\rho)^{1/2}(t-t')]}{C_{cT}k^3(1-d^2k^2/\rho)^{1/2}}e^{-i\vec{k}\cdot(\vec{x}-\vec{x}')}\frac{d^3\vec{k}}{(2\pi)^3}$$

$$-\frac{\partial^2}{\partial x_j\partial x_m}\iiint_{\infty}^{\infty} e^{-1/2D_Lk^2(t-t')}\frac{\sin[C_Lk(1-h^2k^2/\rho)^{1/2}(t-t')]}{C_Lk^3(1-h^2k^2/\rho)^{1/2}}e^{-i\vec{k}\cdot(\vec{x}-\vec{x}')}\frac{d^3\vec{k}}{(2\pi)^3}\},$$

(7.1)

where

$$D_{cT} = \frac{\eta"k^2+\mu"}{\rho}, \quad C_{cT}^2 = C_T^2(1+\ell^2k^2), \quad d^2 = \frac{(\eta"k^2+\mu")^2}{4\mu'(1+\ell^2k^2)}$$

$$D_L = \frac{\lambda"+2\mu"}{\rho}, \quad h^2 = \frac{(\lambda"+2\mu")^2}{4(\lambda'+2\mu')}$$

$$C_T^2 = \frac{\mu'}{\rho}, \quad \ell^2 = \frac{\eta'}{\mu'}, \quad C_L^2 = \frac{\lambda'+2\mu'}{\rho} \qquad (7.1a)$$

and $u(t-t')$ represents the unit step function. These integrals are to be evaluated over the entire space of $\vec{k}$-vectors.

A convenient approach for the evaluation of integrals of this type, which utilizes a spatial representation in spherical coordinates, was outlined previously for the integrals in equation (6.1). Accordingly, a volume element in $\vec{k}$-space is expressed as $d^3\vec{k} = k^2 \sin\theta \, dk \, d\theta \, d\phi$, and when the polar axis is chosen along the direction of $\vec{x}-\vec{x}'$, the quantity $\vec{k}\cdot(\vec{x}-\vec{x}')$, which appears in the exponential term within each integrand, can be replaced by $k|\vec{x}-\vec{x}'|\cos\theta$, where $k = |\vec{k}|$. Integrating with respect to the angles θ and ϕ first, the Green's function assumes the form

$$G_{jm}(\vec{x}-\vec{x}';t-t') = u(t-t') \times$$

$$\{\delta_{jm}\left[\frac{-i}{(2\pi)^2|\vec{x}-\vec{x}'|}\int_0^\infty e^{-1/2D_{cT}k^2(t-t')} \frac{\sin[C_{cT}k(1-d^2k^2/\rho)^{1/2}(t-t')]}{C_{cT}(1-d^2k^2/\rho)^{1/2}} \times \right.$$

$$\left. [e^{ik|\vec{x}-\vec{x}'|} - e^{-ik|\vec{x}-\vec{x}'|}]dk\right]$$

$$+ \frac{\partial^2}{\partial x_j \partial x_m}\left[\frac{-i}{(2\pi)^2|\vec{x}-\vec{x}'|}\int_0^\infty e^{-1/2D_{cT}k^2(t-t')} \frac{\sin[C_{cT}k(1-d^2k^2/\rho)^{1/2}(t-t')]}{C_{cT}k^2(1-d^2k^2/\rho)^{1/2}} \times \right.$$

$$\left. [e^{ik|x-x'|} - e^{-ik|x-x'|}]dk\right]$$

$$- \frac{\partial^2}{\partial x_j \partial x_m}\left[\frac{-i}{(2\pi)^2|\vec{x}-\vec{x}'|}\int_0^\infty e^{-1/2D_{L}k^2(t-t')} \frac{\sin[C_{L}k(1-h^2k^2/\rho)^{1/2}(t-t')]}{C_{L}k^2(1-h^2k^2/\rho)^{1/2}} \times \right.$$

$$\left. [e^{ik|\vec{x}-\vec{x}'|} - e^{-ik|\vec{x}-\vec{x}'|}]dk]\right\} . \qquad (7.2)$$

Performing the change of variables $k \to -k$ on the first exponential function in the integrand of each of the integrals permits the limits of integration to be extended from $-\infty$ to ∞, leaving the following integration over k:

$$G_{jm}(\vec{x}-\vec{x}';t-t') = u(t-t')\{\delta_{jm}[\frac{i}{(2\pi)^2|\vec{x}-\vec{x}'|} I_1] + \frac{\partial^2}{\partial x_j \partial x_m}[\frac{i}{(2\pi)^2|\vec{x}-\vec{x}'|} I_2] - \frac{\partial^2}{\partial x_j \partial x_m}[\frac{i}{(2\pi)^2|\vec{x}-\vec{x}'|} I_3]\} , \quad (7.3)$$

where I_1, I_2, and I_3 denote the integrals

$$I_1 = \int_{-\infty}^{\infty} e^{-1/2D_{cT}k^2(t-t')} \frac{\sin[C_{cT}k(1-d^2k^2/\rho)^{1/2}(t-t')]}{C_{cT}(1-d^2k^2/\rho)^{1/2}} e^{-ik|\vec{x}-\vec{x}'|} dk , \quad (7.3a)$$

$$I_2 = \int_{-\infty}^{\infty} e^{-1/2D_{cT}k^2(t-t')} \frac{\sin[C_{cT}k(1-d^2k^2/\rho)^{1/2}(t-t')]}{C_{cT}k^2(1-d^2k^2/\rho)^{1/2}} e^{-ik|\vec{x}-\vec{x}'|} dk , \quad (7.3b)$$

and

$$I_3 = \int_{-\infty}^{\infty} e^{-1/2D_{L}k^2(t-t')} \frac{\sin[C_{L}k(1-h^2k^2/\rho)^{1/2}(t-t')]}{C_{L}k^2(1-h^2k^2/\rho)^{1/2}} e^{-ik|\vec{x}-\vec{x}'|} dk . \quad (7.3c)$$

One method of evaluating the remaining integrals consists of first expressing the integrands in more integrable forms by the use of series expansions. After interchanging the order of the integration and summation operations, the resultant integrals are evaluated analytically. This approach leads to a representation for the Green's function in the $\vec{x},t$

domain as a superposition of damped harmonic oscillator wave functions in the form of a series of Hermite polynomials and Gaussian functions. The analytical procedure outlined here for the evaluation of integrals I_1, I_2, and I_3 proves to be rather cumbersome in application, however, due to the algebraic forms of the integrands, and the resultant series are inefficient for numerical evaluation by computer.

It is more productive in this case to evaluate the integrals I_1, I_2, and I_3 in equations (7.3a - c) by numerical methods. An approach is suggested whereby each element of the tensorial Green's function is evaluated separately. First the operations on I_1, I_2, and I_3 indicated in equation (7.3) must be performed. Then the altered integrals can be evaluated numerically by computer and combined by use of equation (7.3) to give $G_{jm}(\vec{x}-\vec{x}';t-t')$. It should be noted that the tensorial Green's function in equation (7.3) is symmetric under an interchange of "j" and "m" indices and also symmetric with respect to an interchange of $\vec{x}$ and $\vec{x}'$. Consequently, only six elements, or subsidiary Green's functions, need to be determined in order to completely specify $G_{jm}(\vec{x}-\vec{x}';t-t')$.

Viscoelastic Medium

The Green's function representation that appropriately describes the properties of wave propagation for the special case of a viscoelastic medium may be obtained directly from the corresponding representation for the general case of a viscoelastic medium with couple-stresses by disregarding the contribution due to couple-stresses. Since couple-stresses affect only the transverse mode of wave propagation, characteristics of the longitudinal mode of wave propagation do not undergo alteration in

the transition to this special case. When the terms that account for the effects of couple-stresses in the medium are eliminated by setting the material parameters $\ell = \eta'' = 0$, the Green's function representation for the general case reduces to the form

$$G^{v}_{jm}(\vec{x}-\vec{x}';t-t') = u(t-t')\{\delta_{jm}[\frac{i}{(2\pi)^2|\vec{x}-\vec{x}'|} I^{v}_{1}] + \frac{\partial^2}{\partial x_j \partial x_m}[\frac{i}{(2\pi)^2|\vec{x}-\vec{x}'|} I^{v}_{2}]$$

$$- \frac{\partial^2}{\partial x_j \partial x_m}[\frac{i}{(2\pi)^2|\vec{x}-\vec{x}'|} I^{v}_{3}]\} , \qquad (7.4)$$

where I^{v}_{1}, I^{v}_{2}, and I^{v}_{3} denote the integrals

$$I^{v}_{1} = \int_{-\infty}^{\infty} e^{-1/2D_T k^2(t-t')} \frac{\sin[C_T k(1-g^2k^2/\rho)^{1/2}(t-t')]}{C_T(1-g^2k^2/\rho)^{1/2}} e^{-ik|\vec{x}-\vec{x}'|} dk, \qquad (7.4a)$$

$$I^{v}_{2} = \int_{-\infty}^{\infty} e^{-1/2D_T k^2(t-t')} \frac{\sin[C_T k(1-g^2k^2/\rho)^{1/2}(t-t')]}{C_T k^2(1-g^2k^2/\rho)^{1/2}} e^{-ik|\vec{x}-\vec{x}'|} dk, \qquad (7.4b)$$

and

$$I^{v}_{3} = \int_{-\infty}^{\infty} e^{-1/2D_L k^2(t-t')} \frac{\sin[C_L k(1-h^2k^2/\rho)^{1/2}(t-t')]}{C_L k^2(1-h^2k^2/\rho)^{1/2}} e^{-ik|\vec{x}-\vec{x}'|} dk \; . \qquad (7.4c)$$

The new quantities D_T and g, which were defined earlier following equations (5.14a - f), are given by $D_T = \mu''/\rho$ and $g^2 = \mu''^2/4\mu'$.

Elastic Medium with Couple-Stresses

The Green's function representation that appropriately describes the properties of wave propagation for the special case of an elastic medium with couple-stresses may be obtained directly from the corresponding representation for the general case of a viscoelastic medium with couple-stresses by disregarding the contribution due to viscoelasticity. When the terms that account for the effects of viscoelasticity in the medium are eliminated by setting the material parameters $\eta'' = \lambda'' = \mu'' = 0$, the Green's function representation for the general case reduces to the form

$$G_{jm}^{ec}(\vec{x}-\vec{x}';t-t') = u(t-t')\{\delta_{jm}[\frac{i}{(2\pi)^2|\vec{x}-\vec{x}'|} I_1^{ec}] + \frac{\partial^2}{\partial x_j \partial x_m}[\frac{i}{(2\pi)^2|\vec{x}-\vec{x}'|} I_2^{ec}]$$

$$- \frac{\partial^2}{\partial x_j \partial x_m}[\frac{i}{(2\pi)^2|\vec{x}-\vec{x}'|} I_3^{ec}]\} , \qquad (7.5)$$

where I_1^{ec}, I_2^{ec}, and I_3^{ec} denote the integrals

$$I_1^{ec} = \int_{-\infty}^{\infty} \frac{\sin[C_{cT}k(t-t')]}{C_{cT}} e^{-ik|\vec{x}-\vec{x}'|} dk , \qquad (7.5a)$$

$$I_2^{ec} = \int_{-\infty}^{\infty} \frac{\sin[C_{cT}k(t-t')]}{C_{cT}k^2} e^{-ik|\vec{x}-\vec{x}'|} dk , \qquad (7.5b)$$

and

$$I_3^{ec} = \int_{-\infty}^{\infty} \frac{\sin[C_L k(t-t')]}{C_L k^2} e^{-ik|\vec{x}-\vec{x}'|} dk . \qquad (7.5c)$$

Elastic Medium

The Green's function representation that appropriately describes the properties of wave propagation for the special case of an elastic medium may be obtained directly from the corresponding representation for the general case of a viscoelastic medium with couple-stresses by disregarding the contributions due to viscoelasticity and couple-stresses. It may also be obtained from the special case of a viscoelastic medium or the special case of an elastic medium with couple-stresses by disregarding, respectively, the contributions due to viscoelasticity and couple-stresses. Since couple-stresses influence only the transverse mode of wave propagation, characteristics of the longitudinal mode of wave propagation for this special case are identical to those for the previous special case of an elastic medium with couple-stresses. When the terms that account for the effects of viscoelasticity and couple-stresses are eliminated by setting the material parameters $\ell = \eta'' = \lambda'' = \mu'' = 0$, the Green's function representation for the general case reduces to the form

$$G^{e}_{jm}(\vec{x}-\vec{x}';t-t') = u(t-t')\{\delta_{jm}[\frac{i}{(2\pi)^2|\vec{x}-\vec{x}'|} I^{e}_{1}] + \frac{\partial^2}{\partial x_j \partial x_m}[\frac{i}{(2\pi)^2|\vec{x}-\vec{x}'|} I^{e}_{2}]$$

$$- \frac{\partial^2}{\partial x_j \partial x_m}[\frac{i}{(2\pi)^2|\vec{x}-\vec{x}'|} I^{e}_{3}]\} , \qquad (7.6)$$

where I_1^e, I_2^e, and I_3^e denote the integrals

$$I_1^e = \int_{-\infty}^{\infty} \frac{\sin[C_T k(t-t')]}{C_T} e^{-ik|\vec{x}-\vec{x}'|} dk \ , \tag{7.6a}$$

$$I_2^e = \int_{-\infty}^{\infty} \frac{\sin[C_T k(t-t')]}{C_T k^2} e^{-ik|\vec{x}-\vec{x}'|} dk \ , \tag{7.6b}$$

and

$$I_3^e = \int_{-\infty}^{\infty} \frac{\sin[C_L k(t-t')]}{C_L k^2} e^{-ik|\vec{x}-\vec{x}'|} dk \ . \tag{7.6c}$$

CHAPTER VIII

NUMERICAL ANALYSIS

In this chapter, numerical analysis is performed on the analytical Green's function representations in the $\vec{k},\omega$, $\vec{k},t$, and $\vec{x},t$ domains for the general case of a viscoelastic medium with couple-stresses and for the special cases of a viscoelastic medium, an elastic medium with couple-stresses, and an elastic medium. Numerical results based on this analysis are presented in the form of graphical illustrations which include the isolated contributions from the transverse and longitudinal components of the Green's function in addition to the total Green's function. Tables of numerical values that correspond to various properties characteristic of the transverse and longitudinal modes of wave propagation are also included.

An analytical basis for a comparison of the properties characteristic of wave propagation in these media, whereby inspection of analytical structure of the Green's function representations provided valuable information concerning wave phenomena, was developed in the foregoing chapters. It is also desirable to establish a numerical basis for comparison. Since this investigation concerns a relatively unexplored area of mechanics, however, there is no experimental data available upon which to base a numerical analysis. Despite the lack of available data, an attempt is made here to graphically illustrate the analytical Green's function expressions obtained earlier in order to gain insight into the propagation of waves in these media. Numerical analysis is particularly helpful for interpreting the Green's function representations in the $\vec{x},t$

domain, which are left in integral form following the analytical development. Comparisons of the viscoelastic medium with couple-stresses with the viscoelastic medium, the elastic medium with couple-stresses with the elastic medium, and the viscoelastic medium with the elastic medium, where either the effects of couple-stresses or viscoelasticity are isolated, should be most useful for identifying these effects.

It was mentioned earlier that the derivation of the Cosserat field equations takes into account the effects of a surface couple per unit area in addition to the usual surface force per unit area, and that such a consideration seems appropriate for materials with granular or crystalline structure, where the interaction between adjacent elements may introduce internal couples. In view of this argument, the selection of one of the major marine-sediment types as the medium upon which to base the numerical analysis on couple-stresses that follows seems justifiable. Marine sediments are classified according to the general environment in which they are found in addition to various of their physical properties which are either measured or computed. Coarse sand, a major marine-sediment type that occurs in the continental terrace (shelf and slope) environment, is chosen here as the medium for numerical analysis.

The material parameters used in this analysis to characterize the marine-sediment type coarse sand are summarized as follows:

$$\rho = 2.30 \times 10^{3} \text{kg/m}^{3}$$

$$\eta' = 3.33 \times 10^{8} \text{nt} \quad , \quad \eta'' = 6.67 \times 10^{4} \text{nt-sec}$$

$$\lambda' = 6.00 \times 10^{9} \text{nt/m}^{2} \quad , \quad \lambda'' = 6.00 \times 10^{5} \text{nt-sec/m}^{2}$$

$$\mu' = 1.00 \times 10^{9} \text{nt/m}^{2} \quad , \quad \mu'' = 2.00 \times 10^{5} \text{nt-sec/m}^{2} \quad . \qquad (8.1)$$

Values for the elastic material parameters ρ, λ', and μ' correspond closely to the data on the elastic properties of coarse sand reported by Hamilton (1974a). Numerous investigations have been performed to model and measure internal energy dissipation in marine sediments. Yet, the damping mechanisms in marine sediments are not well understood and no universally accepted model for damping exists which is valid over the frequency range of interest. In view of the conflicting data on compressional-wave attenuation in marine sediments and the lack of available data on shear-wave attenuation, values for the viscous material parameters λ'' and μ'', which correspond to Lamé's parameters λ' and μ', are chosen by the author. With regard to the material parameters for couple-stresses, since there are no experimental values available for the elastic bending-twisting parameter η', and there is no previous mention in the literature of the corresponding viscous parameter η'', these values were also chosen by the author. If the values selected for the material parameters that account for the effects of couple-stresses and viscoelasticity in the medium are somewhat exaggerated due to the lack of available data, it serves the purpose of clearly illustrating these effects in the graphical results that follow. Since special cases where these effects are disregarded are also treated here, it is desirable to emphasize these effects, when they are present in the medium, as a basis for comparison.

In the graphical illustrations that follow, in each case the trace of the tensorial Green's function G_{jm}, G_{jj}, is plotted versus either frequency or time. The trace represents the sum of the elements along the principal diagonal of the matrix formed by the subsidiary Green's functions of the tensorial Green's function G_{jm}. It is convenient to

plot the trace of the tensorial Green's function, since the projection operators which accompany the transverse and longitudinal components of the Green's function are eliminated.

Taking the trace of the tensorial Green's function representations in the $\vec{k},\omega$ and $\vec{k},t$ domains affects only the projection operators P^T_{jm} and P^L_{jm}, which precede the transverse and longitudinal components of the Green's function. Setting $j = m$, one finds that

$$P^T_{jm} = (\delta_{jm} - \frac{k_j k_m}{k^2}) \rightarrow P^T_{jj} = 2 \qquad (8.2a)$$

and

$$P^L_{jm} = \frac{k_j k_m}{k^2} \rightarrow P^L_{jj} = 1 \quad . \qquad (8.2b)$$

In order to obtain graphical representations of the Green's functions in the $\vec{k},\omega$ and $\vec{k},t$ domains, which are to be plotted versus ω and t, respectively, the spatial wavenumber k is arbitrarily fixed at $k = 1m^{-1}$, or wavelength $\lambda = 2\pi m$. Figures 7, 8, 9, and 10 illustrate the Green's function representations in the $\vec{k},\omega$ and $\vec{k},t$ domains for all the media previously considered in the analytical development. The transverse and longitudinal components of the Green's functions are illustrated separately in order to obtain a measure of their respective contributions to the Green's function. Tables 1A and 1B give numerical values for the transverse and longitudinal wave properties summarized in equations (5.9), (5.15), (5.17), and (5.19). It should be mentioned that the odd part of $G_{jj}(k;t-t')$ is plotted in place of $G''_{jj}(k;t-t')$. The The odd and even parts of $G_{jj}(k;t-t')$, denoted, respectively, by

TABLE 1A

TRANSVERSE WAVE PROPERTIES

Medium	ω_{nT} sec^{-1} $\times 10^{2}$	ζ_T $\times 10^{-2}$	γ_T sec^{-1} $\times 10^{1}$	ω_{dT} sec^{-1} $\times 10^{2}$	Q_T	τ_T sec $\times 10^{-3}$	BW_T sec^{-1} $\times 10^{2}$
Viscoelastic with couple-stresses	7.61	7.61	5.80	7.59	6.57	8.28	1.16
Viscoelastic	6.59	6.59	4.35	6.58	7.58	9.55	0.87
Elastic with couple-stresses	7.61	0.00	0.00	7.61	∞	8.25	0.00
Elastic	6.59	0.00	0.00	6.59	∞	9.53	0.00

TABLE 1B

LONGITUDINAL WAVE PROPERTIES

Medium	ω_{nL} sec^{-1} $\times 10^{3}$	ζ_L $\times 10^{-1}$	γ_L sec^{-1} $\times 10^{2}$	ω_{dL} sec^{-1} $\times 10^{3}$	Q_L	τ_L sec $\times 10^{-3}$	BW_L sec^{-1} $\times 10^{2}$
Viscoelastic with couple-stresses	1.87	1.17	2.17	1.85	4.29	3.39	4.35
Viscoelastic	1.87	1.17	2.17	1.85	4.29	3.39	4.35
Elastic with couple-stresses	1.87	0.00	0.00	1.87	∞	3.37	0.00
Elastic	1.87	0.00	0.00	1.87	∞	3.37	0.00

$G^{o}_{jj}(k;t-t')$ and $G^{e}_{jj}(k;t-t')$, are related to the imaginary and real parts of $G_{jj}(k;t-t')$ by the relationships

$$G^{o}_{jj}(k;t-t') = \frac{1}{2}[G_{jj}(k;t-t')-G_{jj}(k;t'-t)] = i\, G''_{jj}(k;t-t') \qquad (8.3a)$$

and

$$G^{e}_{jj}(k;t-t') = \frac{1}{2}[G_{jj}(k;t-t')+G_{jj}(k;t'-t)] = G'_{jj}(k;t-t') \ . \qquad (8.3b)$$

Similar relationships exist for the components $G_T(k;t-t')$ and $G_L(k;t-t')$.

Taking the trace of the tensorial Green's function representation in the $\vec{x},t$ domain has the following effect on the projection operators which precede the transverse and longitudinal components of the Green's function:

$$\delta_{jm} \rightarrow \delta_{jj} = 3 \ , \quad \frac{\partial^2}{\partial x_j \partial x_m} \rightarrow \frac{\partial^2}{\partial x_j^2} = \nabla^2 \ . \qquad (8.4)$$

It follows that the identity

$$\nabla^2\{\frac{e^{-ik|\vec{x}-\vec{x}'|}}{|\vec{x}-\vec{x}'|}\} = -k^2 \frac{e^{-ik|\vec{x}-\vec{x}'|}}{|\vec{x}-\vec{x}'|} \qquad (8.5)$$

helps to reduce the expressions for $G_{jj}(\vec{x}-\vec{x}';t-t')$, $G^{v}_{jj}(\vec{x}-\vec{x}';t-t')$, $G^{ec}_{jj}(\vec{x}-\vec{x}';t-t')$, and $G^{e}_{jj}(\vec{x}-\vec{x}';t-t')$ in equations (7.3 - 6). The trace of the tensorial Green's function representation in equation (7.3) gives

$$G_{jj}(\vec{x}-\vec{x}';t-t') = u(t-t')\{\frac{2i}{(2\pi)^2|\vec{x}-\vec{x}'|} I_1 + \frac{i}{(2\pi)^2|\vec{x}-\vec{x}'|} I_3\} \ , \qquad (8.6)$$

where

$$I_1 = \int_{-\infty}^{\infty} e^{-1/2D_{cT}k^2(t-t')} \frac{\sin[C_{cT}k(1-d^2k^2/\rho)^{1/2}(t-t')]}{C_{cT}(1-d^2k^2/\rho)^{1/2}} e^{-ik|\vec{x}-\vec{x}'|}dk \quad (8.6a)$$

as in equation (7.3a), and now

$$I_3 = \int_{-\infty}^{\infty} e^{-1/2D_{L}k^2(t-t')} \frac{\sin[C_{L}k(1-h^2k^2/\rho)^{1/2}(t-t')]}{C_{L}(1-h^2k^2/\rho)^{1/2}} e^{-ik|\vec{x}-\vec{x}'|}dk \; . \quad (8.6b)$$

The trace of the tensorial Green's function representation in equation (7.4) gives

$$G^{v}_{jj}(\vec{x}-\vec{x}';t-t') = u(t-t')\{\frac{2i}{(2\pi)^2|\vec{x}-\vec{x}'|} I^{v}_1 + \frac{i}{(2\pi)^2|\vec{x}-\vec{x}'|} I^{v}_3\} \; , \quad (8.7)$$

where

$$I^{v}_1 = \int_{-\infty}^{\infty} e^{-1/2D_{T}k^2(t-t')} \frac{\sin[C_{T}k(1-g^2k^2/\rho)^{1/2}(t-t')]}{C_{T}(1-g^2k^2/\rho)^{1/2}} e^{-ik|\vec{x}-\vec{x}'|}dk \quad (8.7a)$$

as in equation (7.4a), and now

$$I^{v}_3 = \int_{-\infty}^{\infty} e^{-1/2D_{L}k^2(t-t')} \frac{\sin[C_{L}k(1-h^2k^2/\rho)^{1/2}(t-t')]}{C_{L}(1-h^2k^2/\rho)^{1/2}} e^{-ik|\vec{x}-\vec{x}'|}dk \; . \quad (8.7b)$$

The trace of the tensorial Green's function representation in equation (7.5) gives

$$G^{ec}_{jj}(\vec{x}-\vec{x}';t-t') = u(t-t')\{\frac{2i}{(2\pi)^2|\vec{x}-\vec{x}'|} I^{ec}_1 + \frac{i}{(2\pi)^2|\vec{x}-\vec{x}'|} I^{ec}_3\} \; , \quad (8.8)$$

where

$$I_1^{ec} = \int_{-\infty}^{\infty} \frac{\sin[C_{cT}k(t-t')]}{C_{cT}} e^{-ik|\vec{x}-\vec{x}'|} dk \qquad (8.8a)$$

as in equation (7.5a), and now

$$I_3^{ec} = \int_{-\infty}^{\infty} \frac{\sin[C_L k(t-t')]}{C_L} e^{-ik|\vec{x}-\vec{x}'|} dk = \frac{-\pi i}{C_L^2} \delta(t-t' - \frac{|\vec{x}-\vec{x}'|}{C_L}) \quad . \qquad (8.8b)$$

Numerical evaluation by computer of I_1^{ec} presents some difficulty since there is no exponential damping factor present in the integrand. Therefore, I_1^{ec} is converted into the equivalent integral (see Appendix B)

$$I_1^{ec} = \frac{-2i}{C_T \ell} e^{-2a} \int_0^{\infty} e^{-4ay^2} \sinh[2^{1/2} b(y^2+1)^{1/2}] \cos[2^{1/2} by] \frac{dy}{(y^2+1)^{1/2}} \quad , \qquad (8.9)$$

where

$$a = \frac{C_T(t-t')}{4\ell} \quad , \qquad b = \frac{|\vec{x}-\vec{x}'|}{2\ell} \quad . \qquad (8.9a)$$

This form is more convenient for numerical evaluation by computer because it contains the Gaussian type convergence factor $\exp(-4ay^2)$. The trace of the tensorial Green's function representation in equation (7.6) gives

$$G_{jj}^e(\vec{x}-\vec{x}';t-t') = u(t-t')\{\frac{2i}{(2\pi)^2|\vec{x}-\vec{x}'|} I_1^e + \frac{i}{(2\pi)^2|\vec{x}-\vec{x}'|} I_3^e\} \quad , \qquad (8.10)$$

where

$$I_1^e = \int_{-\infty}^{\infty} \frac{\sin[C_T k(t-t')]}{C_T} e^{-ik|\vec{x}-\vec{x}'|} dk = -\frac{i\pi}{C_T^2} \delta\left(t-t' - \frac{|\vec{x}-\vec{x}'|}{C_T}\right) \quad (8.10a)$$

as in equation (7.6a), and now

$$I_3^e = \int_{-\infty}^{\infty} \frac{\sin[C_L k(t-t')]}{C_L} e^{-ik|\vec{x}-\vec{x}'|} dk = -\frac{i\pi}{C_L^2} \delta\left(t-t' - \frac{|\vec{x}-\vec{x}'|}{C_L}\right) . \quad (8.10b)$$

Upon substituting the right-hand sides of equations (8.10a) and (8.10b) for I_1^e and I_3^e into equation (8.10), $G_{jj}^e(\vec{x}-\vec{x}';t-t')$ may be expressed as

$$G_{jj}^e(\vec{x}-\vec{x}';t-t') = u(t-t')\left\{\frac{2}{C_T^2} \frac{\delta\left(t-t' - \frac{|\vec{x}-\vec{x}'|}{C_T}\right)}{4\pi|\vec{x}-\vec{x}'|} + \frac{1}{C_L^2} \frac{\delta\left(t-t' - \frac{|\vec{x}-\vec{x}'|}{C_L}\right)}{4\pi|\vec{x}-\vec{x}'|}\right\} . \quad (8.11)$$

Figures 11, 12, 13, and 14 illustrate the Green's function representation in the $\vec{x},t$ domain for all the media previously considered in the analytical development. The transverse and longitudinal components of the Green's functions are illustrated separately in order to obtain a measure of their respective contributions to the Green's function. In each case the Green's function is plotted versus time, and the source point is fixed at $\vec{x}' = 0$, $t' = 0$, while the observation point is taken to be $|\vec{x}| = 10m$. The transverse and longitudinal components $G_T(\vec{x}-\vec{x}';t-t')$ and $G_L(\vec{x}-\vec{x}';t-t')$ are defined according to the relation

$$G_{jj}(\vec{x}-\vec{x}';t-t') = 2G_T(\vec{x}-\vec{x}';t-t') + G_L(\vec{x}-\vec{x}';t-t') , \quad (8.12)$$

in order to be consistent with the previous definitions for these components in the Green's function representations in the $\vec{k},\omega$ and $\vec{k},t$ domains.

It was mentioned earlier that the spatial wavenumber k was arbitrarily fixed at $k = 1m^{-1}$ in order to obtain the graphical illustrations of the analytical Green's function representations in the $\vec{k},\omega$ and $\vec{k},t$ domains. Thus, only one spatial component is plotted here for each of these Green's function representations. With the aid of Tables 1A and 1B, a comparison of the numerical results in Figures 7, 8, 9, and 10 for the viscoelastic medium with and without couple-stresses and the elastic medium with and without couple-stresses indicates that the elastic and viscous effects of couple-stresses are small for this spatial component. The reason for this is clear when one inspects equations (5.17a) and (5.19a) for the transverse wave properties of an elastic medium with couple-stresses and an elastic medium, respectively. It is observed that the nondimensional product ℓk carries with it all of the difference between the elastic equations with and without couple-stresses. In the numerical analysis performed here, $\ell k < 1$. If the value for k was selected such that the wavelength $\lambda = 2\pi/k$ was on the order of the material length ℓ (for example, $\lambda = \ell$ gives $\ell k = 2\pi$), the product ℓk would be much larger and the effect of couple-stresses would be more noticeable in the graphical illustrations. An inspection of equations (5.9a) and (5.15a) for the transverse wave properties of a viscoelastic medium with couple-stresses and a viscoelastic medium, respectively, illustrates the same effect for the elastic couple-stress parameter ℓ . However, in order to complete the comparison in this instance, one must also take into consideration the presence of the viscous parameter η'' in the damping factor ζ .

This parameter also occurs as a product with the spatial wavenumber k in these forms. Thus, it appears that the numerical value of the spatial wavenumber k is a critical factor in determining the magnitude of the elastic and viscous effects of couple-stresses in the graphical representations in the $\vec{k},\omega$ and $\vec{k},t$ domains. The observations here support the earlier statement that influence of couple-stresses might become important as wavelengths diminish to the order of the material length ℓ .

Graphical illustrations of the analytical Green's function representation in the $\vec{x},t$ domain contain all of the spatial components due to the modal synthesis (integration) or inverse transform procedure. In accordance with this procedure, in order to obtain the Green's function representations in the $\vec{x},t$ domain, the Green's function representations in the $\vec{k},t$ domain are integrated with respect to k over all k $(-\infty<k<\infty)$, including all the spatial components of these continuous media during the process. The numerical results in Figures 11, 12, 13, and 14 clearly illustrate the effects of couple-stresses and viscoelasticity in the $\vec{x},t$ domain. In the elastic medium there is no response at $|\vec{x}| = 10m$ to the disturbance created at $x' = 0$, $t' = 0$ until the time intervals $t_T = |\vec{x}|/C_T$ and $t_L = |\vec{x}|/C_L$ required, respectively, for the transverse and longitudinal waves to travel $|\vec{x}| = 10m$ have elapsed. As soon as each wave passes, the Green's function returns to its original value (zero) instead of being permanently changed. In contrast, the response in the viscoelastic medium occurs in the form of two Gaussian curves whose peaks occur at $t = t_T$ and $t = t_L$, and correspond, respectively, to the transverse and longitudinal waves. The broadening of the elastic response about the times $t = t_T$ and $t = t_L$ is due to viscous effects introduced by viscoelasticity and depends on the degree of damping in the medium. Larger values of damping give broader responses. The presence of couple-stresses in the elastic medium and the viscoelastic medium does not influence the longitudinal components of the responses in these media. However, the transverse components of the responses in these media are altered by the presence of couple-stresses. The transverse component of the response in the elastic medium with couple-stresses is

a damped oscillatory curve, even though there is no damping mechanism in the elastic medium. Somehow the bending and twisting which accompany couple-stresses are responsible for creating this damping in the absence of a damping mechanism. Except for the slightly smaller amplitude of the oscillations, the transverse component of the response in the viscoelastic medium with couple-stresses closely resembles that in the elastic medium with couple-stresses. Of course, there exists an actual damping mechanism in this case.

Further numerical analysis should be performed to better understand the behavior of the elastic medium with couple-stresses. By varying the numerical value for η' while keeping μ' fixed, one effectively changes the material parameter ℓ for couple-stresses and permits a study to be performed where the sensitivity of the response to ℓ is isolated. This would allow one to better observe the manner in which the delta function response of the elastic medium is altered by the presence of couple-stresses.

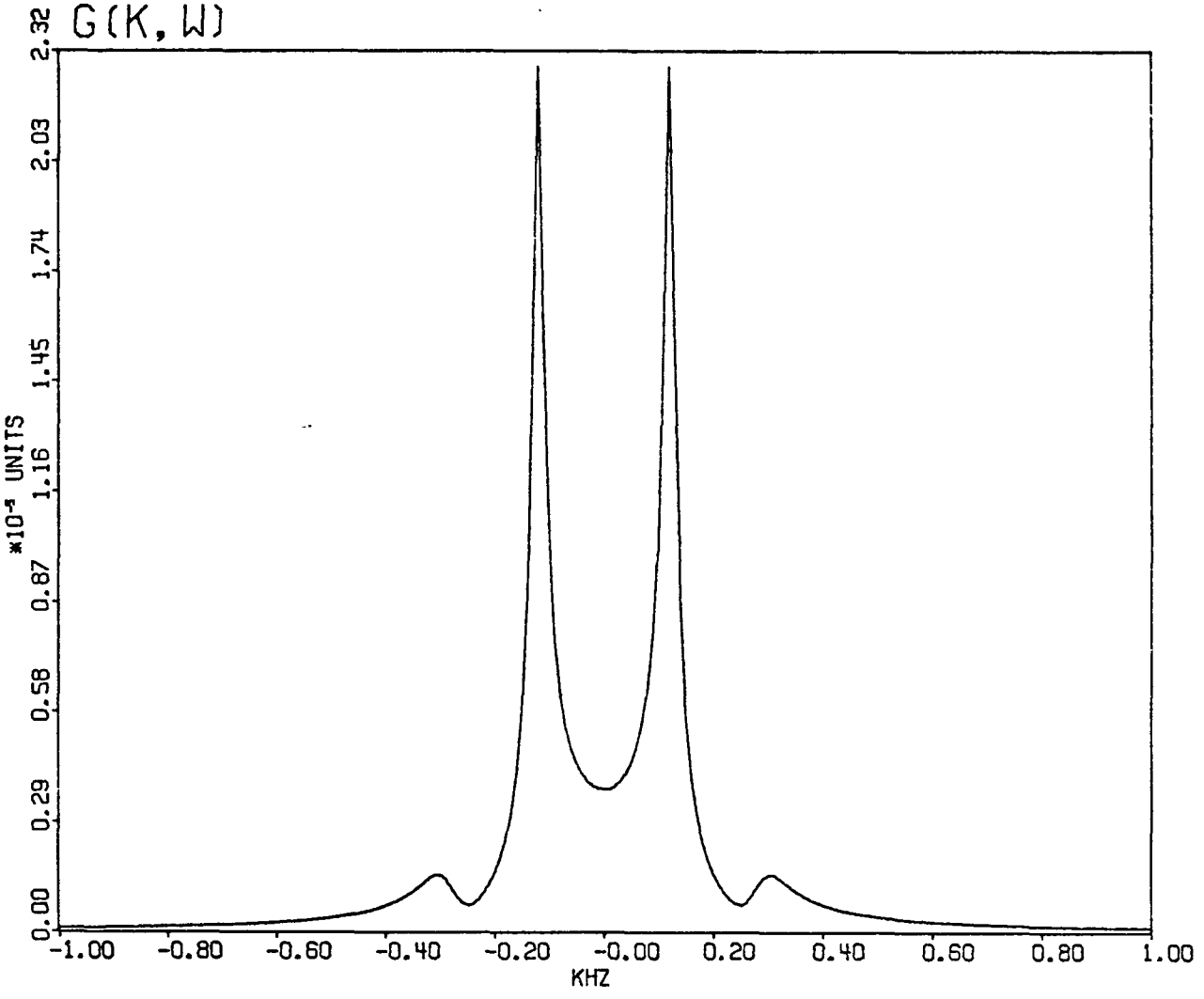

Figure 7a. The absolute value of the retarded response in the frequency domain, $|G_{jj}(k;\omega)|$.

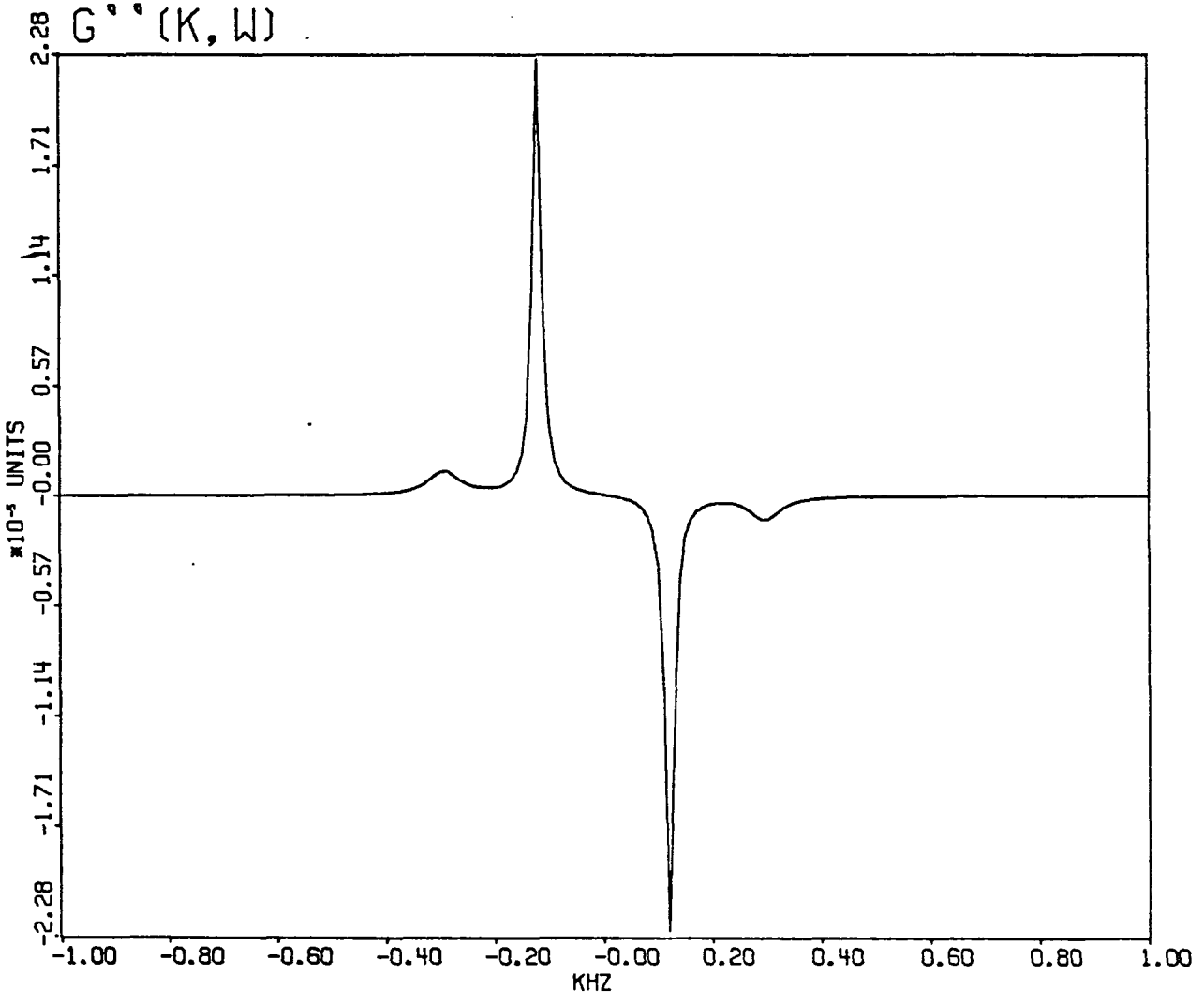

Figure 7b. The absorptive response, $G''_{jj}(k;\omega)$, which is the imaginary part of the retarded response in the frequency domain.

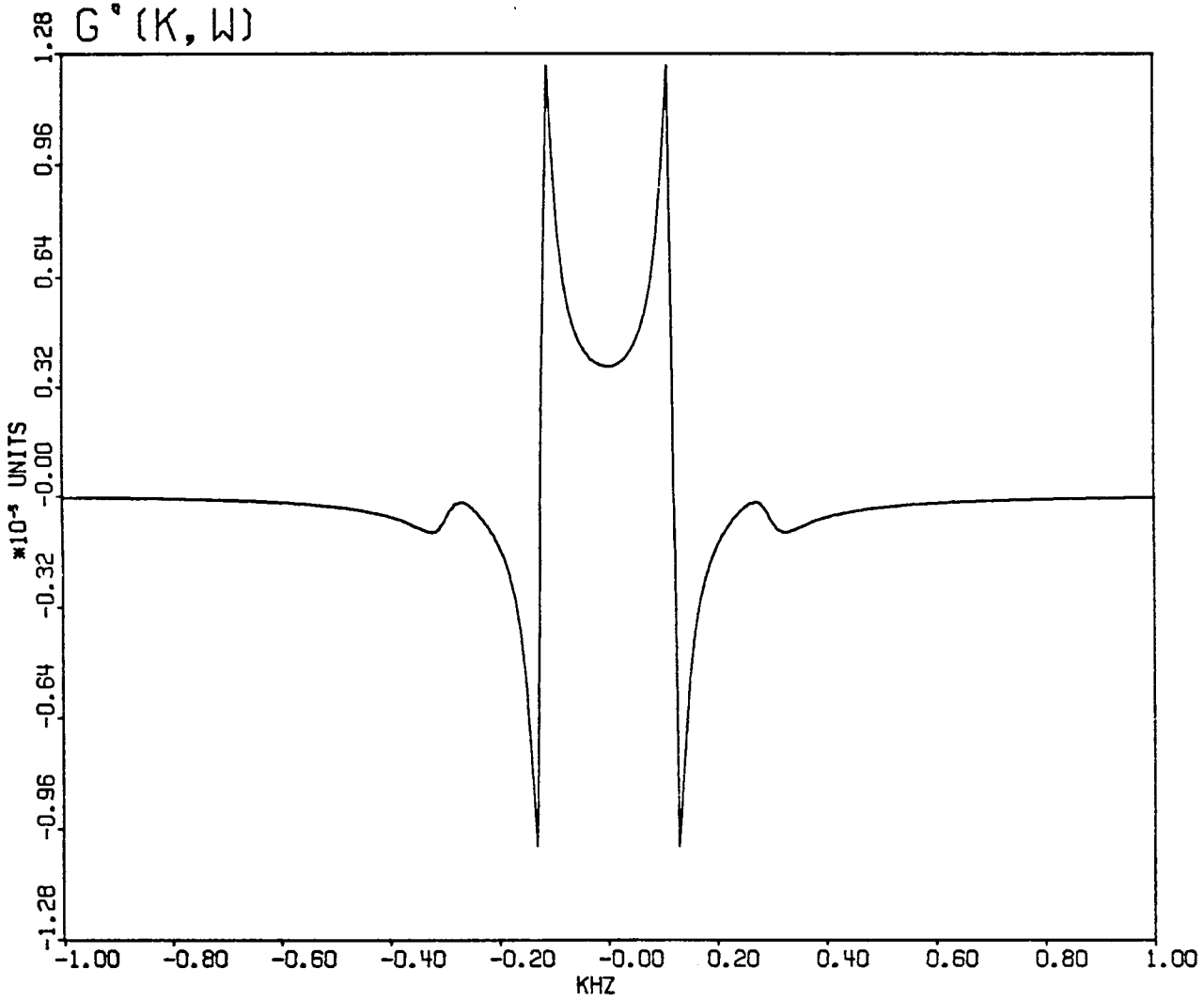

Figure 7c. The dispersive response, $G'_{jj}(k;\omega)$, which is the real part of the retarded response in the frequency domain.

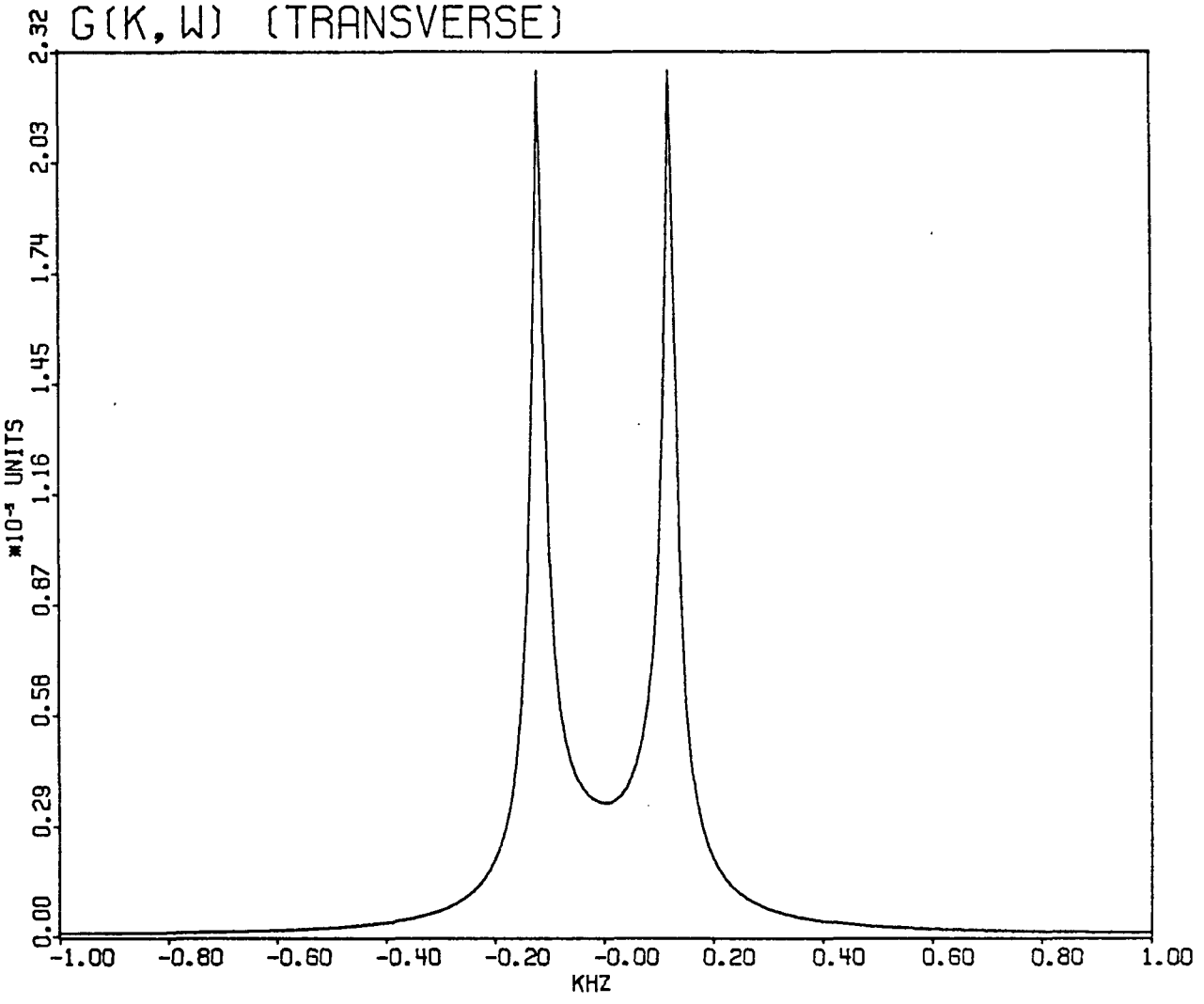

Figure 7d. The absolute value of the transverse component of the retarded response, $|G_T(k;\omega)|$. Plotted is $|2G_T(k;\omega)|$.

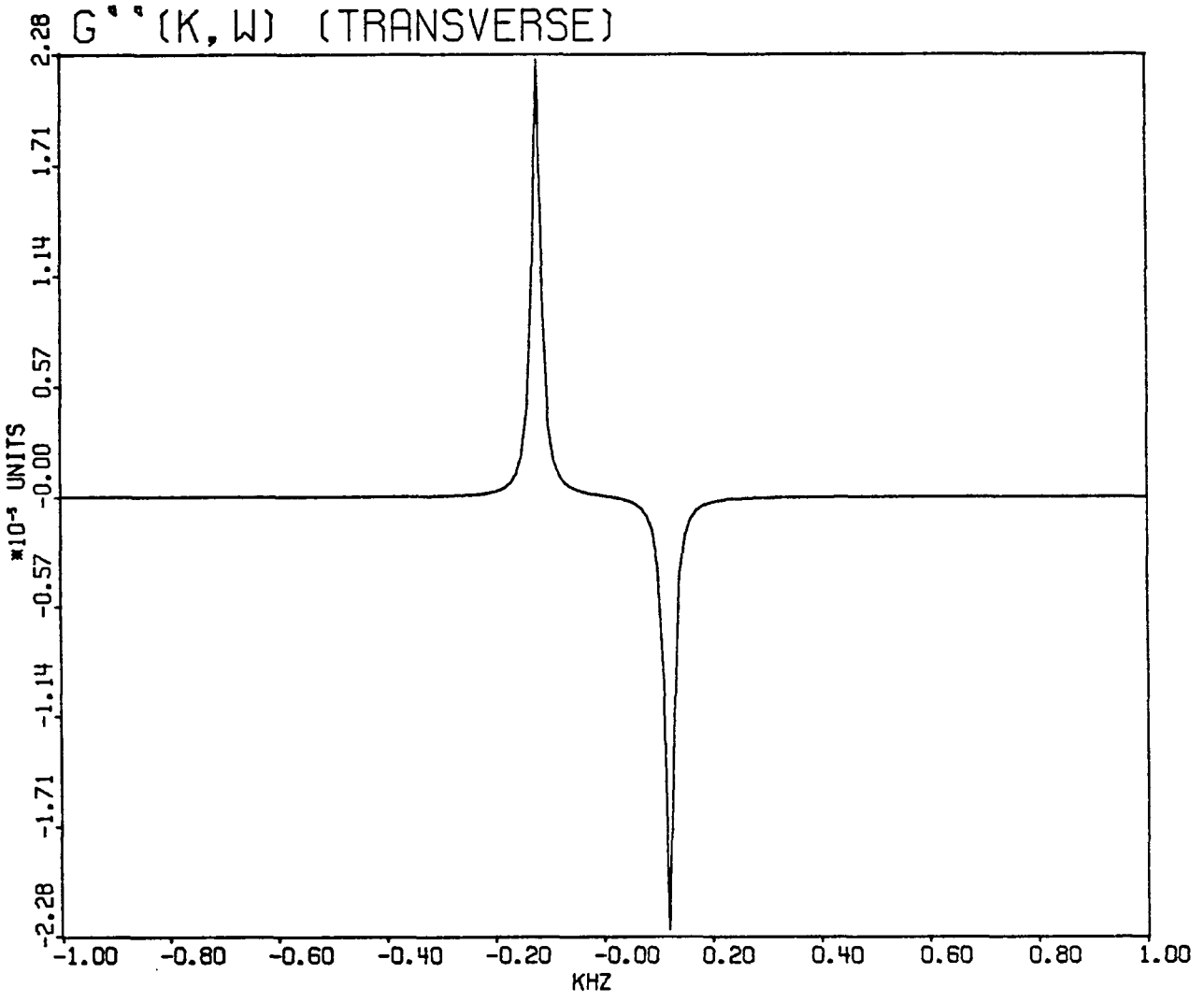

Figure 7e. The transverse component of the absorptive response, $G''_T(k;\omega)$. Plotted is $2G''_T(k;\omega)$.

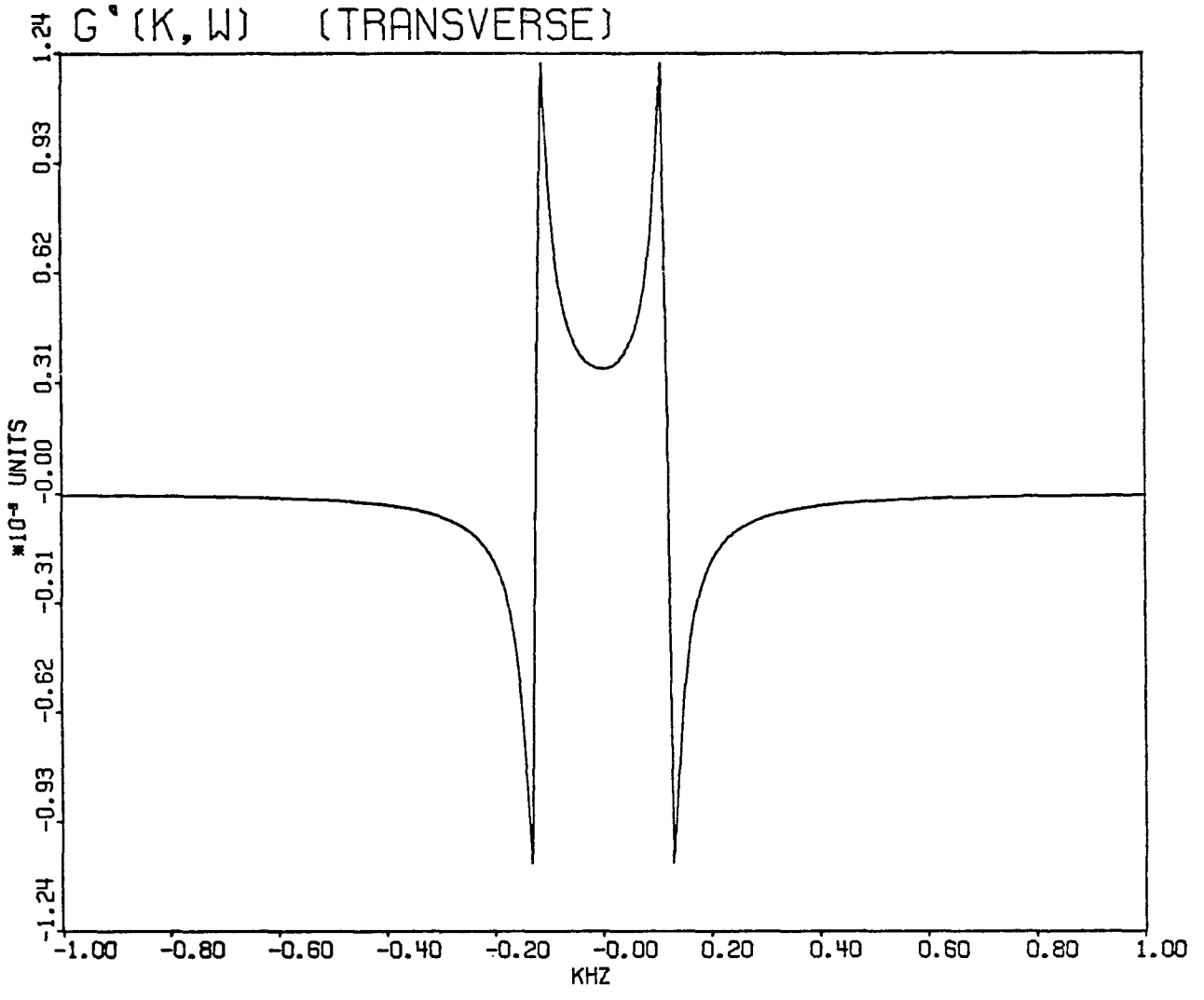

Figure 7f. The transverse component of the dispersive response, $G'_T(k;\omega)$. Plotted is $2G'_T(k;\omega)$.

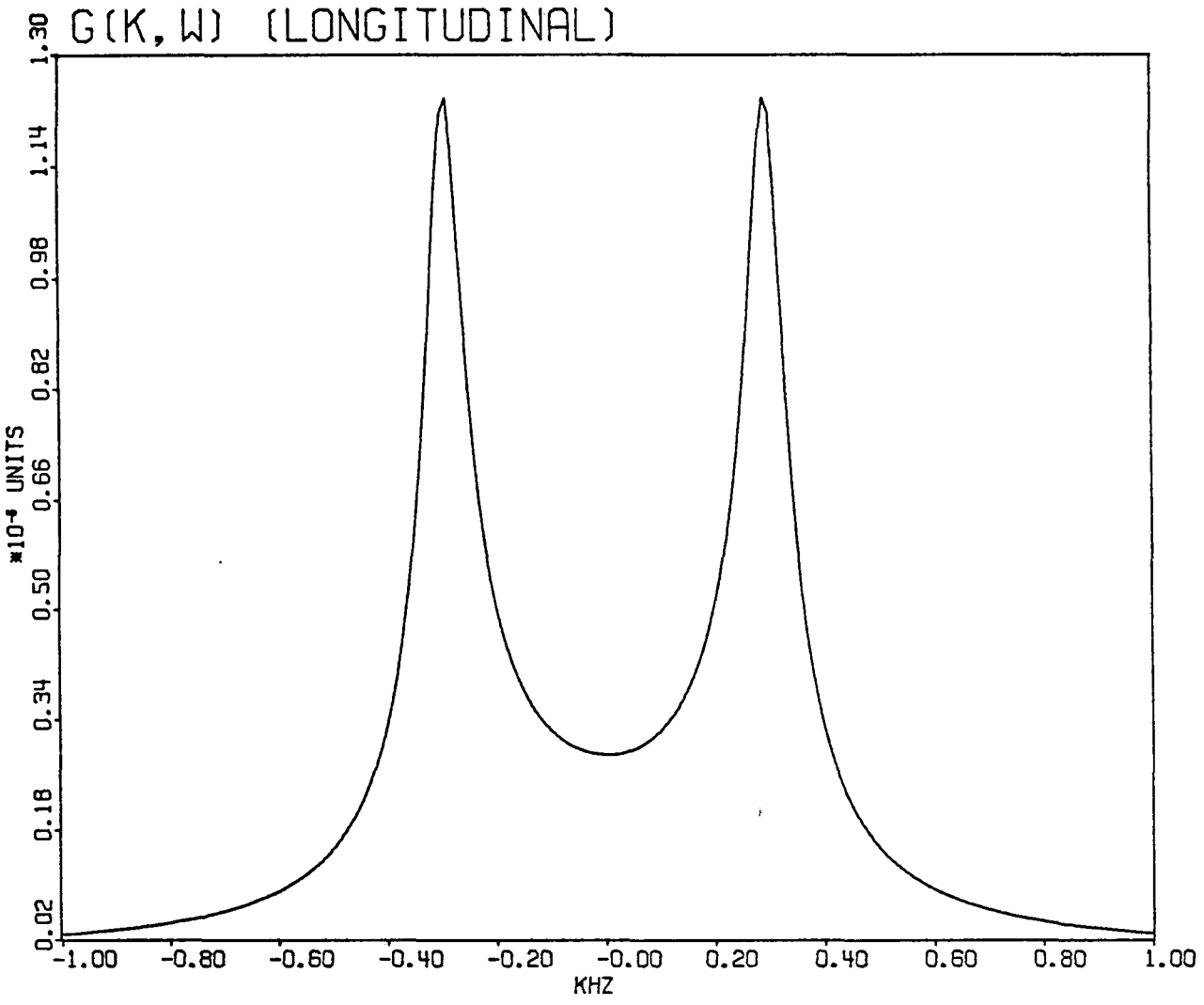

Figure 7g. The absolute value of the longitudinal component of the retarded response, $|G_L(k;\omega)|$.

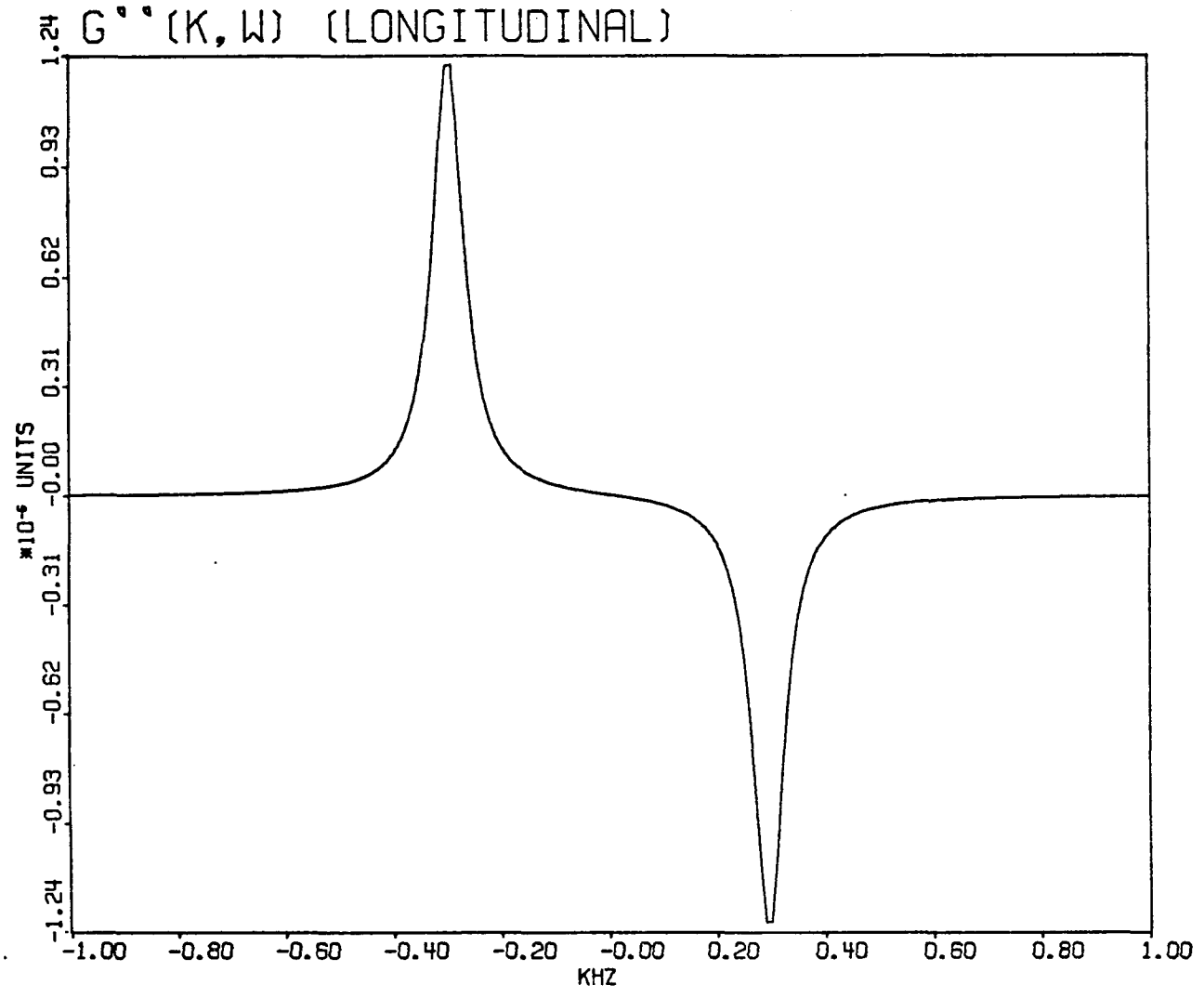

Figure 7h. The longitudinal component of the absorptive response, $G''_L(k;\omega)$.

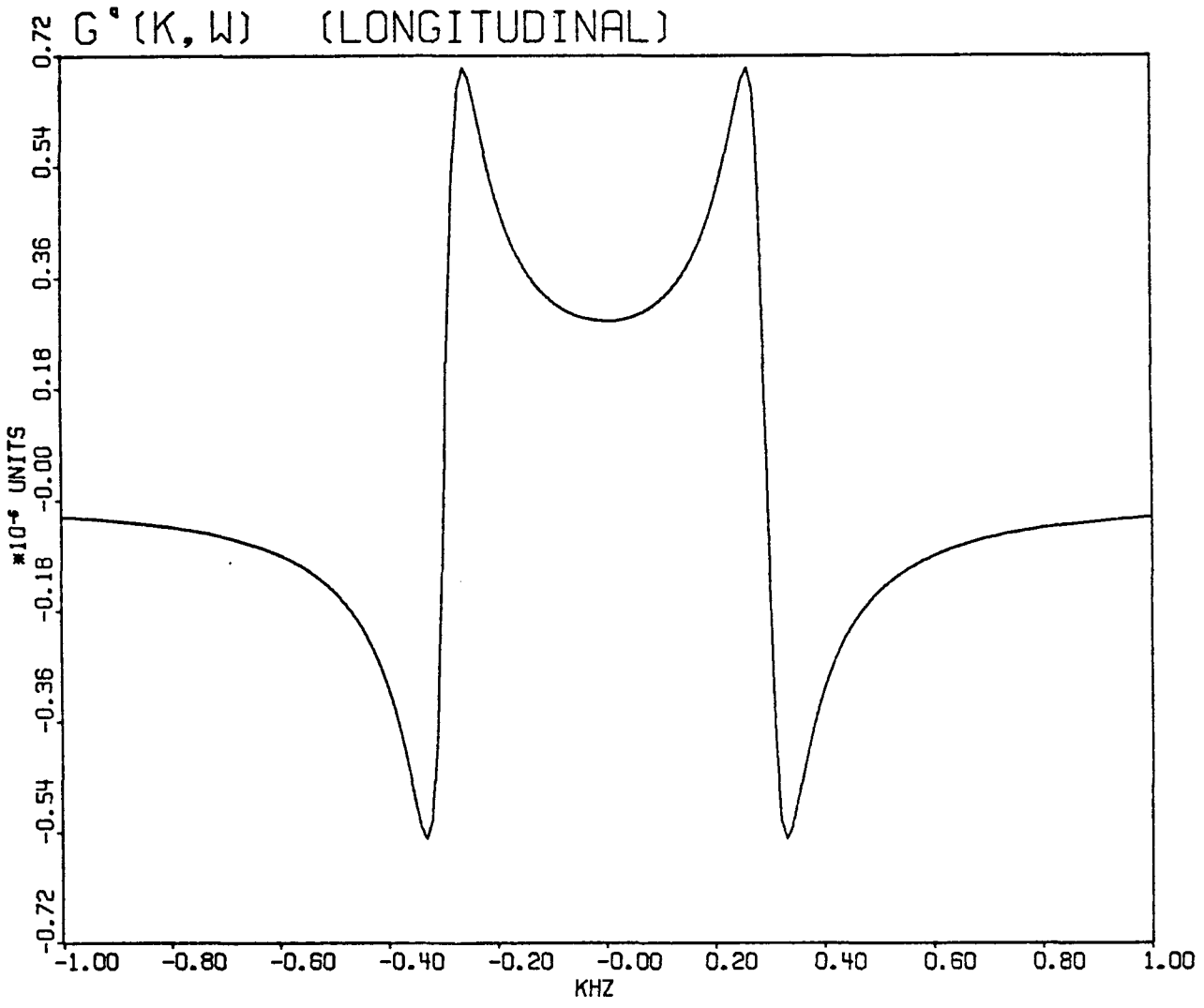

Figure 7i. The longitudinal component of the dispersive response, $G'_L(k;\omega)$.

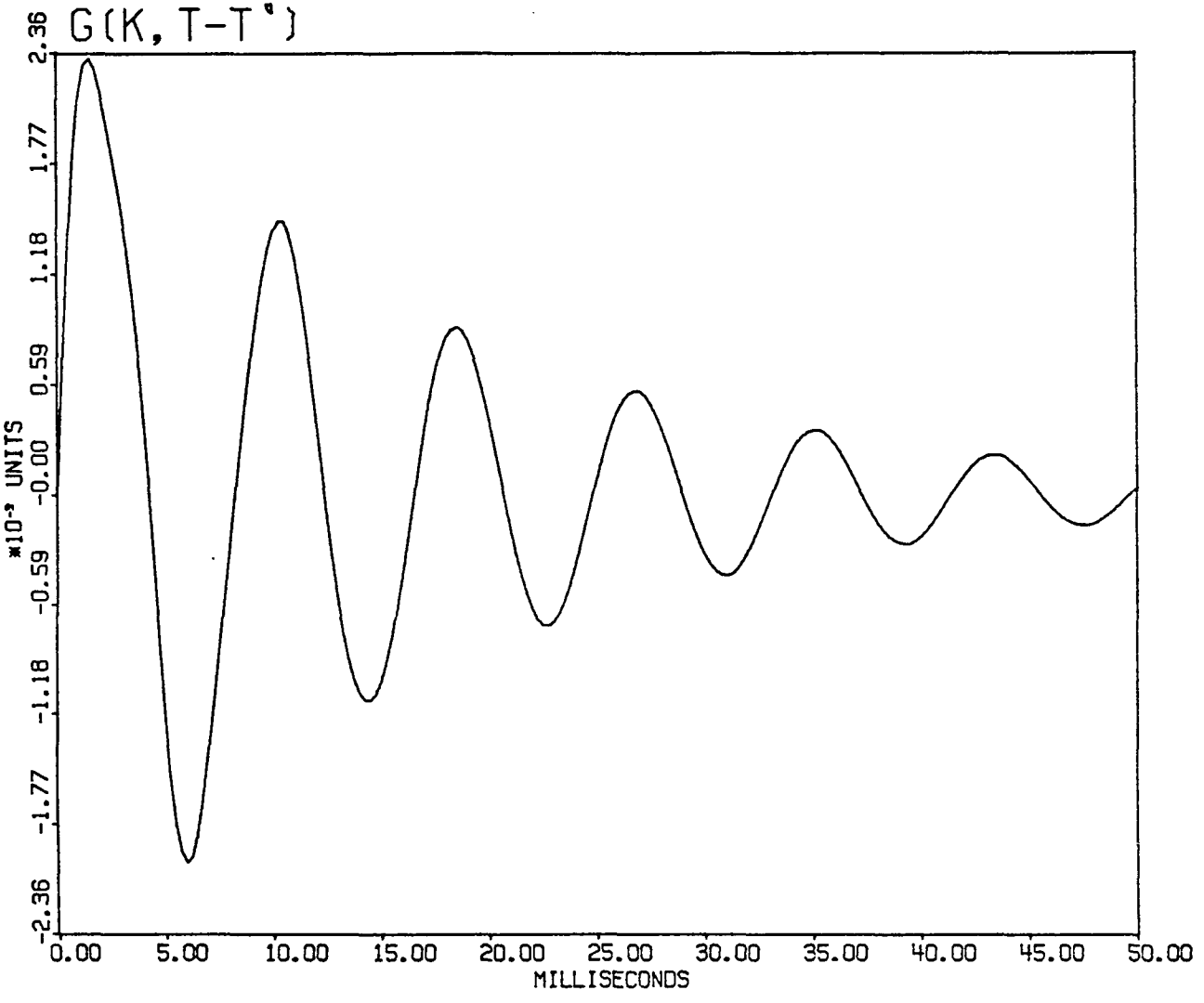

Figure 7j. The retarded response in the time domain, $G_{jj}(k;t-t')$.

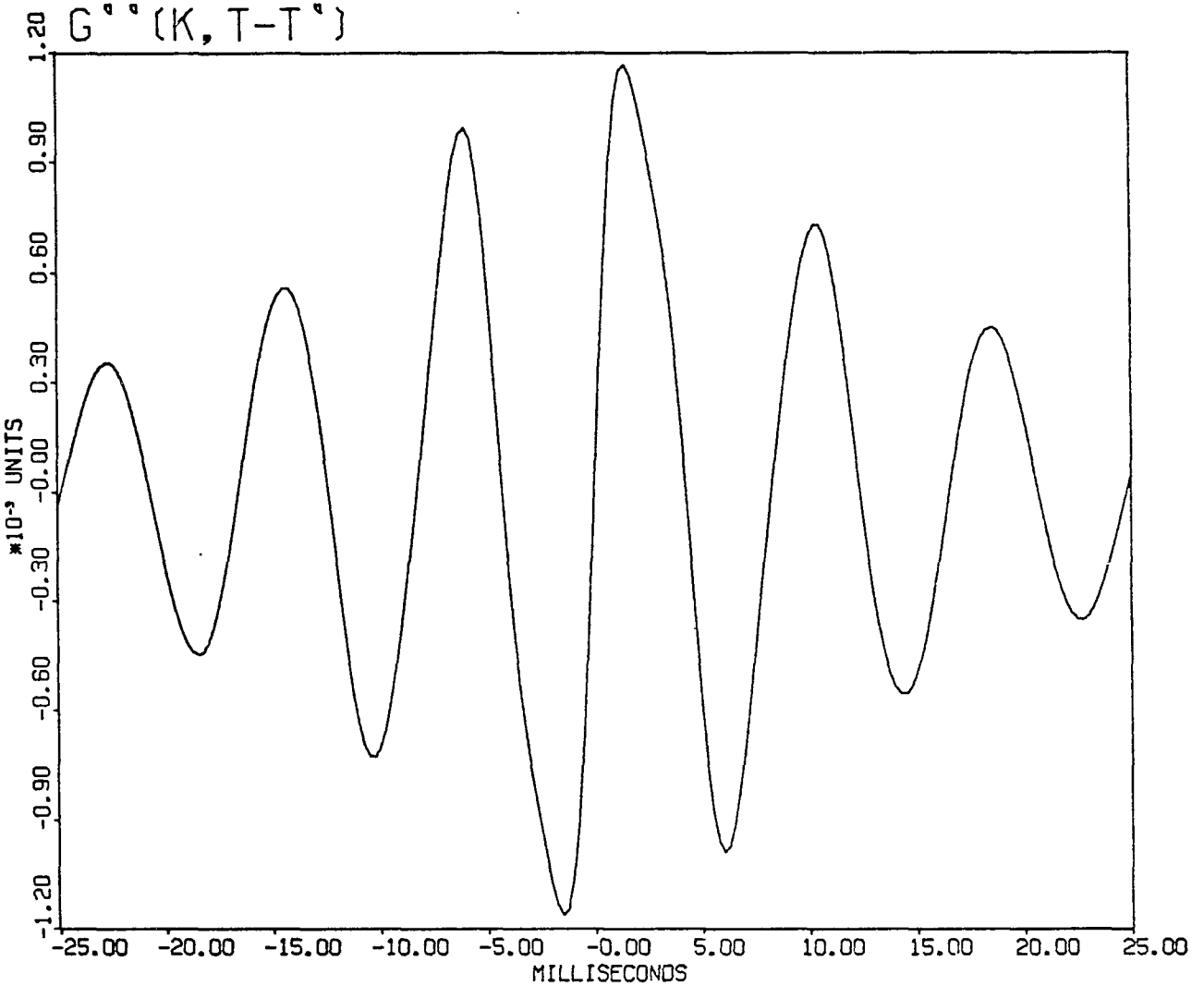

Figure 7k. The absorptive response, $G''_{jj}(k;t-t')$. Plotted is $i\,G''_{jj}(k;t-t')$, an odd function of time corresponding to $G_{jj}(k;t-t')$.

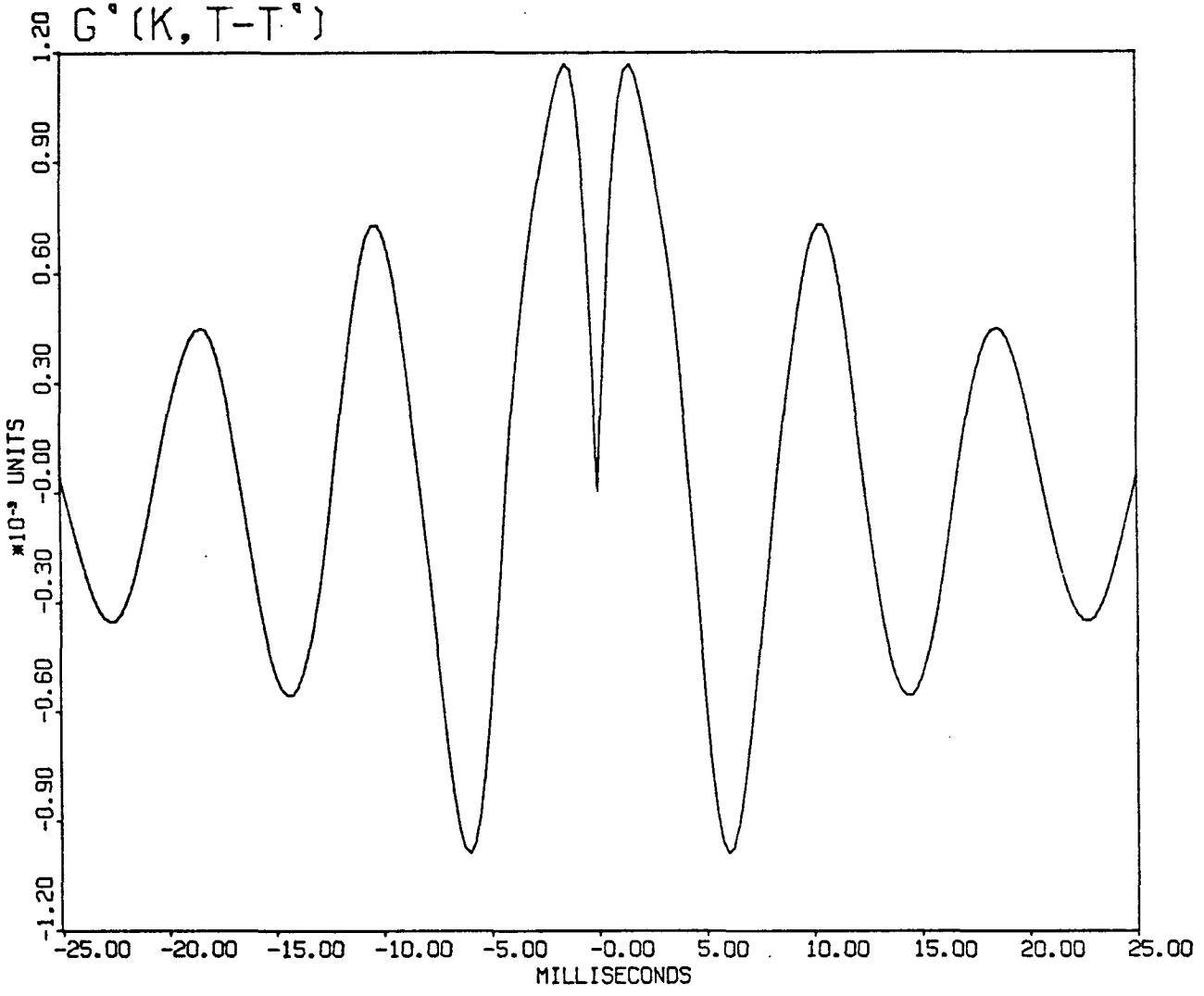

Figure 71. The dispersive response, $G'_{jj}(k;t-t')$, which is an even function of time corresponding to $G_{jj}(k;t-t')$.

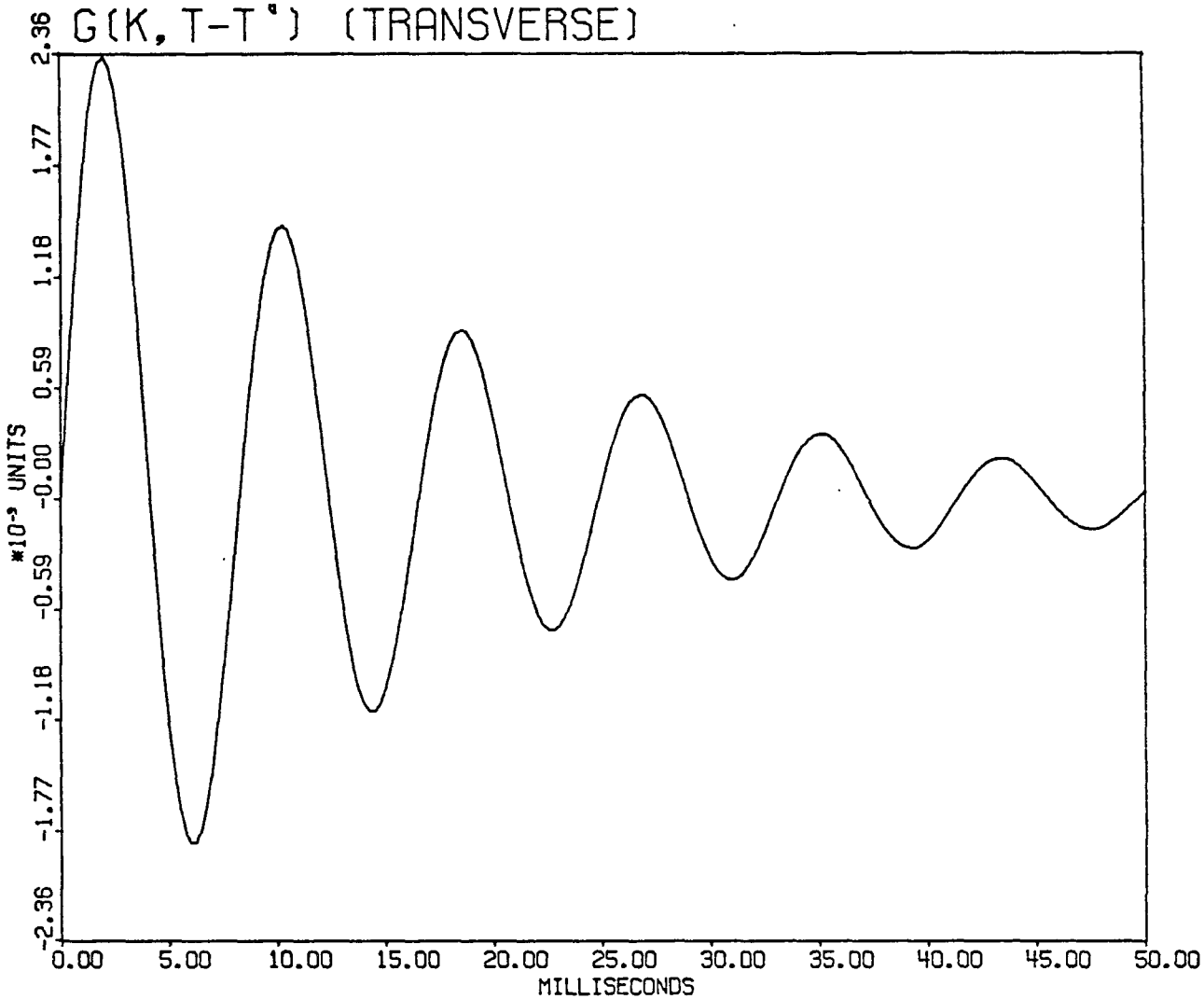

Figure 7m. The transverse component of the retarded response, $G_T(k;t-t')$. Plotted is $2G_T(k;t-t')$.

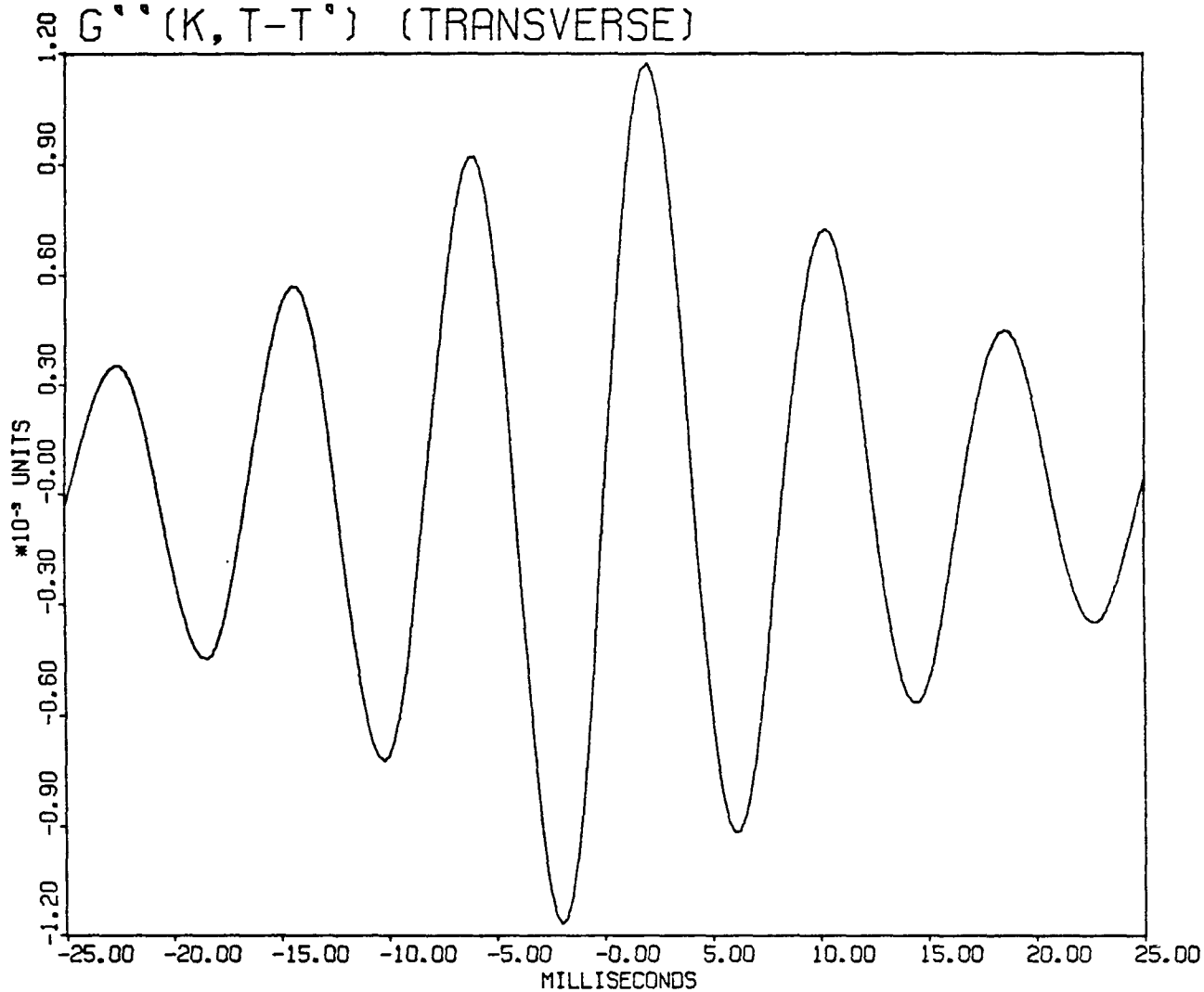

Figure 7n. The transverse component of the absorptive response, $G''_T(k;t-t')$. Plotted is $2i\ G''_T(k;t-t')$, an odd function of time.

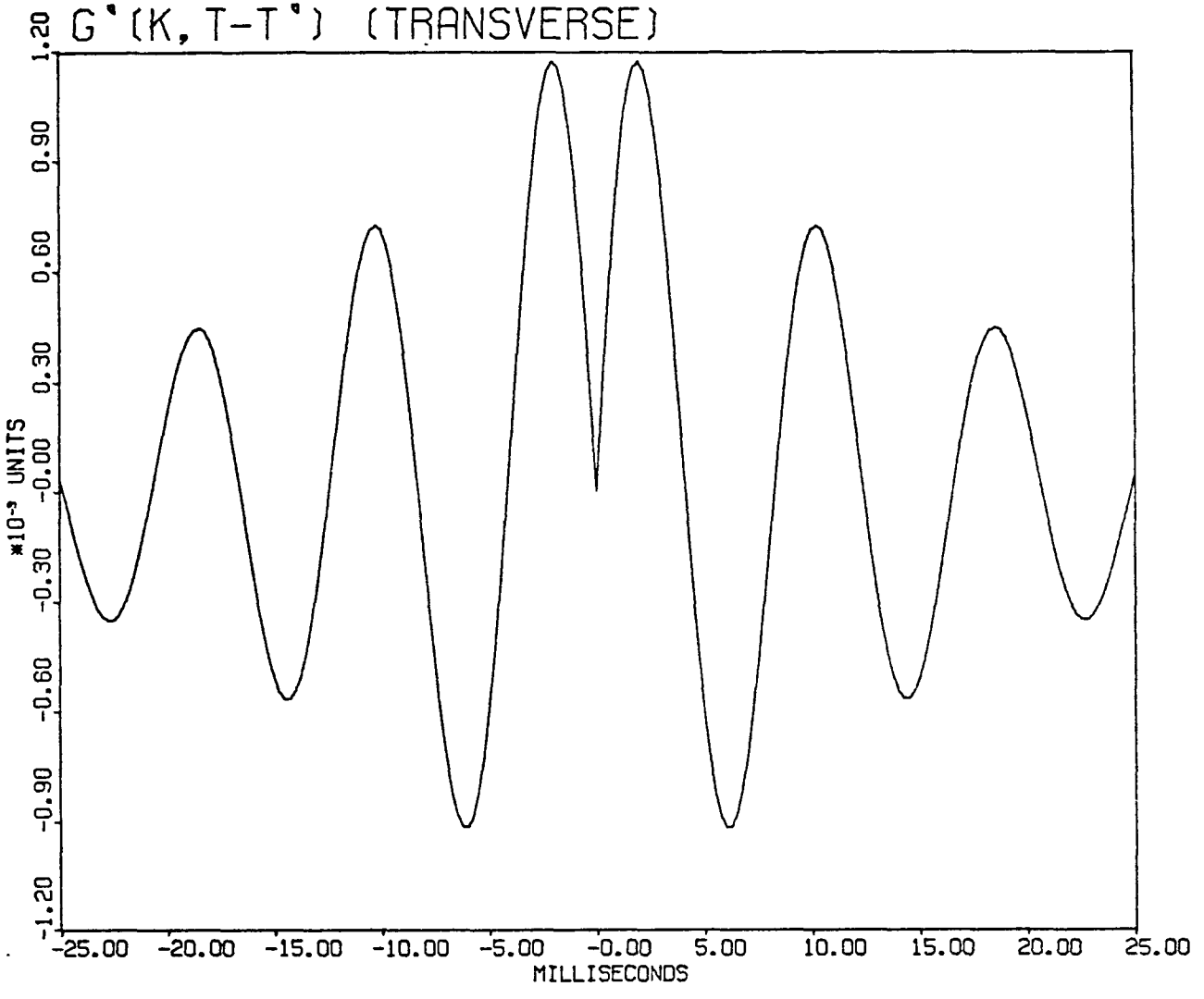

Figure 7o. The transverse component of the dispersive response, $G'_T(k;t-t')$. Plotted is $2G'_T(k;t-t')$, an even function of time.

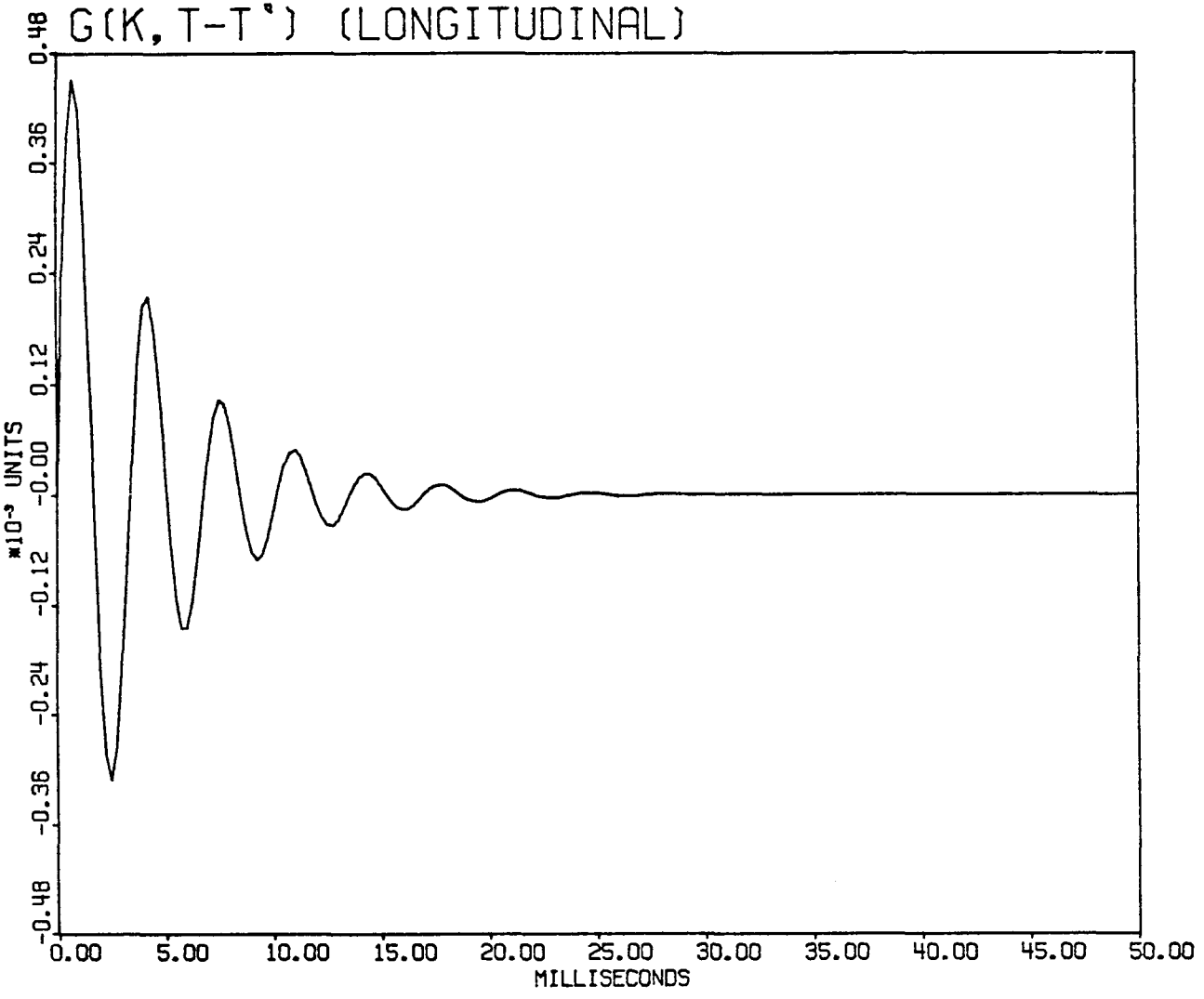

Figure 7p. The longitudinal component of the retarded response, $G_L(k;t-t')$.

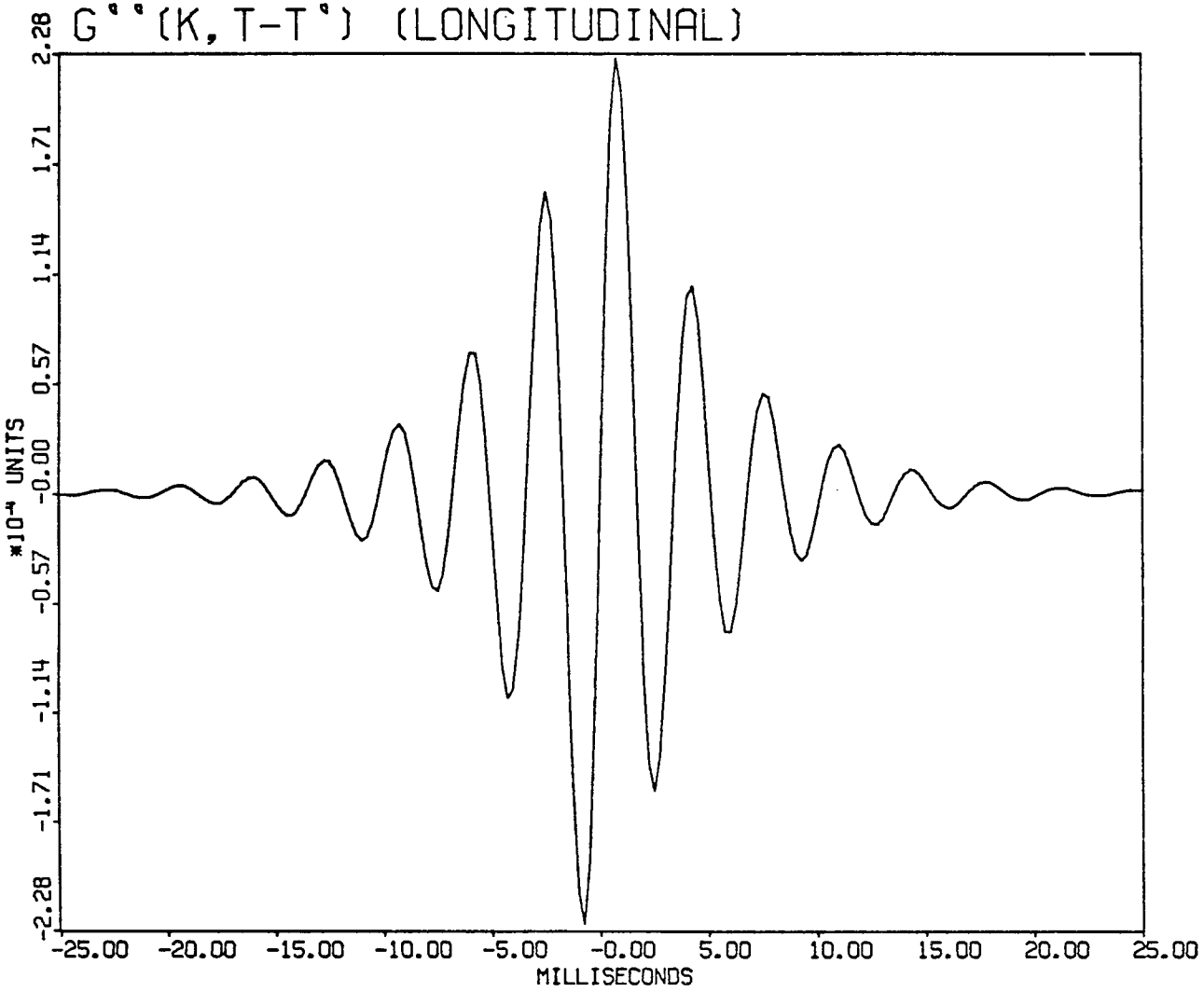

Figure 7q. The longitudinal component of the absorptive response, $G''_L(k;t-t')$. Plotted is $i\,G''_L(k;t-t')$, an odd function of time.

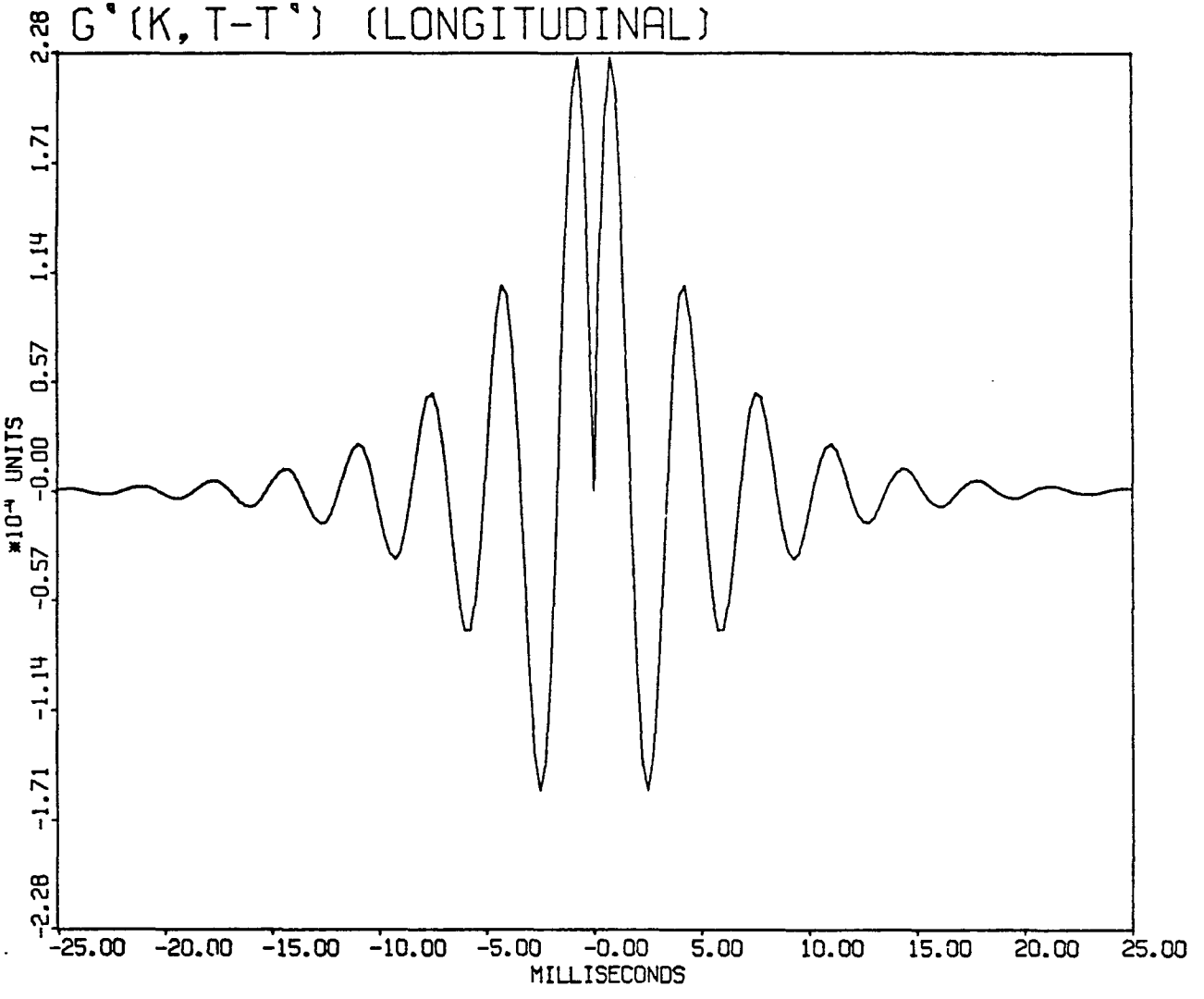

Figure 7r. The longitudinal component of the dispersive response, $G'_L(k;t-t')$, an even function of time.

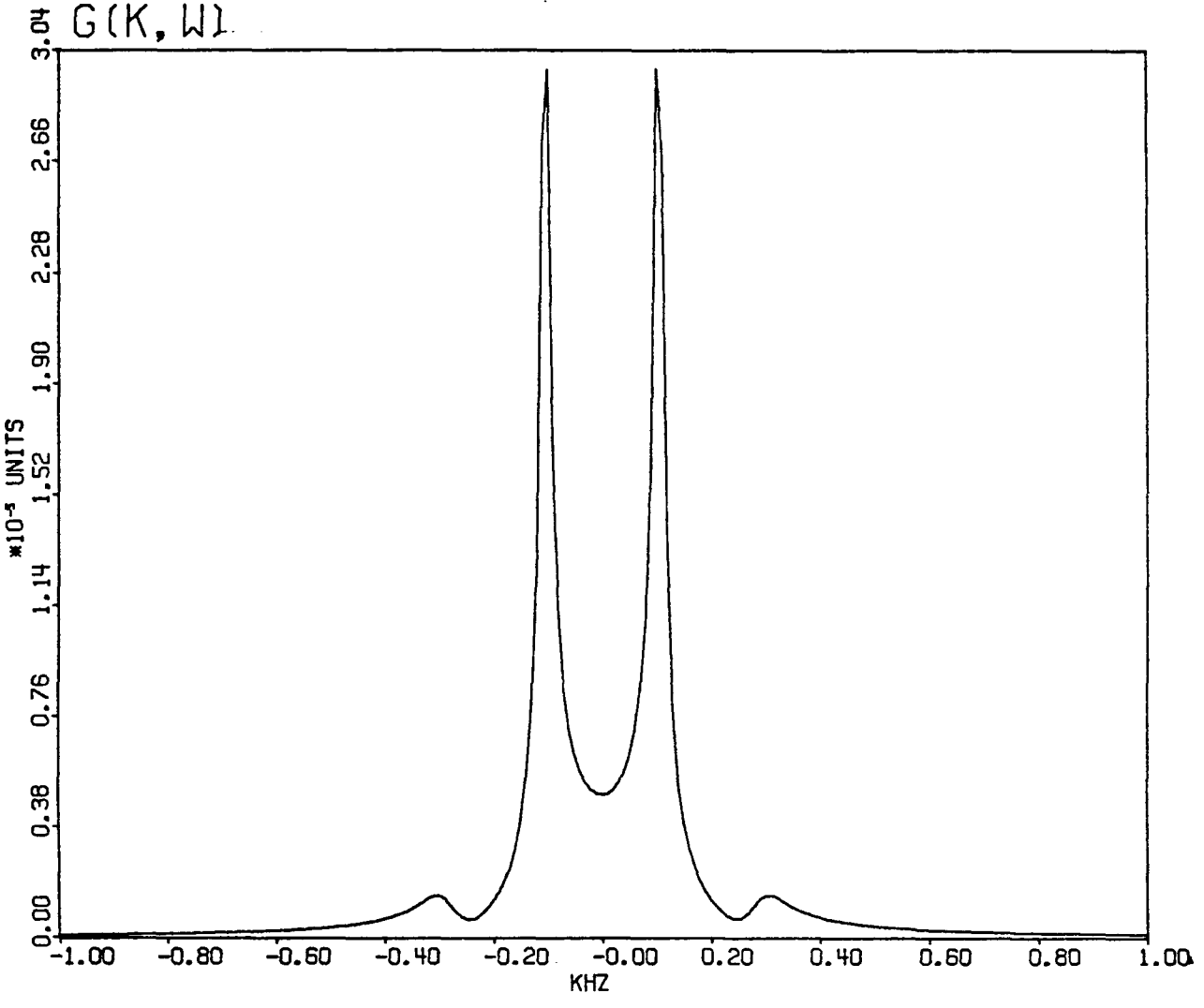

Figure 8a. The absolute value of the retarded response in the frequency domain, $|G^{v}_{jj}(k;\omega)|$.

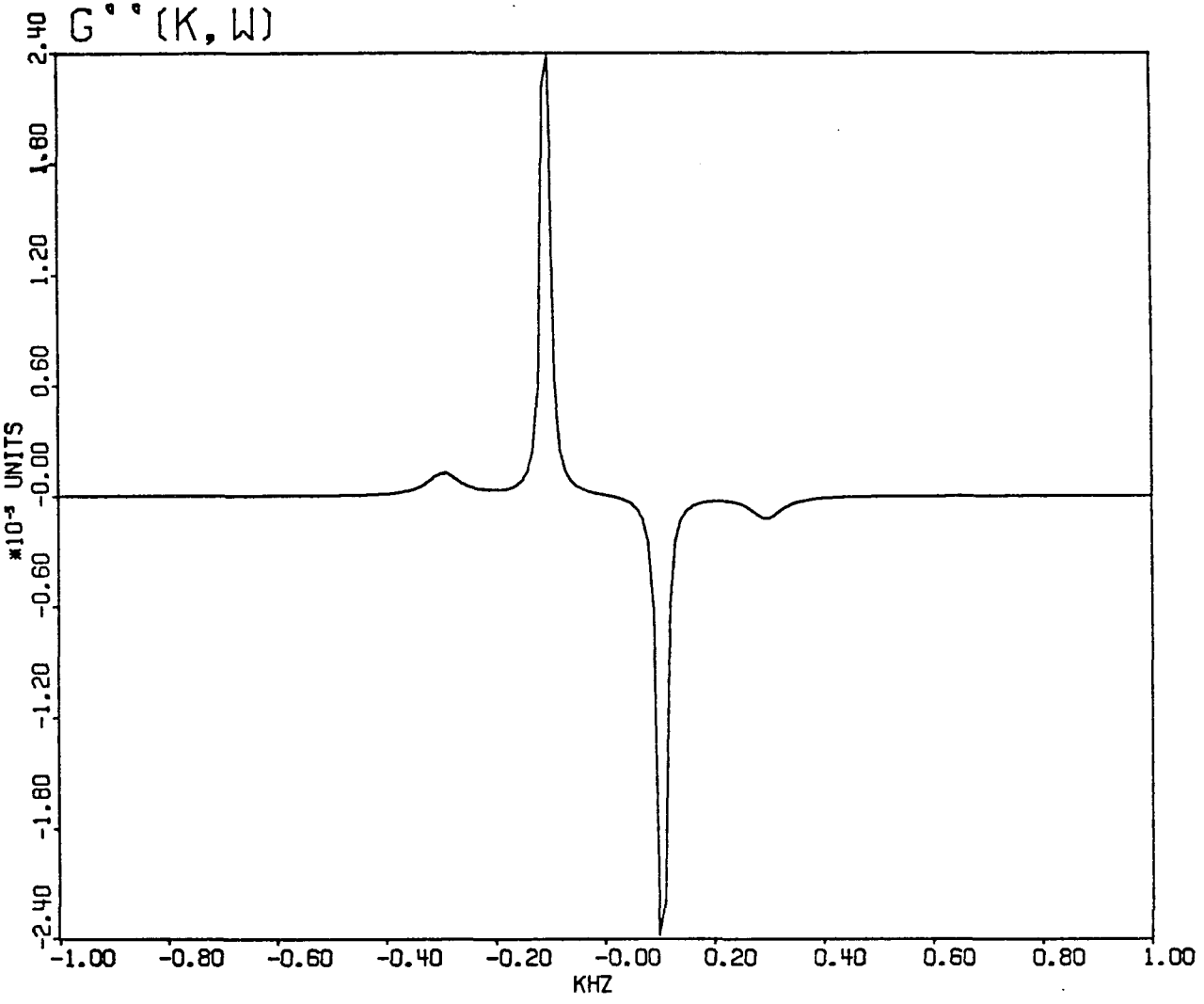

Figure 8b. The absorptive response, $G''^{v}_{jj}(k;\omega)$, which is the imaginary part of the retarded response in the frequency domain.

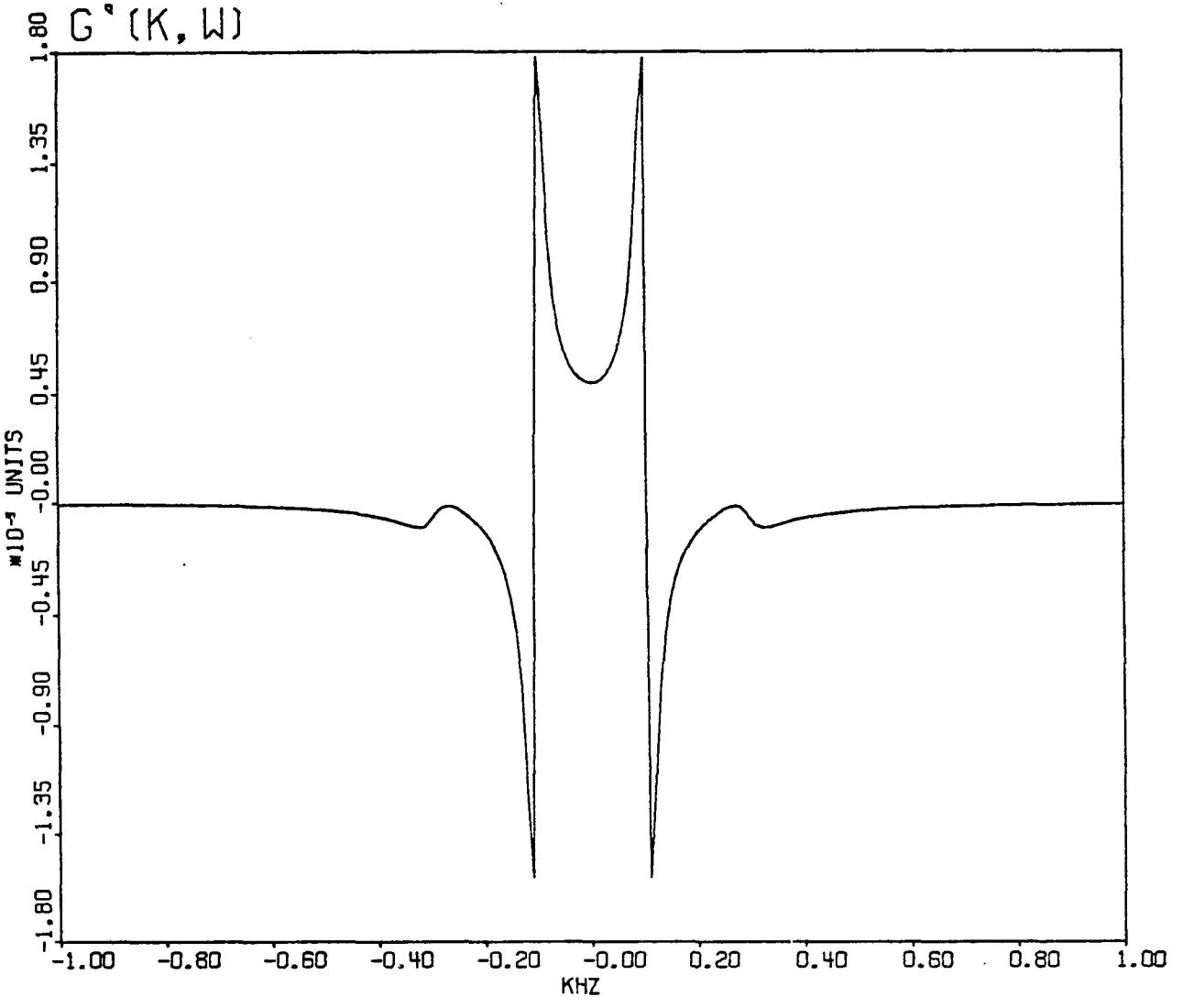

Figure 8c. The dispersive response, $G'^{v}_{jj}(k;\omega)$, which is the real part of the retarded response in the frequency domain.

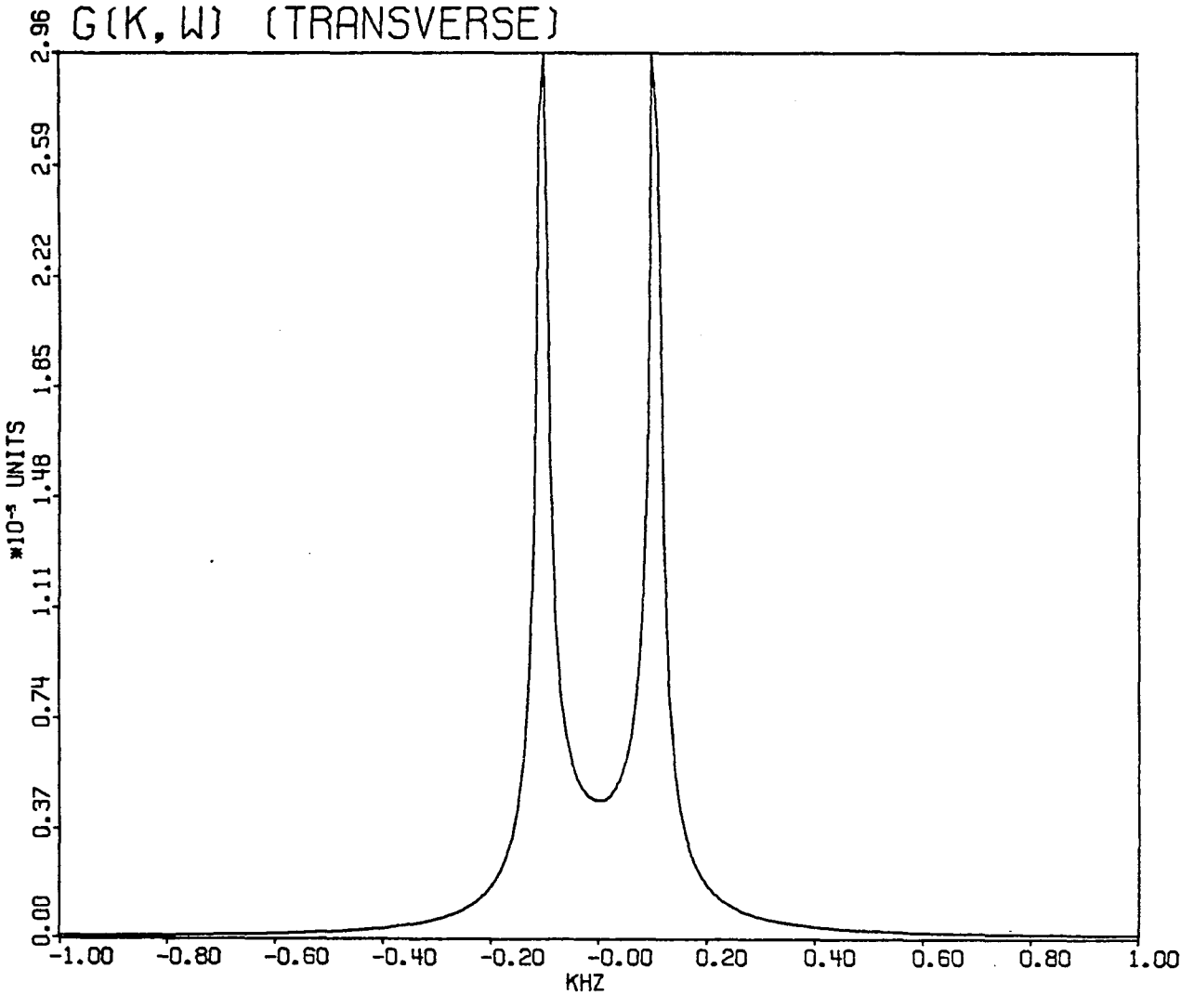

Figure 8d. The absolute value of the transverse component of the retarded response, $|G_T^V(k;\omega)|$. Plotted is $|2G_T^V(k;\omega)|$.

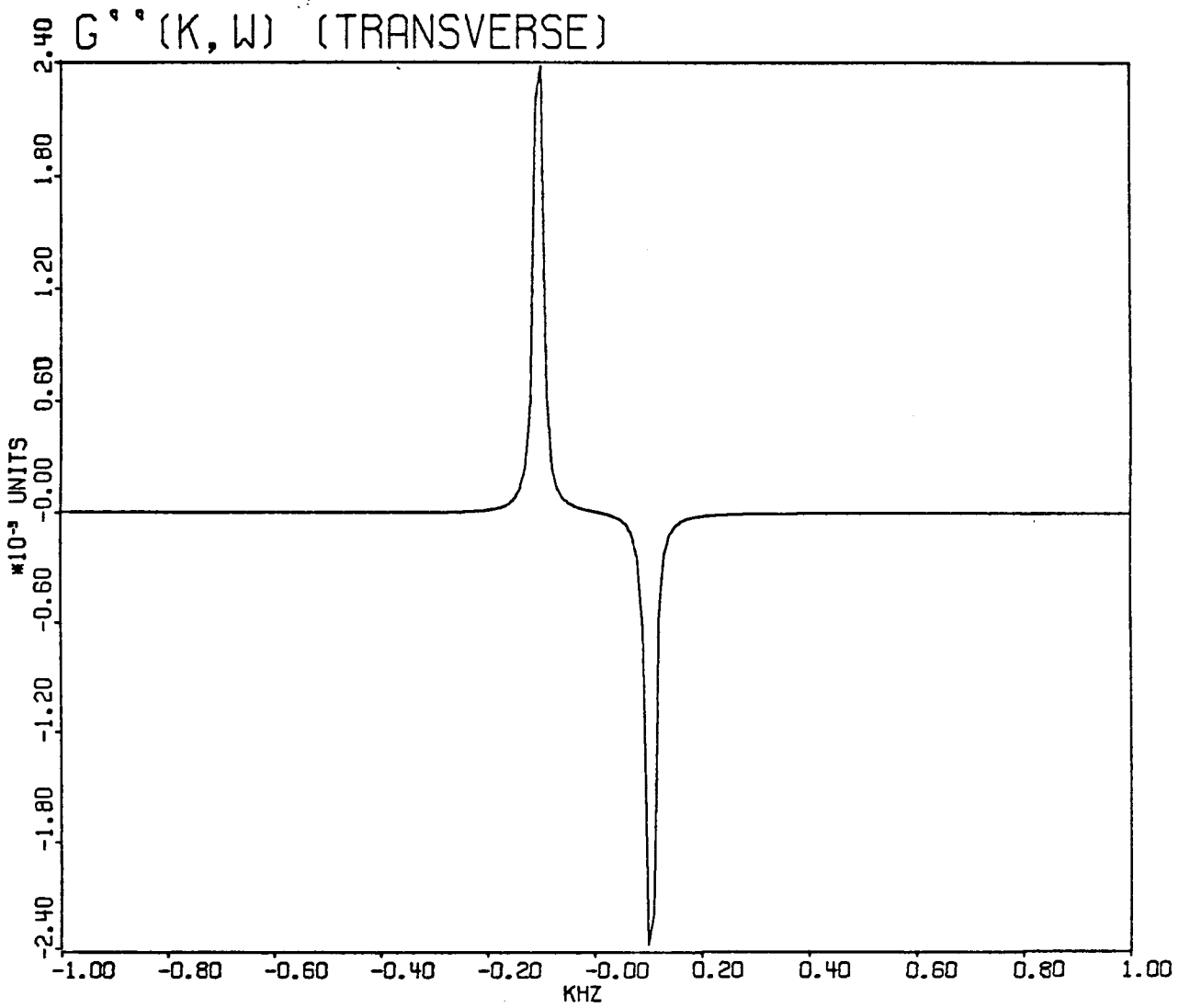

Figure 8e. The transverse component of the absorptive response, $G_T''^{V}(k;\omega)$. Plotted is $2G_T''^{V}(k;\omega)$.

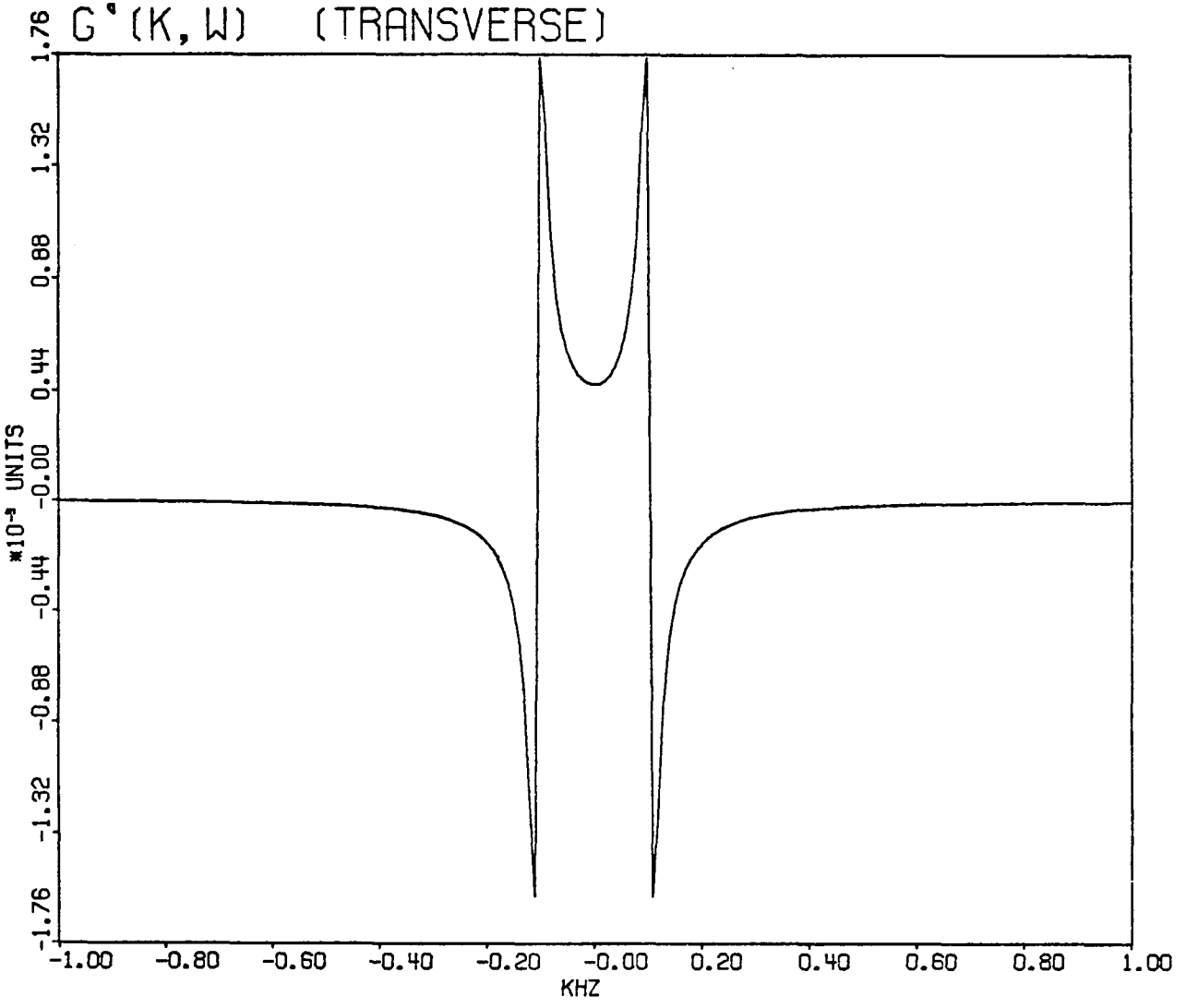

Figure 8f. The transverse component of the dispersive response, $G_T'^{V}(k;\omega)$. Plotted is $2G_T'^{V}(k;\omega)$.

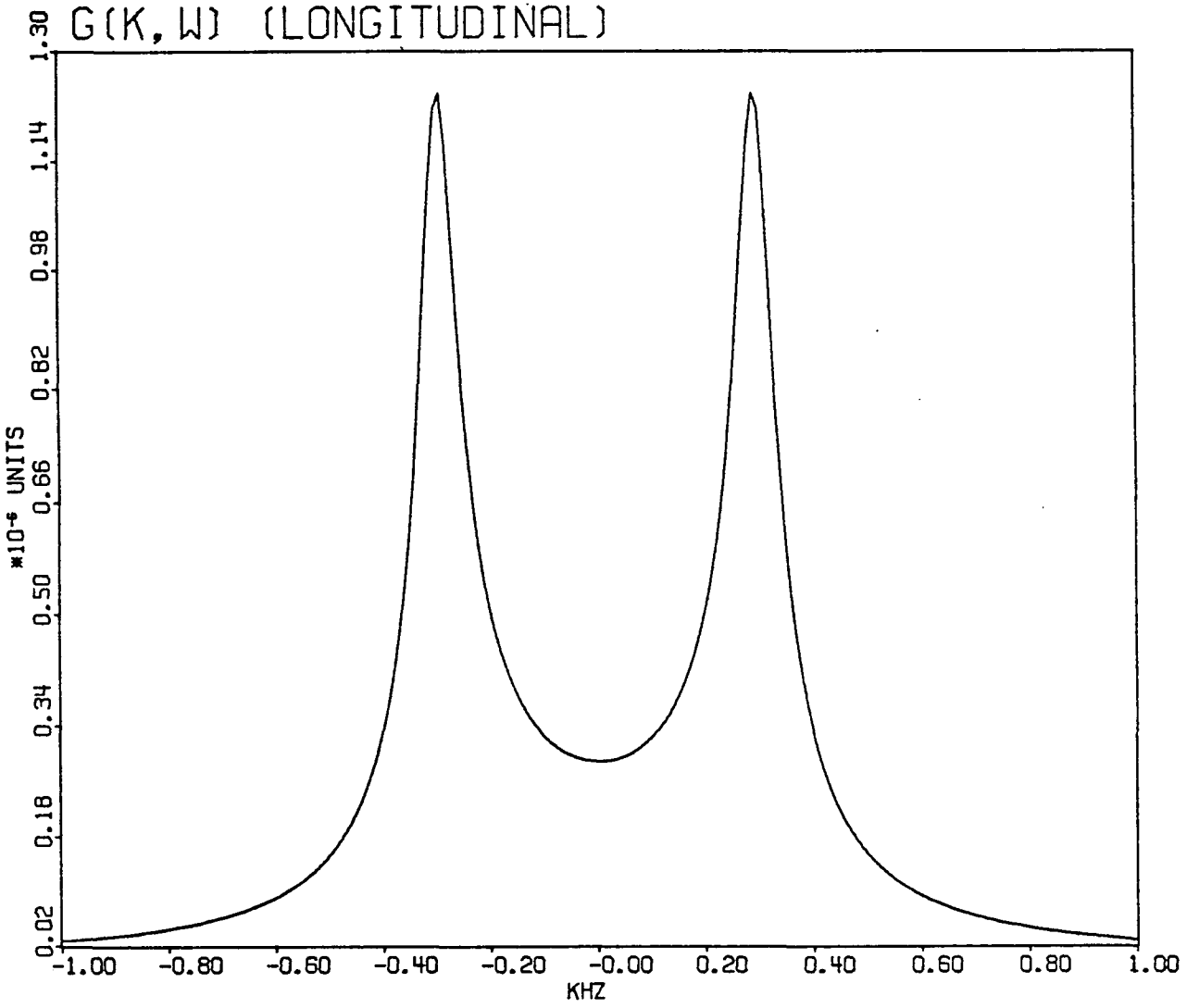

Figure 8g. The absolute value of the longitudinal component of the retarded response, $|G_L^V(k;\omega)|$.

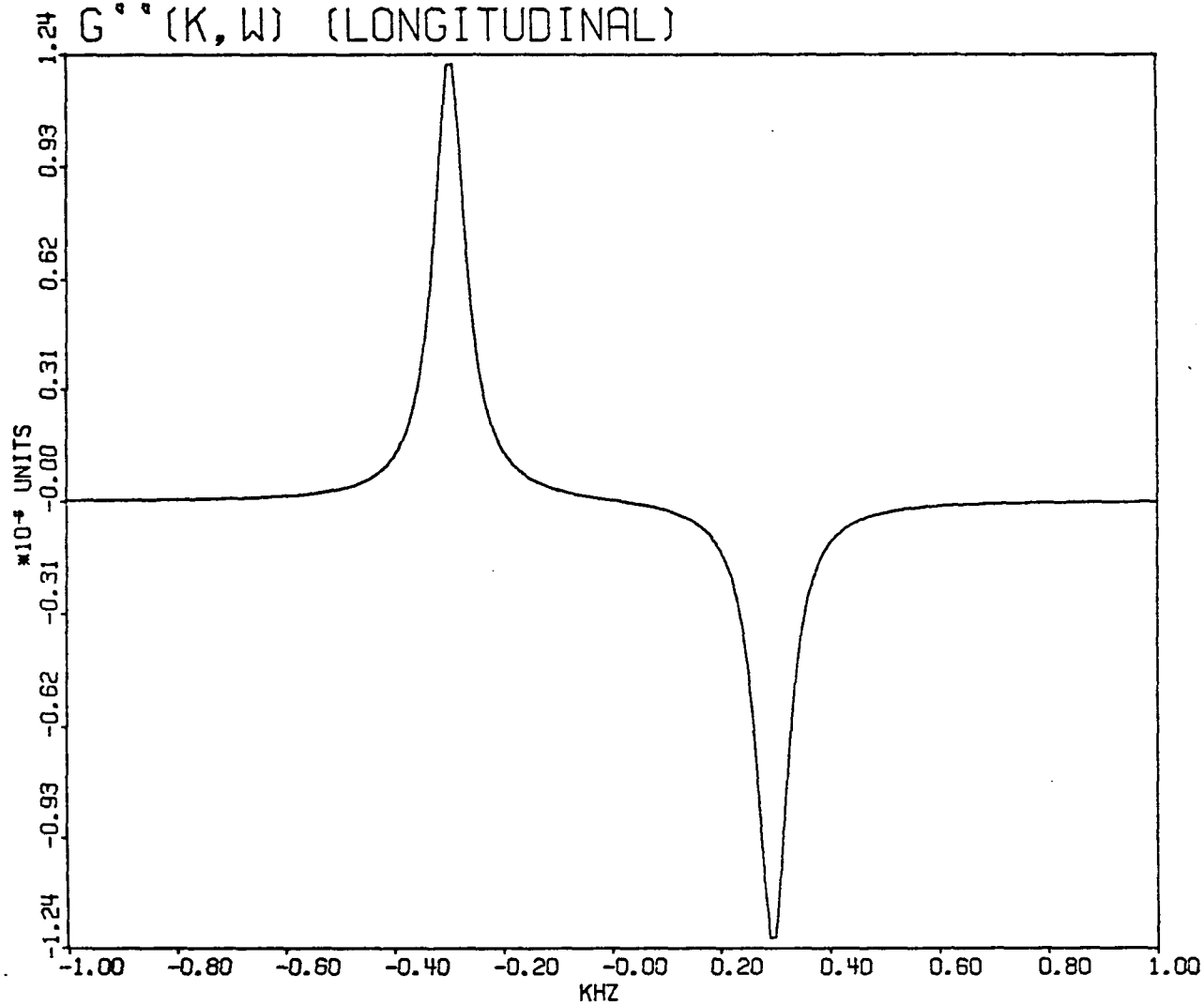

Figure 8h. The longitudinal component of the absorptive response, $G''^{V}_{L}(k;\omega)$.

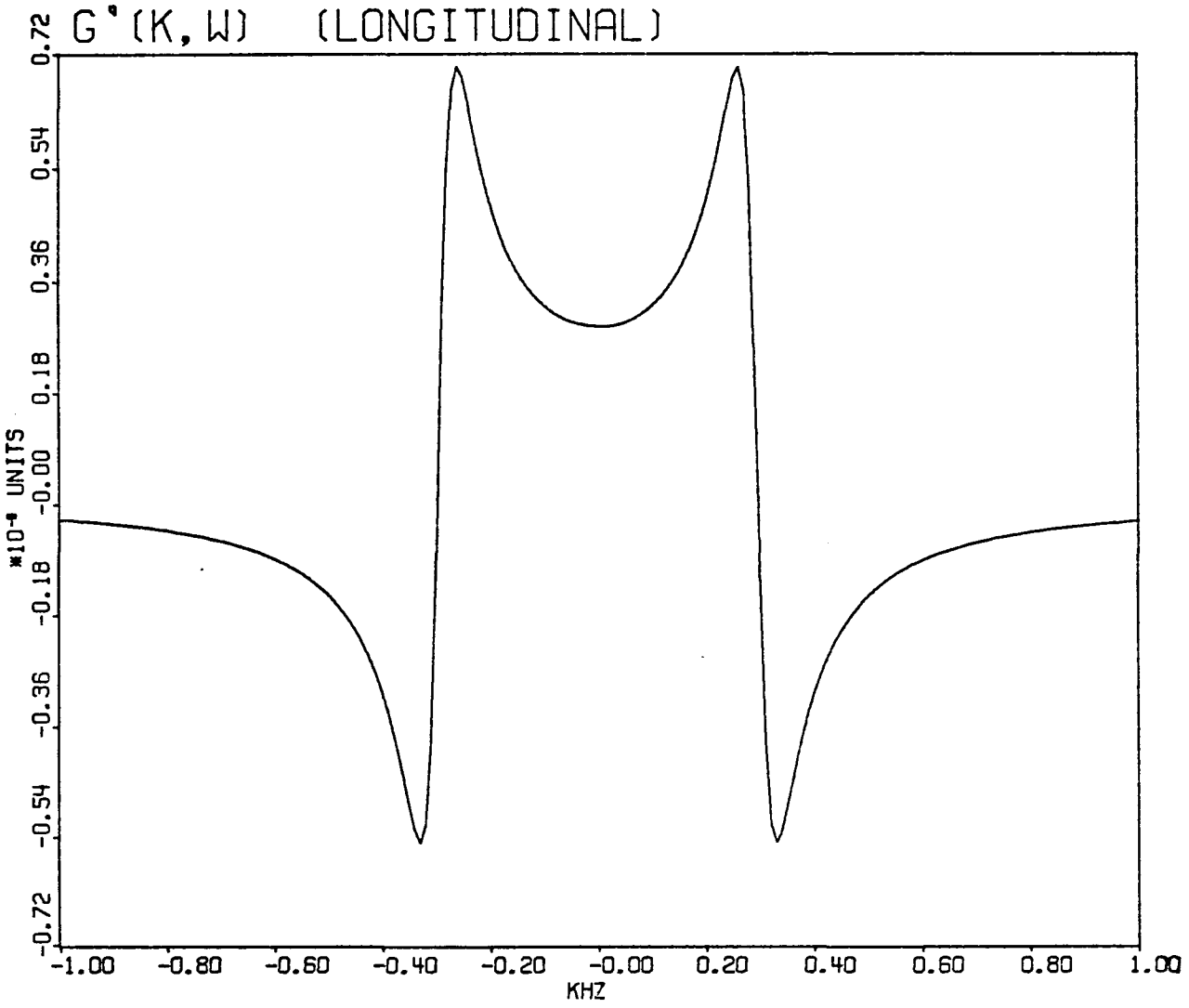

Figure 8i. The longitudinal component of the dispersive response, $G_L'^{V}(k;\omega)$.

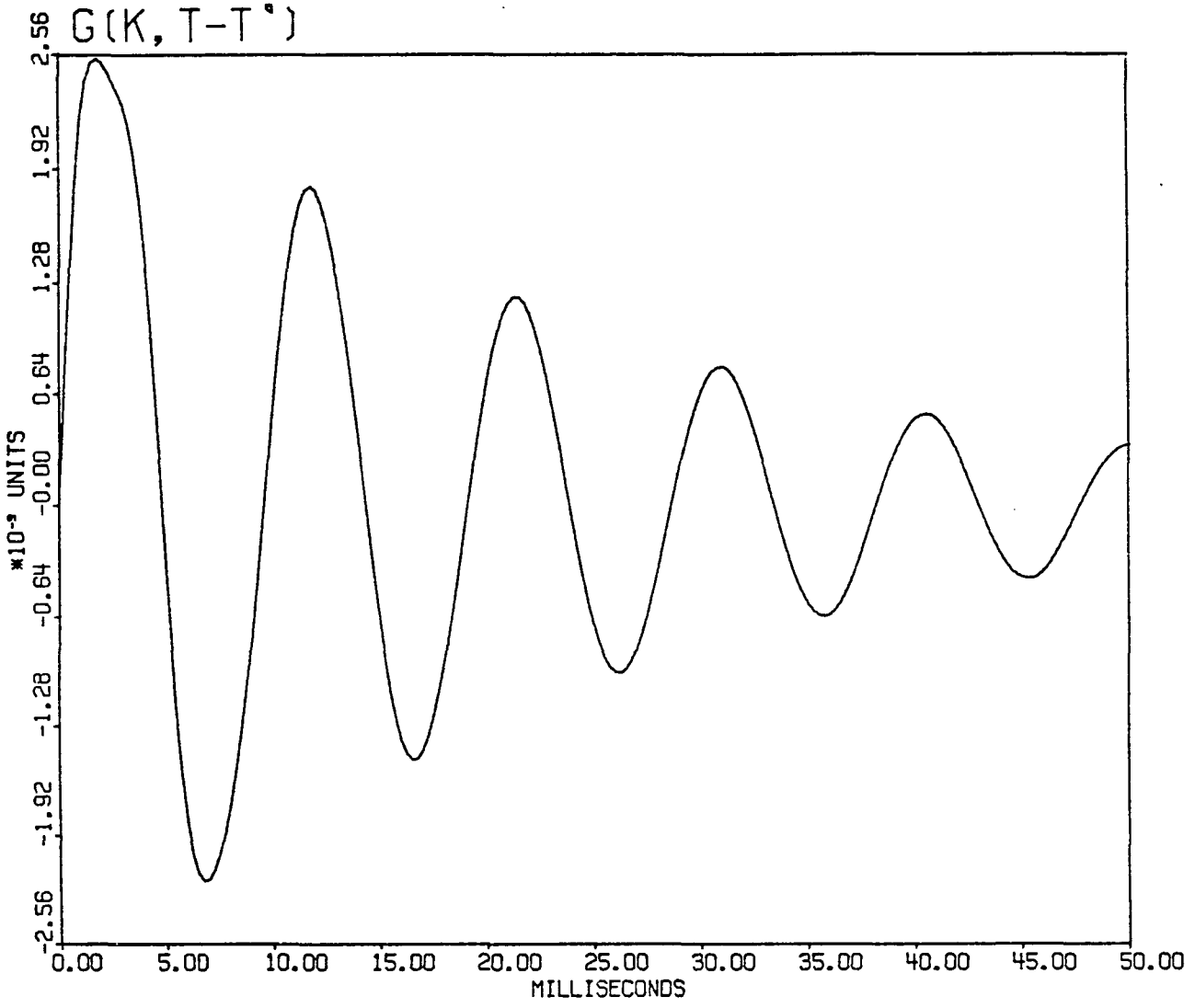

Figure 8j. The retarded response in the time domain, $G^{v}_{jj}(k;t-t')$.

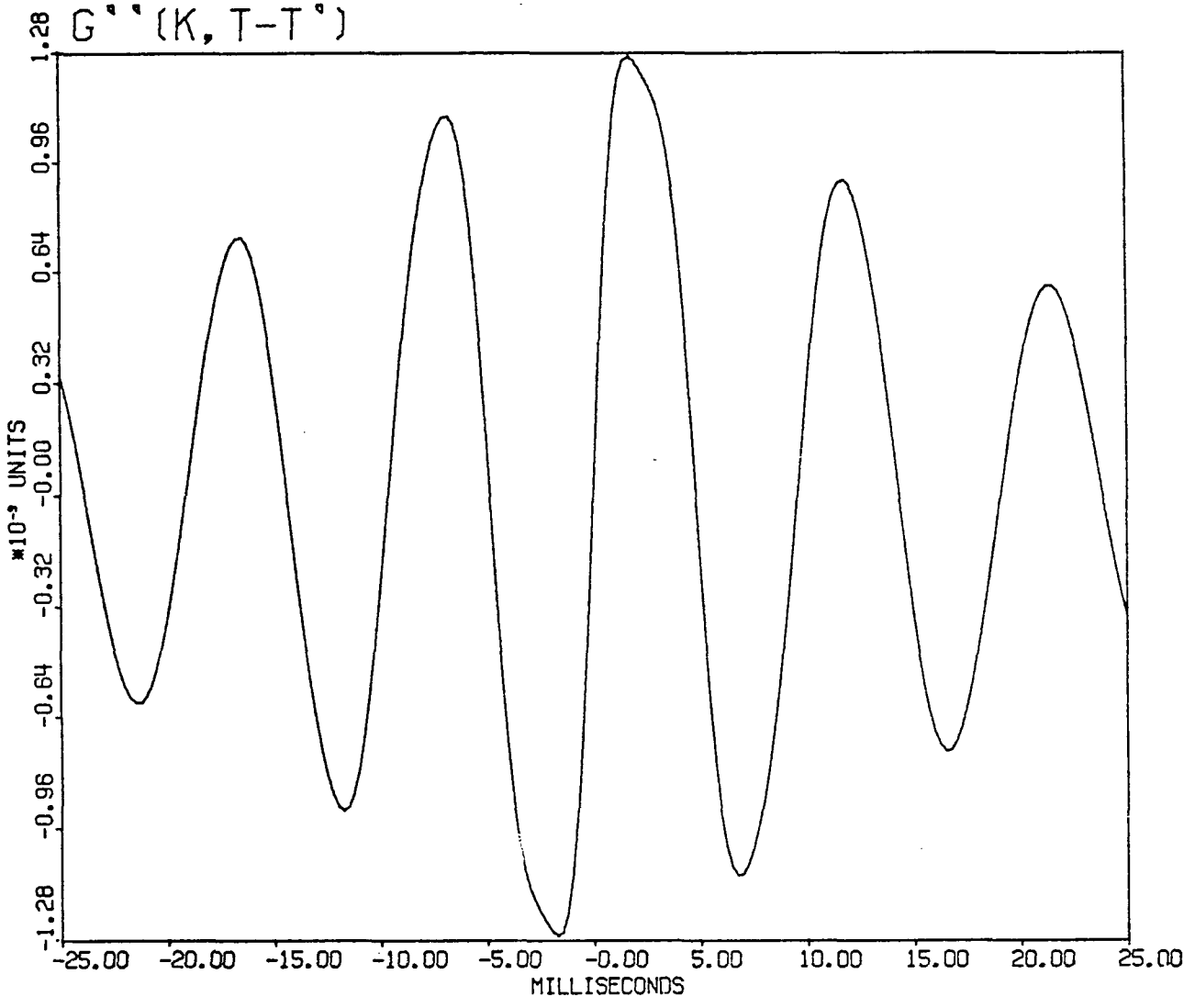

Figure 8k. The absorptive response, $G''^{V}_{jj}(k;t-t')$. Plotted is $i\,G''^{V}_{jj}(k;t-t')$, an odd function of time corresponding to $G^{V}_{jj}(k;t-t')$.

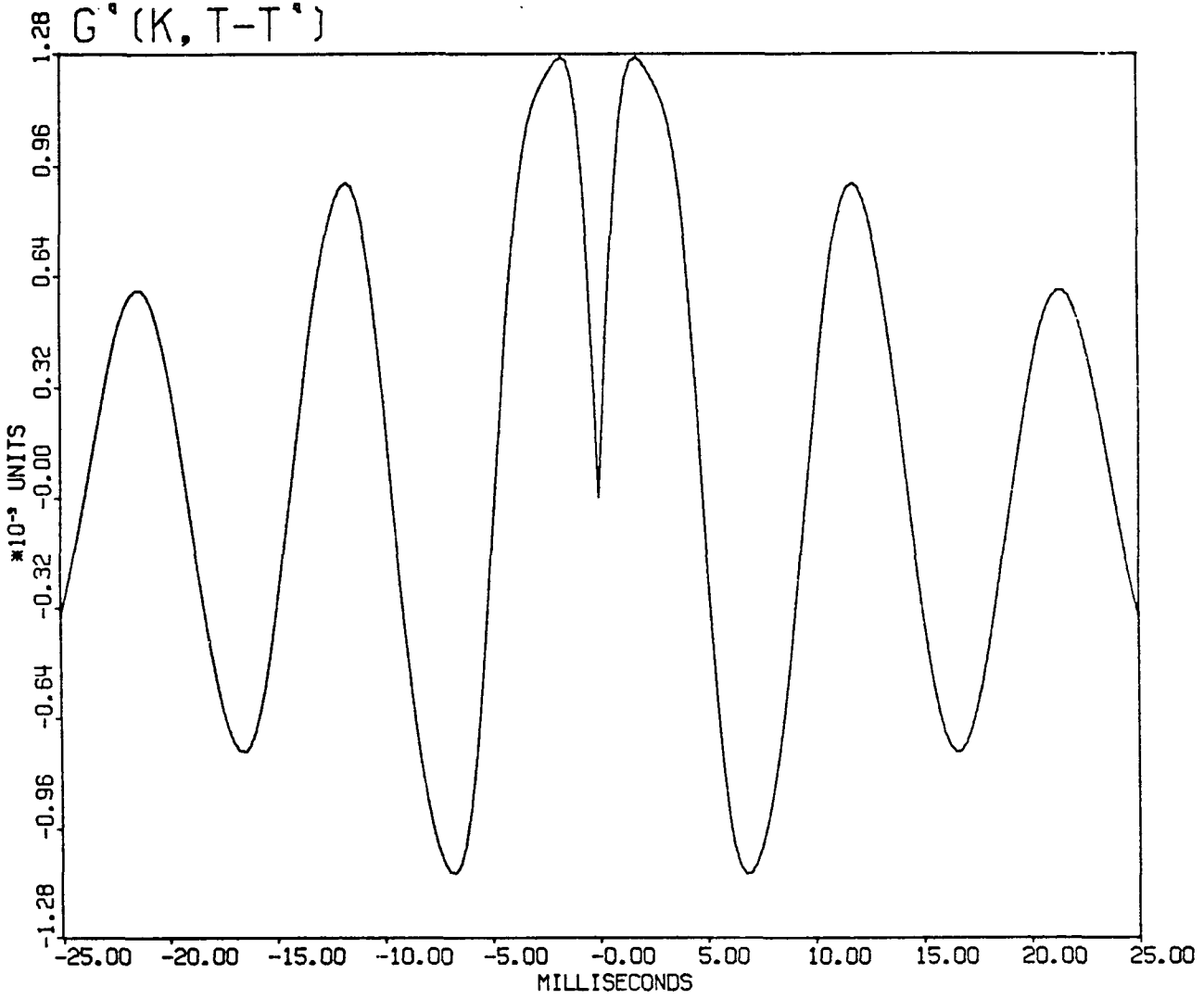

Figure 81. The dispersive response, $G'^{V}_{jj}(k;t-t')$, which is an even function of time corresponding to $G^{V}_{jj}(k;t-t')$.

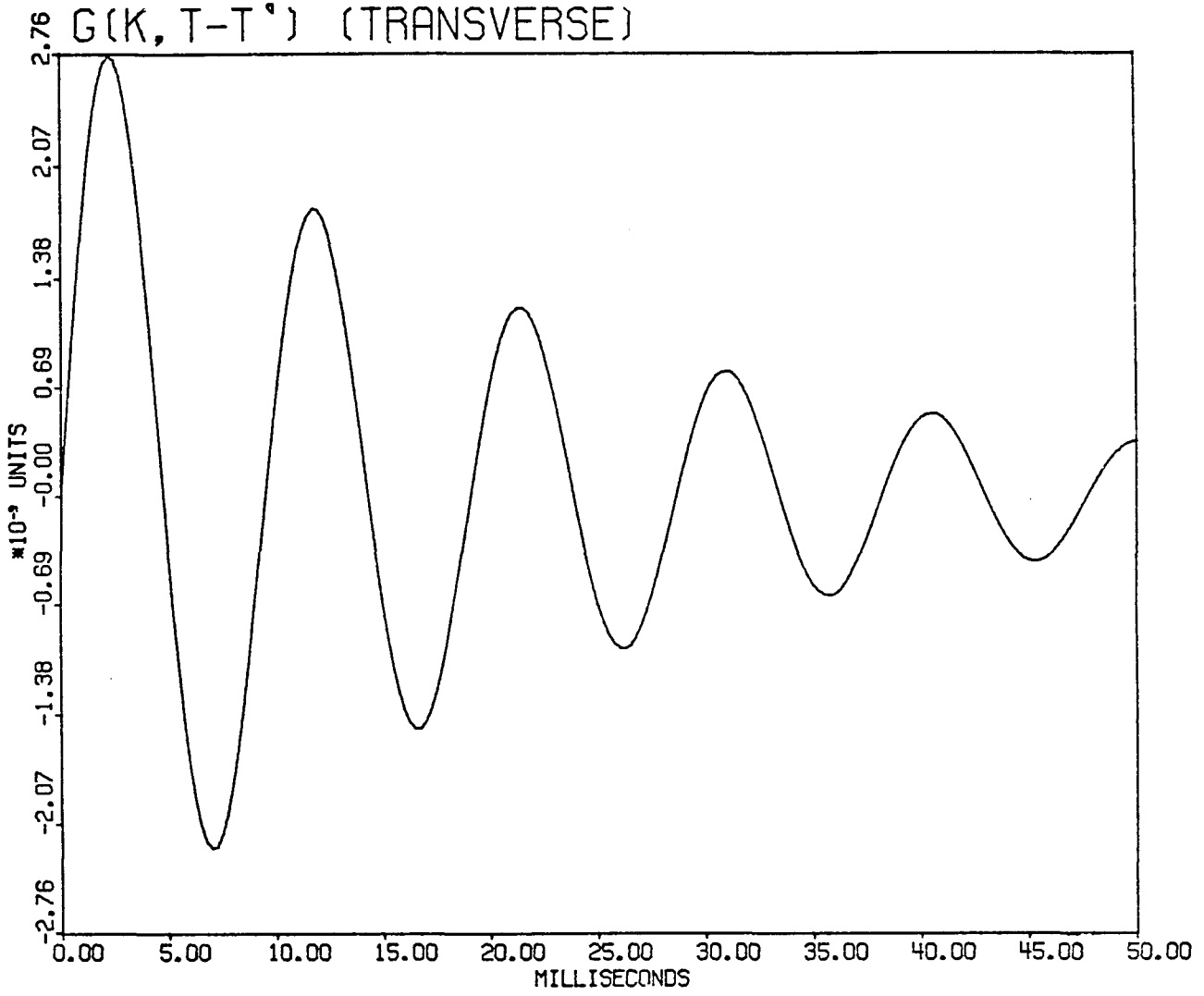

Figure 8m. The transverse component of the retarded response, $G_T^V(k;t-t')$.

Plotted is $2\ G_T^V(k;t-t')$.

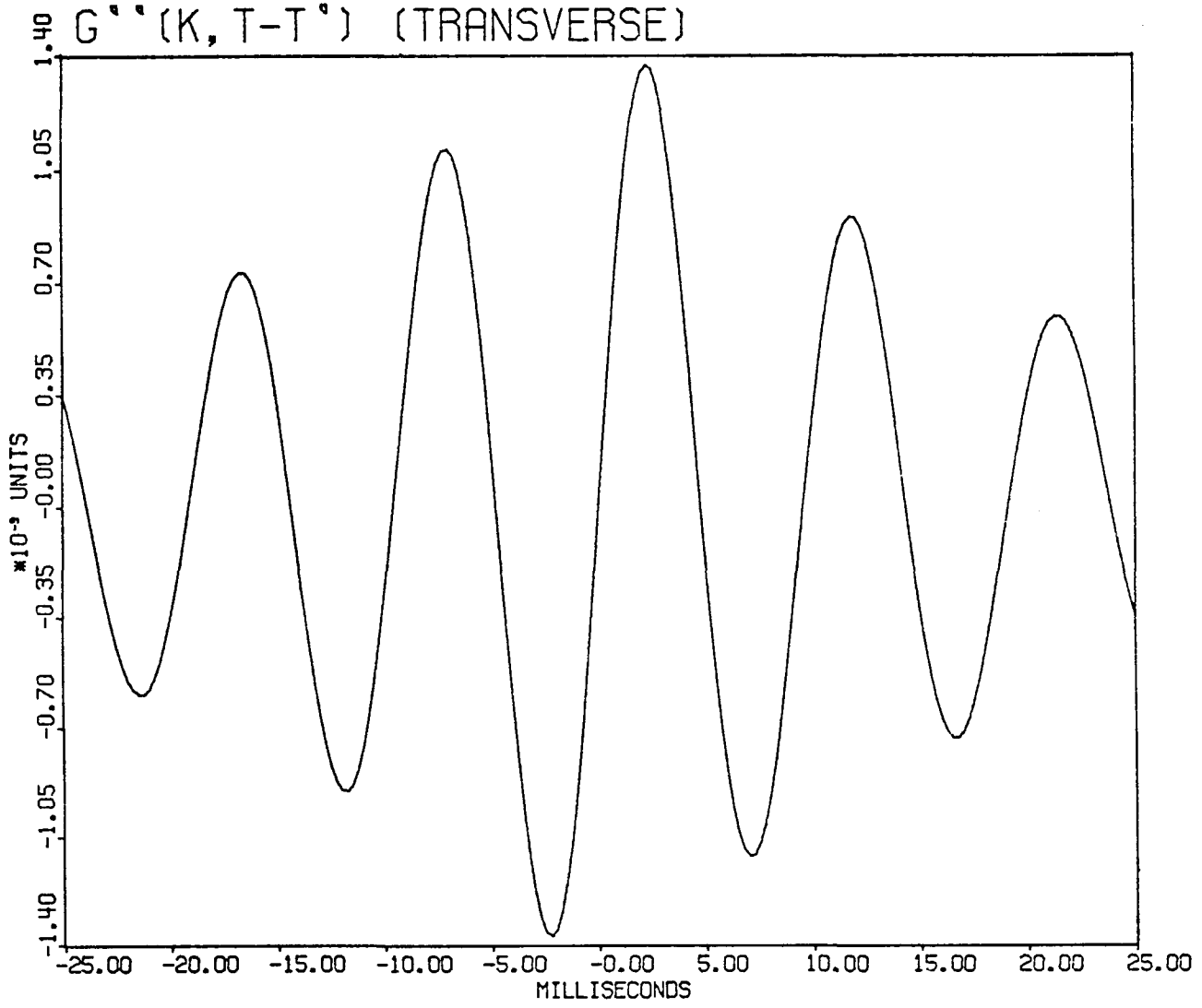

Figure 8n. The transverse component of the absorptive response, $G''^{V}_{T}(k;t-t')$.

Plotted is $2i\, G''^{V}_{T}(k;t-t')$, an odd function of time.

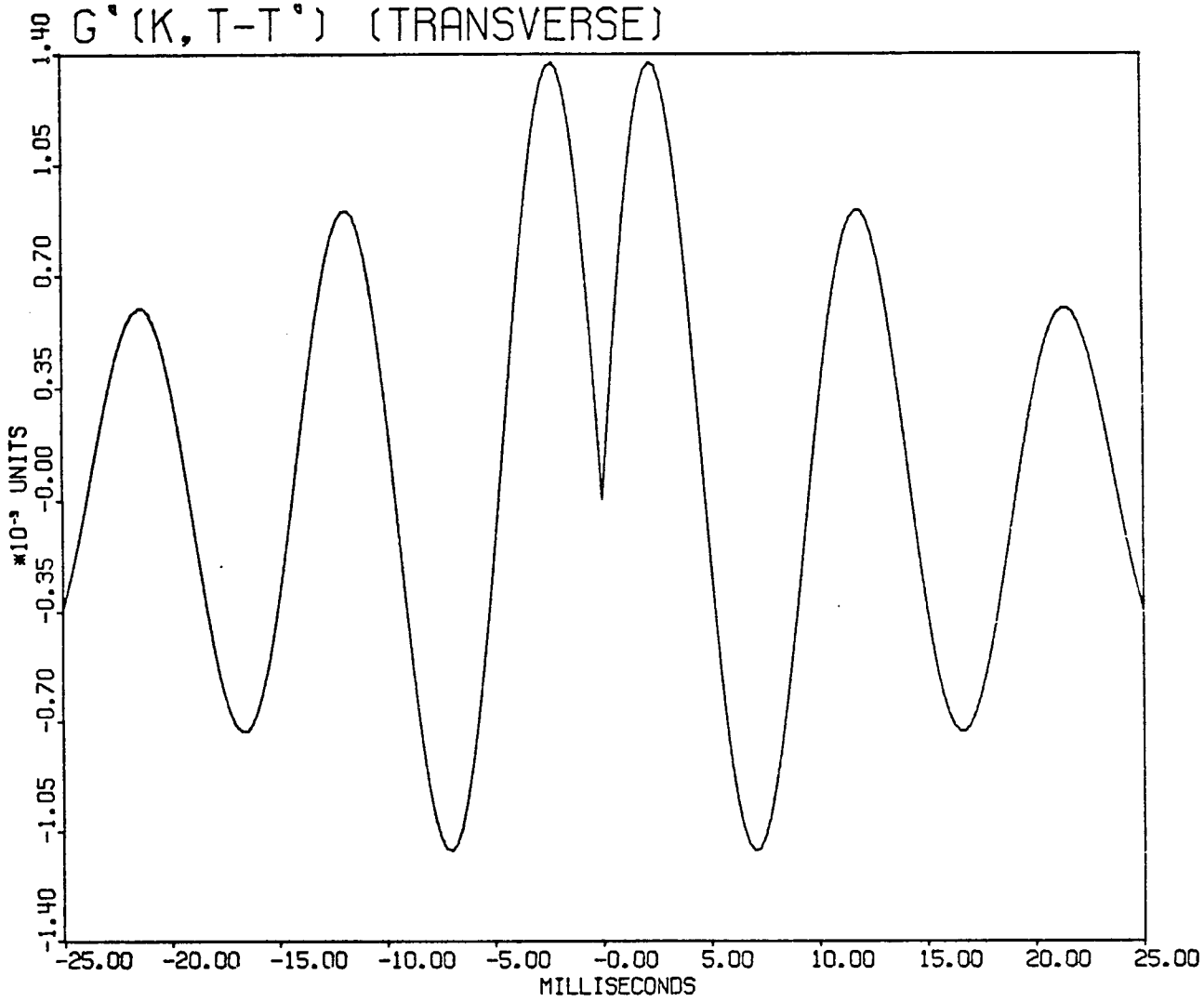

Figure 8o. The transverse component of the dispersive response, $G_T'^{V}(k;t-t')$.

Plotted is $2\ G_T'^{V}(k;t-t')$, an even function of time.

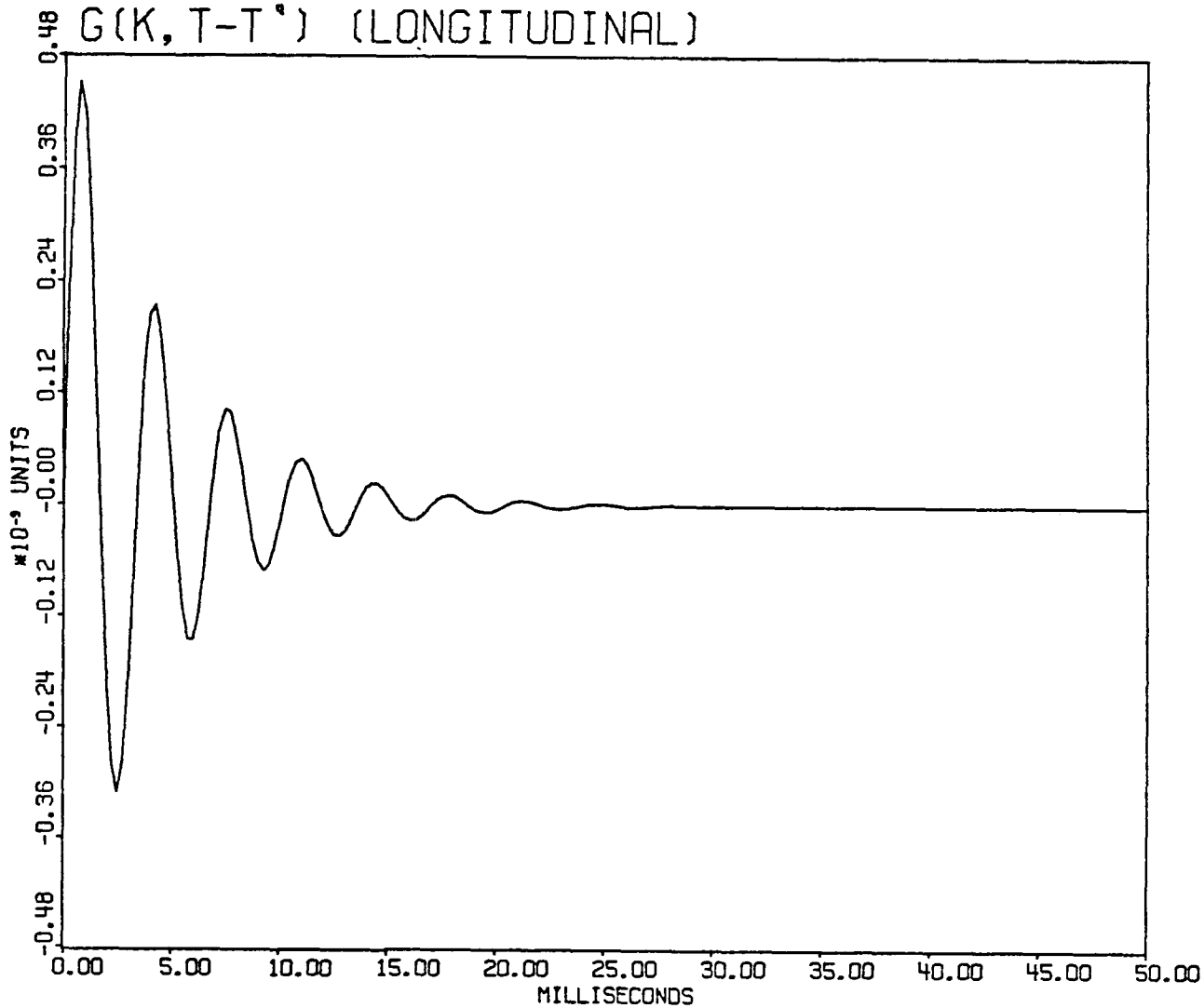

Figure 8p. The longitudinal component of the retarded response, $G_L^V(k;t-t')$.

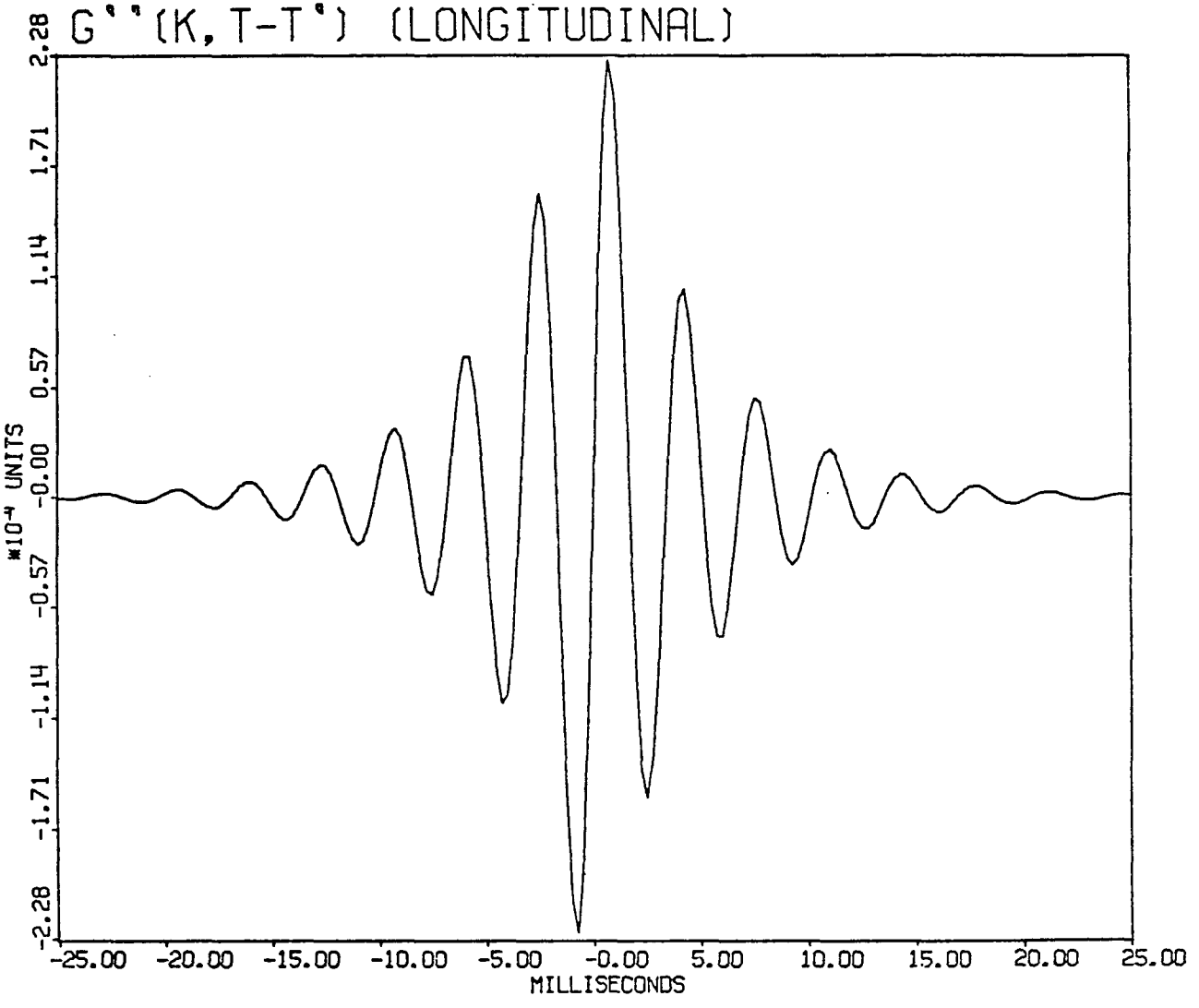

Figure 8q. The longitudinal component of the absorptive response, $G_L''^{V}(k;t-t')$.

Plotted is $i\, G_L''^{V}(k;t-t')$, an odd function of time.

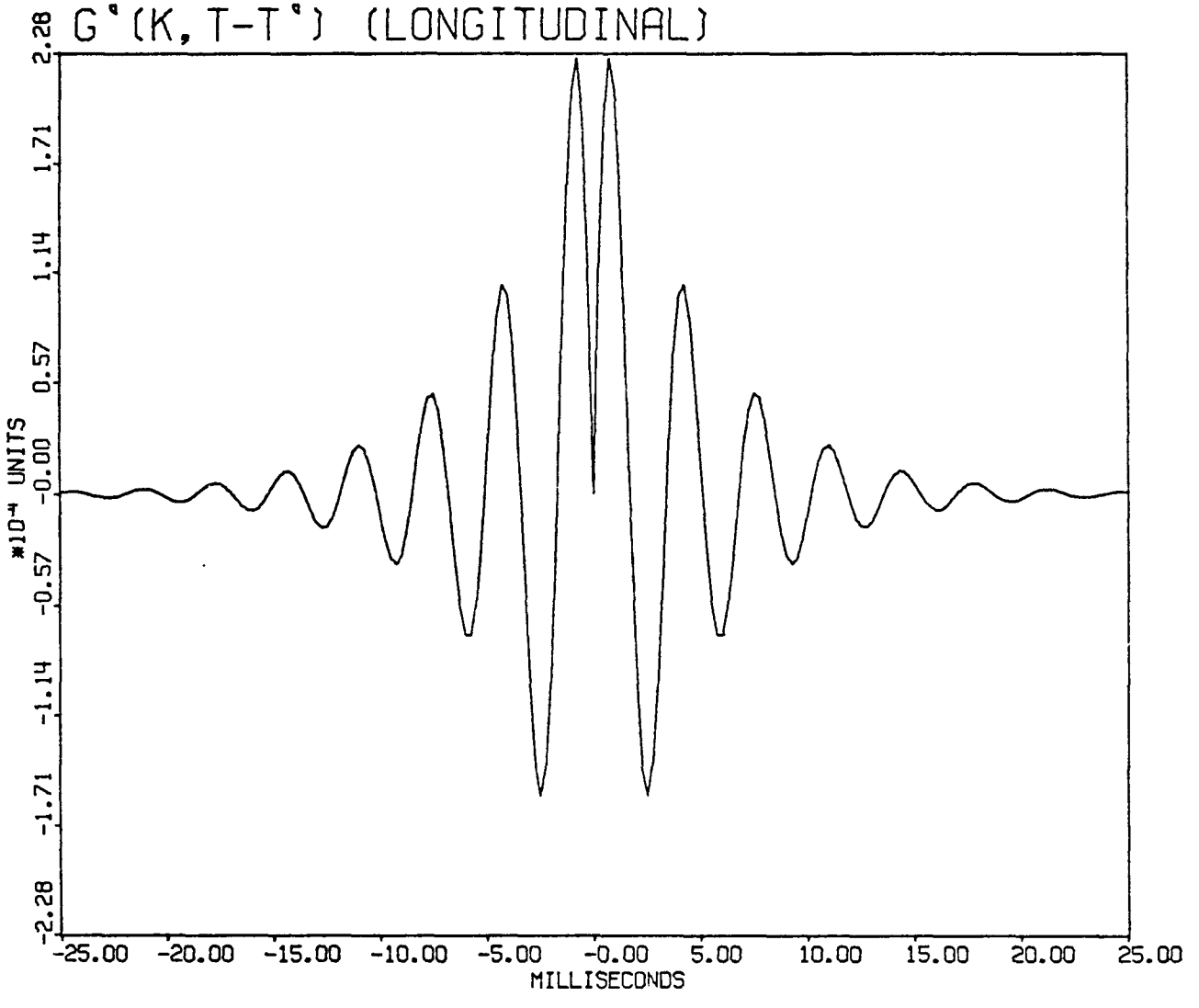

Figure 8r. The longitudinal component of the dispersive response, $G_L'^{v}(k;t-t')$, an even function of time.

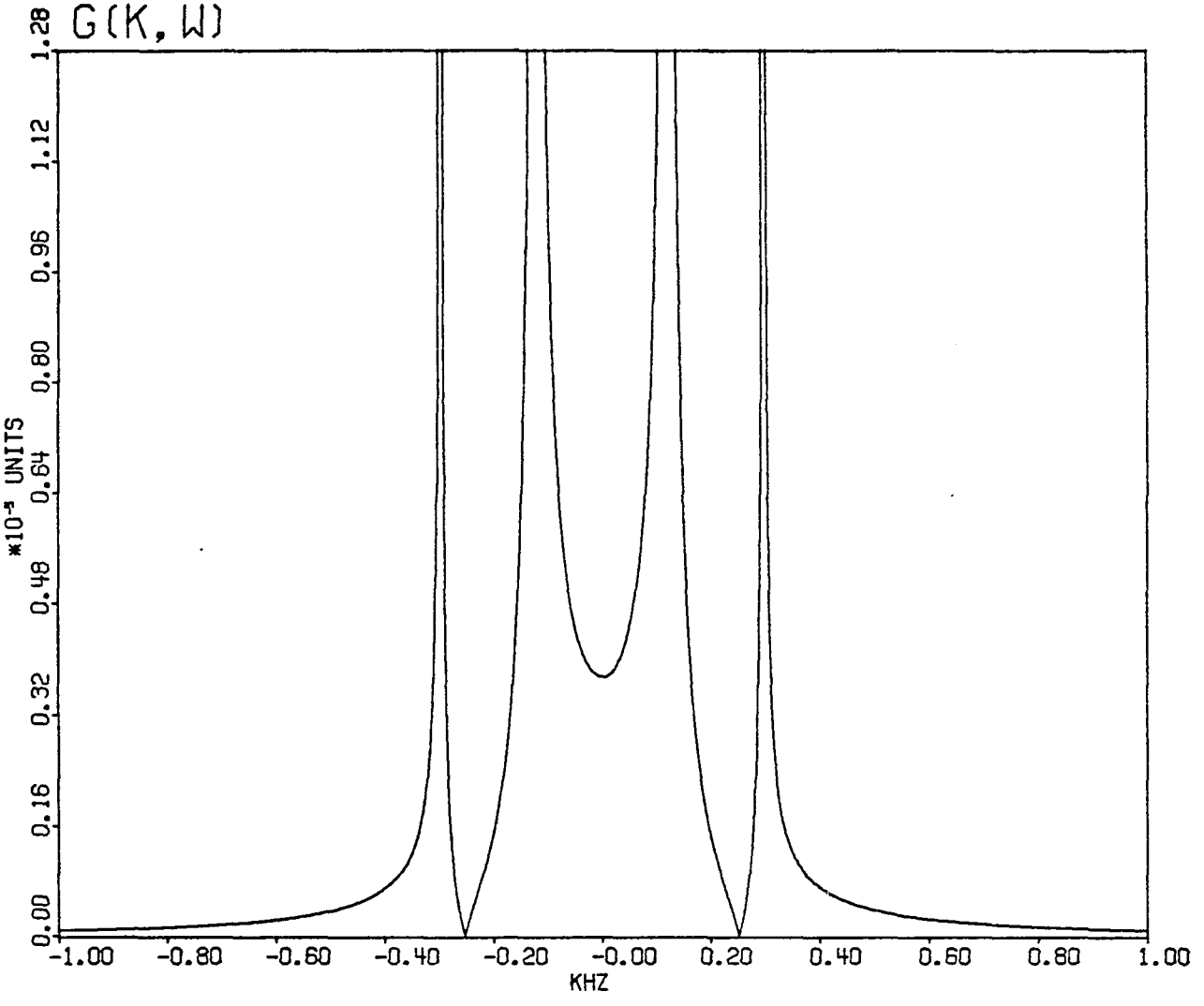

Figure 9a. The absolute value of the retarded response in the frequency domain, $|G^{ec}_{jj}(k;\omega)|$.

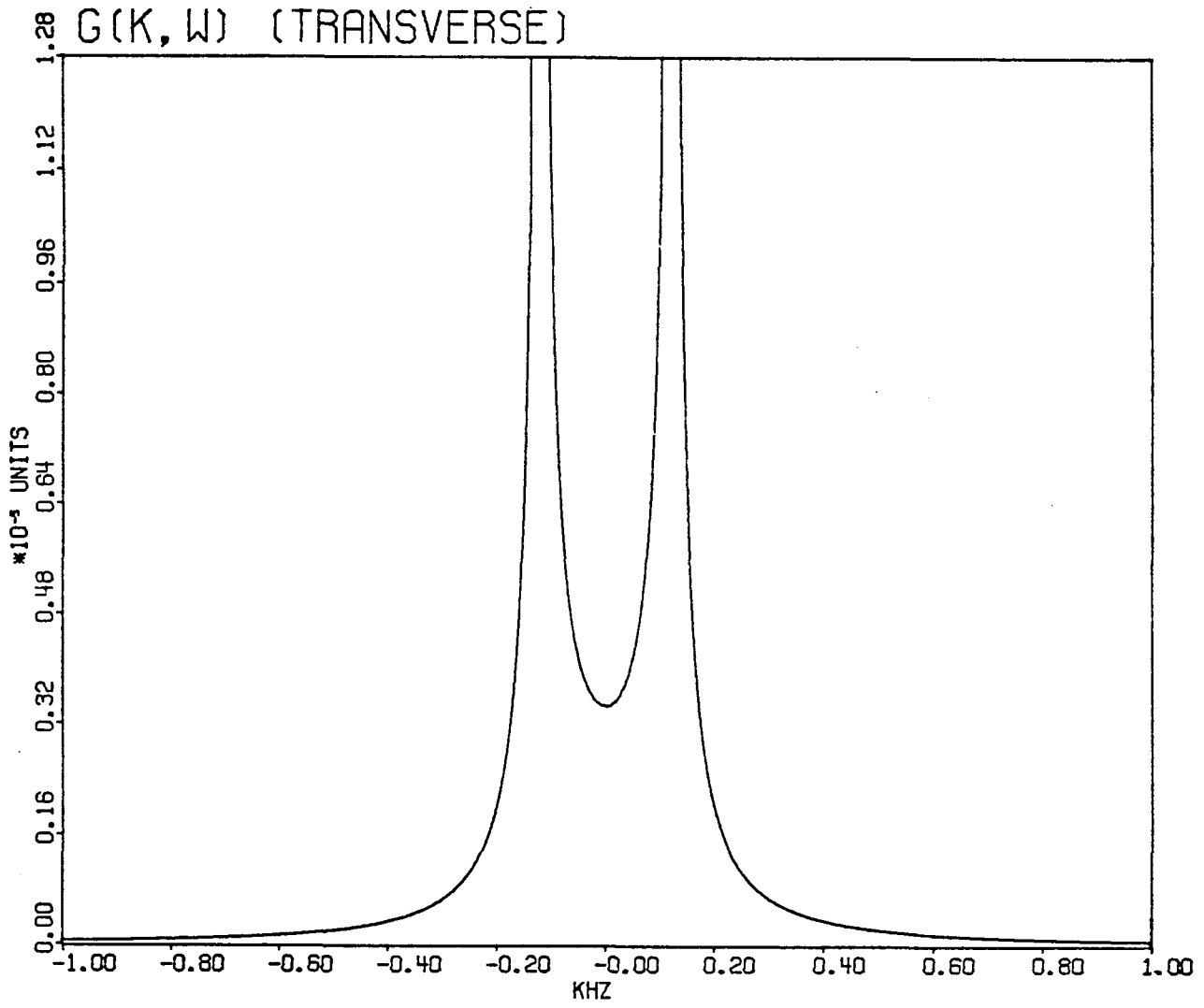

Figure 9b. The absolute value of the transverse component of the retarded response, $|G_T^{ec}(k;\omega)|$. Plotted is $|2G_T^{ec}(k;\omega)|$.

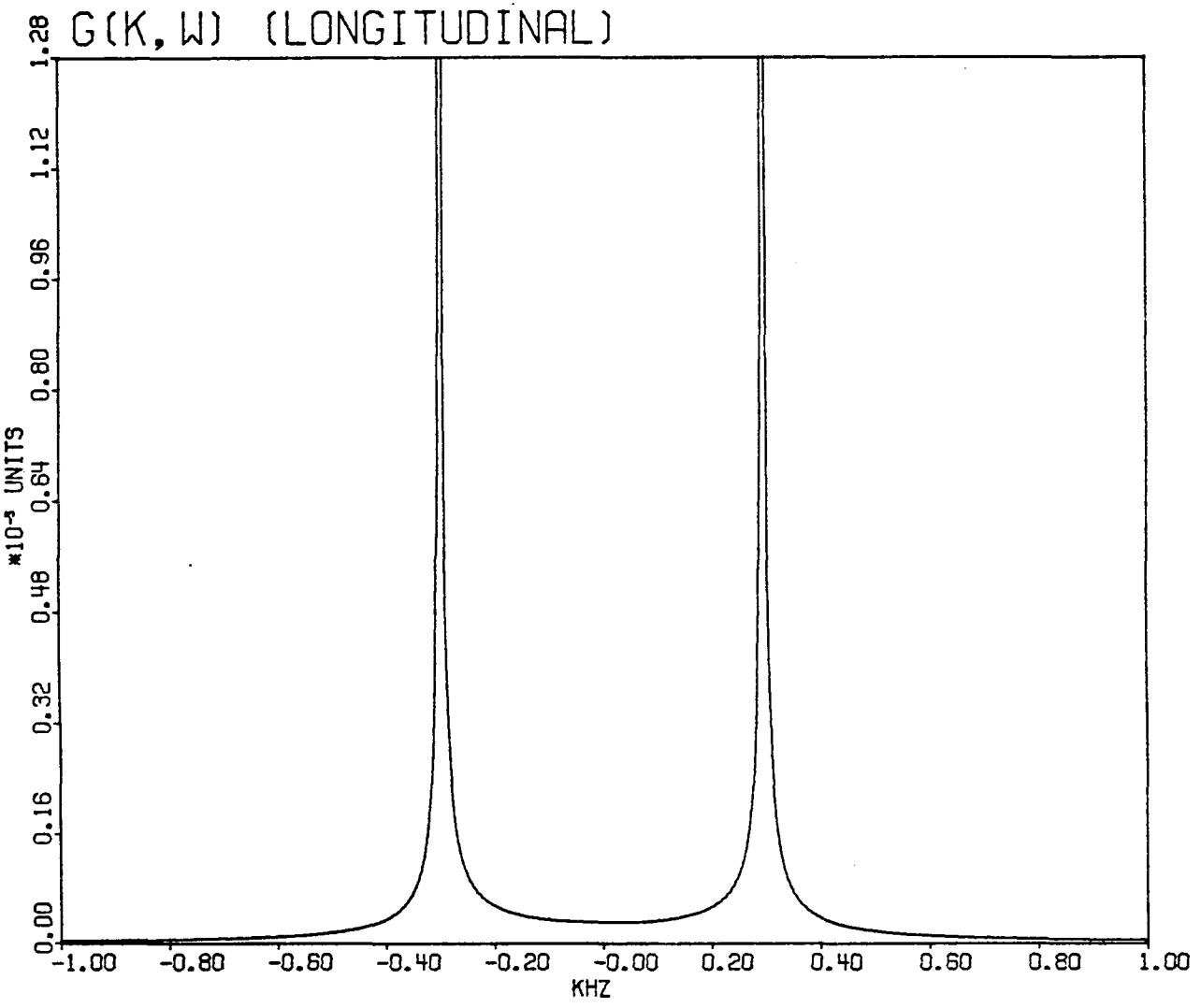

Figure 9c. The absolute value of the longitudinal component of the retarded response, $|G_L^{ec}(k;\omega)|$.

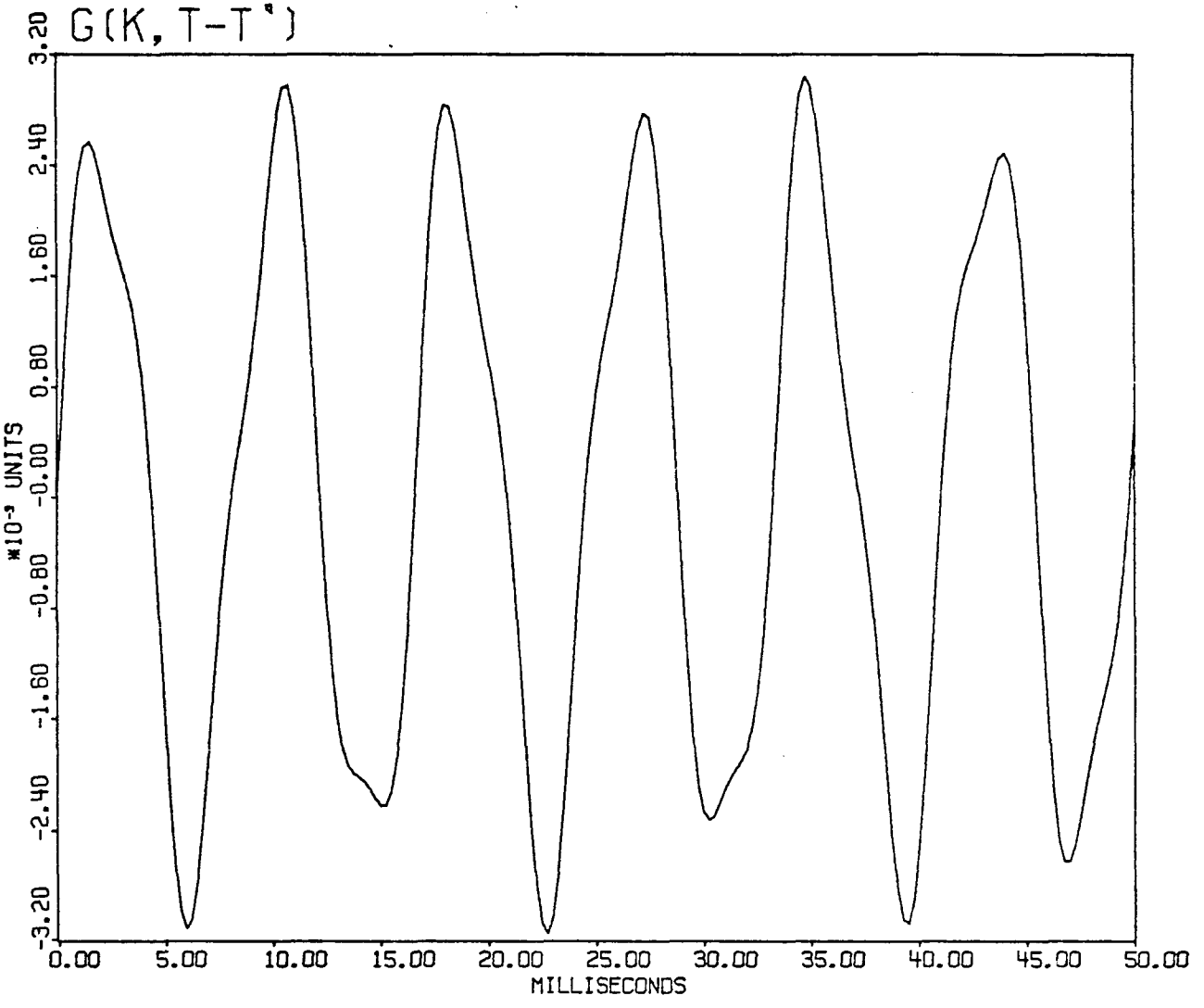

Figure 9d. The retarded response in the time domain, $G^{ec}_{jj}(k;t-t')$.

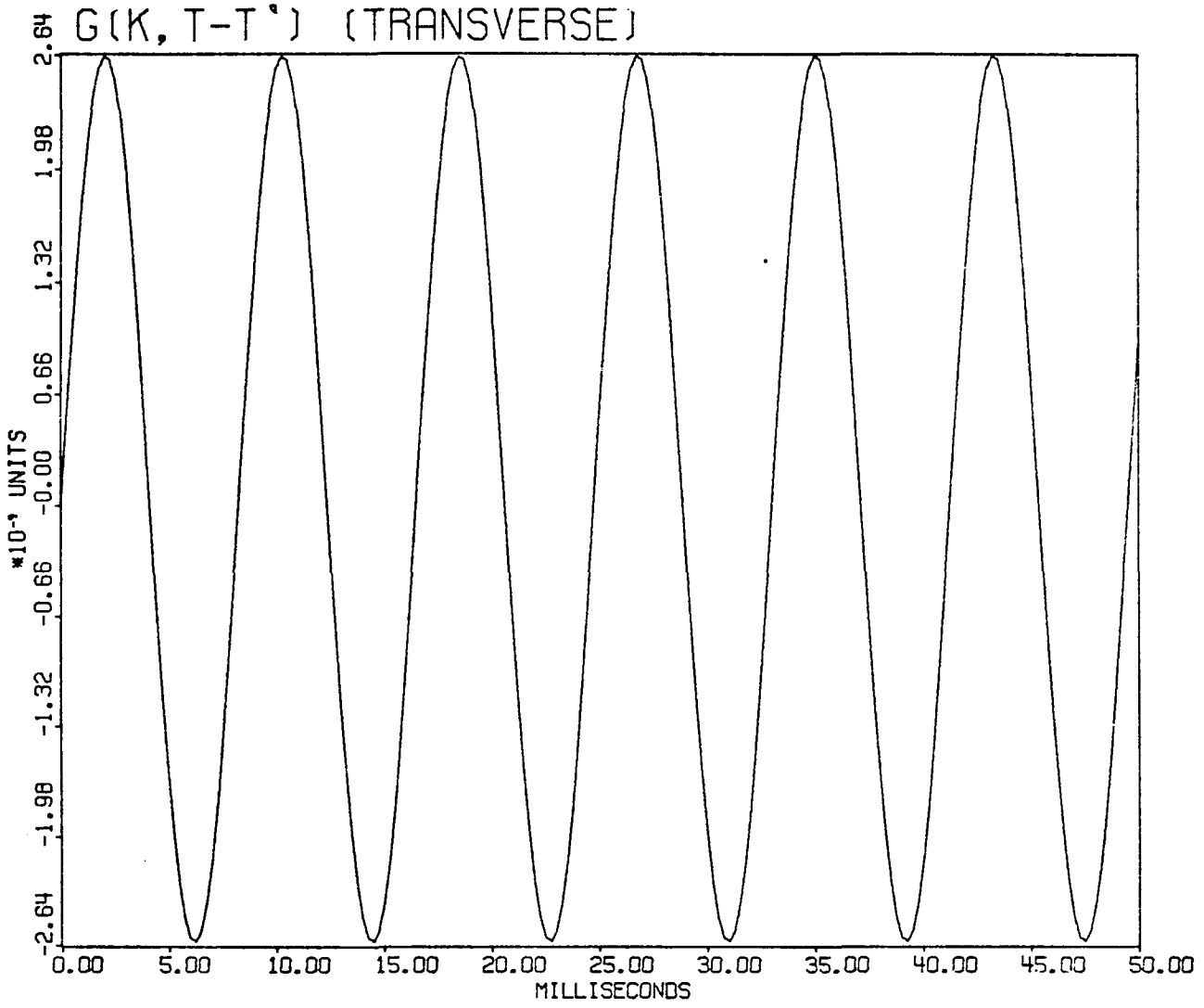

Figure 9e. The transverse component of the retarded response, $G_T^{ec}(k;t-t')$.

Plotted is $2\ G_T^{ec}(k;t-t')$.

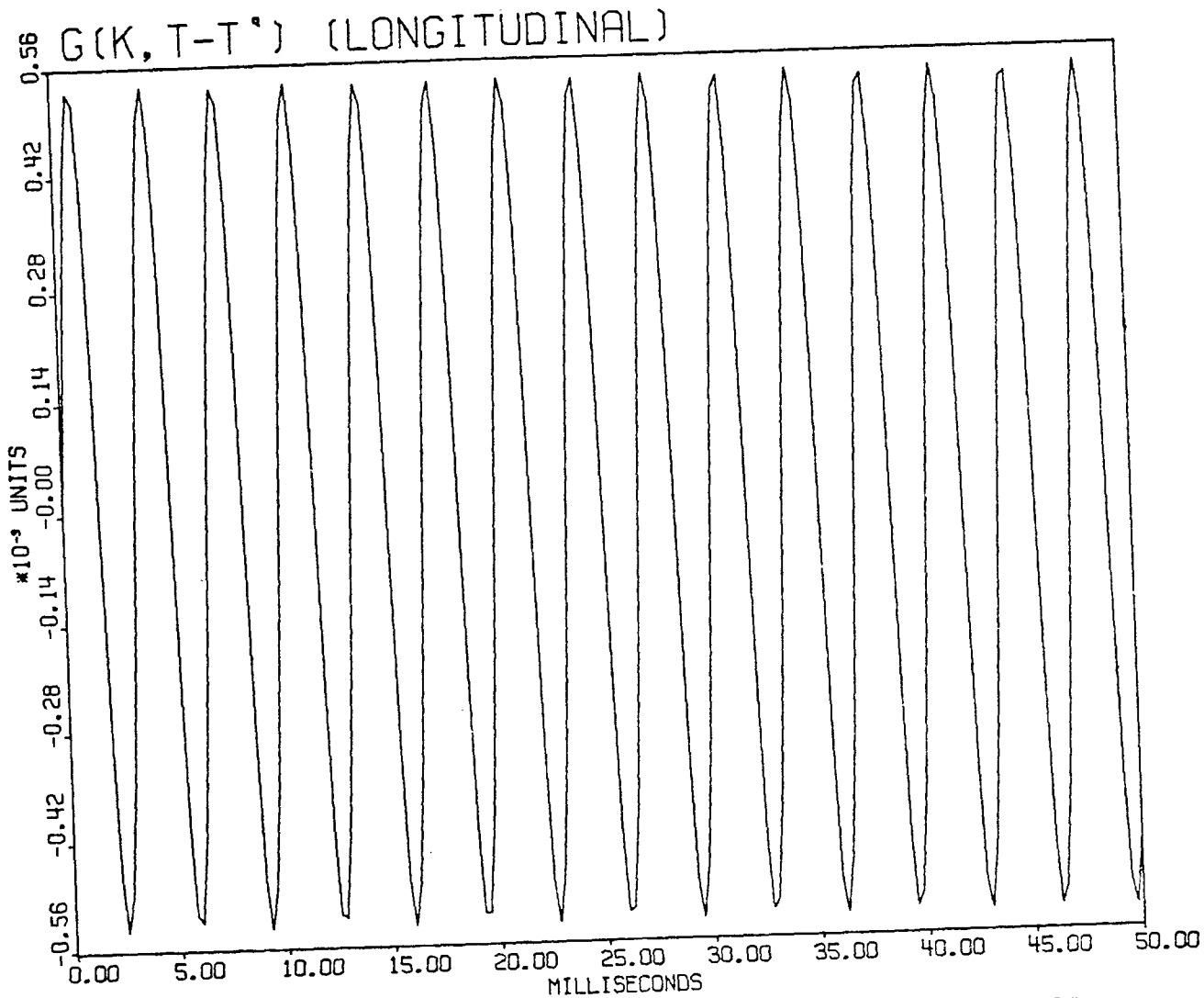

Figure 9f. The longitudinal component of the retarded response, $G_L^{ec}(k;t-t')$.

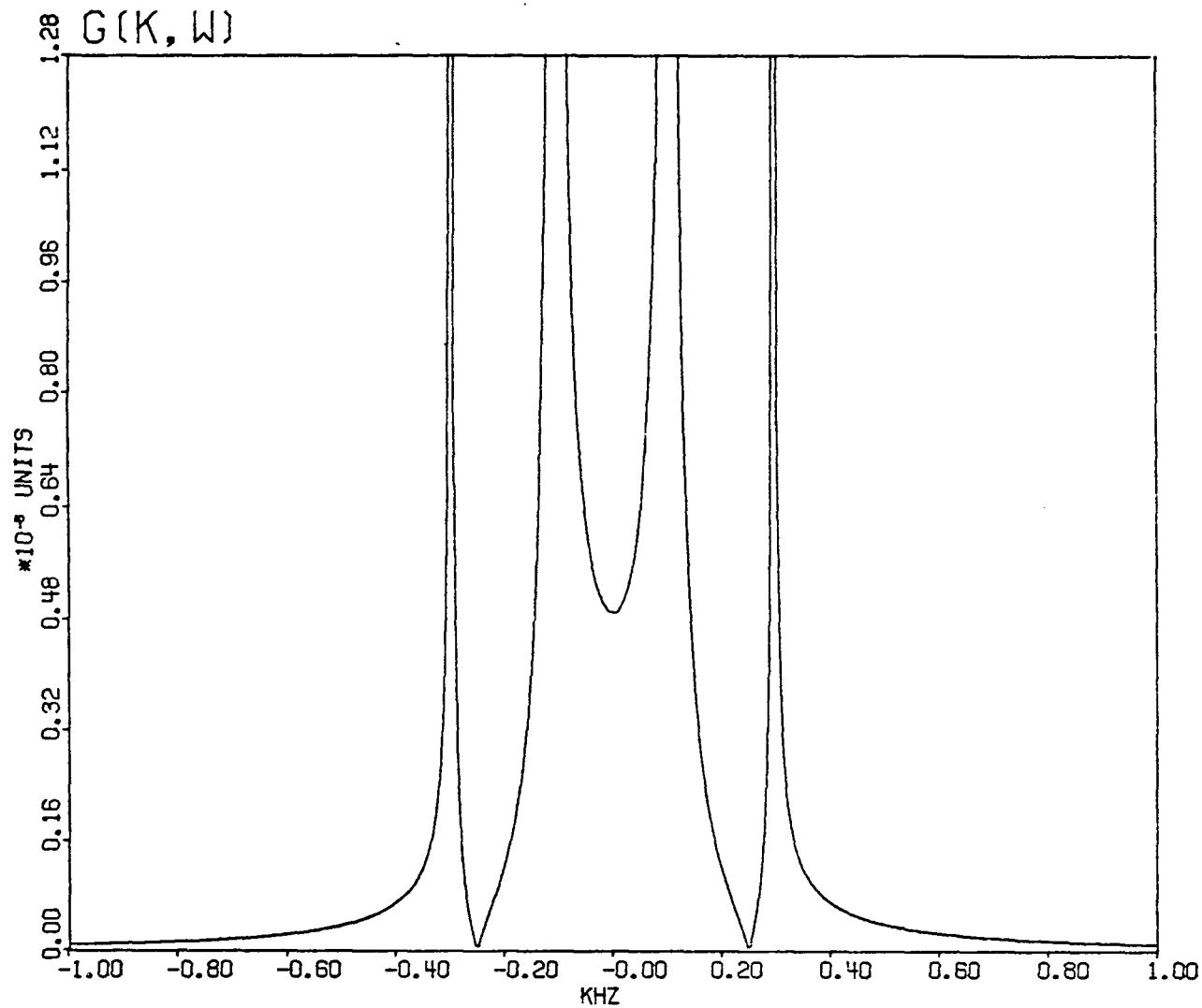

Figure 10a. The absolute value of the retarded response in the frequency domain, $|G^{e}_{jj}(k;\omega)|$.

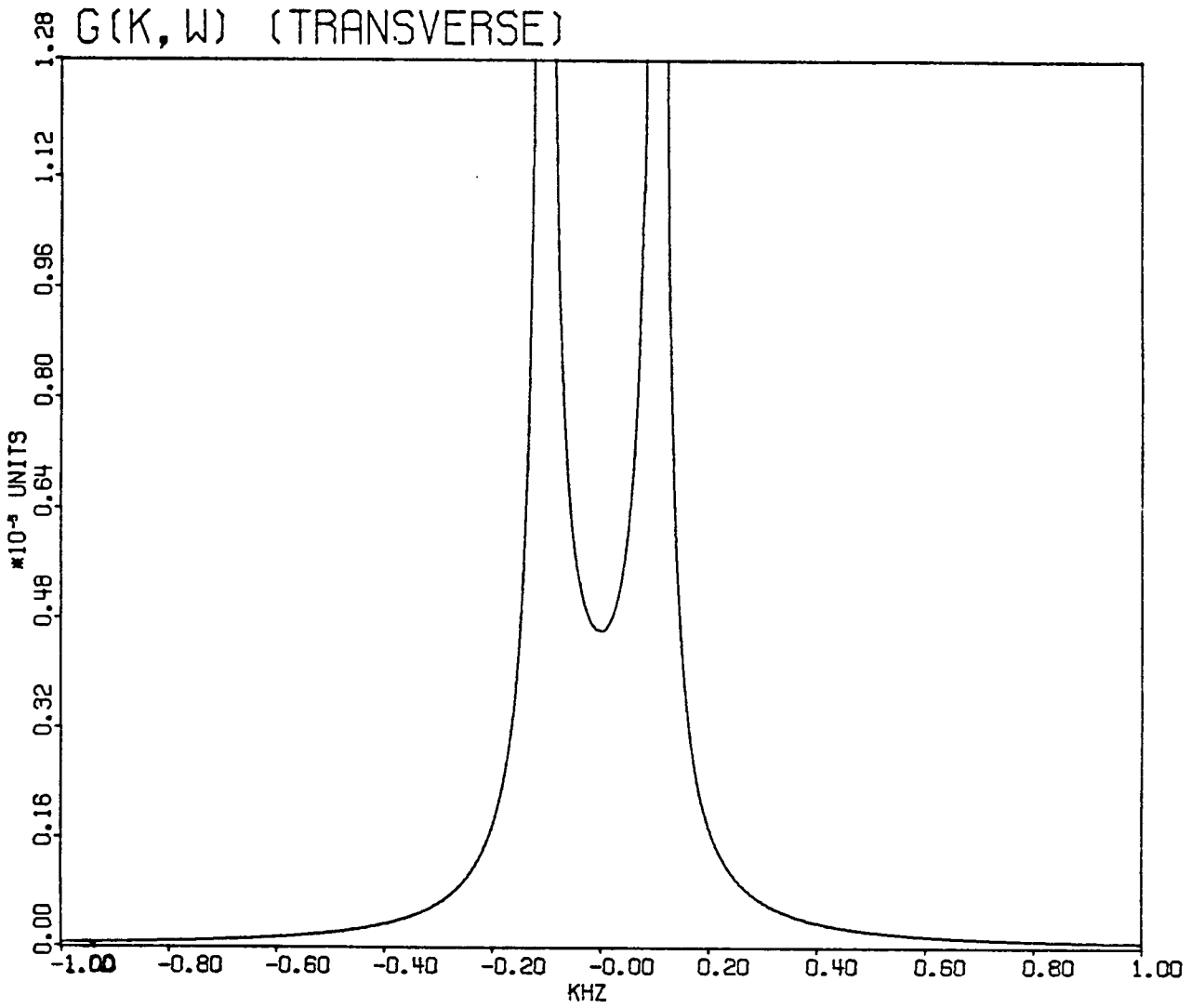

Figure 10b. The absolute value of the transverse component of the retarded response, $|G_T^e(k;\omega)|$. Plotted is $|2G_T^e(k;\omega)|$.

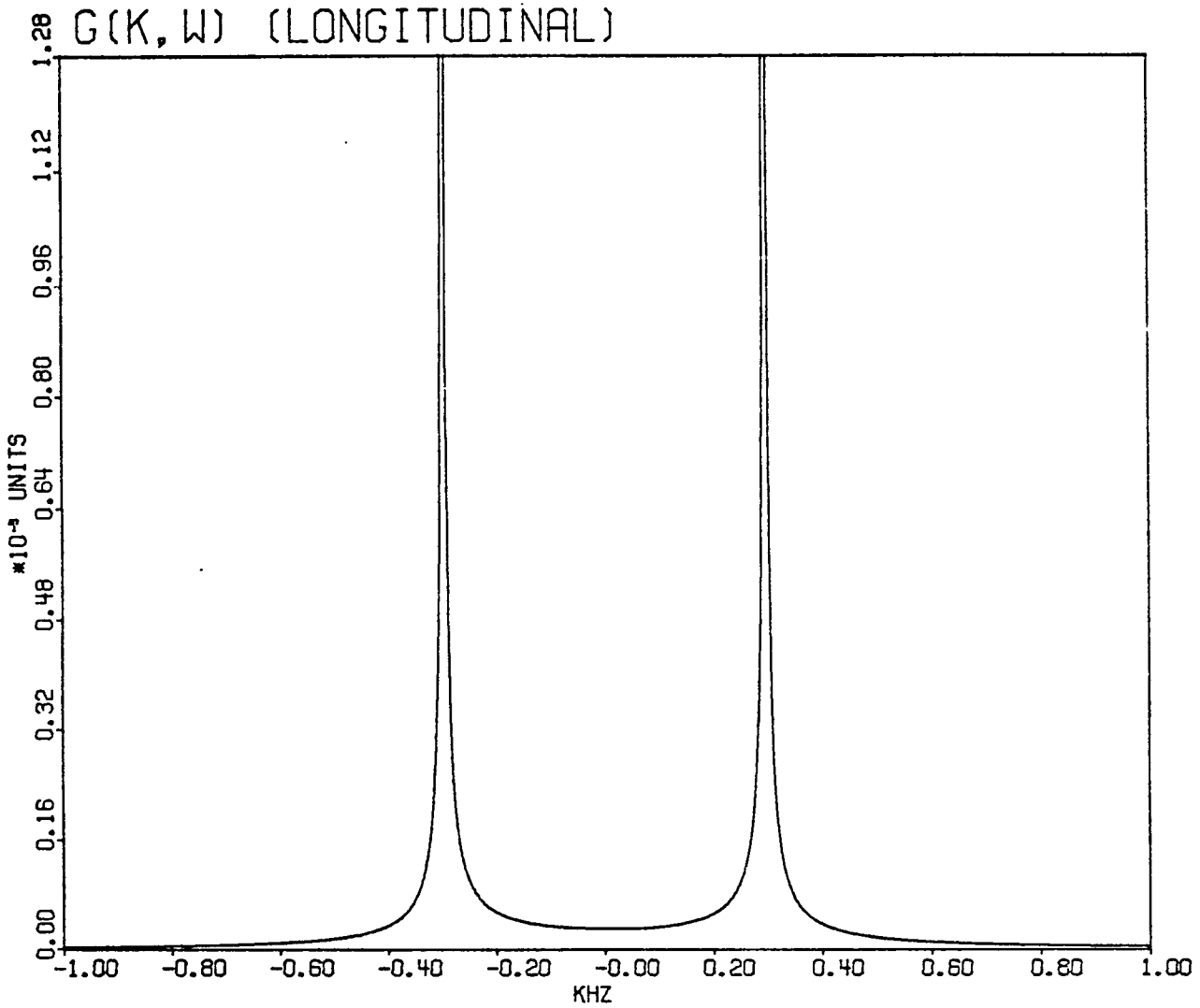

Figure 10c. The absolute value of the longitudinal component of the retarded response, $|G_L^e(k;\omega)|$.

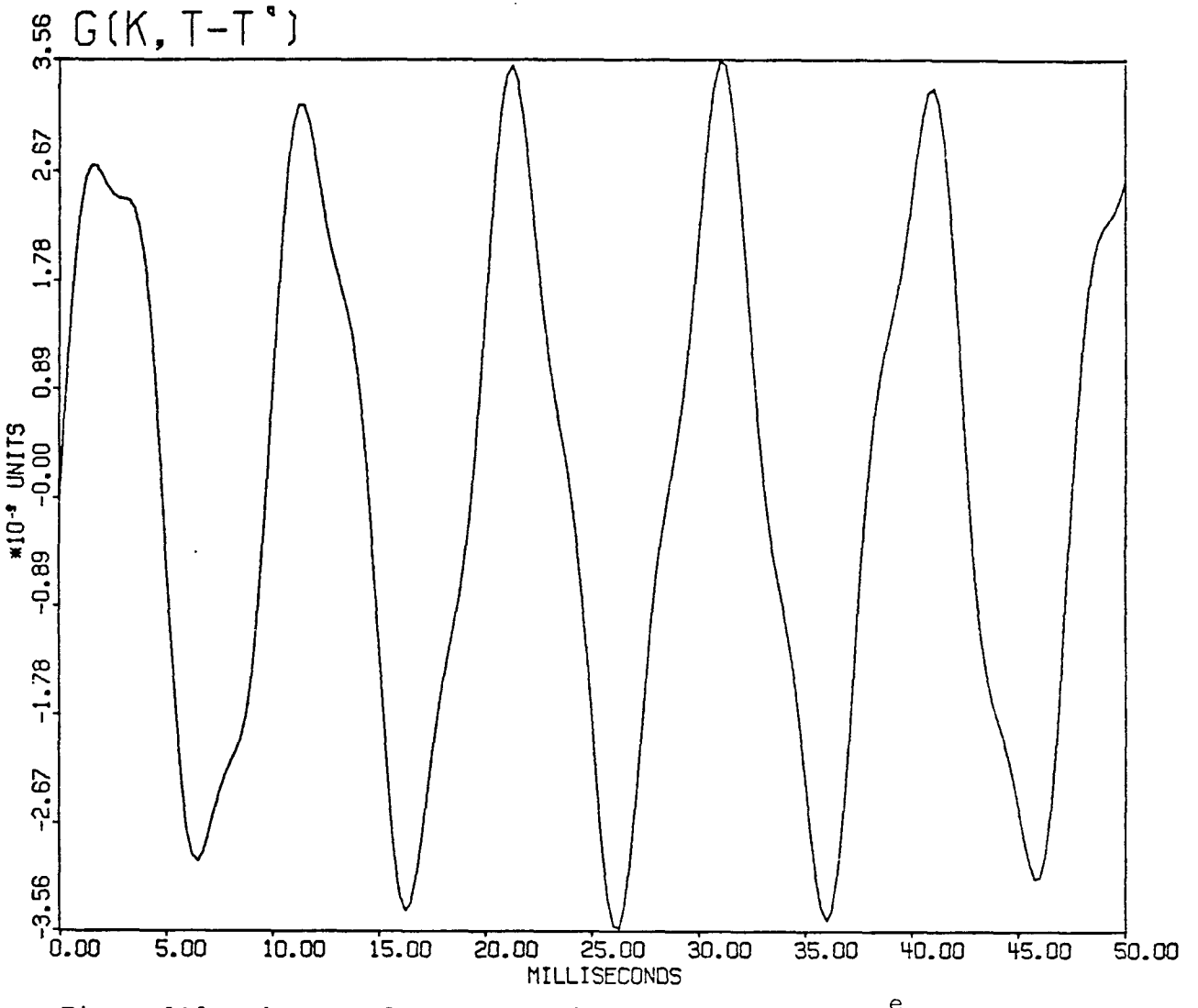

Figure 10d. The retarded response in the time domain, $G^{e}_{jj}(k;t-t')$.

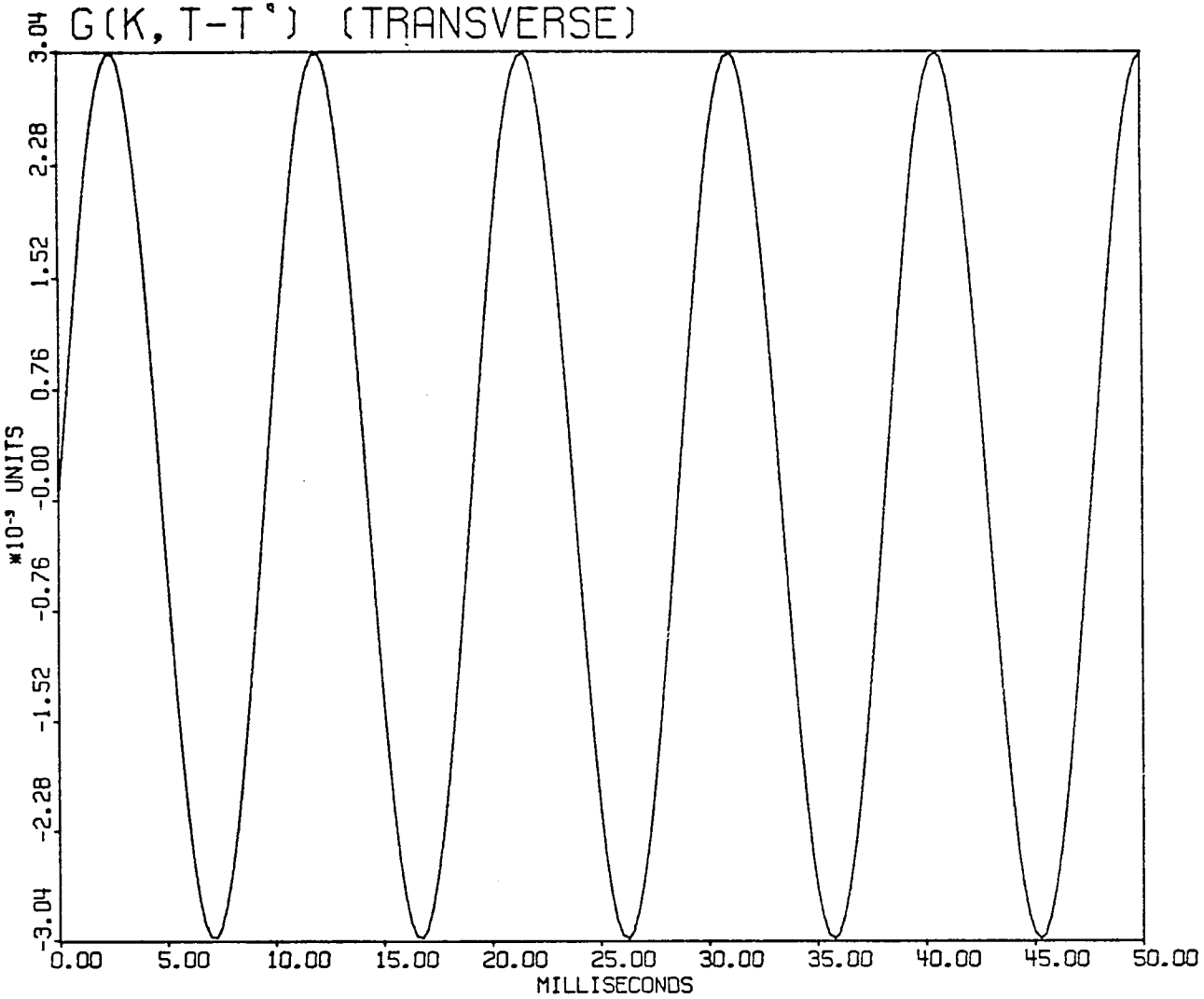

Figure 10e. The transverse component of the retarded response, $G_T^e(k;t-t')$.

Plotted is $2\ G_T^e(k;t-t')$.

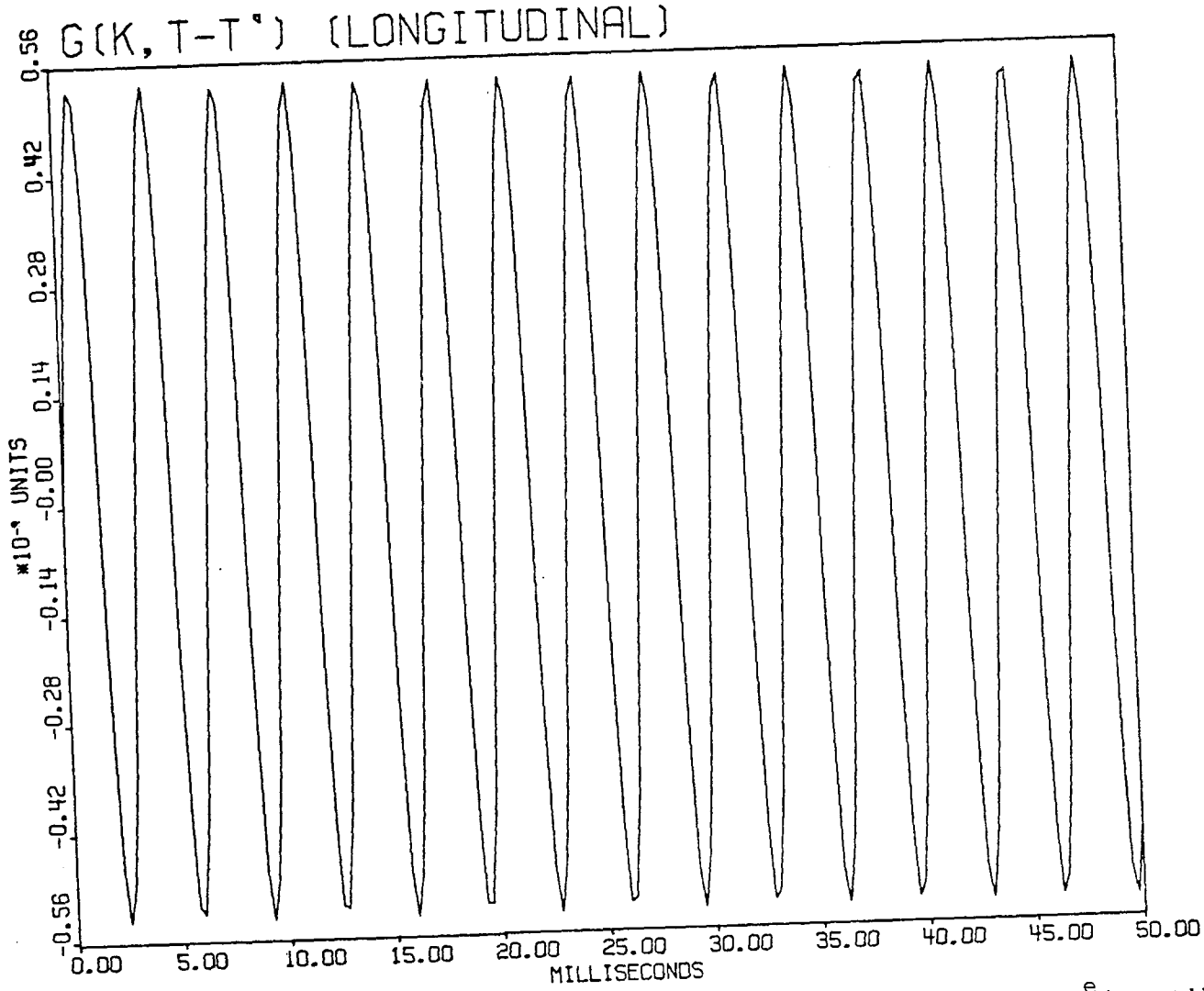

Figure 10f. The longitudinal component of the retarded response, $G_L^e(k;t-t')$.

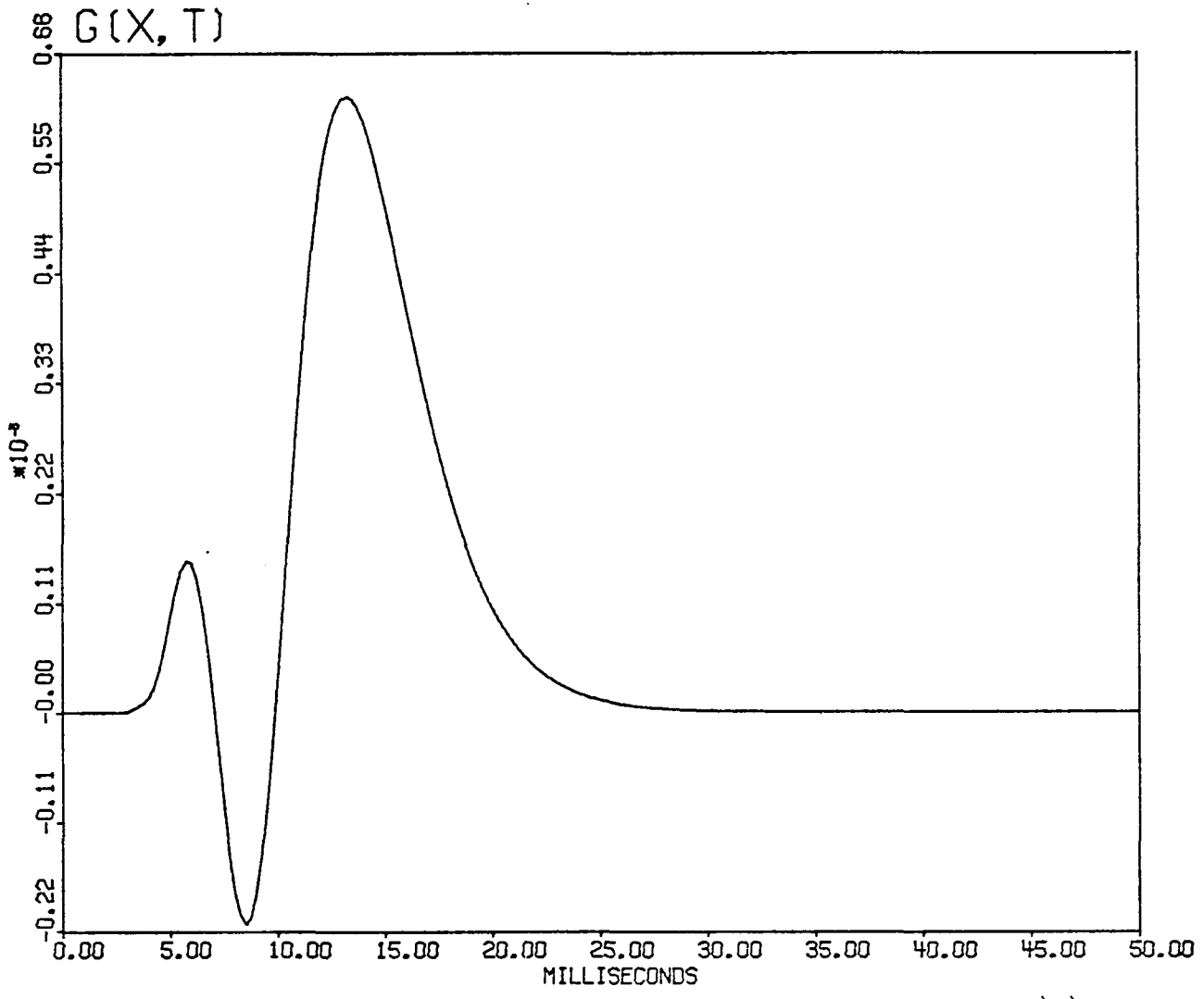

Figure 11a. The retarded response in the space-time domain, $G_{jj}(\vec{x}-\vec{x}';t-t')$.

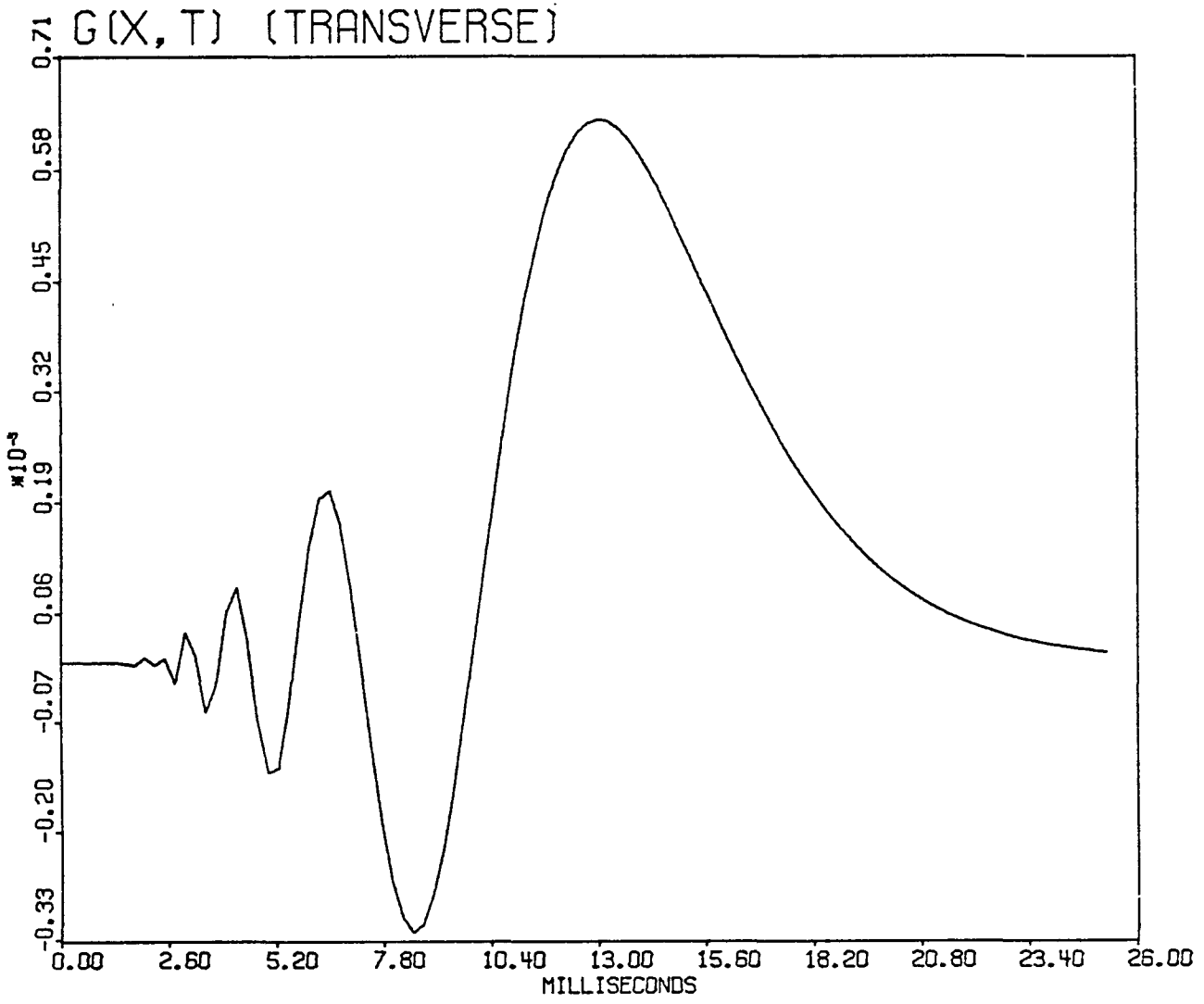

Figure 11b. The transverse component of the retarded response, $G_T(\vec{x}-\vec{x}';t-t')$.

Plotted is $2\ G_T(\vec{x}-\vec{x}';t-t')$.

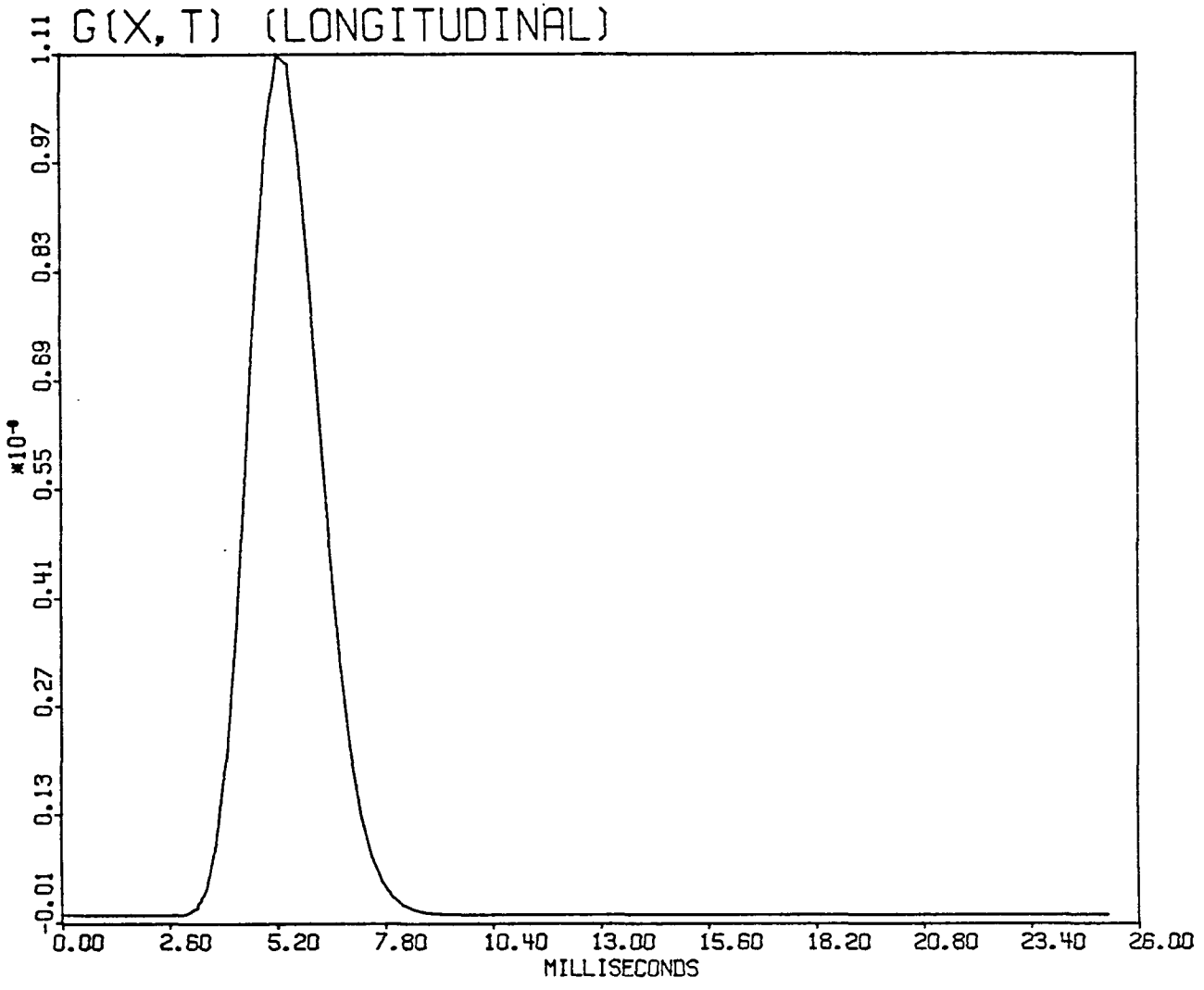

Figure 11c. The longitudinal component of the retarded response, $G_L(\vec{x}-\vec{x}';t-t')$.

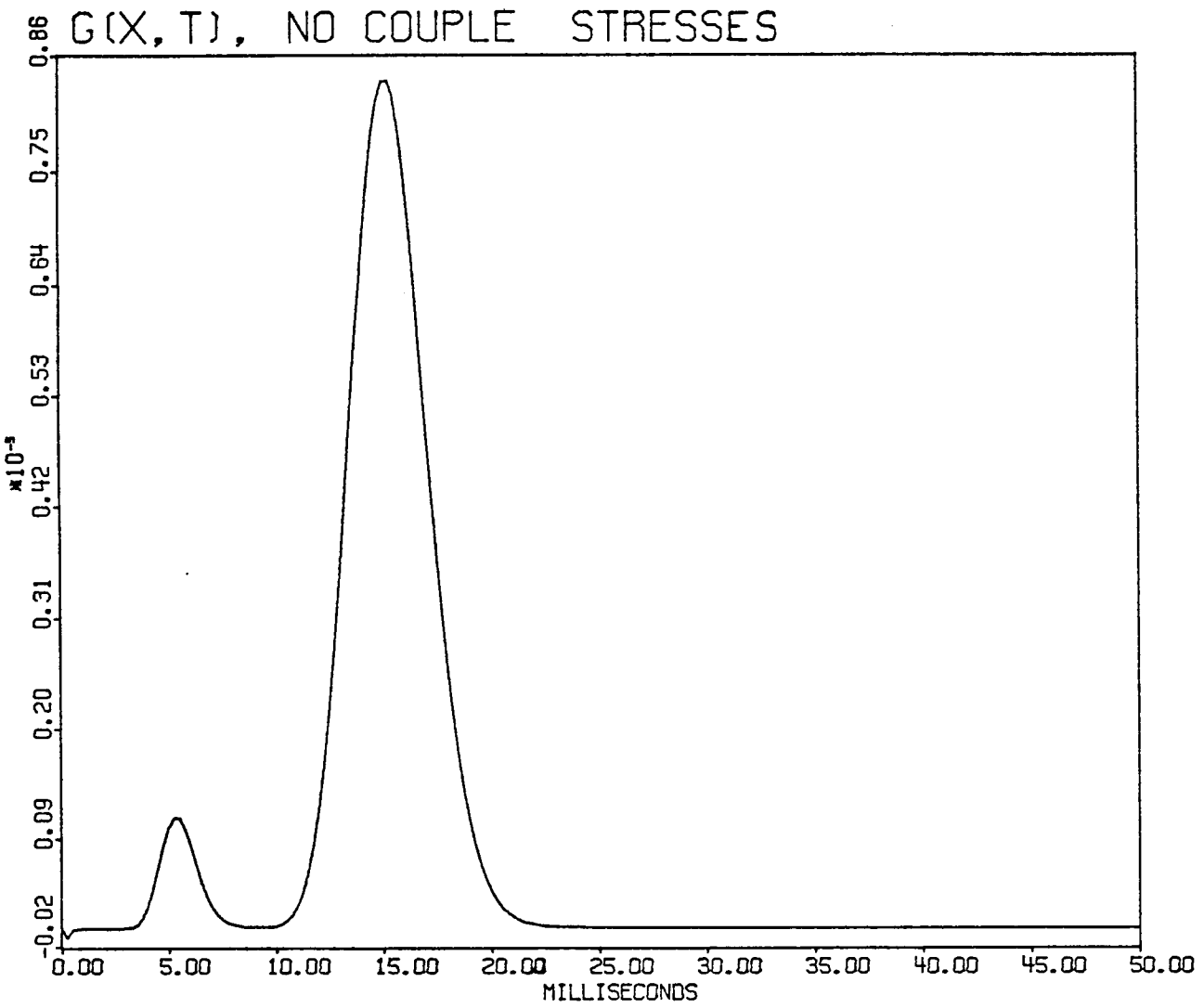

Figure 12a. The retarded response in the space-time domain, $G^{v}_{jj}(\vec{x}-\vec{x}';t-t')$.

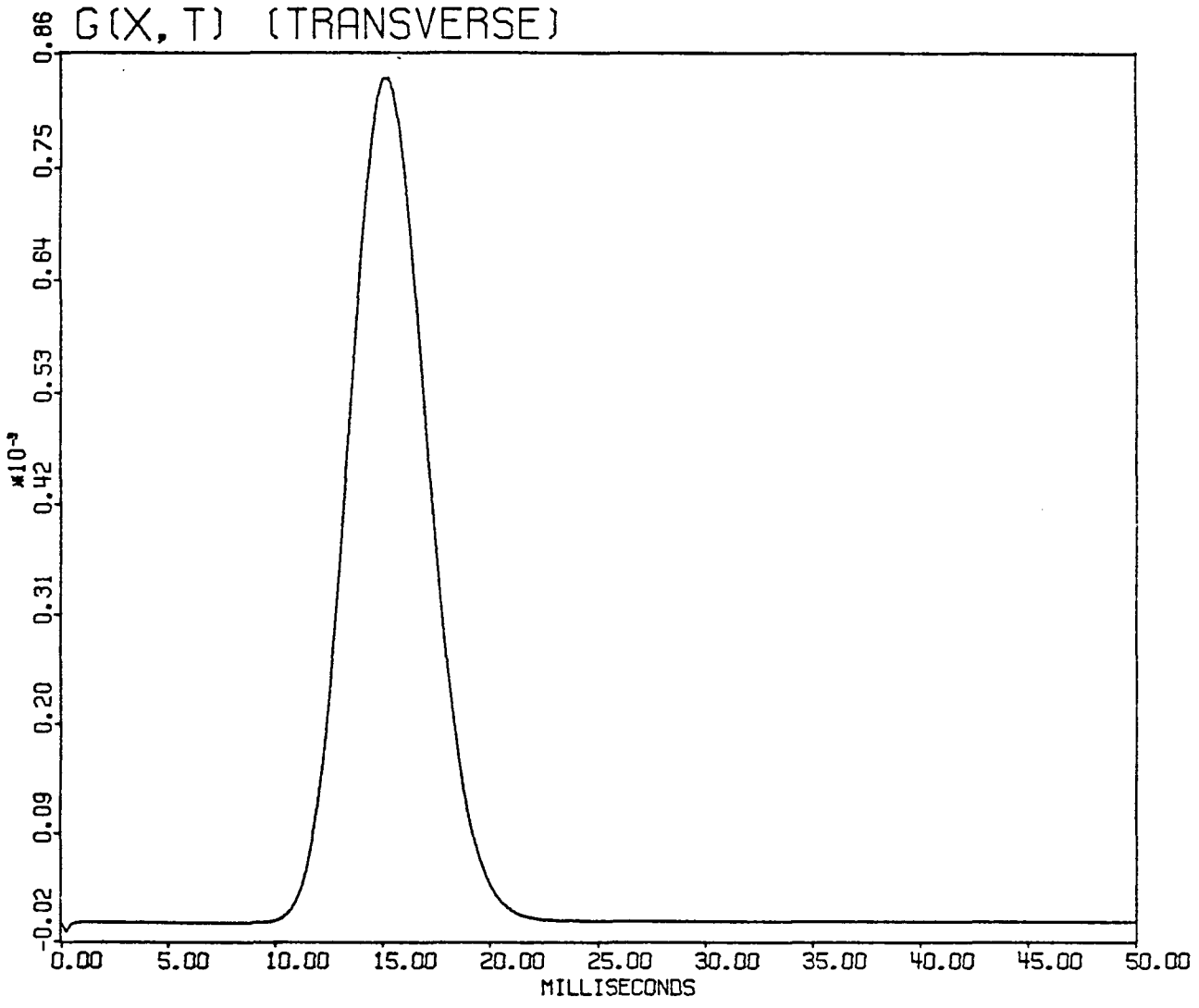

Figure 12b. The transverse component of the retarded response, $G_T^V(\vec{x}-\vec{x}';t-t')$.

Plotted is $2\ G_T^V(\vec{x}-\vec{x}';t-t')$.

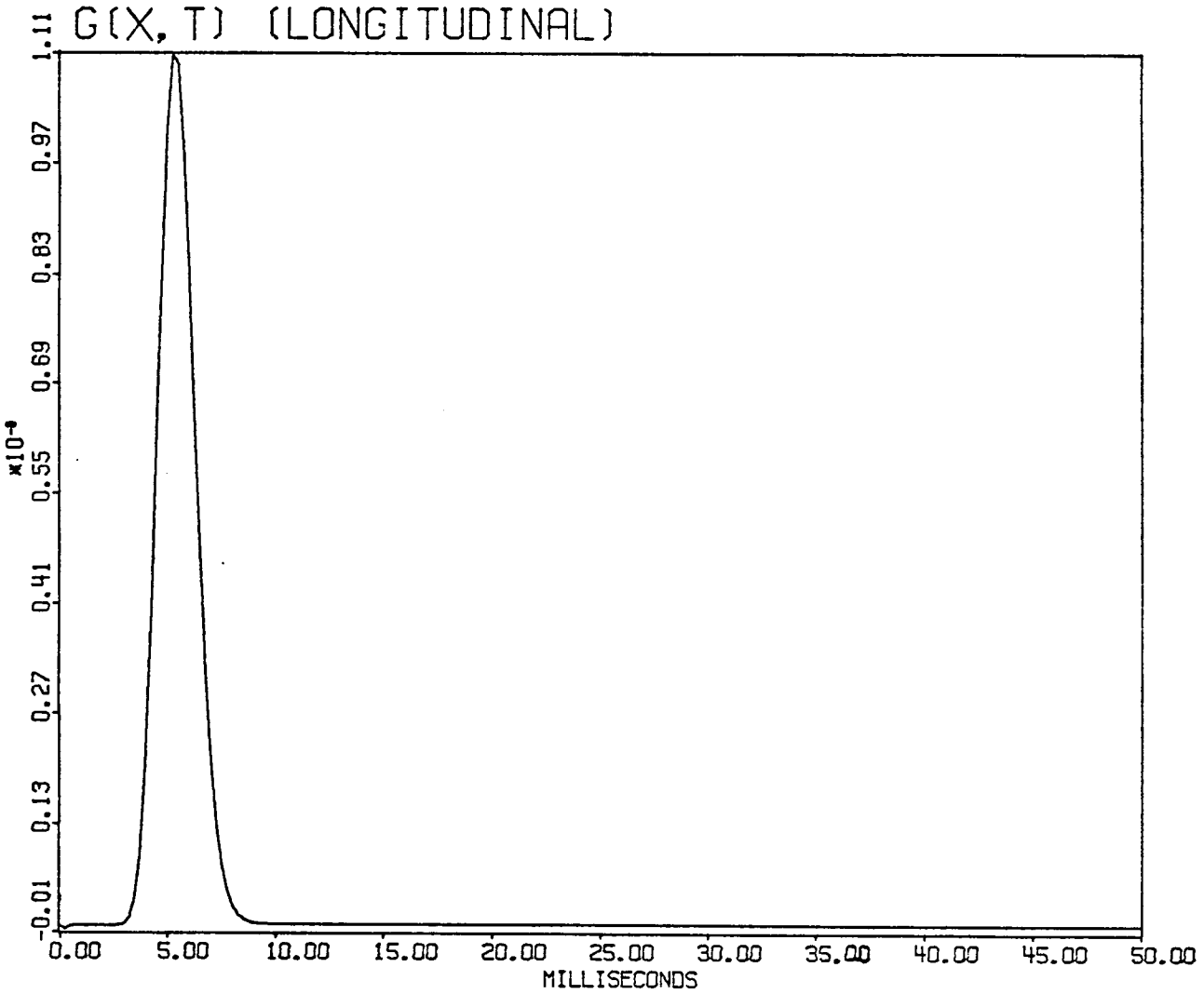

Figure 12c. The longitudinal component of the retarded response, $G_L^V(\vec{x}-\vec{x}';t-t')$.

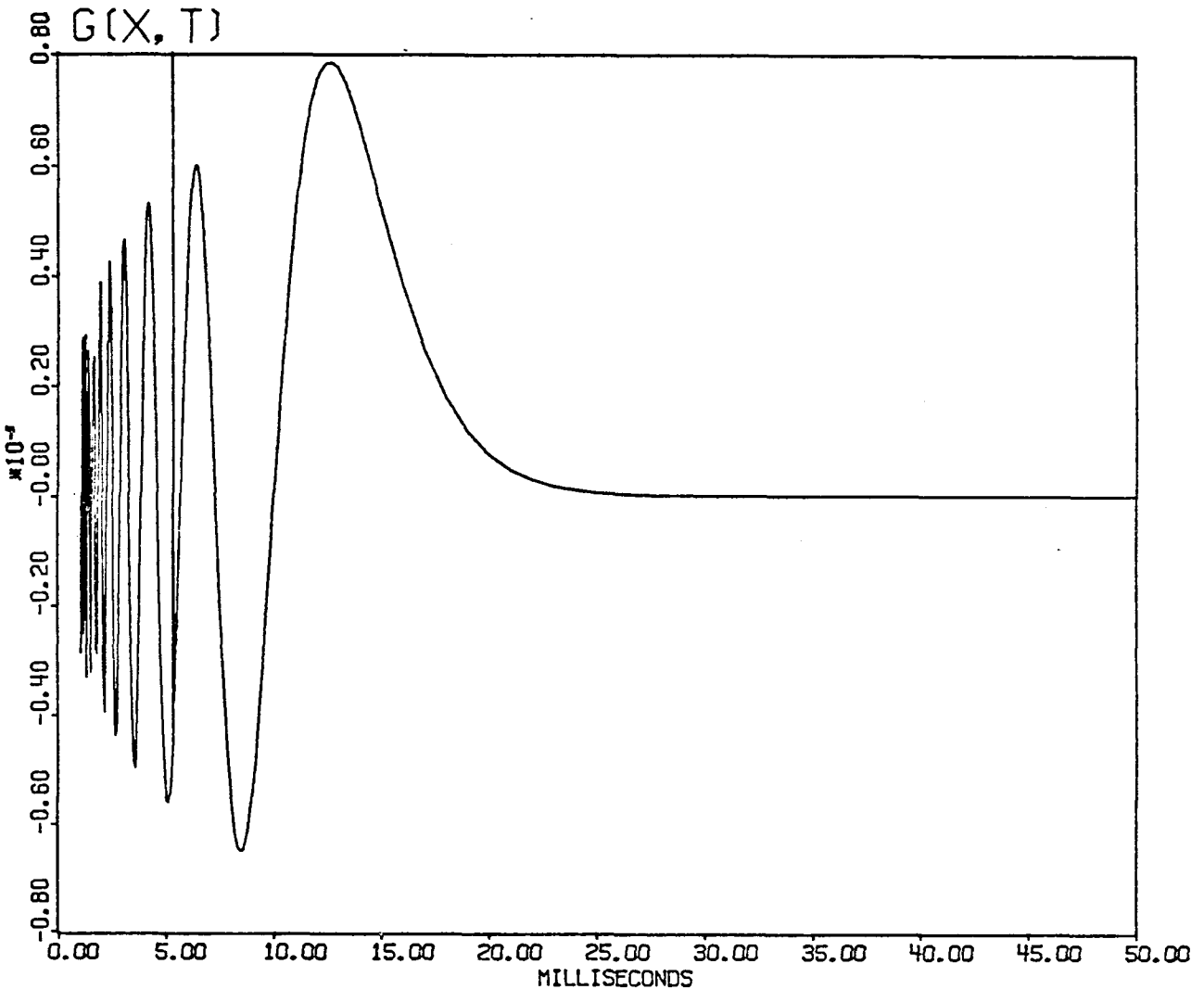

Figure 13a. The retarded response in the space-time domain, $G^{ec}_{jj}(\vec{x}-\vec{x}';t-t')$.

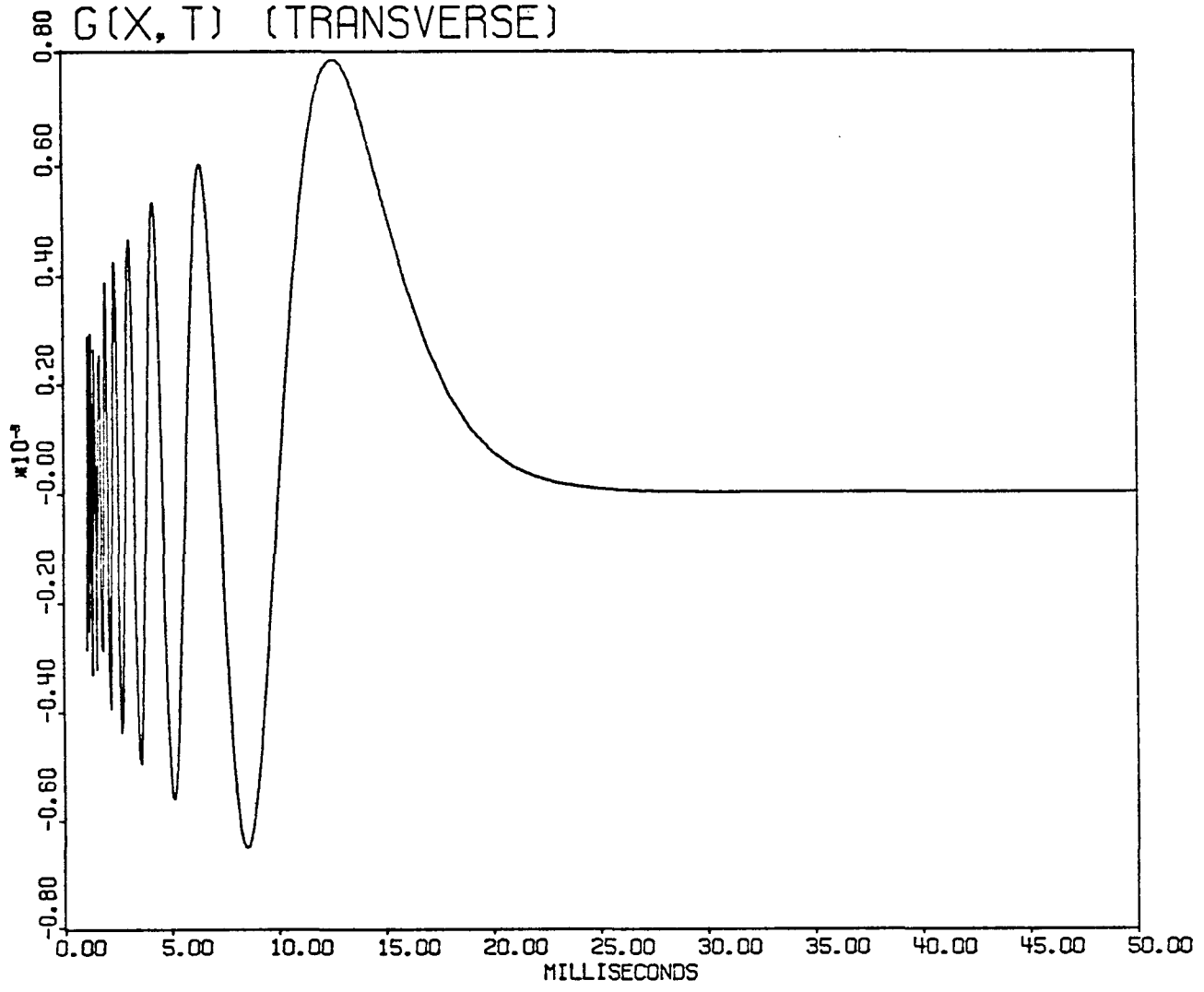

Figure 13b. The transverse component of the retarded response, $G_T^{ec}(\vec{x}-\vec{x}';t-t')$.

Plotted is $2\ G_T^{ec}(\vec{x}-\vec{x}';t-t')$.

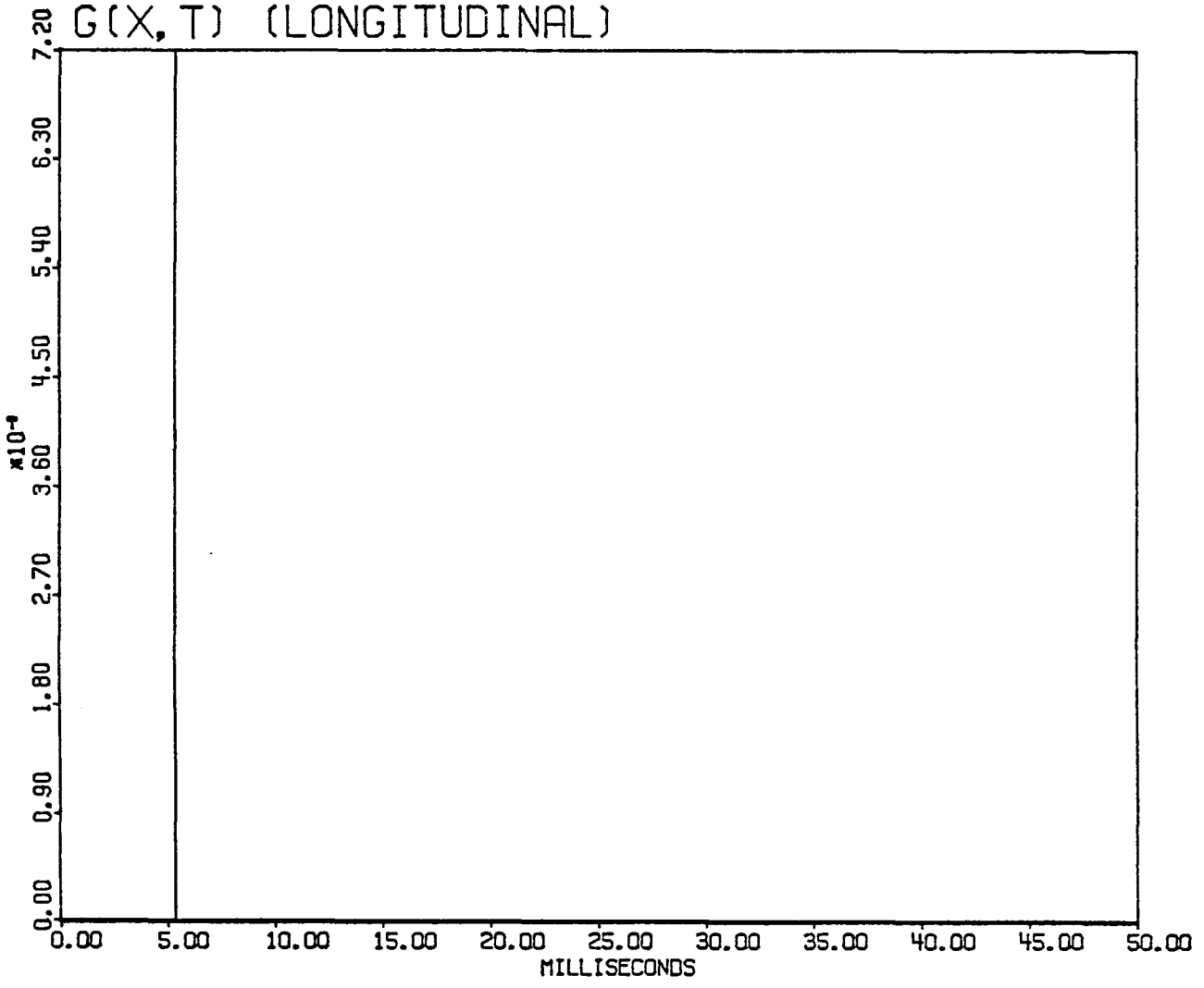

Figure 13c. The longitudinal component of the retarded response, $G_L^{ec}(\vec{x}-\vec{x}';t-t')$.

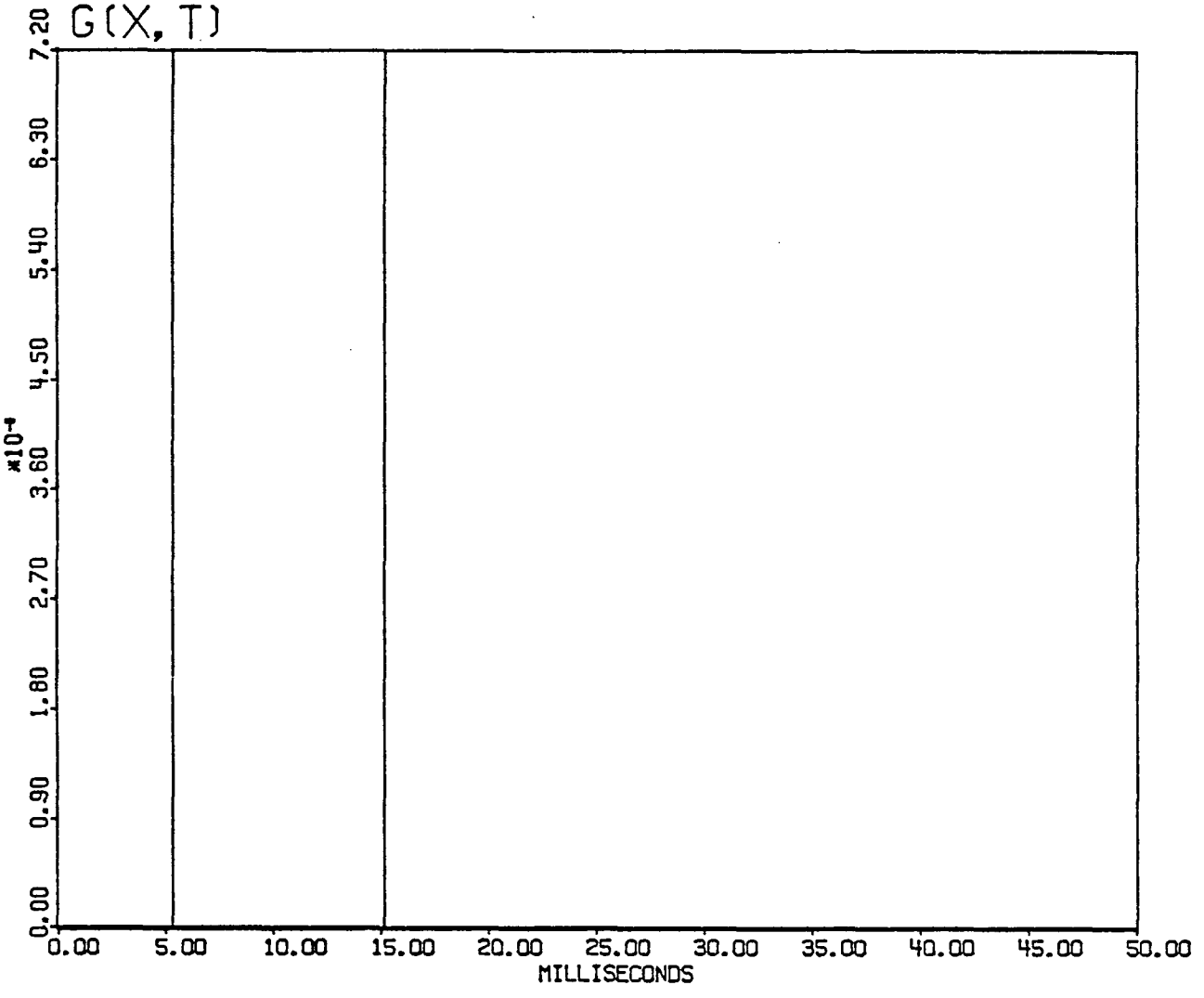

Figure 14a. The retarded response in the space-time domain, $G^{e}_{jj}(\vec{x}-\vec{x}';t-t')$.

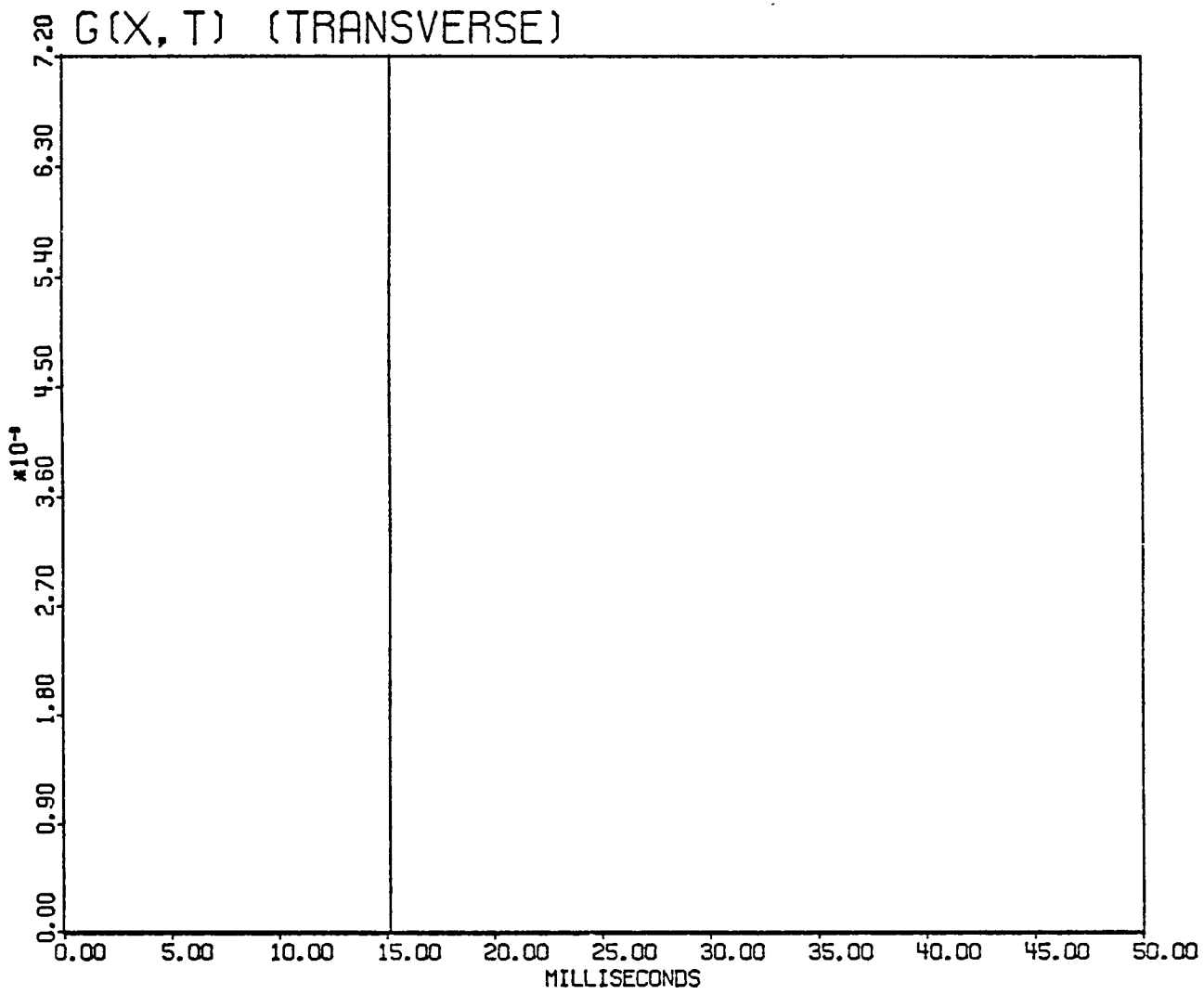

Figure 14b. The transverse component of the retarded response, $G_T^e(\vec{x}-\vec{x}';t-t')$.

Plotted is $2\ G_T^e(\vec{x}-\vec{x}';t-t')$.

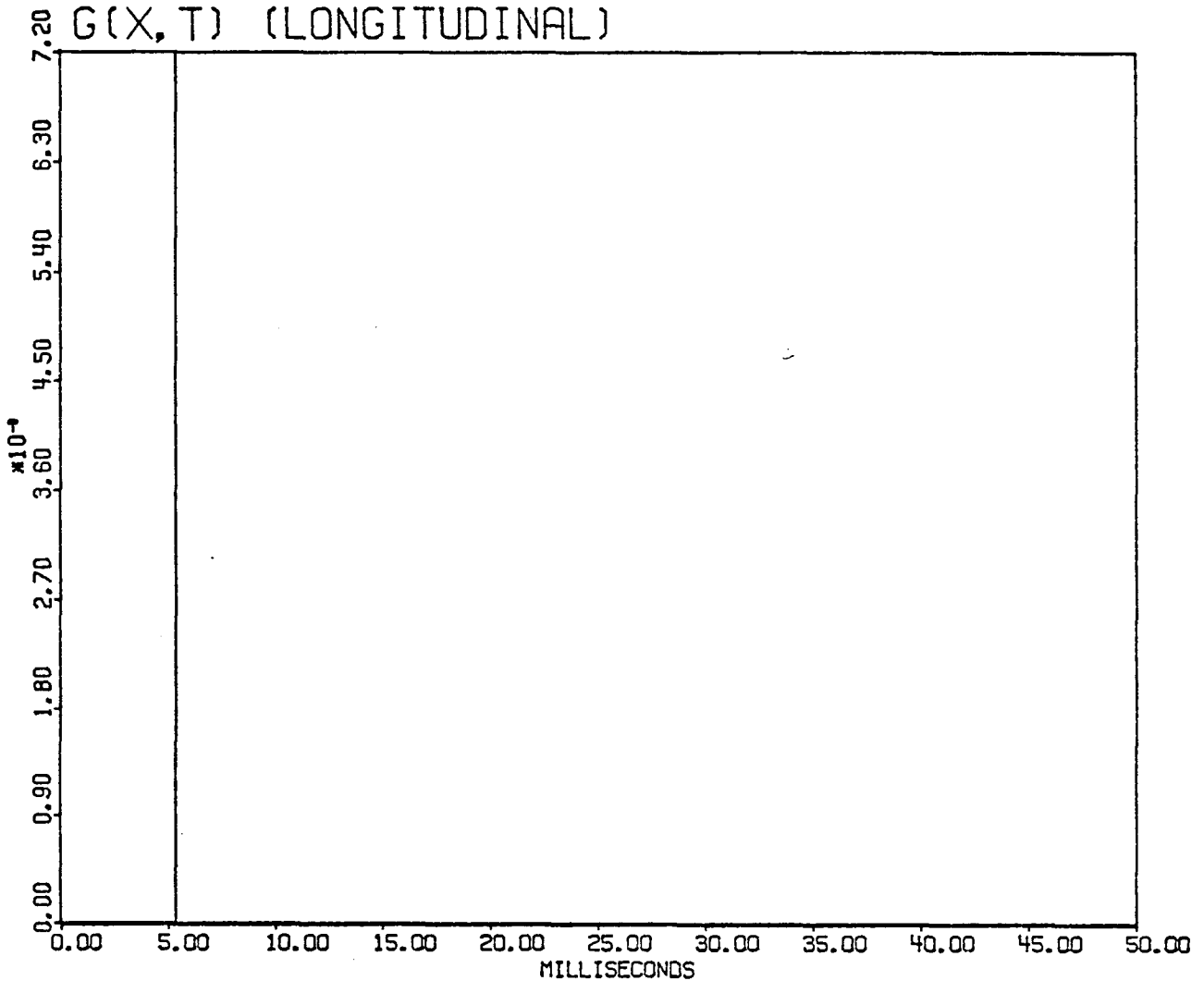

Figure 14c. The longitudinal component of the retarded response, $G_L^e(\vec{x}-\vec{x}';t-t')$.

PART II

THE REFLECTION OF ACOUSTIC WAVES

FROM A LIQUID-VISCOELASTIC MULTILAYERED MEDIUM

CHAPTER IX

GREEN'S FUNCTION REPRESENTATION FOR THE ACOUSTIC RESPONSE IN THE LIQUID MEDIUM

The acoustic response due to a point source in a liquid medium overlying a multilayered liquid-viscoelastic medium, which correspond to the ocean and its subbottom, respectively, is to be determined. The point source has varying strength and is located as shown in Figure 15. The response can be characterized by a displacement potential ϕ_0, from which the vector displacement $\vec{u}_0$ is given by $\vec{u}_0 = \nabla\phi_0$, where ∇ is the gradient operator. The potential ϕ_0 satisfies the scalar wave equation

$$(\nabla^2 - \frac{1}{c_0^2}\frac{\partial^2}{\partial t^2})\phi_0(\vec{x},\vec{x}';t) = -\delta(\vec{x}-\vec{x}')h(t) \quad , \tag{9.1}$$

where ∇^2 is the Laplacian operator, c_0 is the adiabatic sound velocity, $h(t)$ is the time dependence of the source strength, $\vec{x}$ is the field point, and $\vec{x}'$ is the source point.

One may define the Green's function for equation (9.1) as

$$(\nabla^2 - \frac{1}{c_0^2}\frac{\partial^2}{\partial t^2})g(\vec{x},\vec{x}';t,t') = -\delta(\vec{x}-\vec{x}')\delta(t-t') \quad . \tag{9.2}$$

Equation (9.2) implies that the Green's function $g(\vec{x},\vec{x};t,t')$ represents the response at $\vec{x},t$ arising from an impulsive point-source excitation applied at $\vec{x} = \vec{x}'$, $t = t'$. Introducing the temporal Fourier transform

pair

$$G(\omega) = \int_{-\infty}^{\infty} g(t)e^{-i\omega t}dt \tag{9.3a}$$

$$g(t) = \frac{1}{2\pi}\int_{-\infty}^{\infty} G(\omega)e^{i\omega t}d\omega \ , \tag{9.3b}$$

according to which time differentiation in the transform domain corresponds to $\partial/\partial t \equiv i\omega$, and transforming equations (9.1) and (9.2), one obtains

$$(\nabla^2+k_0^2)\Phi_0(\vec{x},\vec{x}';\omega) = -\delta(\vec{x}-\vec{x}')H(\omega) \tag{9.4a}$$

and

$$(\nabla^2+k_0^2)G(\vec{x},\vec{x}';\omega) = -\delta(\vec{x}-\vec{x}') \ , \tag{9.4b}$$

where Φ_0,H, and G are the transforms of ϕ_0,h, and g , respectively. The wavenumber k_0 is defined by $k_0 = \omega/c_0$. Combining equations (9.4a) and (9.4b), the transformed potential Φ_0 may be expressed as

$$\Phi_0(\vec{x},\vec{x}';\omega) = G(\vec{x},\vec{x}';\omega)H(\omega) \ . \tag{9.5}$$

The time domain response for arbitrary $h(t)$ or $H(\omega)$ is obtained by taking the inverse transform of equation (9.5)

$$\phi_0(\vec{x},\vec{x}';t) = \frac{1}{2\pi}\int_{-\infty}^{\infty} G(\vec{x},\vec{x}';\omega)H(\omega)e^{i\omega t}dt \ . \tag{9.6}$$

It is observed that obtaining the response $\phi_0(\vec{x},\vec{x};t)$ for any pulse shape $h(t)$ is dependent upon the determination of the Green's function $G(\vec{x},\vec{x}';\omega)$ which satisfies equation (9.4b) and the appropriate boundary

conditions for the liquid layer. The scope of this investigation does not include the explicit determination of $\phi_0(\vec{x},\vec{x};t)$, however. The primary objective is to construct an analytical expression for $G(\vec{x},\vec{x}';\omega)$.

In order to solve differential equation (9.4b), the following modal representation for the Green's function

$$G(\vec{x},\vec{x}';\omega) = \sum_j \Phi_j(\vec{\rho})\Phi_j(\vec{\rho}')G(\kappa_j,z,z';\omega) \tag{9.7}$$

shall be employed, where $\Phi_j(\vec{\rho})$ are the two-dimensional set of mode functions defined by the two-dimensional scalar eigenvalue problem

$$(\nabla_t^2+k_{tj}^2)\phi_j = 0 , \tag{9.7a}$$

and $G(\kappa_j,z,z';\omega)$ satisfies the differential equation

$$(\frac{d^2}{dz^2} + \kappa_j^2)G(\kappa_j,z,z';\omega) = -\delta(z-z') , \quad \kappa_j^2 = k_0^2 - k_{tj}^2 , \tag{9.7b}$$

subject to appropriate boundary conditions in the z domain. The subscript t in equations (9.7a) and (9.7b) denotes that the mode functions are for the coordinates transverse to the z-direction.

Since the configuration to be analyzed (see Figure 15) possesses a transversely unbounded cross section, the transverse eigenvalue problem is highly degenerate and many alternative choices of coordinate systems are possible for the modal representation of the unbounded cross section. The most useful for a point-source excitation are the circular cylindrical and rectangular, respectively, since they account in the most direct manner for the symmetry properties of the associated field. For the rectangular and circular waveguide descriptions of the unbounded cross

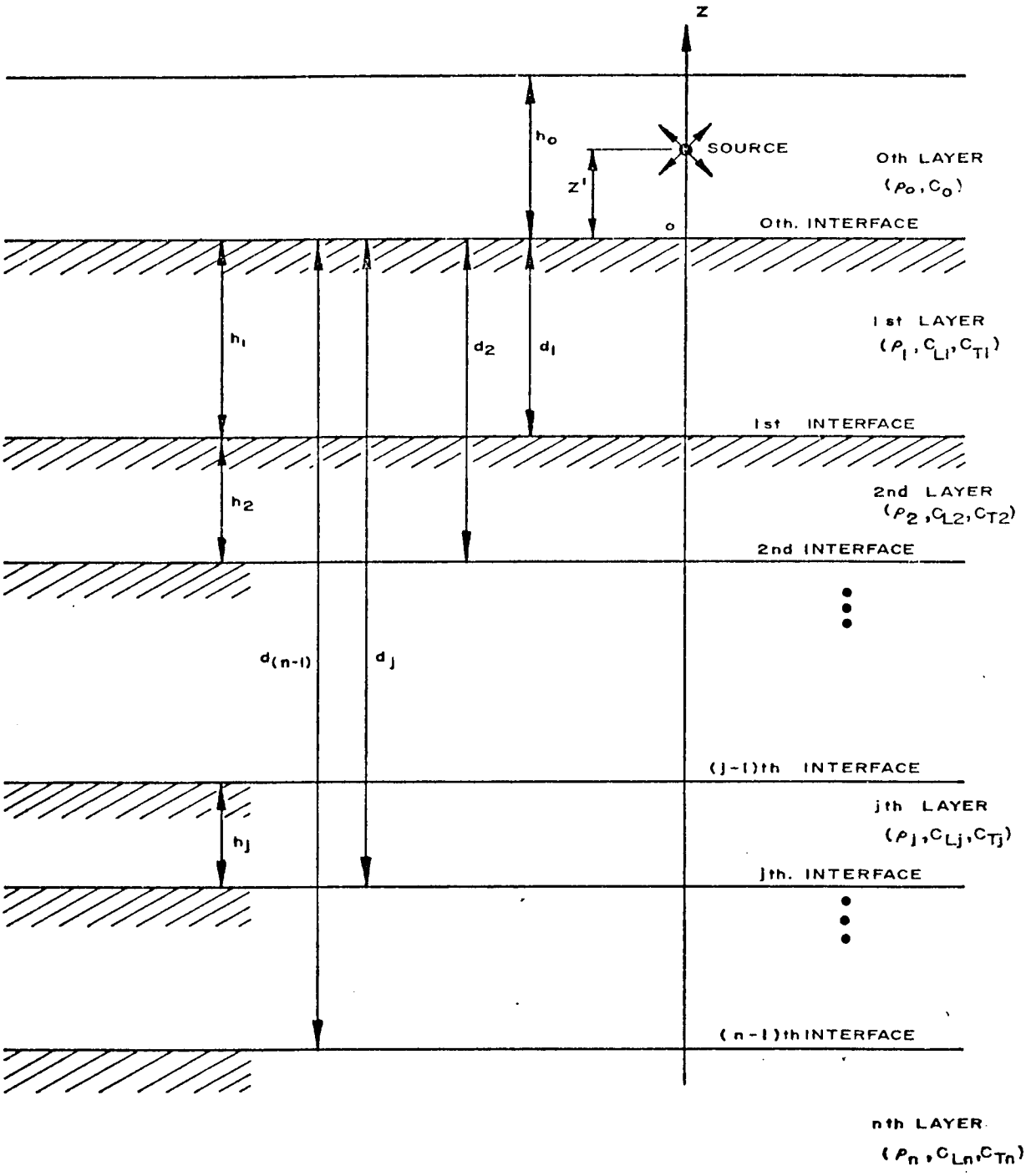

Figure 15. Geometry of the liquid layer and the multilayered subbottom.

section, one has (M. Yildiz, 1975):

Rectangular Waveguide Representation

$$\Phi_j(\vec{\rho}) = \frac{1}{2\pi} e^{-i(\xi x+\eta y)} , \quad -\infty < \xi < \infty , \quad -\infty < \eta < \infty$$

$$\nabla_t^2 = \frac{\partial^2}{\partial x^2} + \frac{\partial^2}{\partial y^2} , \quad k_{ti}^2 = \xi^2 + \eta^2 , \quad \kappa_j^2 = k_0^2 - \xi^2 - \eta^2$$

$$\delta(\vec{\rho}-\vec{\rho}') = \delta(x-x')\delta(y-y')$$

$$= \sum_j \Phi_j(\vec{\rho})\Phi_j(\vec{\rho}')$$

$$= \frac{1}{4\pi^2} \int_{-\infty}^{\infty} d\xi \int_{-\infty}^{\infty} e^{-i(\xi x+\eta y)} e^{i(\xi x'+\eta y')} d\eta$$

$$G(\vec{x},\vec{x}';\omega) = \frac{1}{4\pi^2} \int_{-\infty}^{\infty} \int_{-\infty}^{\infty} e^{-i\xi(x-x')-i\eta(y-y')} G(\kappa_j,z,z';\omega) d\xi d\eta \qquad (9.8a)$$

Circular Waveguide Representation

$$\Phi_j(\vec{\rho}) = \left(\frac{\xi}{2\pi}\right)^{1/2} e^{-im\phi} J_m(\xi\rho) \ , \qquad m = 0, \pm 1, \pm 2, \cdots \ , \qquad 0 < \xi < \infty$$

$$\nabla_t^2 = \frac{1}{\rho}\frac{\partial}{\partial\rho}\left(\rho\,\frac{\partial}{\partial\rho}\right) + \frac{1}{\rho^2}\frac{\partial^2}{\partial\phi^2} \ , \qquad k_{ti}^2 = \xi^2 \ , \qquad \kappa_j^2 = k_0^2 - \xi^2$$

$$\delta(\vec{\rho}-\vec{\rho}') = \frac{\delta(\rho-\rho')\delta(\phi-\phi')}{\rho'}$$

$$= \sum_j \Phi_j(\vec{\rho})\Phi_j(\vec{\rho}')$$

$$= \frac{1}{2\pi}\sum_{m=-\infty}^{\infty}\int_0^{\infty} \xi e^{-im\phi} J_m(\xi\rho) e^{-im\phi'} J_m(\xi\rho')\,d\xi$$

$$G(\vec{x},\vec{x}';\omega) = \frac{1}{2\pi}\sum_{m=-\infty}^{\infty} e^{-im(\phi-\phi')}\int_0^{\infty} \xi J_m(\xi\rho) J_m(\xi\rho') G(\kappa_j,z,z';\omega)\,d\xi \ .$$

(9.8b)

For each of these representations the transverse wavenumber k_{tj} is expressed in terms of the "separation" constants. The eigenvalue problem in x and y leads to a double Fourier integral representation for $\delta(x-x')\delta(y-y')$ in equations (9.8a), so that the two-dimensional free-space representation constitutes the two-dimensional Fourier integral theorem. The transform theorem associated with the integral representation for $\delta(\rho-\rho')/\rho'$ in equations (9.8b) is referred to as the Fourier-Bessel or Hankel transformation.

The suitability of the circular waveguide representation for this point-source excitation problem may be made manifest if the coordinate system is chosen so that $\rho' = 0$, that is, the source is located on the z-axis at $\rho = 0$, $z = z'$. This is the case for azimuthal symmetry $(\partial/\partial\phi = 0)$ of the field, where only the $m = 0$ mode contributes to the Green's function. In view of the relation $J_0(0) = 1$, the expression for $G(\vec{x},\vec{x}';\omega)$ in equations (9.8b) reduces to

$$G(\vec{x},\vec{x}';\omega) = \frac{1}{2\pi}\int_0^\infty G(\xi,z,z';\omega)J_0(\xi\rho)\xi d\xi \ . \tag{9.9}$$

If κ_j^2 is redefined as $\kappa_j^2 = -a_0^2$, equation (9.7b) can be rewritten as

$$(\frac{d^2}{dz^2} - a_0^2)G(\xi,z,z';\omega) = -\delta(z-z') \ , \tag{9.10}$$

where

$$a_0^2 = \xi^2 - k_0^2 \ . \tag{9.10a}$$

After solving equation (9.10) for the transformed Green's function $G(\xi,z,z';\omega)$, one may apply the inverse transform of equation (9.9) to obtain the Green's function $G(\rho,z,z';\omega)$.

It remains to solve equation (9.10) for appropriate boundary conditions at the top $(z = h_0)$ and bottom $(z = 0)$ of the liquid layer. The Green's function may be written in two parts: one for the region above the source and one for the region below the source, or

$$G(\xi,z,z';\omega) = \begin{cases} G_>(\xi,z,z';\omega) \ , & h_0 \geq z \geq z' \\ G_<(\xi,z,z';\omega) \ , & z' \geq z \geq 0 \ . \end{cases} \tag{9.11}$$

The Green's function can be constructed from a knowledge of the two solutions $G_>$ and $G_<$ of the homogeneous form of equation (9.10)

$$\left(\frac{d^2}{dz^2} - a_0^2\right)\begin{Bmatrix} G_> \\ G_< \end{Bmatrix} = 0 \ , \tag{9.12}$$

satisfying the required boundary conditions at $z = h_0$ and $z = 0$, respectively, and the required conditions at $z = z'$. The behavior of G and dG/dz in the vincinity of the source at $z = z'$ is given by

$$G_> = G_< \quad \text{at} \quad z = z' \tag{9.13a}$$

and

$$\frac{dG_>}{dz} - \frac{dG_<}{dz} = -1 \quad \text{at} \quad z = z' \ . \tag{9.13b}$$

The former expression requires that the Green's function be continuous at $z = z'$. The latter expression for the discontinuity in the first derivative of the Green's function, referred to as the jump condition, is obtained by integrating governing equation (9.10) across an infinitesimal interval from just below the source to just above it.

If solutions of the form

$$G(\xi,z,z';\omega) = \begin{matrix} G_> = c_2 V(z) \ , & z > z' \\ G_< = c_1 U(z) \ , & z' > z \end{matrix} \tag{9.14}$$

are assumed for homogeneous equations (9.12), then conditions (9.13) yield

$$c_2 = \frac{U(z')}{W(U,V)} \ , \quad c_1 = \frac{V(z')}{W(U,V)} \tag{9.15}$$

for the constants c_1 and c_2, where $W(U,V)$ is the Wronskian

determinant

$$W(U,V) = \begin{vmatrix} V(z') & U(z') \\ \dfrac{dV(z')}{dz'} & \dfrac{dU(z')}{dz'} \end{vmatrix} . \qquad (9.15a)$$

Equations (9.15) can be substituted into equation (9.14) to give

$$G(\xi,z,z';\omega) = \begin{matrix} G_{>} = \dfrac{U(z')V(z)}{W(U,V)} \\ \\ G_{<} = \dfrac{U(z)V(z')}{W(U,V)} \end{matrix} , \qquad (9.16)$$

or, using a more compact notation:

$$G(\xi,z,z';\omega) = \frac{U(z_{<})V(z_{>})}{W(U,V)} , \qquad (9.17)$$

where $z_{<}$ and $z_{>}$ denote, respectively, the lesser and greater of the quantities z and z'. Now only the functions $V(z)$ and $U(z)$, which satisfy the homogeneous equations (9.12) in the regions above and below the source, respectively, and the yet to specified boundary conditions at the top $(z = h_0)$ and bottom $(z = 0)$ of the liquid layer, need to be determined in order to obtain the Green's function $G(\xi,z,z';\omega)$.

The displacement $\vec{u}_0$ and pressure p in the liquid layer are related to the transformed Green's function as follows:

$$\vec{u}_0 = \nabla G \qquad (9.18a)$$

and

$$p = \rho_0 \omega^2 G , \qquad (9.18b)$$

where ρ_0 is the mass density of the liquid. Assuming that the first layer of the multilayered subbottom is a viscoelastic solid, the boundary conditions on the Green's function are as follows:

1. At $z = h_0$, the water's free surface, the pressure release condition holds

$$[p(z)]_{z=h_0} = 0 , \tag{9.19a}$$

or, from equation (9.18b),

$$[G_>]_{z=h_0} = 0 . \tag{9.19b}$$

2. At $z = 0$, the liquid-solid interface, the stress and normal component of the displacement are continuous. Since $\sigma_{zz} = -p$ and $\sigma_{\rho z} = 0$ in the inviscid liquid, from equations (9.18) one has:

$$[(u_z)_0]_{z=0} = [\frac{dG_<}{dz}]_{z=0} = [(u_z)_1]_{z=0} , \tag{9.20a}$$

$$[(\sigma_{zz})_0]_{z=0} = [-\rho_0\omega^2 G_<]_{z=0} = [(\sigma_{zz})_1]_{z=0} , \tag{9.20b}$$

and

$$[(\sigma_{\rho z})_0]_{z=0} = 0 = [(\sigma_{\rho z})_1]_{z=0} . \tag{9.20c}$$

The subscript "0" refers to the liquid layer while the subscript "1" refers to the first layer of the multilayered subbottom. The right-hand sides of equations (9.20a - c) are the transformed expressions for the normal displacement, normal stress, and shear stress at the surface of the multilayered subbottom. These expressions are only functions of the

spectral variables, ξ and ω, and the physical parameters of the subbottom. Next it is shown that by employing the definition of acoustic impedance, boundary conditions (9.20a) and (9.20b) can be combined into a single boundary condition.

The acoustic impedance Z is defined by $Z = p/v_n$, where p is the acoustic pressure and v_n is the velocity normal to the interface. This definition may be generalized for a solid medium by replacing p with the normal stress σ_{zz}, where $p = -\sigma_{zz}$. In the frequency domain the normal velocity v_z is expressed as $v_z = i\omega u_z$. According to these definitions, the impedance of the first layer of the multilayered subbottom is

$$Z_1(\xi;\omega) = \left[\frac{-(\sigma_{zz})_1}{i\omega(u_z)_1}\right]_{z=0} . \tag{9.21}$$

Now the two boundary conditions (9.20a) and (9.20b) can be replaced by the single condition

$$G_< - \frac{i}{\rho_0\omega} Z_1 \frac{dG_<}{dz} = 0 \quad \text{at} \quad z = 0 . \tag{9.22}$$

Thus, the use of the impedance concept simplifies the boundary conditions.

One now constructs eigenfunctions $V(z)$ and $U(z)$ for the regions above and below the source, respectively, satisfying the boundary conditions (9.19), (9.20), and (9.22) and homogeneous equations (9.12). A suitable set of functions is given by

$$V(z) = \sinh[a_0(h_0-z)] , \quad z > z' \tag{9.23a}$$

and

$$U(z) = \sinh(a_0 z) + \frac{ia_0}{\rho_0 \omega} Z_1 \cosh(a_0 z) \ , \quad z' > z \ . \tag{9.23b}$$

When these functions are substituted into the expression for $W(U,V)$ in equation (9.15a), one obtains

$$W(U,V) = a_0[\sinh(a_0 h_0) + \frac{ia_0}{\rho_0 \omega} Z_1 \cosh(a_0 h_0)] \ . \tag{9.24}$$

The final expression for the Green's function is obtained by substituting equations (9.23) and (9.24) into equation (9.17)

$$G(\xi,z,z';\omega) = \frac{\sinh[a_0(h_0 - z_>)]}{a_0} \left\{ \frac{\sinh(a_0 z_<) + \frac{ia_0}{\rho_0 \omega} Z \cosh(a_0 z_<)}{\sinh(a_0 h_0) + \frac{ia_0}{\rho_0 \omega} Z \cosh(a_0 h_0)} \right\} \ , \tag{9.25}$$

where Z_1 is now generalized, $Z_1 \to Z$, to represent the effective impedance of the multilayered subbottom. It is observed that an expression for the acoustic response may be developed without explicitly solving for the subbottom impedance Z characterizing the interaction of the acoustic medium with the multilayered medium. To calculate the effective impedance of the multilayered subbottom, first the propagation of waves in adjoining layers is characterized by the successive application of a recurrence relation generated from a consideration of the appropriate boundary conditions at each interface. Following that, the interaction of the acoustic medium with the multilayered medium is determined, using the boundary conditions in equation (9.20), to obtain an explicit expression for the subbottom impedance Z .

CHAPTER X

WAVE PROPAGATION IN THE LIQUID-VISCOELASTIC MULTILAYERED MEDIUM

It was mentioned earlier that the multilayered subbottom to be considered here consists of layers that are modeled as either viscoelastic solids or viscous liquids. If the problem of wave propagation in the subbottom is formulated for the case of a multilayered viscoelastic subbottom, it is shown here that any viscoelastic layer can be converted to a layer of viscous liquid by a simple transition. The transition involves only the alteration of the velocities of wave propagation in the medium through changes in the material parameters of the medium, and may be accomplished after the effective impedance of the multilayered subbottom is determined. For this reason, an approach is taken which treats the subbottom as a series of viscoelastic layers. After the propagation of waves in the n-layered viscoelastic subbottom is characterized, the method for converting any layer to a viscous liquid is discussed.

An expression for the dynamic behavior of a homogeneous, isotropic, Voigt viscoelastic solid is to be derived. The linear equation of motion applicable to both a linear elastic solid and a linear viscoelastic solid is given by

$$\rho \frac{\partial^2 u_i}{\partial t^2} - \frac{\partial \sigma_{ji}}{\partial x_j} = \rho f_i \ , \qquad (10.1)$$

where ρ is the mass density of the solid, u_i is the displacement vector, σ_{ji} is the stress tensor, $\partial/\partial x_j$ is the spatial gradient operator, and f_i is the extrinsic body force per unit mass. The specialization of

equation of motion (10.1) to describe either of these media is effected by inserting the appropriate constitutive relation into this form. The constitutive relation for a homogeneous, isotropic, Voigt viscoelastic solid is expressed as

$$\sigma_{ij} = \lambda \varepsilon_{\ell\ell} \delta_{ij} + 2\mu \varepsilon_{ij} \ , \tag{10.2}$$

where ε_{ij} is the strain tensor

$$\varepsilon_{ij} = \frac{1}{2}\left(\frac{\partial u_i}{\partial x_j} + \frac{\partial u_j}{\partial x_i}\right) \tag{10.2a}$$

and λ and μ are the Lamé operators

$$\lambda = \lambda' + \lambda'' \frac{\partial}{\partial t} \ , \quad \mu = \mu' + \mu'' \frac{\partial}{\partial t} \ . \tag{10.2b}$$

This constitutive relation is similar to the one which characterizes an elastic solid, except that the time-differential operators $\lambda' + \lambda''(\partial/\partial t)$ and $\mu' + \mu''(\partial/\partial t)$ take the place of λ' and μ', respectively. Here λ' and μ' are the usual Lame parameters for an elastic solid, while λ'' and μ'' denote the viscous parameters which correspond to Lame's parameters in the Voigt viscoelastic model. After combining equations (10.2), (10.2a), and (10.2b) and substituting the resultant form into equation (10.1), one obtains

$$\rho \frac{\partial^2 \vec{u}}{\partial t^2} - \left(\mu' + \mu'' \frac{\partial}{\partial t}\right)\nabla^2 \vec{u} - \left[\lambda' + \mu' + (\lambda'' + \mu'')\frac{\partial}{\partial t}\right]\nabla(\nabla \cdot \vec{u}) = \rho \vec{f} \tag{10.3}$$

for the displacement-equation of motion for a homogeneous, isotropic, Voigt viscoelastic solid.

The dynamic field equation governing each viscoelastic layer in the subbottom may be written from equation (10.3) as

$$\rho \frac{\partial^2 \vec{u}}{\partial t^2} - \left(\mu' + \mu'' \frac{\partial}{\partial t}\right)\nabla^2 \vec{u} - \left[\lambda' + \mu' + (\lambda'' + \mu'')\frac{\partial}{\partial t}\right]\nabla(\nabla \cdot \vec{u}) = 0 \ . \tag{10.4}$$

The homogeneous form of equation (10.3), obtained by setting the body force $\vec{f} = 0$, is assumed here, since no direct form of excitation is present within any of the viscoelastic layers. After taking the Fourier

transform with respect to time, according to the basis defined in equations (9.3), equation (10.4) may be expressed in the frequency domain as

$$(\nabla^2+k_T^2)\vec{u} - (1 - \frac{k_T^2}{k_L^2})\nabla(\nabla\cdot\vec{u}) = 0 , \qquad (10.5)$$

where k_L and k_T are the wavenumber for the longitudinal(compressional)-wave and transverse(shear)-wave fields defined by

$$k_L^2 = \frac{\omega^2}{c_L^2} = \frac{\omega^2}{c_{Le}^2(1+i\omega b_L)} , \qquad k_T^2 = \frac{\omega^2}{c_T^2} = \frac{\omega^2}{c_{Te}^2(1+i\omega b_T)}$$

$$c_{Le}^2 = \frac{\lambda'+2\mu'}{\rho} , \qquad c_{Te}^2 = \frac{\mu'}{\rho}$$

$$b_L = \frac{\lambda''+2\mu''}{\lambda'+2\mu'} , \qquad b_T = \frac{\mu''}{\mu'} . \qquad (10.5a)$$

Here c_{Le} and c_{Te} are the elastic compressional-wave and shear-wave velocities for a typical viscoelastic layer in the subbottom, and b_L and b_T are the damping coefficients which represent the modification that the velocities of elastic waves undergo when an elastic layer is generalized to include the effects of Voigt viscoelasticity. The damping coefficients b_L and b_T account, respectively, for compressional-wave attenuation and shear-wave attenuation in the viscoelastic layer. It is observed that the wave velocities become complex quantitities in the frequency domain when damping or viscoelasticity is introduced due to the time-dependent form of the Lamé parameters.

Consider that it is always possible to separate the displacement vector $\vec{u}$ into longitudinal (irrotational) and transverse (divergenceless) components as follows:

$$\vec{u} = \vec{u}_L + \vec{u}_T \ , \tag{10.6}$$

where

$$\nabla \times \vec{u}_L = 0 \ , \quad \nabla \cdot \vec{u}_T = 0 \ . \tag{10.7}$$

Taking the divergence of equation (10.5), one obtains

$$\nabla \cdot (\nabla^2 \vec{u}_L + k_L^2 \vec{u}_L) = 0 \ . \tag{10.8a}$$

Also, according to the relation $\nabla \times \vec{u}_L = 0$, the curl of the quantity in parentheses vanishes. If the divergence and the curl of a vector vanish, the vector also vanishes in the entire space. Therefore,

$$(\nabla^2 + k_L^2)\vec{u}_L = 0 \ . \tag{10.9a}$$

Returning to equation (10.5) and performing the curl, one obtains

$$\nabla \times (\nabla^2 \vec{u}_T + k_T^2 \vec{u}_T) = 0 \ . \tag{10.8b}$$

Applying the same arguments advanced for divergence equation (10.8a) to equation (10.8b), it is concluded that

$$(\nabla^2 + k_T^2)\vec{u}_T = 0 \ . \tag{10.9b}$$

Thus, the equation of motion for a typical viscoelastic layer in the subbottom has been decomposed into two vector wave equations: one representing the longitudinal-wave field, and the other representing the transverse-wave field.

Solutions for the longitudinal and transverse components of the displacement vector satisfying relations (10.7) may be written as

$$\vec{u}_L = \nabla\chi \ , \quad \vec{u}_T = \nabla \times \vec{A} \ , \tag{10.10}$$

where χ is a scalar displacement potential for the compressional field and $\vec{A}$ is a vector potential. The vector potential is taken to be of the following form, which is appropriate for the cylindrical coordinate system:

$$\vec{A} = \nabla \times \hat{e}_z\psi \ , \tag{10.10a}$$

where $\hat{e}_z$ is the unit vector in the z-direction, and ψ is the scalar displacement potential for the shear field. Only the vertical shear-wave field is excited in the viscoelastic layers due to the point-source excitation in the liquid layer.

The potentials χ and ψ satisfy the following scalar Helmholtz equations (A. Yildiz, 1971):

$$(\nabla^2+k_L^2)\chi = 0 \ , \quad (\nabla^2+k_T^2)\psi = 0 \ . \tag{10.11}$$

It is observed that the introduction of viscoelasticity does not alter the form of the elastic field equations in the frequency domain. Accordingly, any viscoelastic layer can be converted to an elastic layer simply by disregarding the damping coefficients b_L and b_T in the appropriate layer. This is one example where changing the compressional-wave and shear-wave velocities allows one to shift attention from one medium to another without engaging in the derivation of new field equations. Later, this concept is employed to show that any viscoelastic layer can be converted to a layer of viscous liquid by altering the velocities of wave

propagation c_L and c_T, since the field equations governing a viscoelastic solid and a viscous fluid are of the same basic form in the frequency domain.

Solutions of equations (10.11) for the scalar potentials χ and ψ may be obtained by using the method of separation of variables, giving for cylindrical coordinates the following forms:

$$\chi(\rho,\phi,z;\omega) = \sum_m \chi_m(\rho,\phi,z;\omega) \ , \qquad \chi_m \sim J_m(\xi\rho)\cos(m\phi)e^{\pm a_L z} \tag{10.12a}$$

and

$$\psi(\rho,\phi,z;\omega) = \sum_m \psi_m(\rho,\phi,z;\omega) \ , \qquad \psi_m \sim J_m(\xi\rho)\cos(m\phi)e^{\pm a_T z} \ , \tag{10.12b}$$

where

$$a_L^2 = \xi^2 - k_L^2 \ , \qquad a_T^2 = \xi^2 - k_T^2 \ . \tag{10.12c}$$

If one introduces the Fourier-Bessel transform, the potentials may be written in the form

$$\chi(\rho,\phi,z;\omega) = \int_0^\infty \xi J_m(\xi\rho)\underline{\chi}(\xi,\phi,z;\omega)d\xi \tag{10.13a}$$

and

$$\psi(\rho,\phi,z;\omega) = \int_0^\infty \xi J_m(\xi\rho)\underline{\psi}(\xi,\phi,z;\omega)d\xi \ , \tag{10.13b}$$

where $\underline{\chi}$ and $\underline{\psi}$ are the transformed potentials. For azimuthal symmetry of the field $(\partial/\partial\phi=0, m=0)$, these transform relations reduce to

$$\chi(\rho,z;\omega) = \int_0^\infty \underline{\chi}(\xi,z;\omega)J_0(\xi\rho)\xi d\xi \tag{10.14a}$$

and

$$\psi(\rho,z;\omega) = \int_0^\infty \underline{\psi}(\xi,z;\omega)J_0(\xi\rho)\xi d\xi \ . \qquad (10.14b)$$

Equations (10.14) imply that the potentials are obtained by superimposing eigenfunctions $\underline{\chi}(\xi,z;\omega)$ and $\underline{\psi}(\xi,z;\omega)$ over the continuous ξ-spectrum. In order to obtain expressions compatible with the Green's function in the liquid layer, weighting factors are introduced as follows:

$$\underline{\chi}(\xi,z;\omega) = \frac{1}{4\pi a_L}[A(\xi;\omega)e^{-a_L z} + B(\xi;\omega)e^{a_L z}] \ , \qquad (10.15a)$$

and

$$\underline{\psi}(\xi,z;\omega) = \frac{1}{4\pi a_T}[C(\xi;\omega)e^{-a_T z} + D(\xi;\omega)e^{a_T z}] \ . \qquad (10.15b)$$

Due to the choice of time dependence of the form $\exp(i\omega t)$ in equations (9.3), the first and second terms on the right-hand side of equations (10.15) correspond, respectively, to upward and downward traveling waves in a typical layer. The general form for the potentials $\underline{\chi}$ and $\underline{\psi}$ in equations (10.15) must be altered when applied to the $n^{\underline{th}}$ or last visco-elastic layer (a halfspace), since the displacement must vanish as $z \to -\infty$. It follows that this requirement is met by setting the potential coefficients $A(\xi;\omega) = C(\xi;\omega) = 0$ in the halfspace. This is, in essence, a radiation condition since the potential coefficients $A(\xi;\omega)$ and $C(\xi;\omega)$ are paired with exponential terms which represent upward traveling waves, and there are no waves reflected from infinity.

At this point, the boundary conditions used in the solution of the n-layer problem under consideration are formulated. The boundary conditions applicable at each solid-solid interface are the continuity of displacement and stress across the boundary. First the displacement field is developed because stress can be expressed in terms of strain, which in turn is expressed in terms of displacement. It was mentioned earlier that the displacement field may be expressed in terms of longitudinal and transverse components as

$$\vec{u} = \vec{u}_L + \vec{u}_T \ , \tag{10.6}$$

or substituting from equations (10.10),

$$\vec{u} = \nabla\underline{\chi} + \nabla\times\nabla\times\hat{e}_z\underline{\psi} \ . \tag{10.16}$$

The displacement field components are expressed in terms of the potentials as follows:

$$u_\rho = \frac{\partial}{\partial\rho}(\underline{\chi} + \frac{\partial\underline{\psi}}{\partial z}) \ , \tag{10.17a}$$

$$u_\phi = 0 \ , \tag{10.17b}$$

and

$$u_z = \frac{\partial\underline{\chi}}{\partial z} + (\frac{\partial^2}{\partial z^2} + k_T^2)\underline{\psi} \ . \tag{10.17c}$$

The stress tensor σ_{ij} is related to the strain tensor ε_{ij} by the well-known relation in equation (10.2). The only elements of the stress field of interest are those acting on the horizontal surfaces of the layers, that is, σ_{zz} , $\sigma_{\rho z}$, and $\sigma_{\phi z}$. These are expressed

with the use of equation (10.2) as

$$\sigma_{zz} = \lambda\varepsilon_{\ell\ell} + 2\mu\varepsilon_{zz} \ , \tag{10.18a}$$

$$\sigma_{\rho z} = 2\mu\varepsilon_{\rho z} \ , \tag{10.18b}$$

and

$$\sigma_{\phi z} = 2\mu\varepsilon_{\phi z} \ , \tag{10.18c}$$

where ε_{zz} , $\varepsilon_{\rho z}$, and $\varepsilon_{\phi z}$ are strains defined in terms of the displacement components by

$$\varepsilon_{zz} = \frac{\partial u_z}{\partial z} \ , \quad \varepsilon_{\rho z} = \frac{1}{2}\left(\frac{\partial u_\rho}{\partial z} + \frac{\partial u_z}{\partial \rho}\right) \ , \quad \varepsilon_{\phi z} = \frac{1}{2}\left(\frac{\partial u_\phi}{\partial z} + \frac{1}{\rho}\frac{\partial u_z}{\partial \phi}\right) \ , \tag{10.19a}$$

and

$$\varepsilon_{\ell\ell} = \varepsilon_{\rho\rho} + \varepsilon_{\phi\phi} + \varepsilon_{zz} = \nabla \cdot \vec{u} \ . \tag{10.19b}$$

Applying equations (10.17) and (10.19) to equations (10.18) gives the stress components in terms of the potentials:

$$\sigma_{zz} = \left(2\mu \frac{\partial^2}{\partial z^2} - \lambda k_L^2\right)\underline{\chi} + 2\mu \frac{\partial}{\partial z}\left(\frac{\partial^2}{\partial z^2} + k_T^2\right)\underline{\psi} \ , \tag{10.20a}$$

$$\sigma_{\rho z} = \mu \frac{\partial}{\partial \rho}\left[2 \frac{\partial \underline{\chi}}{\partial z} + \left(2 \frac{\partial^2}{\partial z^2} + k_T^2\right)\underline{\psi}\right] \ , \tag{10.20b}$$

and

$$\sigma_{\phi z} = 0 \ . \tag{10.20c}$$

Referring to Figure 15, the appropriate boundary conditions are to be applied at each interface. At the $j^{\underline{th}}$ interface separating the $j^{\underline{th}}$

viscoelastic layer from the $(j+1)^{\underline{th}}$ viscoelastic layer, continuity of the displacement and stress components normal and tangential to the horizontal boundary holds, or:

$$1.\quad [u_{\rho j}]_{z=-d_j} = [u_{\rho (j+1)}]_{z=-d_j} , \tag{10.21a}$$

$$2.\quad [u_{zj}]_{z=-d_j} = [u_{z(j+1)}]_{z=-d_j} , \tag{10.21b}$$

$$3.\quad [\sigma_{zzj}]_{z=-d_j} = [\sigma_{zz(j+1)}]_{z=-d_j} , \tag{10.21c}$$

$$4.\quad [\sigma_{\rho zj}]_{z=-d_j} = [\sigma_{\rho z(j+1)}]_{z=-d_j} . \tag{10.21d}$$

Equations (10.15) are now replaced by the following more general form for the potentials:

$$\underline{\chi}_j(\xi,z;\omega) = \frac{1}{4\pi a_{Lj}}[A_j(\xi;\omega)e^{-a_{Lj}z} + B_j(\xi;\omega)e^{a_{Lj}z}] , \tag{10.22a}$$

$$\underline{\psi}_j(\xi,z;\omega) = \frac{1}{4\pi a_{Tj}}[C_j(\xi;\omega)e^{-a_{Tj}z} + D_j(\xi;\omega)e^{a_{Tj}z}] , \tag{10.22b}$$

where $j = 1, 2, \cdots, n$, and $A_n = C_n = 0$. Applying the expressions for displacement and stress in equations (10.17) and (10.20) and the general form for the potentials in equations (10.22) to the system of boundary conditions given by equations (10.21), one obtains four equations which may be arranged in the following matrix form:

$$[a_j][A_j]\vec{A}_j = [a_{(j+1)}][A_{(j+1)}]\vec{A}_{(j+1)} , \tag{10.23}$$

where

$$[a_j] = \begin{bmatrix} 1 & 1 & -a_{Tj} & a_{Tj} \\ -a_{Lj} & a_{Lj} & \xi^2 & \xi^2 \\ \mu_j(2\xi^2-k_{Tj}^2) & \mu_j(2\xi^2-k_{Tj}^2) & -2\mu_j a_{Tj}\xi^2 & 2\mu_j a_{Tj}\xi^2 \\ -2\mu_j a_{Lj} & 2\mu_j a_{Lj} & \mu_j(2\xi^2-k_{Tj}^2) & \mu_j(2\xi^2-k_{Tj}^2) \end{bmatrix}, \tag{10.23a}$$

$$[A_j] = \begin{bmatrix} e^{a_{Lj}d_j} & 0 & 0 & 0 \\ 0 & e^{-a_{Lj}d_j} & 0 & 0 \\ 0 & 0 & e^{a_{Tj}d_j} & 0 \\ 0 & 0 & 0 & e^{-a_{Tj}d_j} \end{bmatrix}, \tag{10.23b}$$

and

$$\vec{A}_j = \begin{bmatrix} A_j/a_{Lj} \\ B_j/a_{Lj} \\ C_j/a_{Tj} \\ D_j/a_{Tj} \end{bmatrix}. \tag{10.23c}$$

One writes a recurrence relation for the potential coefficients from equation (10.23) as follows:

$$\vec{A}_j = [b_{(j+1),j}]\vec{A}_{(j+1)}, \tag{10.24}$$

where

$$[b_{(j+1),j}] = [A_j]^{-1}[a_j]^{-1}[a_{(j+1)}][A_{(j+1)}] \qquad (10.24a)$$

and

$$[a_j]^{-1} = \frac{1}{2\rho_j\omega^2 a_{Lj}a_{Tj}}\begin{bmatrix} 2\mu_j a_{Lj}a_{Tj}\xi^2 & \mu_j a_{Tj}(2\xi^2-k_{Tj}^2) & -a_{Lj}a_{Tj} & -a_{Tj}\xi^2 \\ 2\mu_j a_{Lj}a_{Tj}\xi^2 & -\mu_j a_{Tj}(2\xi^2-k_{Tj}^2) & -a_{Lj}a_{Tj} & a_{Tj}\xi^2 \\ \mu_j a_{Lj}(2\xi^2-k_{Tj}^2) & 2\mu_j a_{Lj}a_{Tj} & -a_{Lj} & -a_{Lj}a_{Tj} \\ -\mu_j a_{Lj}(2\xi^2-k_{Tj}^2) & 2\mu_j a_{Lj}a_{Tj} & a_{Lj} & -a_{Lj}a_{Tj} \end{bmatrix}. \qquad (10.24b)$$

In order to obtain the acoustic response in the liquid layer, the potential coefficients $\vec{A}_j$ for the intermediate layers $(j=2,3,\cdots,n-1)$ are eliminated by the successive application of equation (10.24). One obtains the following relation for the potential coefficients of the first layer in terms of the last layer:

$$\vec{A}_1 = \{\prod_{\ell=1}^{n-1} [b_{(\ell+1),\ell}]\}\vec{A}_n \ , \qquad (n>1) \ , \qquad (10.25)$$

where it should be recalled that the first and third elements of the column matrix $\vec{A}_n$ are zero due to the physical considerations discussed earlier. Since the repeated product in equation (10.24a) is a (4×4) matrix, it follows that equation (10.25) may be expressed as

$$\vec{A}_1 = [M]\vec{A}_n \ , \qquad (10.26)$$

where

$$[M] = \prod_{\ell=1}^{n-1} [b_{(\ell+1),\ell}] \ , \qquad (n>1) \qquad (10.26a)$$

is a (4×4) matrix whose elements are to be denoted as m_{ij}, i, j = 1,2,3,4 . Recurrence relation (10.24) has been used to successively eliminate the potential coefficients A_j, B_j, C_j, and D_j of the intermediate layers (j=2,3,···,n-1) . As a result, the effect of the layers between the first layer and the halfspace is characterized by the [M] matrix, whose elements are functions of the spectral variables, ξ and ω , and the physical parameters of the intermediate layers.

The explicit calculation of the [M] matrix for more than two viscoelastic layers is impractical due to the algebraic complexity; however, the forms developed here are ideal for computer analysis due to the introduction of the recurrence relation. The recurrence relation reduces all calculations to (4×4) matrix manipulations, which can be performed easily by a computer. The general n-layer problem, if solved without benefit of the recurrence relation, would require the inversion of a (4n-2) square matrix. The order (4n-2) of the matrix is governed by the number of potential coefficients A_j, B_j, C_j, and D_j in equations (10.22) for each layer. The computation time of the analysis would become excessive for a large number of layers. Applying the recurrence relation reduces the computer time for n large due to the cascading feature illustrated in equation (10.25). Another obvious advantage of the recurrence relation is the conciseness of the notation and its generality.

Now, the method for converting any viscoelastic layer in the multilayered subbottom to a layer of viscous liquid is developed. If the layer

of interest is assumed to consist of a linear viscous fluid (a Newtonian fluid), then linearized equation of motion (10.1) governs the dynamic behavior of the fluid layer. The specialization of equation of motion (10.1) to describe a viscous fluid is effected by inserting the appropriate constitutive relation into this form. The constitutive relation for a homogeneous, isotropic, linear viscous fluid is expressed as

$$\sigma_{ij} = -p\delta_{ij} + \bar{\lambda}\dot{\varepsilon}_{\ell\ell}\delta_{ij} + 2\bar{\mu}\dot{\varepsilon}_{ij} , \tag{10.27}$$

where $\dot{(\ )} \equiv \partial(\ )/\partial t$ and the notation with the bar over the constants $\bar{\lambda}$ and $\bar{\mu}$ is employed to avoid confusion with the constants for the viscoelastic solid. The constants $\bar{\lambda}$ and $\bar{\mu}$ are called coefficients of viscosity, and $\bar{\mu}$ is referred to as the dynamic coefficient of viscosity or the shear viscosity. Constitutive relation (10.27) may be expanded in terms of the displacement and velocity fields in the fluid as

$$\sigma_{ij} = \bar{\kappa}\frac{\partial u_\ell}{\partial x_\ell}\delta_{ij} + \bar{\lambda}\frac{\partial \dot{u}_\ell}{\partial x_\ell}\delta_{ij} + \bar{\mu}\left(\frac{\partial \dot{u}_i}{\partial x_j} + \frac{\partial \dot{u}_j}{\partial x_i}\right) , \tag{10.28}$$

where the substitution $p = -\bar{\kappa}\varepsilon_{\ell\ell}$ is made in equation (10.27). The constant $\bar{\kappa}$ denotes the bulk modulus of the fluid.

Constitutive relation (10.2) for the Voigt viscoelastic solid may be expanded with the use of equations (10.2a) and (10.2b) as follows:

$$\sigma_{ij} = \lambda'\frac{\partial u_\ell}{\partial x_\ell}\delta_{ij} + \lambda''\frac{\partial \dot{u}_\ell}{\partial x_\ell}\delta_{ij} + \mu'\left(\frac{\partial u_i}{\partial x_j} + \frac{\partial u_j}{\partial x_i}\right) + \mu''\left(\frac{\partial \dot{u}_i}{\partial x_j} + \frac{\partial \dot{u}_j}{\partial x_i}\right) . \tag{10.29}$$

A comparison of the forms in equations (10.28) and (10.29) illustrates that a transition from the constitutive relation of a viscoelastic solid

to a viscous fluid may be effected through the following changes in the material parameters of the viscoelastic solid:

$$\lambda' \to \bar{\kappa} , \quad \mu' \to 0 , \quad \lambda'' \to \bar{\lambda} , \quad \mu'' \to \bar{\mu} . \tag{10.30}$$

The condition $\mu' \to 0$ denotes that the fluid has no rigidity.

It is convenient, however, to write the constitutive relation for the viscous fluid in a slightly different form, in which the constants $\bar{\lambda}$ and $\bar{\mu}$ are replaced by other constants:

$$\sigma_{ij} = -p\delta_{ij} + \bar{\zeta}\dot{\varepsilon}_{\ell\ell}\delta_{ij} + 2\bar{\eta}(\dot{\varepsilon}_{ij} - \frac{1}{3}\dot{\varepsilon}_{\ell\ell}\delta_{ij}) , \tag{10.31}$$

or, in expanded form,

$$\sigma_{ij} = \bar{\kappa}\frac{\partial u_\ell}{\partial x_\ell}\delta_{ij} + (\bar{\zeta} - \frac{2}{3}\bar{\eta})\frac{\partial \dot{u}_\ell}{\partial x_\ell}\delta_{ij} + \bar{\eta}(\frac{\partial \dot{u}_i}{\partial x_j} + \frac{\partial \dot{u}_j}{\partial x_i}) , \tag{10.32}$$

where the substitution $p = -\bar{\kappa}\varepsilon_{\ell\ell}$ is made again. This alternative form for the constitutive relation for a viscous fluid may be obtained from equation (10.28) by making the substitutions $\bar{\lambda} + \frac{2}{3}\bar{\mu} = \bar{\zeta}$ and $\bar{\mu} = \bar{\eta}$. The constants $\bar{\zeta}$ and $\bar{\eta}$ are also coefficients of viscosity, referred to as the bulk and shear viscosities of the fluid, respectively. Each of these constants precedes a term responsible for a different type of deformation: the constant $\bar{\zeta}$ is related to volume change components of the deformation only without distortion, and the constant $\bar{\eta}$ is related to distortion components of the deformation only without volume change. The transition in equations (10.30) may be expressed alternatively in terms of these different coefficients of viscosity as

$$\lambda' \to \bar{\kappa} , \quad \mu' \to 0 , \quad \lambda'' \to \bar{\zeta} - \frac{2}{3}\bar{\eta} , \quad \mu'' \to \bar{\eta} . \tag{10.33}$$

It should be mentioned that the constitutive relation for an inviscid or perfect fluid may be obtained from the constitutive relation for a viscoelastic solid by the following transition:

$$\lambda' \to \bar{\kappa} \ , \quad \mu' \to 0 \ , \quad \lambda'' \to 0 \ , \quad \mu'' \to 0 \ , \tag{10.34}$$

where the effects of rigidity and viscosity in the fluid are disregarded.

If either of the constitutive relations for the viscous fluid in equations (10.27) or (10.31) was substituted into equation of motion (10.1) and the formal development characterizing wave propagation in the multilayered subbottom was repeated, the new development would lead to expressions of the same form as for the case of a layered viscoelastic subbottom, because the field equations governing a viscoelastic solid and a viscous fluid have the same basic form in the frequency domain. The only differences would occur in the velocities of wave propagation which would undergo the following modifications:

$$k_L^2 = \frac{\omega^2}{c_L^2} = \frac{\rho\omega^2}{\lambda'+2\mu'+i\omega(\lambda''+2\mu'')} \to \bar{k}_L^2 = \frac{\omega^2}{\bar{c}_L^2} = \frac{\bar{\rho}\omega^2}{\bar{\rho}\,\bar{c}^2+i\omega(\bar{\zeta}+\frac{4}{3}\bar{\eta})}$$

$$k_T^2 = \frac{\omega^2}{c_T^2} = \frac{\rho\omega^2}{\mu'+i\omega\mu''} \to \bar{k}_T^2 = \frac{\omega^2}{\bar{c}_T^2} = \frac{\bar{\rho}\omega^2}{i\omega\bar{\eta}} \ . \tag{10.35}$$

The substitution $\bar{\kappa} = \bar{\rho}\,\bar{c}^2$ is made here, where $\bar{\rho}$ is the mass density of the fluid and $\bar{c}$ is the velocity of sound propagation in a perfect fluid. In any layer of the subbottom, the velocities of wave propagation or the respective wavenumbers for the propagation of waves in a viscous fluid may be substituted in place of the corresponding quantities for a viscoelastic solid in order to convert that layer from a viscoelastic

solid to a viscous fluid. A method for specializing the formal development for the propagation of waves in the multilayered viscoelastic subbottom has been discussed here for the cases where any layer in the subbottom may be modeled as an elastic solid, a viscous liquid, or an inviscid liquid.

CHAPTER XI

INTERACTION OF THE ACOUSTIC MEDIUM WITH THE MULTILAYERED MEDIUM

The interaction of the acoustic medium with the multilayered medium is considered at this point, in order to obtain a general expression for the subbottom impedance Z in equation (9.25). One applies the boundary conditions in equation (9.20) and (9.22) at the liquid-solid interface, using the expressions for the potentials in the first viscoelastic layer, that is, equations (10.22) with $j = 1$. Then the recurrence relation in equation (10.26) is applied for the first and last viscoelastic layers.

The three boundary conditions of equations (9.20) are expressed in matrix form in terms of the physical parameters and potential coefficients of the first viscoelastic layer as follows:

$$\begin{bmatrix} \frac{4\pi}{\rho_1 C_{T1}^2}[(\sigma_{zz})_1]_{z=0} \\ 4\pi[(u_z)_1]_{z=0} \\ 0 \end{bmatrix} =$$

$$\begin{bmatrix} (2\xi^2-k_{T1}^2) & (2\xi^2-k_{T1}^2) & -2a_{T1}\xi^2 & 2a_{T1}\xi^2 \\ -a_{L1} & a_{L1} & \xi^2 & \xi^2 \\ -2a_{L1} & 2a_{L1} & (2\xi^2-k_{T1}^2) & (2\xi^2-k_{T1}^2) \end{bmatrix} \begin{bmatrix} A_1/a_{L1} \\ B_1/a_{L1} \\ C_1/a_{T1} \\ D_1/a_{T1} \end{bmatrix} . \quad (11.1)$$

The recurrence relation in equation (10.26), relating the potential

coefficients in the first and last viscoelastic layers, is expanded to give the following:

$$\begin{bmatrix} A_1/a_{L1} \\ B_1/a_{L1} \\ C_1/a_{T1} \\ D_1/a_{T1} \end{bmatrix} = \begin{bmatrix} m_{12} & m_{14} \\ m_{22} & m_{24} \\ m_{32} & m_{34} \\ m_{42} & m_{44} \end{bmatrix} \begin{bmatrix} B_n/a_{Ln} \\ D_n/a_{Tn} \end{bmatrix} , \tag{11.2}$$

where the m_{ij} are the elements of the [M] matrix, and it is recalled that $A_n = C_n = 0$. Substituting equation (11.2) into equation (11.1), one obtains the matrix form

$$\begin{bmatrix} \frac{4\pi}{\rho_1 c_{T1}^2}[(\sigma_{zz})_1]_{z=0} \\ 4\pi[(u_z)_1]_{z=0} \\ 0 \end{bmatrix} = \begin{bmatrix} f_{11} & f_{12} \\ f_{21} & f_{22} \\ f_{31} & f_{32} \end{bmatrix} \begin{bmatrix} B_n/a_{Ln} \\ D_n/a_{Tn} \end{bmatrix} , \tag{11.3}$$

where f_{ij} are the elements of the matrix formed by multiplying the (3×4) matrix in equation (11.1) and the (4×2) matrix in equation (11.2). The f_{ij} elements are given by

$$f_{11} = (2\xi^2 - k_{T1}^2)(m_{12}+m_{22}) + 2a_{T1}\xi^2(m_{42}-m_{32}) , \tag{11.3a}$$

$$f_{12} = (2\xi^2 - k_{T1}^2)(m_{14}+m_{24}) + 2a_{T1}\xi^2(m_{44}-m_{34}) , \tag{11.3b}$$

$$f_{21} = a_{L1}(m_{22}-m_{12}) + \xi^2(m_{32}+m_{42}) , \tag{11.3c}$$

$$f_{22} = a_{L1}(m_{24}-m_{14}) + \xi^2(m_{34}+m_{44}) , \tag{11.3d}$$

$$f_{31} = 2a_{L1}(m_{22}-m_{12}) + (2\xi^2 - k_{T1}^2)(m_{32}+m_{42}) , \tag{11.3e}$$

$$f_{32} = 2a_{L1}(m_{24}-m_{14}) + (2\xi^2 - k_{T1}^2)(m_{34}+m_{44}) . \tag{11.3f}$$

Equation (11.3) may be solved for the subbottom impedance Z, yielding the following result:

$$Z = \frac{i\,\rho_1\,\omega}{k_{T1}^2}\left[\frac{f_{31}f_{12} - f_{32}f_{11}}{f_{31}f_{22} - f_{32}f_{21}}\right] . \tag{11.4}$$

In expanded form, in terms of the m_{ij} elements, equation (11.4) gives

$$Z = \frac{-i\,\rho_1\,\omega}{a_{L1}k_{T1}^4} \times$$

$$\left[\begin{array}{l} 4(2\xi^2-k_{T1}^2)\left[a_{L1}(m_{22}m_{14}-m_{12}m_{24})+a_{T1}\xi^2(m_{32}m_{44}-m_{42}m_{34})\right] \\ +(2\xi^2-k_{T1}^2)^2\left[(m_{32}+m_{42})(m_{14}+m_{24})-(m_{12}+m_{22})(m_{34}+m_{44})\right] \\ \dfrac{-4a_{L1}a_{T1}\xi^2\left[(m_{32}-m_{42})(m_{14}-m_{24})-(m_{12}-m_{22})(m_{34}-m_{44})\right]}{\left[(m_{32}+m_{42})(m_{24}-m_{14})-(m_{22}-m_{12})(m_{34}+m_{44})\right]} \end{array}\right] . \tag{11.5}$$

This process has eliminated the potential coefficients A_j, B_j, C_j, and D_j $(j=1,2,\cdots,n)$ in the viscoelastic layers enabling one to characterize the interaction of the acoustic medium with the multilayered medium by the subbottom impedance Z. The subbottom impedance Z is a function only of the physical parameters for the viscoelastic layers $(\rho_j,\lambda_j',\mu_j',\lambda_j'',\mu_j'')$, the geometry of the layering (h_j), and the spectral variables (ξ,ω).

Upon substituting equation (11.5) into equation (9.25), one obtains a Green's function expression for the n-layered subbottom. The appropriate m_{ij} elements, which are dependent upon the number of viscoelastic layers under consideration, must be inserted into this expression.

It is interesting to note that only the eight elements comprising the second and the fourth columns of the [M] matrix are required in order to obtain the impedance Z for any subbottom. The methodology set forth here to determine the subbottom impedance Z is applied to special cases of the n-layered subbottom in the development to follow. After the subbottom impedances for these special cases of interest are determined, Green's functions for the acoustic responses from these subbottoms are obtained with the use of equations (9.9) and (9.25).

CHAPTER XII

SPECIAL CASES

The general expression for the Green's function obtained by substituting equation (11.5) into equation (9.25) is too complex to analyze further. Some special cases that are of interest are now examined.

One Viscoelastic Layer

The first special case examined is that for one viscoelastic layer (n=1), where the subbottom consists of a single homogeneous, isotropic viscoelastic material occupying the lower halfspace. This problem has been analyzed previously by Press and Ewing (1950) for an elastic subbottom. The result for this case may be developed directly from equation (11.1) or a degenerate form of recurrence relation (10.26) may be used.

According to the former approach, one sets $A_1 = C_1 = 0$ in equation (11.1) and solves this system of three equations directly for the subbottom impedance Z. This procedure yields

$$Z = \frac{-i\rho_1\omega}{a_{L1}k_{T1}^4}[(2\xi^2-k_{T1}^2)^2-4a_{L1}a_{T1}\xi^2] \qquad (12.1)$$

for the impedance of the subbottom. Employing the latter approach, one sets $n = 1$ in equation (11.2), expands for the appropriate values for m_{ij}, and substitutes these values into equation (11.5). Following this

procedure, one finds that the [M] matrix reduces to $m_{22} = m_{44} = 1$, the other elements $m_{ij} = 0$, $i \neq j$. Using these values in equations (11.5) yields the subbottom impedance in equation (12.1).

An integral expression for the Green's function for this special case is obtained by substituting equation (12.1) into equation (9.25) and inserting the latter expression into equation (9.9). Following this procedure, after some rearranging one obtains

$$G(\vec{x},\vec{x}';\omega) = \frac{1}{2\pi}\int_0^\infty \frac{\sinh[a_0(h_0-z_>)]}{a_0\Delta(\xi)}\{\rho_1 a_0[(2\xi^2-k_{T1}^2)^2-4a_{L1}a_{T1}\xi^2]\cosh(a_0 z_<)$$

$$+\rho_0 a_{L1}k_{T1}^4\sinh(a_0 z_<)\}J_0(\xi\rho)\xi d\xi \ , \qquad (12.2)$$

where

$$\Delta(\xi) = \rho_1 a_0[(2\xi^2-k_{T1}^2)^2-4a_{L1}a_{T1}\xi^2]\cosh(a_0 h_0)+\rho_0 a_{L1}k_{T1}^4\sinh(a_0 h_0) \ . \qquad (12.2a)$$

After changing coordinate systems, converting notation, and disregarding the contribution due to viscoelasticity in the viscoelastic halfspace, this result is consistent with Press and Ewing's (1950) result for the case where the subbottom is an elastic solid halfspace. This result also agrees with Pekeris's (1948) result for a two-layered liquid halfspace, if one disregards the contributions due to viscoelasticity and rigidity in the viscoelastic halfspace. This may be accomplished by setting the material parameters $\mu_1' = \lambda_1'' = \mu_1'' = 0$ in the integral in equation (12.2). In each case the present result contains an additional $1/4\pi$ factor due to the Green's function formalism.

Two Viscoelastic Layers

To obtain the Green's function for the more general case where the subbottom consists of two viscoelastic layers (n=2) requires the use of the multilayer techniques developed earlier. The recurrence relation for the special case where the subbottom is a two-layered solid halfspace is obtained by writing equation (10.26) for n = 2:

$$\vec{A}_1 = [M]\vec{A}_2 \ , \tag{12.3}$$

where, from equations (10.24a) and (10.26a), the appropriate [M] matrix is given by

$$[M] = [b_{2,1}] = [A_1]^{-1}[a_1]^{-1}[a_2][A_2] \ . \tag{12.3a}$$

The eight elements of the [M] matrix which appear in the general form for the impedance in equation (11.5) must be computed. After considerable algebra these elements are expressed as follows:

$$m_{12} = \frac{e^{-(a_{L1}+a_{L2})d_1}}{\Delta}\{a_{L1}[2(\mu_2-\mu_1)\xi^2-\rho_2\omega^2]+a_{L2}[2(\mu_2-\mu_1)\xi^2+\rho_1\omega^2]\} \ , \tag{12.4a}$$

$$m_{22} = \frac{e^{(a_{L1}-a_{L2})d_1}}{\Delta}\{a_{L1}[2(\mu_2-\mu_1)\xi^2-\rho_2\omega^2]-a_{L2}[2(\mu_2-\mu_1)\xi^2+\rho_1\omega^2]\} \ , \tag{12.4b}$$

$$m_{32} = \frac{e^{-(a_{T1}+a_{L2})d_1}}{\Delta}\{[2(\mu_2-\mu_1)\xi^2-(\rho_2-\rho_1)\omega^2]+2(\mu_2-\mu_1)a_{T1}a_{L2}\} \ , \tag{12.4c}$$

$$m_{42} = \frac{e^{(a_{T1}-a_{L2})d_1}}{\Delta}\{[2(\mu_2-\mu_1)\xi^2-(\rho_2-\rho_1)\omega^2]-2(\mu_2-\mu_1)a_{T1}a_{L2}\} \ , \tag{12.4d}$$

$$m_{14} = \frac{e^{-(a_{L1}+a_{T2})d_1}}{\Delta}\{[2(\mu_2-\mu_1)\xi^2-(\rho_2-\rho_1)\omega^2]+2(\mu_2-\mu_1)a_{L1}a_{T2}\} \ , \tag{12.4e}$$

$$m_{24} = \frac{a_{T1}\xi^2 e^{(a_{L1}-a_{T2})d_1}}{\Delta}\{[2(\mu_2-\mu_1)\xi^2-(\rho_2-\rho_1)\omega^2]-2(\mu_2-\mu_1)a_{L1}a_{T2}\} , \quad (12.4f)$$

$$m_{34} = \frac{-a_{L1}e^{-(a_{T1}+a_{T2})d_1}}{\Delta}\{a_{T1}[2(\mu_2-\mu_1)\xi^2-\rho_2\omega^2]+a_{T2}[2(\mu_2-\mu_1)\xi^2+\rho_1\omega^2]\} , \quad (12.4g)$$

$$m_{44} = \frac{-a_{L1}e^{(a_{T1}-a_{T2})d_1}}{\Delta}\{a_{T1}[2(\mu_2-\mu_1)\xi^2-\rho_2\omega^2]-a_{T2}[2(\mu_2-\mu_1)\xi^2+\rho_1\omega^2]\} , \quad (12.4h)$$

where Δ is the determinant of the $[a_1]$ matrix given by

$$\Delta = 2\rho_1\omega^2 a_{L1}a_{T1} . \quad (12.4i)$$

Substituting these elements of the [M] matrix into equation (11.5), one obtains

$$Z = \frac{-i\rho_1\omega}{a_{L1}k_{T1}^4}\left\{\frac{4(2\xi^2-k_{T1}^2)P_1+(2\xi^2-k_{T1}^2)^2P_2-4a_{L1}a_{T1}\xi^2P_3}{P_4}\right\} , \quad (12.5)$$

where

$$P_1 = a_{L1}a_{T1}\xi^2\{[2(\mu_2-\mu_1)\xi^2-(\rho_2-\rho_1)\omega^2][2(\mu_2-\mu_1)\xi^2-\rho_2\omega^2]\}$$

$$-2(\mu_2-\mu_1)a_{L2}a_{T2}[2(\mu_2-\mu_1)\xi^2+\rho_1\omega^2] , \quad (12.5a)$$

$$P_2 = \{\xi^2[2(\mu_2-\mu_1)\xi^2-(\rho_2-\rho_1)\omega^2]^2-a_{L2}a_{T2}[2(\mu_2-\mu_1)\xi^2+\rho_1\omega^2]^2\}\sinh(a_{L1}h_1)\sinh(a_{T1}h_1)$$

$$-a_{L1}a_{T1}\{[2(\mu_2-\mu_1)\xi^2-\rho_2\omega^2]^2-4(\mu_2-\mu_1)^2a_{L2}a_{T2}\xi^2\}\cosh(a_{L1}h_1)\cosh(a_{T1}h_1)$$

$$-\rho_1\rho_2\omega^4\{a_{L1}a_{T2}\cosh(a_{L1}h_1)\sinh(a_{T1}h_1)+a_{T1}a_{L2}\sinh(a_{L1}h_1)\cosh(a_{T1}h_1)\} , \quad (12.5b)$$

$$P_3 = \{\xi^2[2(\mu_2-\mu_1)\xi^2-(\rho_2-\rho_1)\omega^2]^2-a_{L2}a_{T2}[2(\mu_2-\mu_1)\xi^2+\rho_1\omega^2]^2\}\cosh(a_{L1}h_1)\cosh(a_{T1}h_1)$$

$$-a_{L1}a_{T1}\{[2(\mu_2-\mu_1)\xi^2-\rho_2\omega^2]^2-4(\mu_2-\mu_1)^2a_{L2}a_{T2}\xi^2\}\sinh(a_{L1}h_1)\sinh(a_{T1}h_1)$$

$$-\rho_1\rho_2\omega^4\{a_{L1}a_{T2}\sinh(a_{L1}h_1)\cosh(a_{T1}h_1)+a_{T1}a_{L2}\cosh(a_{L1}h_1)\sinh(a_{T1}h_1)\} , \quad (12.5c)$$

$$P_4 = \{\xi^2[2(\mu_2-\mu_1)\xi^2-(\rho_2-\rho_1)\omega^2]^2-a_{L2}a_{T2}[2(\mu_2-\mu_1)\xi^2+\rho_1\omega^2]^2\}\cosh(a_{L1}h_1)\sinh(a_{T1}h_1)$$

$$-a_{L1}a_{T1}\{[2(\mu_2-\mu_1)\xi^2-\rho_2\omega^2]^2-4(\mu_2-\mu_1)^2a_{L2}a_{T2}\xi^2\}\sinh(a_{L1}h_1)\cosh(a_{T1}h_1)$$

$$-\rho_1\rho_2\omega^4\{a_{L1}a_{T2}\sinh(a_{L1}h_1)\sinh(a_{T1}h_1)+a_{T1}a_{L2}\cosh(a_{L1}h_1)\cosh(a_{T1}h_1)\} . \quad (12.5d)$$

It should be noted that d_1 is replaced by h_1 in these forms since they are equivalent (see Figure 15). The expression for the subbottom impedance in equation (12.5) represents the effective impedance of the two-layered subbottom.

An integral expression for the Green's function for this special case is obtained by substituting equation (12.5) into equation (9.25) and inserting the latter equation into equation (9.9). This form is omitted here because it is rather cumbersome. It can be shown that the result for the special case where the subbottom is a two-layered solid halfspace is consistent with the previous result for the special case where the subbottom is a solid halfspace. One simply allows the physical parameters in both viscoelastic layers to be the same, whereby there is effectively one layer (a halfspace). Upon setting $\rho_2 = \rho_1$, $\lambda_2' = \lambda_1'$, $\mu_2' = \mu_1'$, $\lambda_2'' = \lambda_1''$, and $\mu_2'' = \mu_1''$ in equations (12.5), the expression for the effective impedance of the two-layered subbottom reduces to a

form which, upon substitution into equation (9.25), yields the expression for the Green's function in equation (12.2). A second method of check consists of allowing the thickness of the first viscoelastic layer to approach infinity, whereby the presence of the second viscoelastic layer is effectively disregarded. Upon taking the limit as $h_1 \to \infty$, the expression for the Green's function for the two-layered subbottom reduces to the form in equation (12.2), where the subbottom is a halfspace. This result also agrees with Pekeris's (1948) result for a three-layered liquid halfspace, if one disregards the contributions due to viscoelasticity and rigidity in both layers of the two-layered viscoelastic halfspace. This may be accomplished by setting the material parameters $\mu_1' = \lambda_1'' = \mu_1'' = \mu_2' = \lambda_2'' = \mu_2'' = 0$ in the integral expression for the Green's function for the two-layered subbottom. The present result also contains an additional $1/4\pi$ factor due to the Green's function formalism.

Liquid Layer of Infinite Depth

A special case of practical interest is the limiting case where the depth, h_0, of the liquid layer covering the viscoelastic subbottom becomes infinite. This case provides a model useful where reflections from the water surface are unimportant: for bottom-bounce testing where $h_0 \to \rho$, or for near-bottom pulse testing. Consequently, this special case is treated in detail here, and the numerical analysis that follows is based on the analytical expressions developed herein.

The Green's function for this special case may be obtained directly from the general expression for the Green's function in equation (9.25). Upon taking the limit as $h_0 \to \infty$, the Green's function

in equation (9.25) reduces to

$$G(\xi,z,z';\omega) = \frac{e^{-a_0 z_>}}{a_0}\left\{\frac{\sinh(a_0 z_<) + \frac{ia_0}{\rho_0\omega} Z \cosh(a_0 z_<)}{1 + \frac{ia_0}{\rho_0\omega} Z}\right\} . \quad (12.6)$$

After expanding the hyperbolic functions in the numerator and rearranging terms, this equation may be rewritten in the following form:

$$G(\xi,z,z';\omega) = \frac{e^{-a_0(z_>-z_<)}}{2a_0} - \left\{\frac{1 - \frac{ia_0}{\rho_0\omega} Z}{1 + \frac{ia_0}{\rho_0\omega} Z}\right\} \frac{e^{-a_0(z_>+z_<)}}{2a_0} . \quad (12.7)$$

Each of these terms is physically significant. The first term is the free-space Green's function for the liquid medium, and represents the response from the direct wave propagating through the water from the source to the receiver. The second term is expressive of the boundary effect, representing the response due to the presence of the subbottom. After integration, this term yields the reflected wave, surface (Stonely) waves, and refraction arrivals. It should be pointed out that the Green's function in equation (12.7) is also applicable to any subbottom.

Equation (12.7) is the Fourier-Bessel transformed form of the Green's function. To obtain the Green's function in the space domain, $G(\vec{x},\vec{x}';\omega)$, one must apply the inverse Fourier-Bessel transformation given in equation (9.9). Substituting the transformed expression for the Green's function in equation (12.7) into the inverse Fourier-Bessel transformation in equation (9.9) yields

$$G(\vec{x},\vec{x}';\omega) = G_f(\vec{x},\vec{x}';\omega) + G_b(\vec{x},\vec{x}';\omega) , \quad (12.8)$$

where

$$G_f = \frac{1}{4\pi} \int_0^\infty \frac{e^{-a_0|z-z'|}}{a_0} J_0(\xi\rho)\xi d\xi \quad , \tag{12.8a}$$

$$G_b = \frac{1}{4\pi} \int_0^\infty \frac{e^{-a_0(z+z')}}{a_0} \Gamma(\xi) J_0(\xi\rho)\xi d\xi \quad , \tag{12.8b}$$

and

$$\Gamma(\xi) = \frac{\frac{ia_0}{\rho_0\omega} Z - 1}{\frac{ia_0}{\rho_0\omega} Z + 1} \quad . \tag{12.8c}$$

The notation employed earlier in the development is resumed here. The integration for $G_f(\vec{x},\vec{x}';\omega)$ may be performed readily following Sommerfeld (1949), giving:

$$G_f(\vec{x},\vec{x}';\omega) = \frac{e^{-ik_0R}}{4\pi R} \quad , \tag{12.9}$$

where

$$R = [\rho^2+(z-z')^2]^{1/2} \tag{12.9a}$$

is the distance from the source to the receiver. The evaluation of the integral for $G_b(\vec{x},\vec{x}';\omega)$, which corresponds to reflected sound waves, is more difficult, however. This integral is the subject of the analytical development that follows.

The integral G_b in equation (12.8b) can be evaluated analytically by performing a contour integration in the complex ξ-plane, or numerically

on a digital computer. Efforts to evaluate this integral exactly by performing a numerical integration on the computer, have proven to be rather expensive, rendering this method of evaluation impractical. This difficulty is attributed to the behavior of the integrand, which, when plotted versus the variable of integration ξ, displays large, rapid fluctuations. The fluctuations result in large computation times, serving to make the exact integration procedure an expensive undertaking. The efforts referred to here were directed toward the special cases where the ocean subbottom was modeled as a solid halfspace and a two-layered solid halfspace.

The analytical approach for the evaluation of G_b employs complex variable techniques, involving analytical continuation of the integrand and choosing an appropriate path of integration in the complex plane. The analytical approach does not lead to a closed-form solution for G_b due to the presence of poles and branch points in the integrand. However, there exist several analytical techniques for the approximate evaluation of integrals of this type. The saddle-point method, an analytical technique for the asymptotic evaluation of radiation integrals of the form given in equation (12.8b) for G_b, entails deforming the original path of integration in the complex plane in such a way that the integrand is significant for only a small region in the new path of integration. This method is applicable when one of the parameters in the integrand becomes large. In this case, an asymptotic expansion of the term containing the large parameter is made, and the leading term is integrated to yield the result. The saddle-point method yields the reflected field, which is of primary importance for the identification of the ocean subbottom. The pole and branch-point wave contributions,

which include surface waves, leaky waves, lateral waves and refracted waves, are disregarded by this method of evaluation. The saddle-point method has been discussed by many of the investigators mentioned in the introduction in relation to special cases of the present field problem. More recently, Magnuson (1972, 1972b, 1975) applied this technique to the integral expression he developed for a liquid halfspace overlying a viscoelastic halfspace. An enlightening illustration of the principles fundamental to the application of this technique to wave propagation problems is provided by M. Yildiz (1964, 1966).

For subsequent application of the saddle-point method, it is desirable to cast the Fourier-Bessel transformation in equation (12.8b) into an alternative form in which the integration over ξ extends from $-\infty$ to ∞. Upon introducing the relation

$$J_0(\xi\rho) = \frac{1}{2}[H_0^{(1)}(\xi\rho)+H_0^{(2)}(\xi\rho)] \ , \tag{12.10}$$

where $H_0^{(1,2)}(x)$ is the Hankel function of the first (second) kind of order zero and argument x, one may write equation (12.8b) as

$$G_b(\vec{x},\vec{x}';\omega) = I_1 + I_2 \ , \tag{12.11}$$

$$I_1 = \frac{1}{8\pi}\int_0^\infty \frac{e^{-a_0(z+z')}}{a_0}\Gamma(\xi)H_0^{(1)}(\xi\rho)\xi d\xi \ , \tag{12.11a}$$

$$I_2 = \frac{1}{8\pi}\int_0^\infty \frac{e^{-a_0(z+z')}}{a_0}\Gamma(\xi)H_0^{(2)}(\xi\rho)\xi d\xi \ . \tag{12.11b}$$

When one introduces the circuital relation

$$H_0^{(1)}(xe^{i\pi}) = -H_0^{(2)}(x) \tag{12.12}$$

and the change of variables $\bar{\xi} = \xi \exp(-i\pi)$ in the integrand of I_1 in equation (12.11a), the representation in equation (12.11) becomes

$$G_b = \frac{1}{8\pi} \int_{-\infty}^{\infty} \frac{e^{-a_0(z+z')}}{a_0} \Gamma(\xi) H_0^{(2)}(\xi\rho)\xi d\xi \quad . \tag{12.13}$$

This integral is valid provided that $\Gamma(\xi)$ is an even function of ξ, a requirement satisfied by every special case developed from the multilayer formalism herein. The choice of transformation involving $H_0^{(2)}$ instead of $H_0^{(1)}$ is motivated by the fact that, for a time dependence $\exp(i\omega t)$, the former satisfies the radiation condition at $\rho \to \infty$ in a natural manner and facilitates the subsequent asymptotic evaluation of the integral.

To illustrate the saddle-point method, the exponential terms in the integrand of the integral for G_b in equation (12.13) are examined more closely. First, the nondimensional variable of integration x is defined in terms of the wavenumber k_0 in the liquid by $x = \xi/k_0$. In addition, the nondimensional parameters $\gamma_\rho = k_0\rho$ and $\gamma_z = k_0(z+z')$ are introduced. Upon applying the high frequency assumption by using the asymptotic expression for the Hankel function, the exponential terms in the integrand of G_b in equation (12.13) can be expressed as

$$e^{-i[\gamma_\rho x + (1-x^2)^{1/2}\gamma_z]} \quad . \tag{12.14}$$

Then one introduces the angle of incidence θ (see Figure 16) defined by

$$\theta = \tan^{-1}\left(\frac{\rho}{z+z'}\right) = \tan^{-1}\left(\frac{\gamma_\rho}{\gamma_z}\right) . \tag{12.15}$$

The quantities ρ and $(z+z')$ may be expressed as

$$\rho = R_I \sin\theta , \quad z + z' = R_I \cos\theta , \tag{12.16}$$

where

$$R_I = [\rho^2 + (z+z')^2]^{1/2} . \tag{12.16a}$$

Expression (12.14) may be written using these results as follows:

$$e^{-k_0 R_I f(x)} , \tag{12.17}$$

where

$$f(x) = i[x \sin\theta + (1-x^2)^{1/2} \cos\theta] . \tag{12.17a}$$

The parameter $k_0 R_I$ may be written as γ_I, a ratio of the path length of the reflected wave to the wavelength. Now the parameter $\gamma_I = k_0 R_I$ is assumed to be large, or $\gamma_I >> 1$, defining a radiation zone in the liquid field. In the complex z-plane the exponential term (12.17) decays rapidly due to the large parameter γ_I, provided that the quantity $f(z)$ is not too small. This implies that a portion of the integrand predominates when the integral G_b is evaluated. Upon locating the saddle-point, which occurs at $x = \sin\theta$, or $\xi = k_0 \sin\theta$, and defining the path of integration, the saddle-point integration is

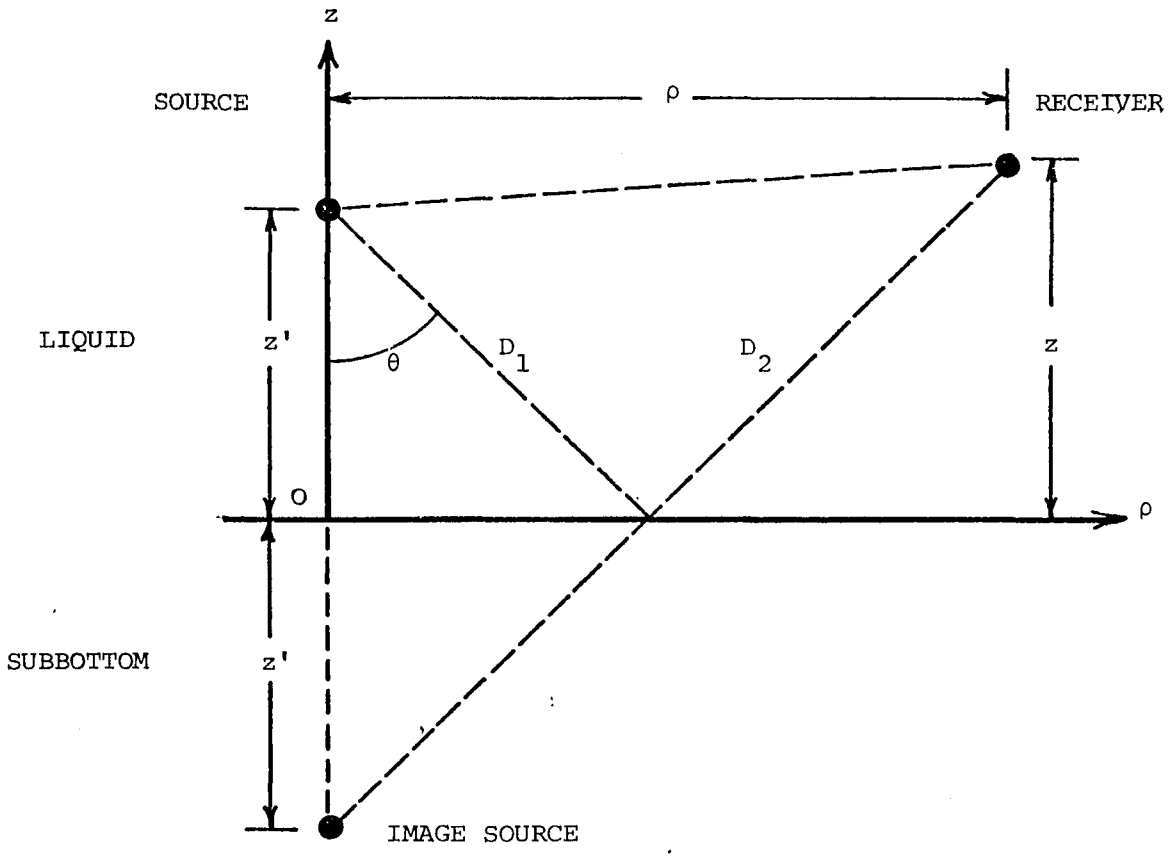

Figure 16. Geometry of the source and receiver in the liquid layer.

performed, yielding

$$G_b(\vec{x},\vec{x}';\omega) = \Gamma(k_0 \sin\theta)\, \frac{e^{-ik_0 R_I}}{4\pi R_I} \quad . \tag{12.18}$$

This is the expression for the reflected wave. It has the spherical spreading factor R_I^{-1}, and propagates along the path shown in Figure 16 with the speed c_0. The result for G_b in equation (12.18) is general in the sense that no characteristics of the subbottom were specified for its evaluation. An expression for $\Gamma(k_0 \sin\theta)$ for the special case where the subbottom is a viscoelastic halfspace is developed explicitly in what follows.

With the use of equations (12.1) and (12.8c), the quantity $\Gamma(k_0 \sin\theta)$ in equation (12.18) may be written for a subbottom consisting of a viscoelastic halfspace as

$$\Gamma(k_0 \sin\theta) = \left\{ \frac{\rho_1 a_0 [(2\xi^2 - k_{T1}^2)^2 - 4a_{L1}a_{T1}\xi^2] - \rho_0 k_{T1}^4 a_{L1}}{\rho_1 a_0 [(2\xi^2 - k_{T1}^2)^2 - 4a_{L1}a_{T1}\xi^2] + \rho_0 k_{T1}^4 a_{L1}} \right\}_{\xi = k_0 \sin\theta} \quad . \tag{12.19}$$

Upon evaluating the right-hand side and rearranging terms, equation (12.19) may be expressed as

$$\Gamma(\theta) = \frac{f_1 - f_2}{f_1 + f_2} \quad , \tag{12.20}$$

where

$$f_1 = \rho_1 c_{L1} \cos\theta \left[\left(2\frac{c_{T1}^2}{c_0^2}\sin^2\theta - 1 \right)^2 + 4\frac{c_{T1}^3}{c_0^2 c_{L1}}\sin^2\theta \left(1 - \frac{c_{L1}^2}{c_0^2}\sin^2\theta\right)^{1/2} \left(1 - \frac{c_{T1}^2}{c_0^2}\sin^2\theta\right)^{1/2} \right] \tag{12.20a}$$

and

$$f_2 = \rho_0 c_0 \left(1 - \frac{c_{L1}^2}{c_0^2} \sin^2\theta\right)^{1/2} \quad . \tag{12.20b}$$

It is observed that the quantity $\Gamma(k_0 \sin\theta)$ in equation (12.19) represents the plane-wave reflection coefficient for a plane sound wave incident from a liquid on a liquid-solid interface (Ewing et al., 1957; Brekhovskikh, 1960). It is concluded that the saddle-point method for the evaluation of G_b yields a result similar to ray theory. The reflection coefficient $\Gamma(\theta)$ is complex here due to the introduction of viscoelasticity into the subbottom. An expression for $\Gamma(k_0 \sin\theta)$ in equation (12.18) can be written for the special case where the subbottom is a two-layered viscoelastic halfspace with the use of equations (12.5) and (12.8c). This expression is omitted here because it is rather lengthy.

In summary, a general expression for the total acoustic response, the sum of the direct wave and the reflected wave, may be written from equations (12.8), (12.9), and (12.18) as

$$G(\vec{x},\vec{x}';\omega) = \frac{e^{-ik_0 R}}{4\pi R} + \Gamma(\theta) \frac{e^{-ik_0 R_I}}{4\pi R_I} \quad . \tag{12.21}$$

This result could also be deduced directly by arguments of geometrical optics. Thus, for the limiting case of a liquid layer of infinite depth, the Green's function for the acoustic response from any subbottom may be written from equation (12.21), provided that the appropriate reflection coefficient $\Gamma(\theta)$, which is dependent upon the acoustic properties of the subbottom, is inserted into this form. It should be kept in mind

that the contribution to this result from the integral for G_b was obtained by the saddle-point method of integration, and provides a good approximation to the exact integration when the condition discussed earlier is satisfied.

CHAPTER XIII

NUMERICAL ANALYSIS

In the foregoing chapters, a sophisticated and realistic analytical model was proposed for application to the remote acoustic sensing of marine sediments on the continental shelf. The approach suggested therein for use in the remote acoustic identification and classification of marine sediments on the continental shelf is based on the usefulness of information that can be obtained by studying the reflection of sound waves from the ocean's subbottom. Accordingly, an acoustic signal is transmitted in the ocean and the return signal from the subbottom is analyzed, the subbottom's property of reflectivity revealing information useful for its identification. In order to accurately model the physical processes which occur in the ocean-subbottom system to form the return signal, the model proposed in the analytical development includes improvements in the model of the subbottom. The improved geoacoustic model of the continental shelf takes into account the effects of rigidity, internal energy dissipation, and stratification in the sedimentary subbottom. In addition, the model proposed here has the capability of accommodating layers of viscous liquids, for example, petroleum, which might occur in the subbottom.

In this chapter, numerical analysis is presented for a study on the reflection of sound waves incident from a liquid halfspace (ocean) on an interface with a liquid-viscoelastic multilayered halfspace (continental shelf), which is described by the improved geoacoustic model discussed above. The integral for G_b in equation (12.8b) and

the saddle-point approximation to this integral in equation (12.18), both of which give the contribution of the wave reflected from the subbottom, are to be evaluated numerically by computer for special cases of the subbottom. A comparison of these numerical results is desired in order to determine the accuracy, and hence, assess the validity of the saddle-point approximation, which is dependent upon yet to be prescribed conditions regarding the frequency of the sound source and the geometry of the source and receiver. In addition, less sophisticated acoustic theories used in the study of the reflection of sound waves from the ocean's subbottom, which disregard the effects of rigidity and internal energy dissipation in their model of the subbottom, are analyzed for the purpose of comparison. Oftentimes these theories express the acoustic return from the subbottom as a plane-wave reflection coefficient of the form for $\Gamma(\theta)$ in equation (12.20), which is independent of the geometry of the source and receiver. Therefore, in order to establish a basis for comparison with results from these acoustic theories, the Green's functions G_b for the exact and approximate estimation of the reflected field are normalized with respect to the reflection coefficient $\Gamma(\theta)$. The magnitudes of these normalized reflection coefficients are then plotted versus the angle of incidence θ . It is anticipated that the variation of the magnitude of the reflection coefficient as a function of the angle of incidence θ may be useful for identifying various sediment types which occur on the continental shelf. Special cases where the subbottom is a halfspace and a two-layered halfspace are analyzed here for subbottoms with varying properties. In particular, the stratification and composition of the subbottom is

varied, using Hamilton's data (1974a) for the properties of marine sediments on the continental shelf.

The present numerical study of the reflection of sound waves from the ocean's subbottom is an extension of the previous studies of Newman (1973) and Magnuson et al. (1973). They numerically evaluated the Green's function for the reflected wave for a subbottom consisting of a viscoelastic halfspace. They also included results for the saddle-point approximation and the less sophisticated acoustic theories discussed earlier. Hamilton's data (1971a) for the properties of marine sediments on the continental shelf was used to characterize the subbottom. Numerical results for the case where the subbottom consists of a two-layered halfspace were not included in their studies. Their results showed that the acoustic return signal from the subbottom is sensitive to changes in the sediment type over a wide range of angles of incidence. The potential usefulness of the results from their preliminary investigation inspired the present extension to their work. The present numerical study is based on corrected laboratory data on the properties of marine sediments published recently by Hamilton (1974a). In addition, in-situ values for compressional- and shear-wave attenuation in these sediments is predicted in accordance with the method outlined by Hamilton (1972).

At this point it is useful to review the analytical forms which are to be analyzed numerically on the computer. The integral expression for G_b in equation (12.8b) for the reflected wave from the subbottom is to be evaluated for the special cases where the subbottom is a halfspace and a two-layered halfspace. For the special case where the subbottom

is a viscoelastic halfspace, one may develop from equations (12.1), (12.8b), and (12.8c) the explicit expression for G_b given by

$$G_b(\vec{x},\vec{x}';\omega) = \int_0^\infty \frac{e^{-a_0(z+z')}}{a_0} \left\{\frac{\rho_1 a_0[(2\xi^2-k_{T1}^2)^2-4a_{L1}a_{T1}\xi^2]-\rho_0 a_{L1}k_{T1}^4}{\rho_1 a_0[(2\xi^2-k_{T1}^2)^2-4a_{L1}a_{T1}\xi^2]+\rho_0 a_{L1}k_{T1}^4}\right\} J_0(\xi\rho)\xi d\xi \ . \tag{13.1}$$

The corresponding expression for the special case of a two-layered viscoelastic halfspace is obtained by the use of equations (12.5), (12.8b), and (12.8c). This expression is too cumbersome to include in the text. The integral expression for G_b contains a complete description of the acoustic return signal as a function of the acoustic properties which describe the water and sediment, the geometry of the source and receiver, and the frequency of the acoustic signal transmitted. The Green's function G_b is a complex quantity due to the introduction of viscoelasticity into the subbottom. In order to introduce the angle of incidence θ into the integral for G_b in equation (13.1), the quantities ρ and $(z+z')$ are replaced by $R_I \sin\theta$ and $R_I \cos\theta$ (see equations (12.16)), respectively. The quantity R_I is fixed at $R_I = 10m$ in the numerical analysis. This implies that the positions of the source and receiver change as the angle of incidence varies. It was mentioned earlier that the numerical evaluation of the integral for G_b for different subbottoms was quite expensive.

The saddle-point approximation for G_b in equation (12.18) is to be evaluated for the special cases where the subbottom is a halfspace and a two-layered halfspace. For the special case where the subbottom is a viscoelastic halfspace, an explicit expression for G_b is

given by

$$G_b(\vec{x},\vec{x}';\omega) = \Gamma(\theta)\,\frac{e^{-ik_0R_I}}{4\pi R_I} = \frac{f_1 - f_2}{f_1 + f_2}\,\frac{e^{-ik_0R_I}}{4\pi R_I} \quad , \qquad (13.2)$$

where

$$f_1 = \rho_1 c_{L1}\cos\theta\left[\left(2\frac{c_{T1}^2}{c_0^2}\sin^2\theta - 1\right)^2 + 4\frac{c_{T1}^3}{c_0^2 c_{L1}}\sin^2\theta\left(1 - \frac{c_{L1}^2}{c_0^2}\sin^2\theta\right)^{1/2}\left(1 - \frac{c_{T1}^2}{c_0^2}\sin^2\theta\right)^{1/2}\right] \qquad (13.2a)$$

and

$$f_2 = \rho_0 c_0\left(1 - \frac{c_{L1}^2}{c_0^2}\sin^2\theta\right)^{1/2} \quad . \qquad (13.2b)$$

The quantity $\Gamma(\theta)$ is recognizable as the plane-wave reflection coefficient for a plane sound wave incident from a liquid on a liquid-solid interface. The compressional- and shear-wave velocities, c_{L1} and c_{T1}, are complex quantities due to the introduction of viscoelasticity into the subbottom. The quantity R_I is fixed at $R_I = 10\text{m}$ in the numerical analysis in order to be consistent with the numerical evaluation of the integral expression for G_b. It was mentioned earlier that a comparison of the numerical results for the integral for G_b and the saddle-point approximation to this integral was desirable.

In addition to the comparison of the numerical results for the integral for G_b and the saddle-point approximation to the integral for G_b, it is of interest to compare these results with those obtained with less sophisticated acoustic theories, which disregard the effects of rigidity and internal energy dissipation in their model of the subbottom. Many of these theories express the acoustic return from the

subbottom as a plane-wave reflection coefficient. If the contribution due to viscoelasticity in the complex compressional- and shear-wave velocities, c_{L1} and c_{T1} is disregarded, the reflection coefficient $\Gamma(\theta)$ in equation (13.2) reduces to the form appropriate for a subbottom that is an elastic halfspace. An expression for $\Gamma(\theta)$ for this case may be developed from equations (10.5a), where for no damping one sets $b_{L1} = b_{T1} = 0$ to effect the transition

$$c_{L1}^2 \to c_{Le1}^2 = \frac{\lambda_1' + 2\mu_1'}{\rho_1}, \quad c_{T1}^2 \to c_{Te1}^2 = \frac{\mu_1'}{\rho_1} \tag{13.3}$$

in equation (13.2). If the contribution due to shear waves in the subbottom is disregarded by setting $\mu_1' = \mu_1'' = 0$, the reflection coefficient $\Gamma(\theta)$ in equation (13.2) reduces to

$$\Gamma(\theta) = \frac{\rho_1 c_{L1}\cos\theta - \rho_0 c_0 \left(1 - \frac{c_{L1}^2}{c_0^2}\sin^2\theta\right)^{1/2}}{\rho_1 c_{L1}\cos\theta + \rho_0 c_0 \left(1 - \frac{c_{L1}^2}{c_0^2}\sin^2\theta\right)^{1/2}}, \tag{13.4}$$

where

$$c_{L1}^2 = \frac{\lambda_1' + i\omega\lambda_1''}{\rho_1}. \tag{13.4a}$$

If the contributions due to both viscoelasticity and rigidity in the subbottom are disregarded, one obtains an expression of the same form as equation (13.4), but now $c_{L1}^2 = \lambda_1'/\rho_1$. This is the classical Rayleigh reflection coefficient, which is the plane-wave reflection coefficient for a plane sound wave incident from a liquid on a liquid-liquid interface. It is observed that the effect of disregarding the

contributions due to viscoelasticity and rigidity in the subbottom is to model the sea floor as a liquid. This is the simplest model of the subbottom which is employed in the study of the reflection of sound waves from the ocean floor. It should be pointed out that for normal incidence ($\theta=0^{o}$), the reflection coefficient $\Gamma(\theta)$ in equation (13.4) assumes the form

$$\Gamma = \frac{\rho_1 c_{L1} - \rho_0 c_0}{\rho_1 c_{L1} + \rho_0 c_0} \quad . \tag{13.5}$$

It is observed from equations (13.2) that, even if the subbottom is capable of supporting and transmitting shear waves, a consequence of using the reflection coefficient for normal incidence is to disregard the effects due to rigidity in the subbottom. In the introduction, it was mentioned that most investigators, in their efforts to use the acoustic return from the ocean floor for determining soil classifications and engineering properties of marine sediments, have studied reflection coefficients obtained for normal incidence.

In order to establish a basis for comparison for the numerical results obtained here with those of less sophisticated acoustic theories, it is necessary to normalize the exact and approximate evaluations of the reflected field, given by G_b, with respect to the reflection coefficients $\Gamma(\theta)$. Therefore, the numerical results for G_b are plotted in the normalized form $4\pi R_I|G_b|\times 100\%$, which gives a reflection coefficient in percent.

The reflection coefficient $4\pi R_I|G_b|\times 100\%$ is to be plotted versus the angle of incidence θ, which is defined in Figure 16, as the angle of incidence θ is varied from $\theta = 0^{o}$ (normal incidence)

to $\theta = 90^{\circ}$ (grazing incidence). Additionally, the bounce distance, BD, is kept constant at BD = 10m in the numerical analysis. The bounce distance is defined as the total distance along the path traveled by the reflected wave in the water. Referring to Figure 16, the distance traveled by the reflected wave from the source to the water-sediment interface to the receiver is given by

$$BD = D_1 + D_2 = R_I = [\rho^2+(z+z')^2]^{1/2} \quad . \tag{13.6}$$

In reference to the integral for G_b and the saddle-point approximation to the integral for G_b, it was mentioned that R_I would be fixed at $R_I = 10m$ in the numerical analysis. Now, this constraint may be viewed as holding the bounce distance BD constant.

The carrier frequency of the signal transmitted from the source is taken to be f = 5kHz for the numerical analysis. Thus, the acoustic waves transmitted from the source are monochromatic waves. The interrelationships between the wavelength λ_0, the wavenumber k_0, the wavevelocity c_0, and frequency ω ($\omega=2\pi f$) in the liquid are given by

$$\lambda_0 = \frac{2\pi}{k_0} = \frac{2\pi c_0}{\omega} \quad . \tag{13.7}$$

The frequency f = 5kHz corresponds to the wavelength $\lambda_0 \sim 0.3m$ in the water. It should be recalled that in the procedure by which the saddle-point approximation to the integral for G_b was obtained, it was assumed that the nondimensional quantity $\gamma_I = k_0 R_I$ is large, that is, $\gamma_I >> 1$. For the given constant values of the frequency of the signal and the bounce distance, $\gamma_I \sim 210$. Although this nondimensional quantity γ_I is much greater than unity, the behavior of exponential term (12.17) is

also dependent upon the exponent $f(x)$, which is a function of the angle of incidence θ. Recalling that the arrangement of the source and receiver change as the angle of incidence θ varies, it is of interest to note what effects different arrangements might have on the accuracy, and therefore, the validity of the saddle-point approximation under the conditions prescribed in this field problem. It is also of interest to note what effects the wavelength of the acoustic signal transmitted from the source might have on detecting layering in the subbottom.

The data used to characterize the elastic properties of the marine sediments, which comprise the various subbottoms considered in the numerical analysis, was taken from laboratory values of data reported by Hamilton (1974a) for the elastic properties of marine sediments on the continental terrace (shelf and slope). The laboratory values for these sediment properties were then corrected to in-situ values by the author according to the methods outlined by Hamilton (1971b). The corrected values for the elastic properties of these marine sediments are given in Table 2A in the text. The in-situ viscoelastic properties of marine sediments were obtained by following a method developed by Hamilton (1972), which allows prediction of compressional-wave attenuation in marine sediments, given the mean grain size or porosity of the sediment. The predicted values for the in-situ viscous properties of the marine sediment types in Table 2A were computed by the author for the Voigt viscoelastic model employed in this investigation. These values are given in Table 2B in the text. In the remainder of this work, the marine sediment types in Tables 2A and 2B are quite often denoted by the numbers which appear beside their names.

TABLE 2A

IN-SITU ELASTIC PROPERTIES OF MARINE SEDIMENTS*

Sediment Type	η %	ρ g/cm^3	c_L m/sec	κ dynes/cm^2 $\times 10^{10}$	λ' dynes/cm^2 $\times 10^{10}$	μ' dynes/cm^2 $\times 10^{10}$	c_T m/sec $\times 10^{1}$
Continental terrace (shelf and slope)							
1. Coarse sand	38.6	2.06	1808	6.69	6.70	0.030	12
2. Fine sand	44.8	1.95	1727	5.51	5.35	0.23	35
3. Very fine sand	49.8	1.86	1672	5.02	4.95	0.14	27
4. Silty sand	53.8	1.80	1642	4.50	4.3	0.26	37
5. Sandy silt	52.5	1.81	1638	4.45	4.2	0.31	41
6. Silt	54.2	1.77	1599	4.33	4.2	0.15	29
7. Sand-silt-clay	67.2	1.58	1555	3.59	3.5	0.17	33
8. Clayey silt	72.6	1.47	1522	3.32	3.28	0.060	20
9. Silty clay	75.9	1.43	1496	3.15	3.12	0.038	16

η, porosity; ρ, bulk saturated density; c_L, compressional-wave velocity; κ, bulk modulus; λ' μ', Lamé's constants; c_T, shear-wave velocity.

*Elastic properties were taken from laboratory values reported by Hamilton (1974a), and corrected to in-situ values by the techniques outlined by Hamilton (1971b). Elastic properties are given for a water depth of 31 meters in the San Diego Trough where the water density $\rho_0 = 1.025$ g/cm^3 and compressional-wave velocity $c_0 = 1505.37$ m/sec.

TABLE 2B

IN-SITU VISCOELASTIC PROPERTIES OF MARINE SEDIMENTS*

Sediment Type	b_L sec $\times 10^{-4}$	b_T sec $\times 10^{-4}$	λ' dynes/cm^2 $\times 10^{10}$	λ'' dyne-sec/cm^2 $\times 10^{6}$	μ' dynes/cm^2 $\times 10^{10}$	μ'' dyne-sec/cm^2 $\times 10^{6}$
Continental terrace (shelf and slope)						
1. Coarse sand	0.010	1.7	6.70	-0.035	0.030	0.051
2. Fine sand	0.010	0.19	5.35	-0.030	0.23	0.045
3. Very fine sand	0.013	0.35	4.95	-0.035	0.14	0.051
4. Silty sand	0.013	0.17	4.3	-0.030	0.26	0.045
5. Sandy silt	0.014	0.17	4.2	-0.035	0.31	0.051
6. Silt	0.013	0.30	4.2	-0.030	0.15	0.045
7. Sand-silt-clay	0.0020	0.035	3.5	-0.0038	0.17	0.0057
8. Clayey silt	0.0016	0.070	3.28	-0.0028	0.060	0.0041
9. Silty clay	0.0014	0.083	3.12	-0.0021	0.038	0.0032

b_L and b_T, damping coefficients; λ' and μ', elastic contribution of complex Lamé constants; λ'' and μ'', viscous contribution of complex Lamé constants.

*In-situ viscous properties were predicted by the method developed by Hamilton (1972), and adjusted to describe the Voigt viscoelastic model for the frequency f = 5kHz .

The physical parameters used in the numerical analysis to characterize petroleum are given by

$$\bar{\rho} = 0.912 \text{ g/cm}^3, \quad \bar{c} = 1326 \text{ m/sec}, \quad \bar{\lambda} = \bar{\rho}\,\bar{c}^2 = 1.60\times10^6 \text{ dynes/cm}^2$$

$$\bar{\zeta} = 0.9 \text{ dyne-sec/cm}^2, \quad \bar{\eta} = 0.3 \text{ dyne-sec/cm}^2, \tag{13.8}$$

where $\bar{\rho}$ is the mass density, $\bar{c}$ is the adiabatic sound velocity, $\bar{\zeta}$ is the bulk viscosity, and $\bar{\eta}$ is the shear viscosity. The values for the viscosities $\bar{\zeta}$ and $\bar{\eta}$ were selected from a wide range of viscosities characteristic of petroleum.

It is observed from a comparison of the graphs in Figures 17, 18a, 19a - c, and 20a - c that the saddle-point approximation to the integral for G_b agrees closely with the result obtained by the exact evaluation of the integral for G_b for small angles of incidence θ, and begins to deviate as the angle of incidence θ approaches grazing incidence. The discrepancy between the numerical results for the saddle-point approximation to the integral for G_b and the exact evaluation of the integral for G_b at higher angles of incidence is due to the closeness of the source and receiver to the liquid-solid interface. For a constant bounce distance, the source and receiver approach the water-sediment interface as the angle of incidence θ approaches grazing incidence ($\theta=90^o$). For angles of incidence approaching grazing incidence, higher order terms, which were deemed small in the asymptotic expansion discussed earlier, begin to make a significant contribution to G_b. It should be recalled that only the leading term in the asymptotic expansion discussed earlier was considered in order to obtain the expression for the saddle-point approximation for G_b which was used

in this numerical analysis. This phenomenon, where the geometrical optics approximation becomes less and less applicable as the receiver approaches the interface is discussed at length by Brekhovskikh (1960). If the bounce distance $BD = R_I$ was fixed at a value greater than $BD = 10m$, the approximation would be improved at larger angles of incidence.

It is observed from a comparison of Figures 19a - c and 20a - c that when the wavelength of the signal transmitted from the acoustic source is on the order of the thickness of the layer of sediment with finite thickness, the acoustic return signal is sensitive to the presence of both layers in the subbottom. However, as the thickness of this intermediate layer is increased and the wavelength of the signal remains fixed, the return from the subbottom detects only the intermediate layer. At a thickness of $h_1 = 3m$ for the intermediate layer, the return signal closely resembles that as if the intermediate layer was a halfspace. It is difficult to draw conclusions from a comparison of Figures 20a,b and 21a,b, regarding the sensitivity of the acoustic return to replacing the halfspace of sediment #1 with a halfspace of petroleum, since the scales on these graphs are different. A comparison of Figures 18a - d indicates that the acoustic return signal is more sensitive to effects of internal energy dissipation than it is to the effects of rigidity.

In general, it is observed that the magnitude of the acoustic return signal is greater at larger angles of incidence. The increased magnitude of the acoustic return signal at large oblique angles indicates that as the angle of incidence θ is increased, more acoustic energy is scattered back to the receiver, and less is transmitted away from the water-sediment interface into the sediment.

Additionally, it is observed that the sensitivity of the acoustic return signal to distinguishing between subbottoms composed of varying sediment types is improved at oblique angles of incidence as compared with the return at normal incidence. The quasi-periodic small variations in the magnitude of the curves in Figures 17 - 21 are due to the accurate modeling of the physical processes which occur in the ocean-subbottom system to form the return signal as the angle of incidence varies.

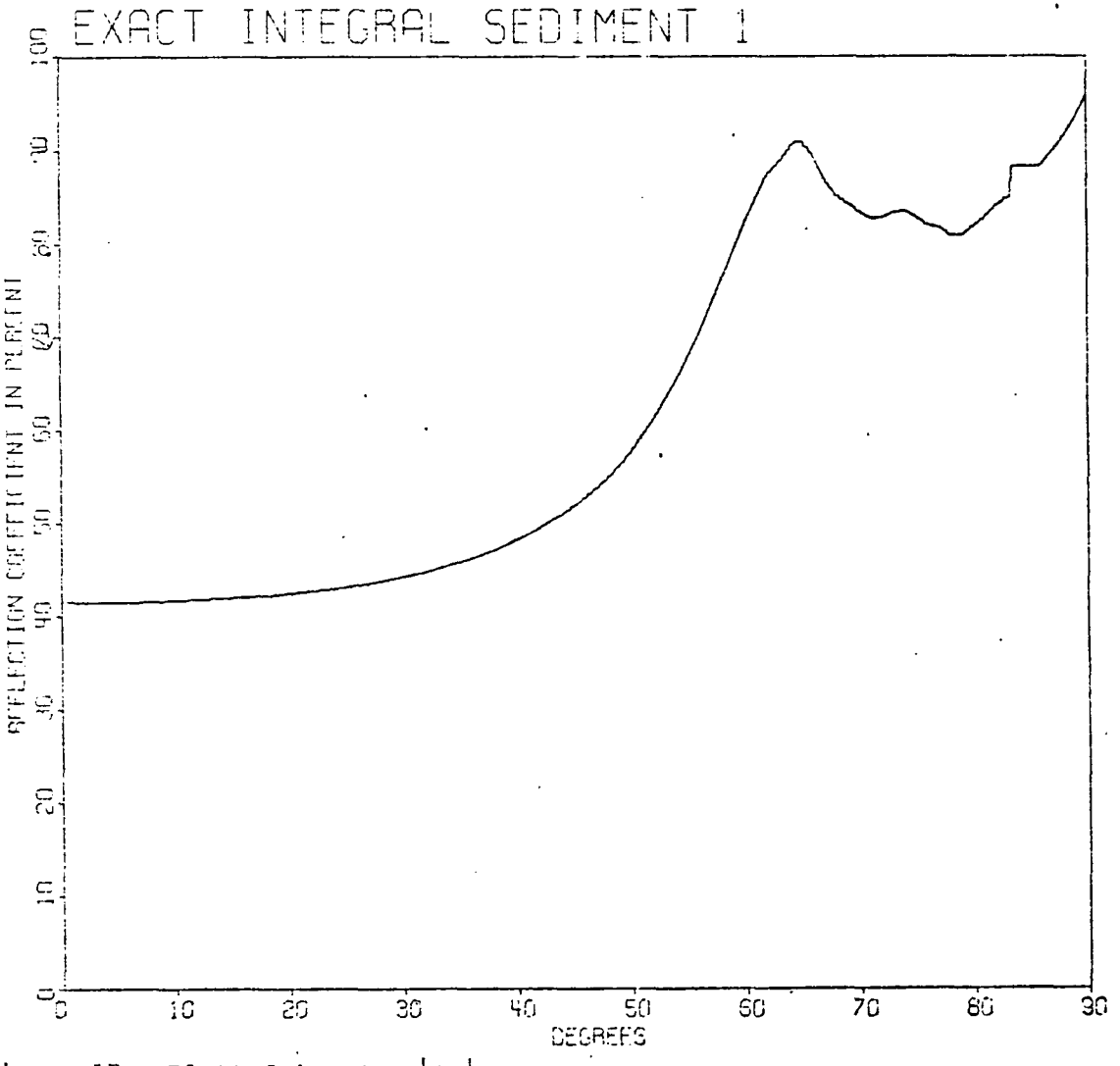

Figure 17. Plotted is $4\pi R_I|G_b|\times 100\%$ vs. θ for the exact integral for G_b, where the subbottom consists of a halfspace of sediment #1.

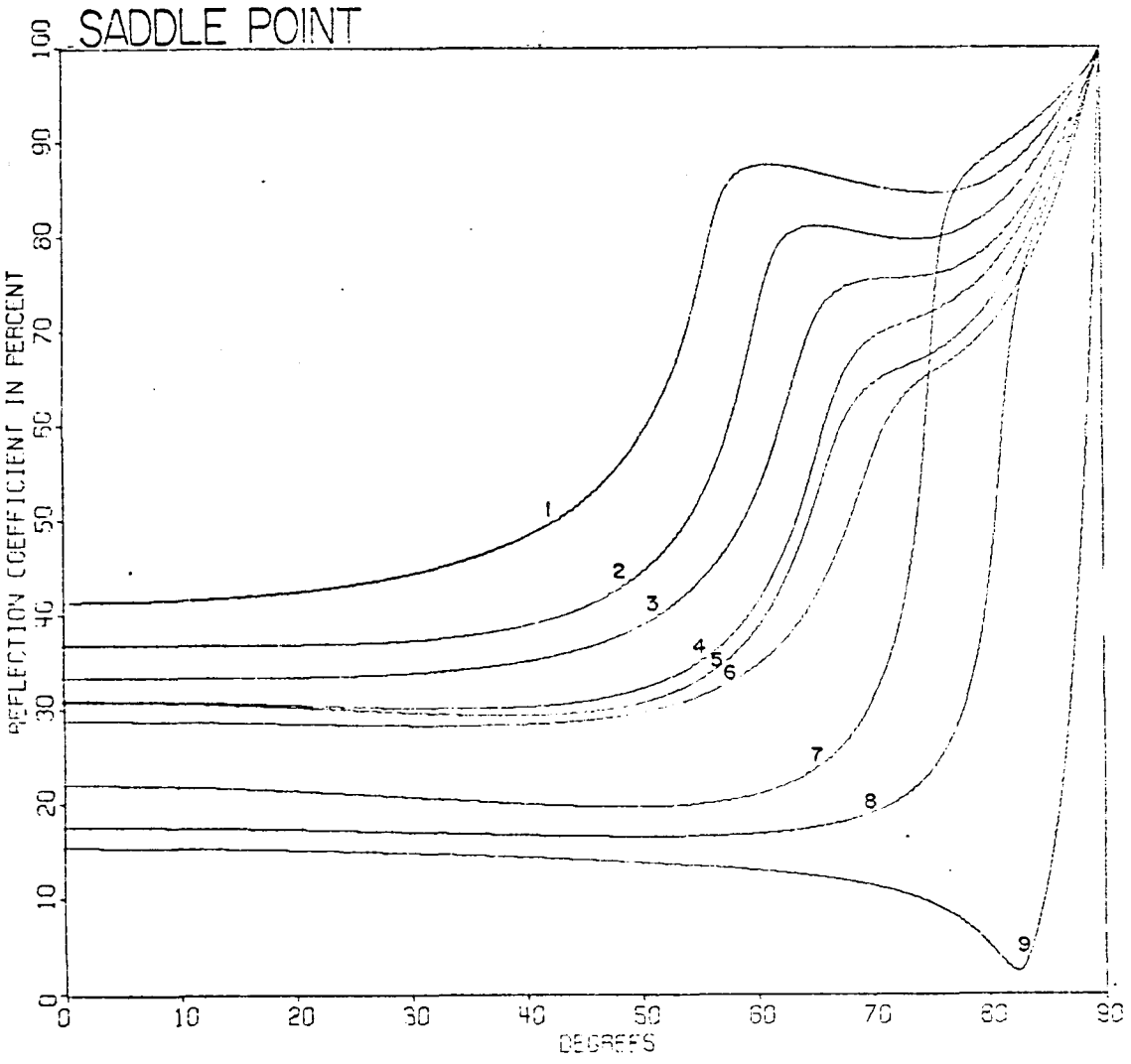

Figure 18a. Plotted is $4\pi R_I |G_b| \times 100\%$ vs. θ for the saddle-point approximation for G_b, where the subbottom consists of a halfspace of sediments #1-9.

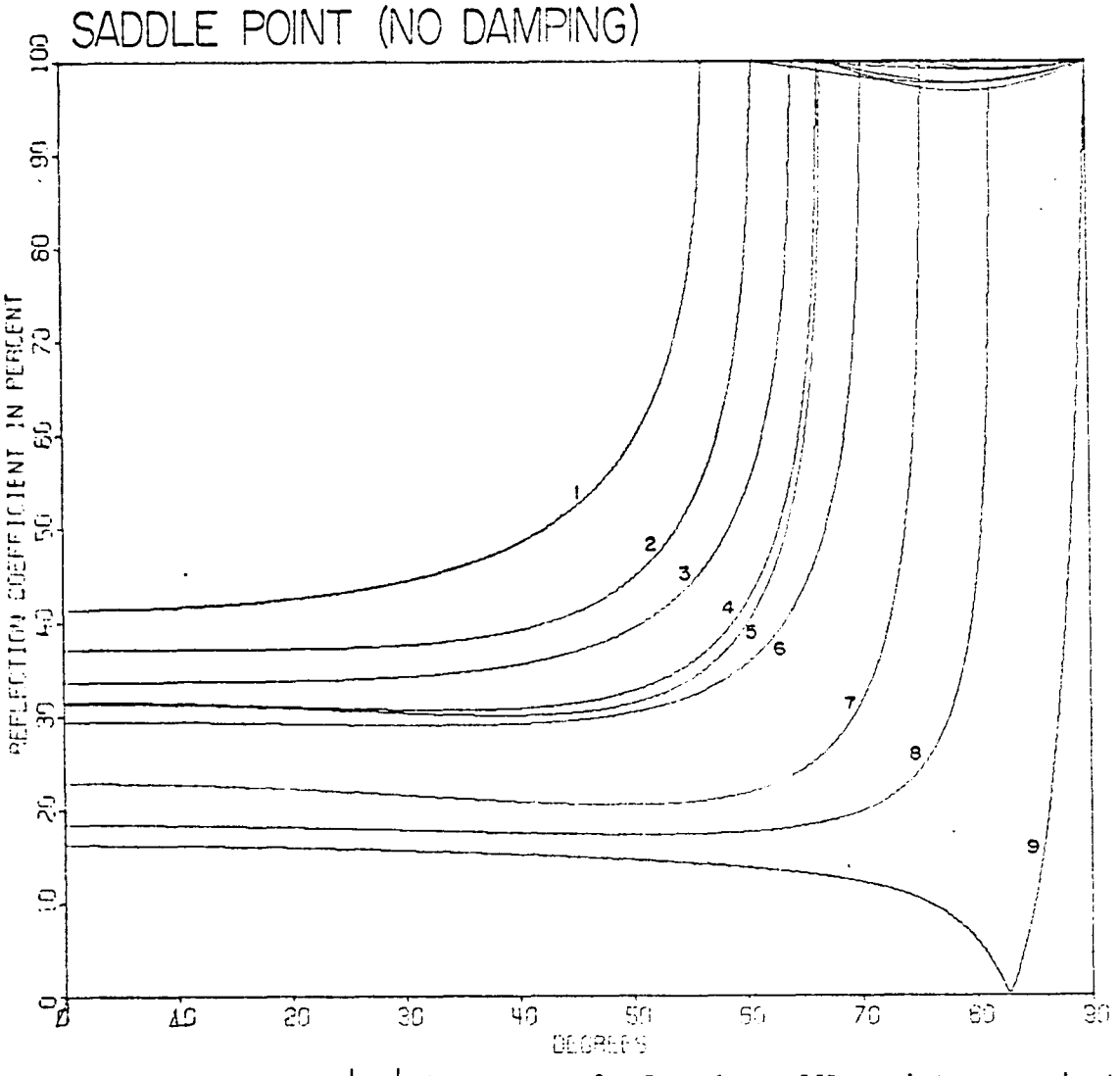

Figure 18b. Plotted is $4\pi R_I |G_b| \times 100\%$ vs. θ for the saddle-point approximation for G_b, where the subbottom (no damping) consists of a halfspace of sediments #1-9.

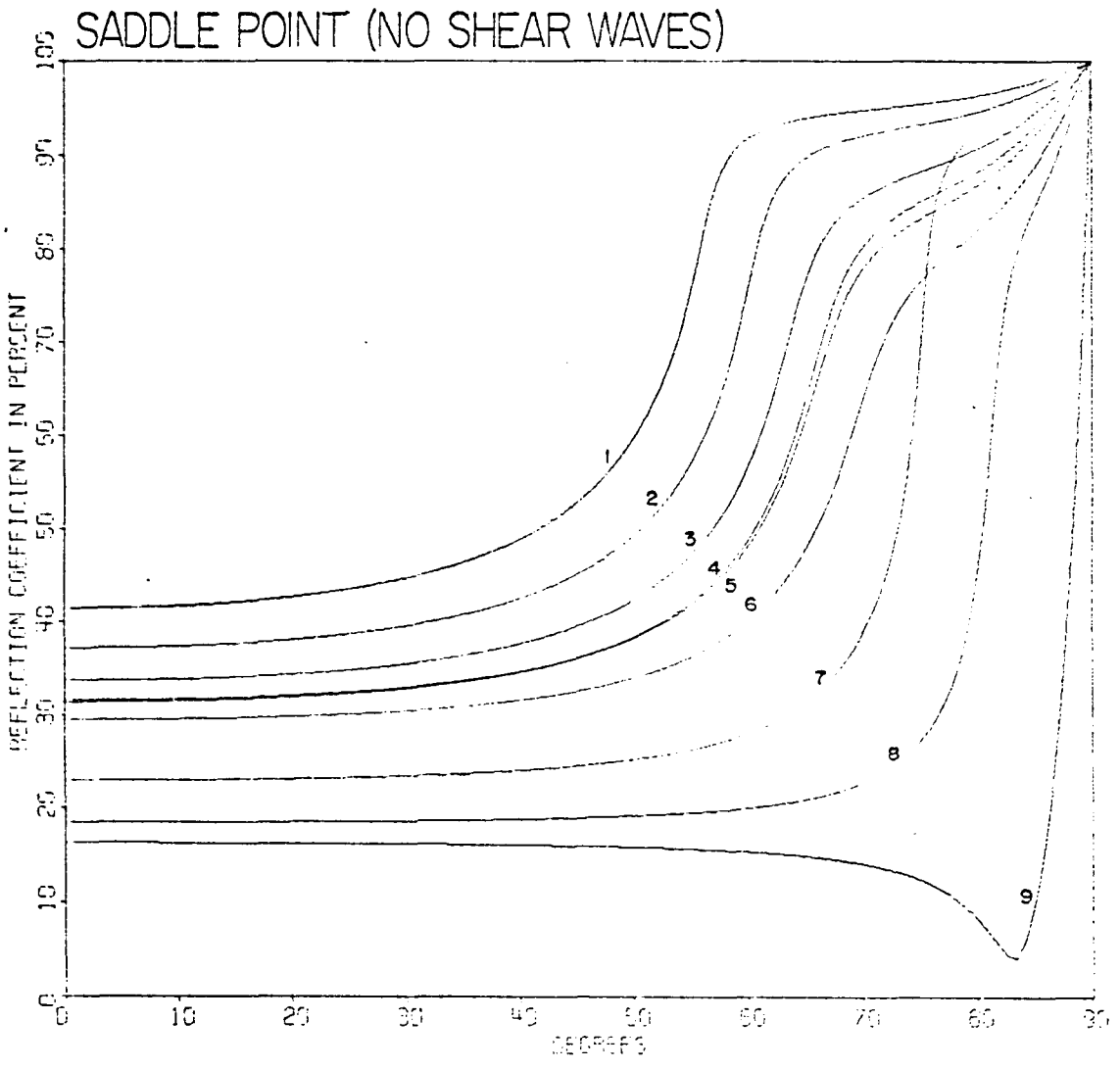

Figure 18c. Plotted is $4\pi R_I |G_b| \times 100\%$ vs. θ for the saddle-point approximation for G_b, where the subbottom (no shear waves) consists of a halfspace of sediments #1-9.

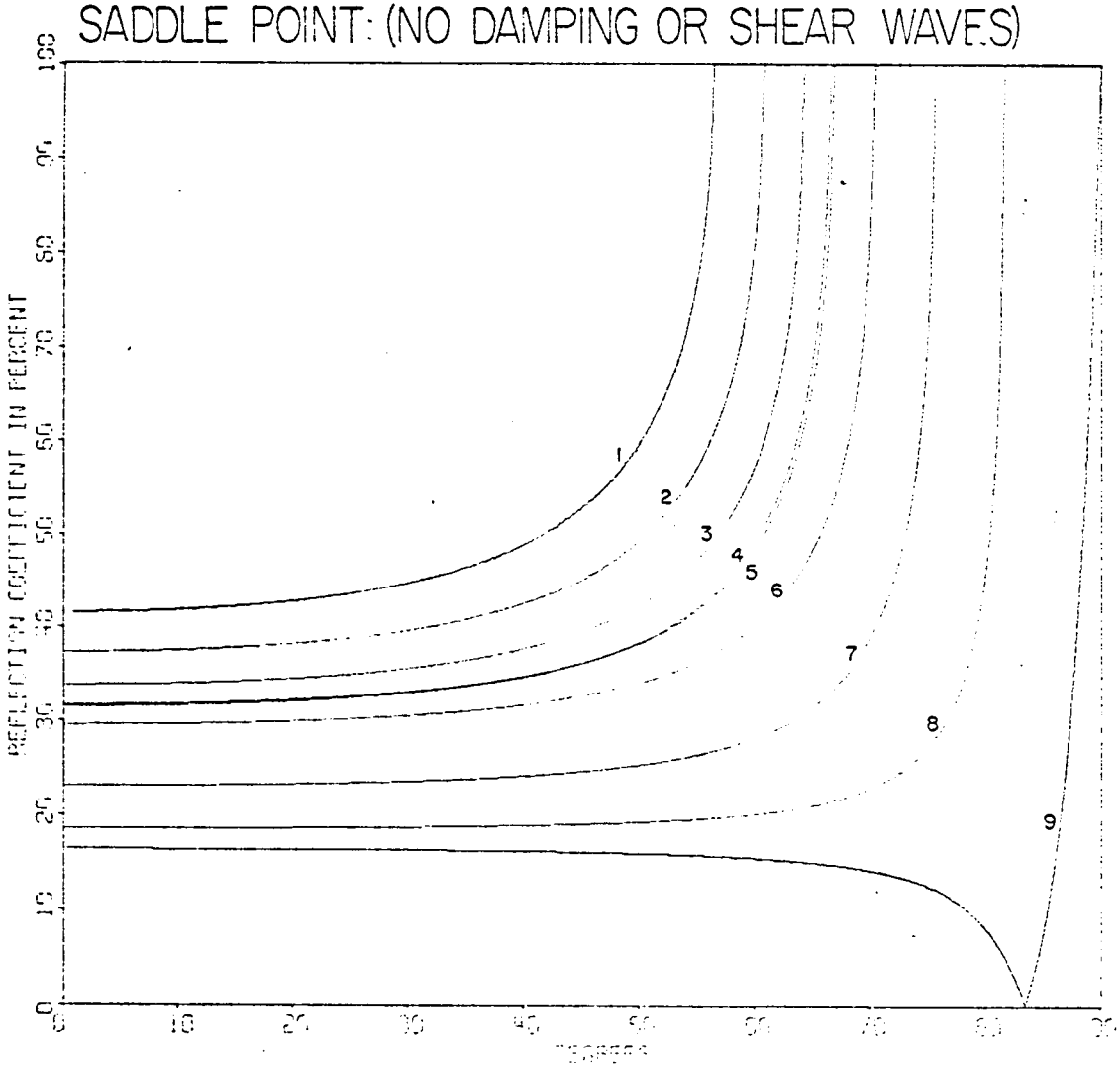

Figure 18d. Plotted is $4\pi R_I |G_b| \times 100\%$ vs. θ for the saddle-point approximation for G_b, where the subbottom (no damping, no shear waves) consists of a halfspace of sediments #1-9.

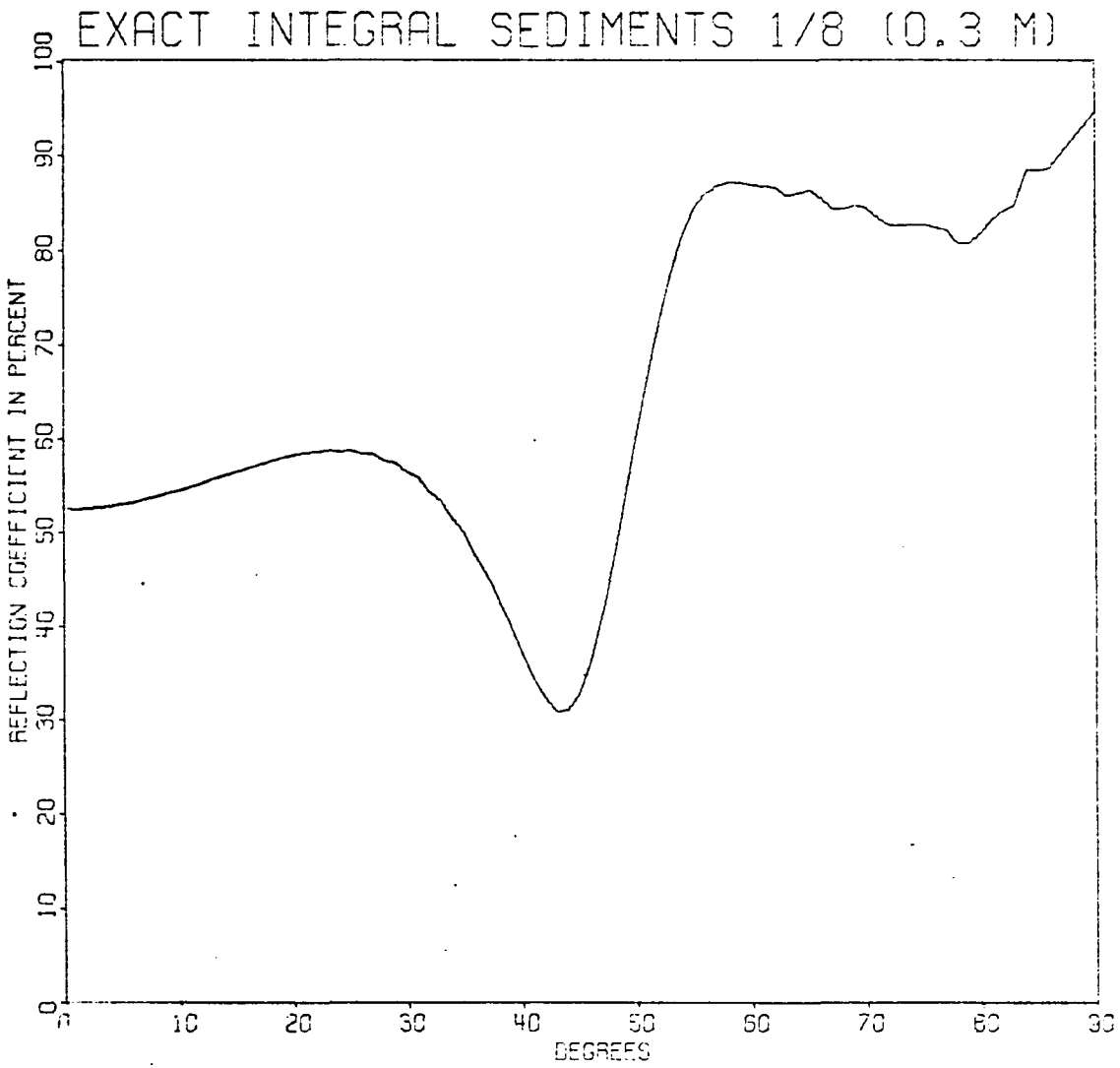

Figure 19a. Plotted is $4\pi R_I |G_b| \times 100\%$ vs. θ for the exact integral for G_b, where the subbottom consists of 0.3m of sediment #1 overlying a halfspace of sediment #8.

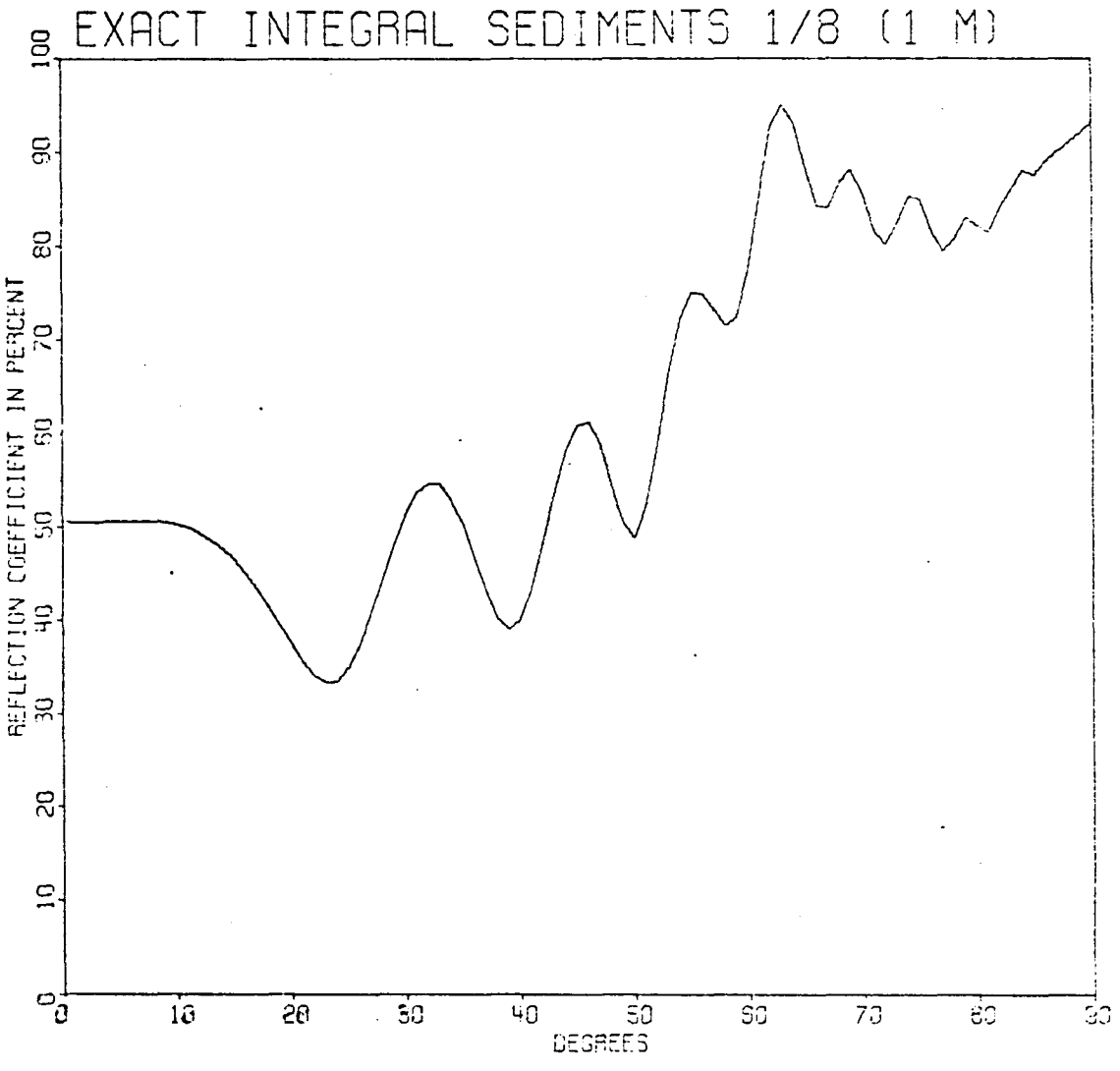

Figure 19b. Plotted is $4\pi R_I |G_b| \times 100\%$ vs. θ for the exact integral for G_b, where the sub-bottom consists of 1m of sediment #1 overlying a halfspace of sediment #8.

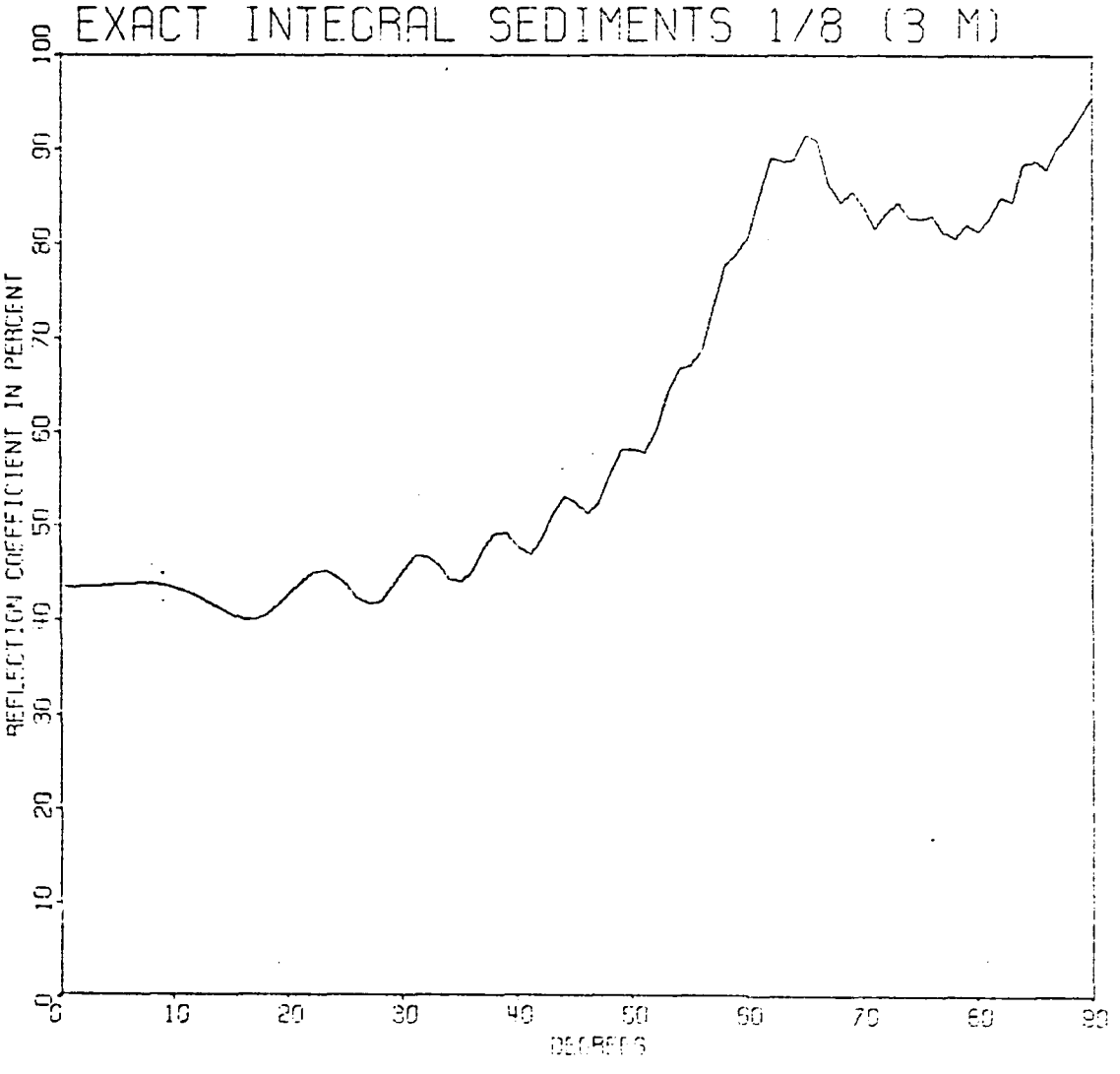

Figure 19c. Plotted is $4\pi R_I |G_b| \times 100\%$ vs. θ for the exact integral for G_b, where the sub-bottom consists of 3m of sediment #1 overlying a halfspace of sediment #8.

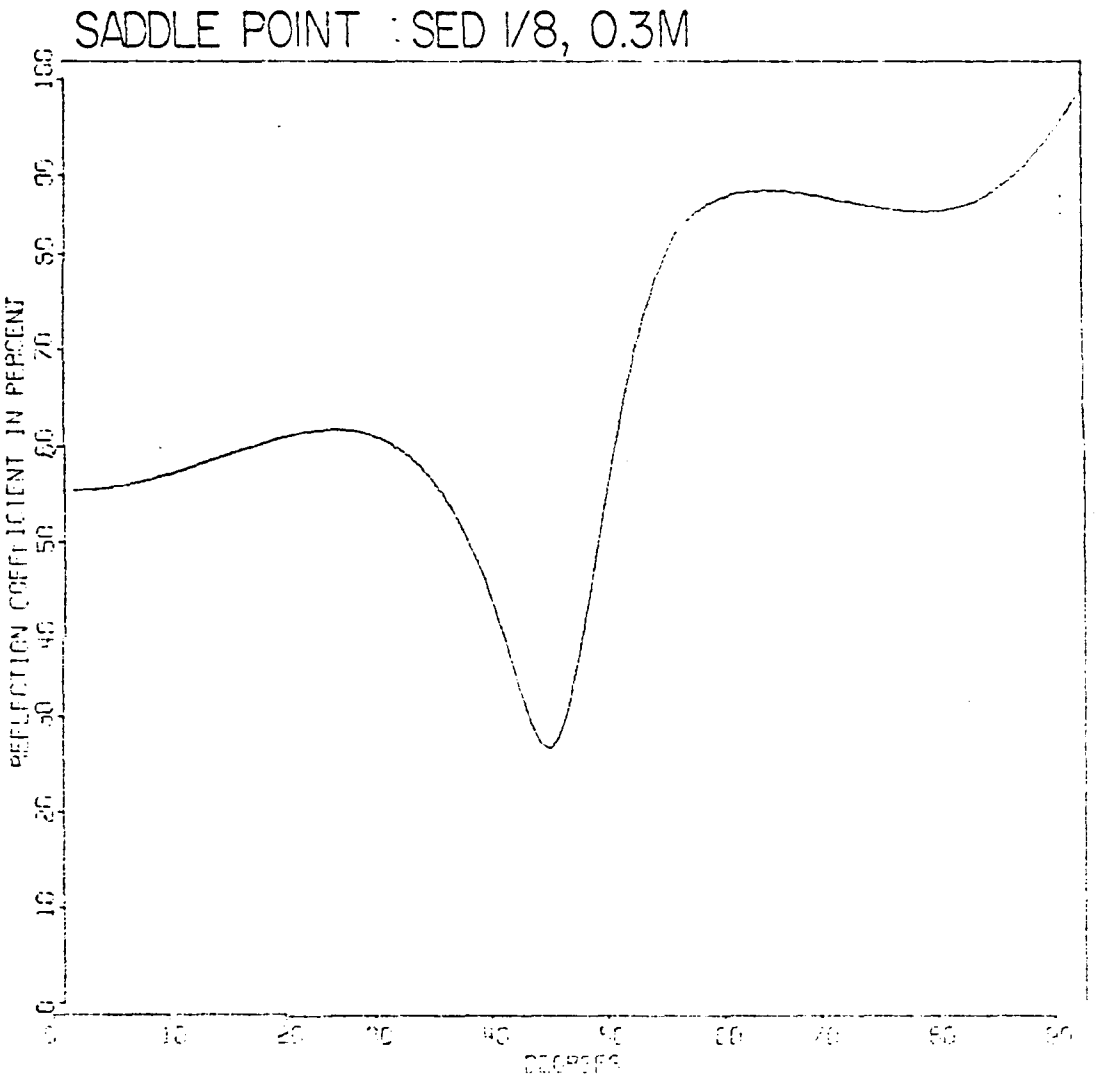

Figure 20a. Plotted is $4\pi R_I |G_b| \times 100\%$ vs. θ for the saddle-point approximation for G_b, where the subbottom consists of 0.3m of sediment #1 overlying a halfspace of sediment #8.

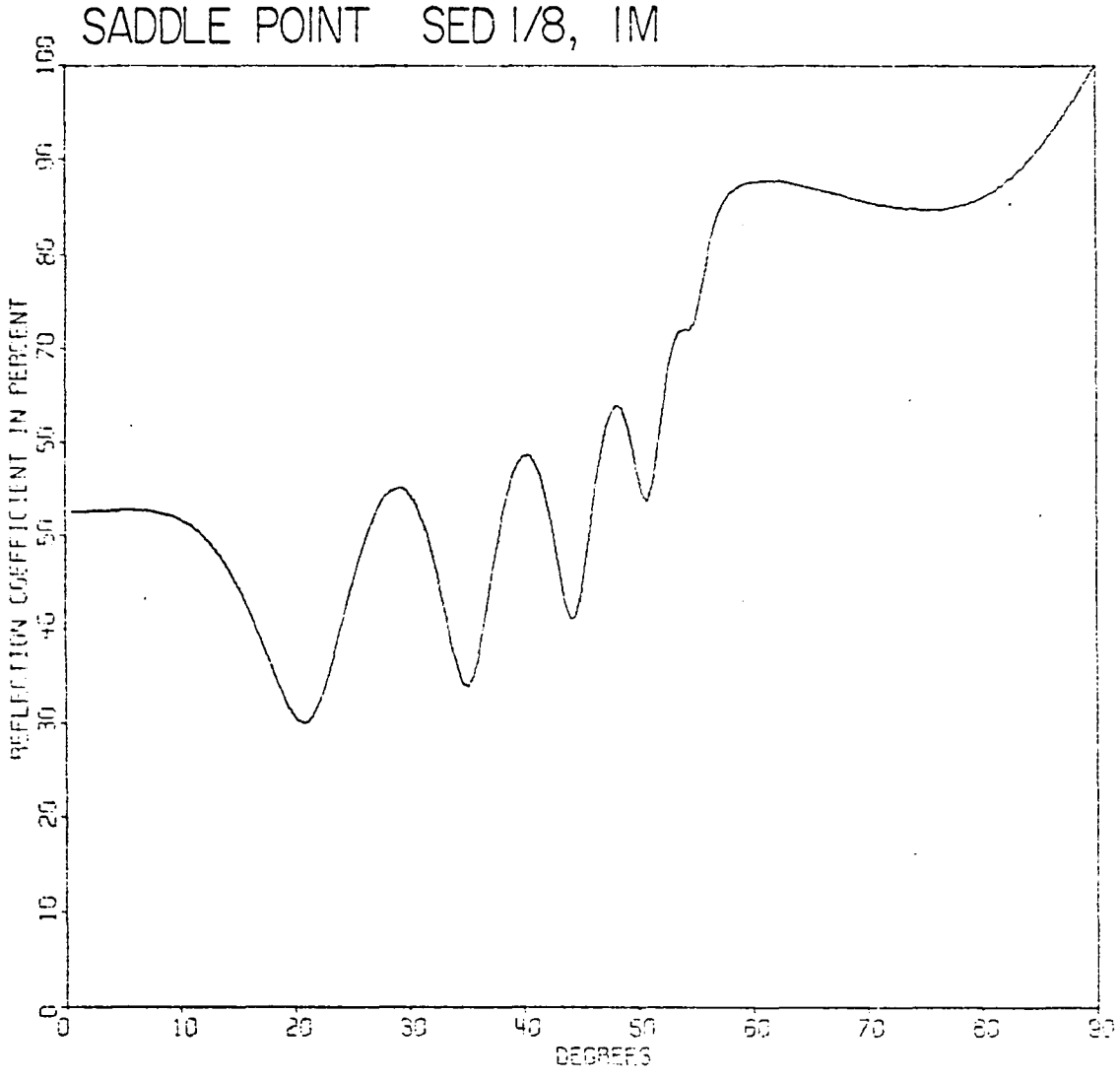

Figure 20b. Plotted is $4\pi R_I |G_b| \times 100\%$ vs. θ for the saddle-point approximation for G_b, where the subbottom consists of 1m of sediment #1 overlying a halfspace of sediment #8.

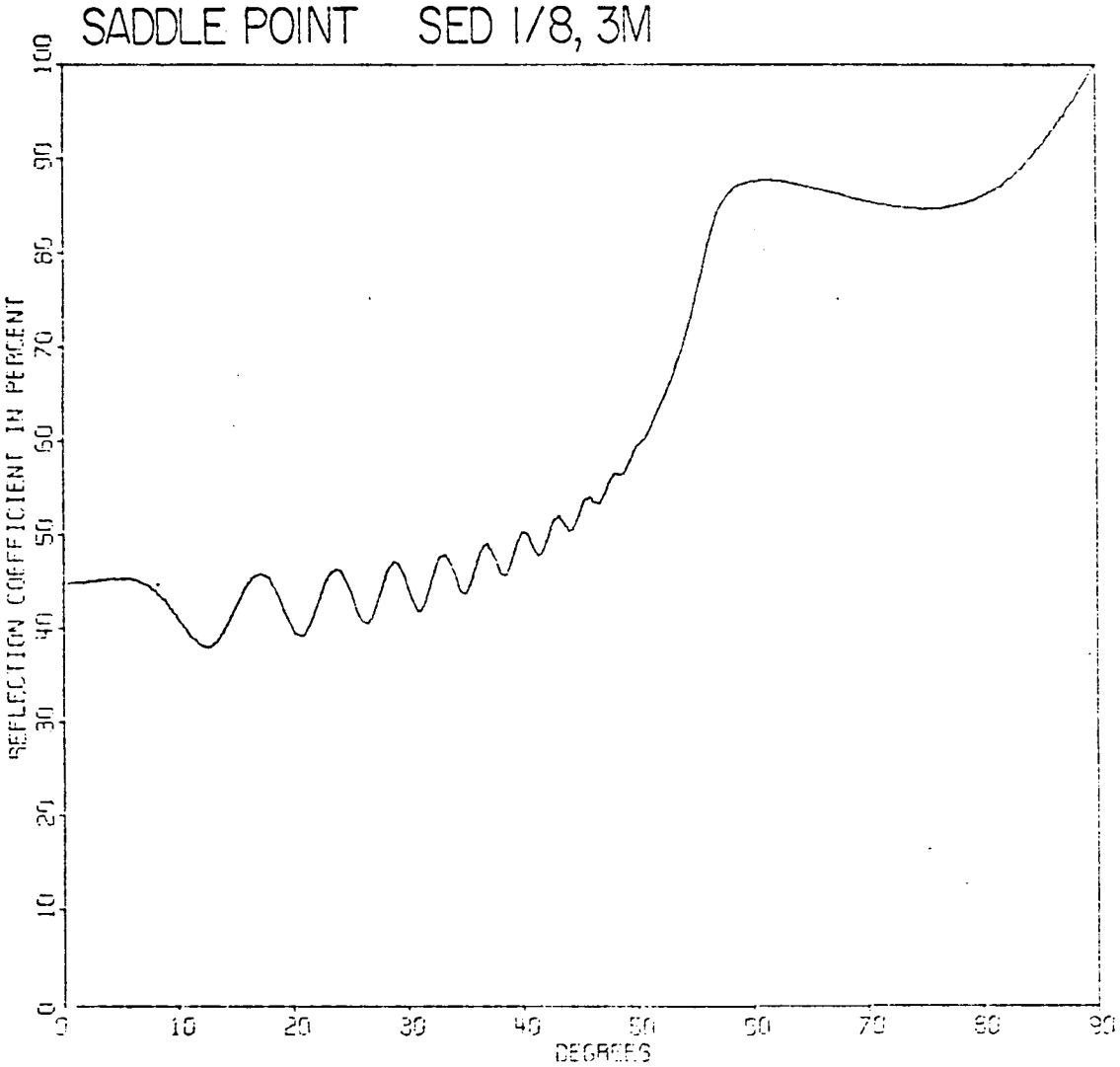

Figure 20c. Plotted is $4\pi R_I|G_b|\times 100\%$ vs. θ for the saddle-point approximation for G_b, where the subbottom consists of 3m of sediment #1 overlying a halfspace of sediment #8.

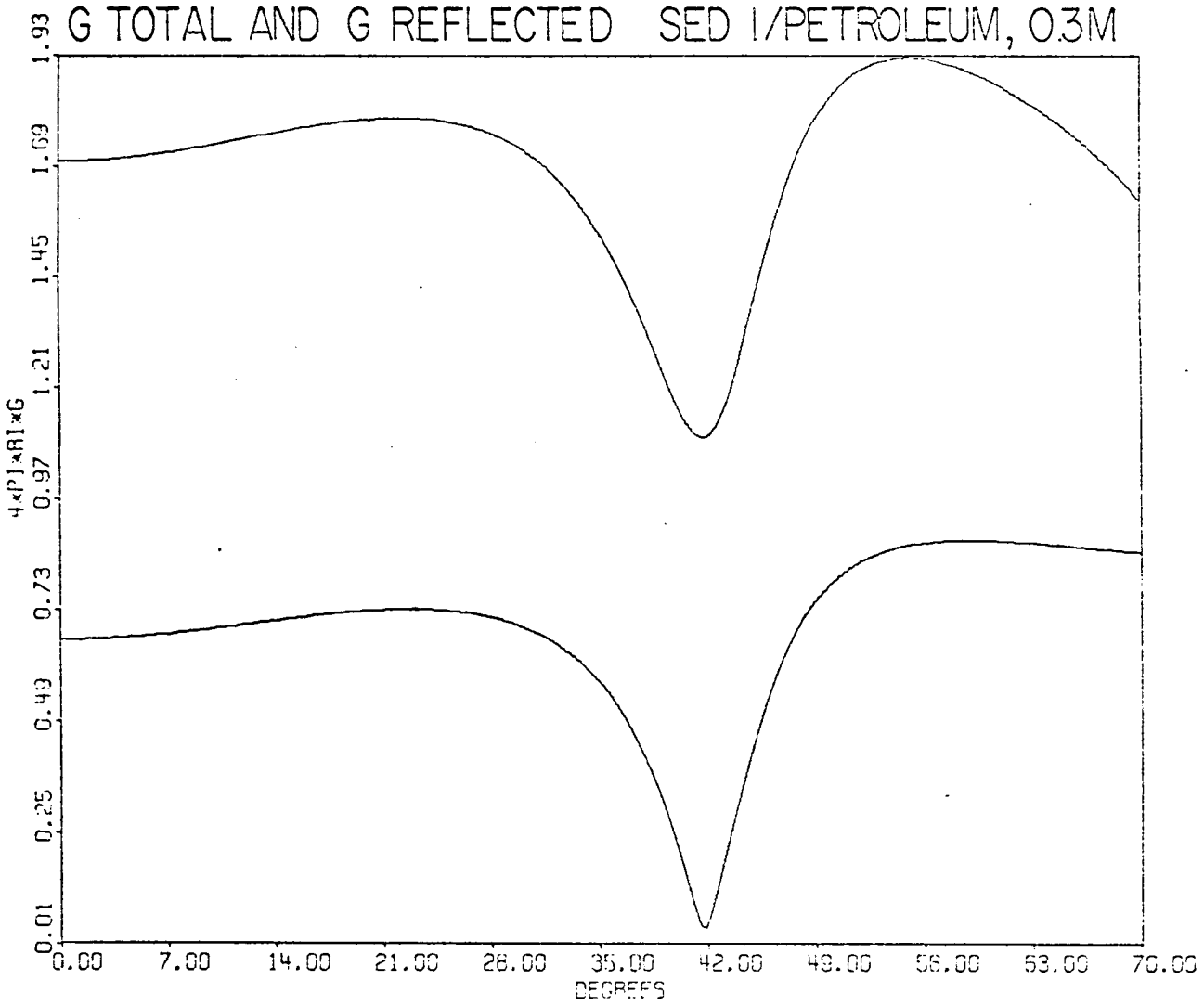

Figure 21a. Plotted is $4\pi R_I|G_b|\times 100\%$ vs. θ for the saddle-point approximation for G_b, where the subbottom consists of 0.3m of sediment #1 overlying a halfspace of petroleum.

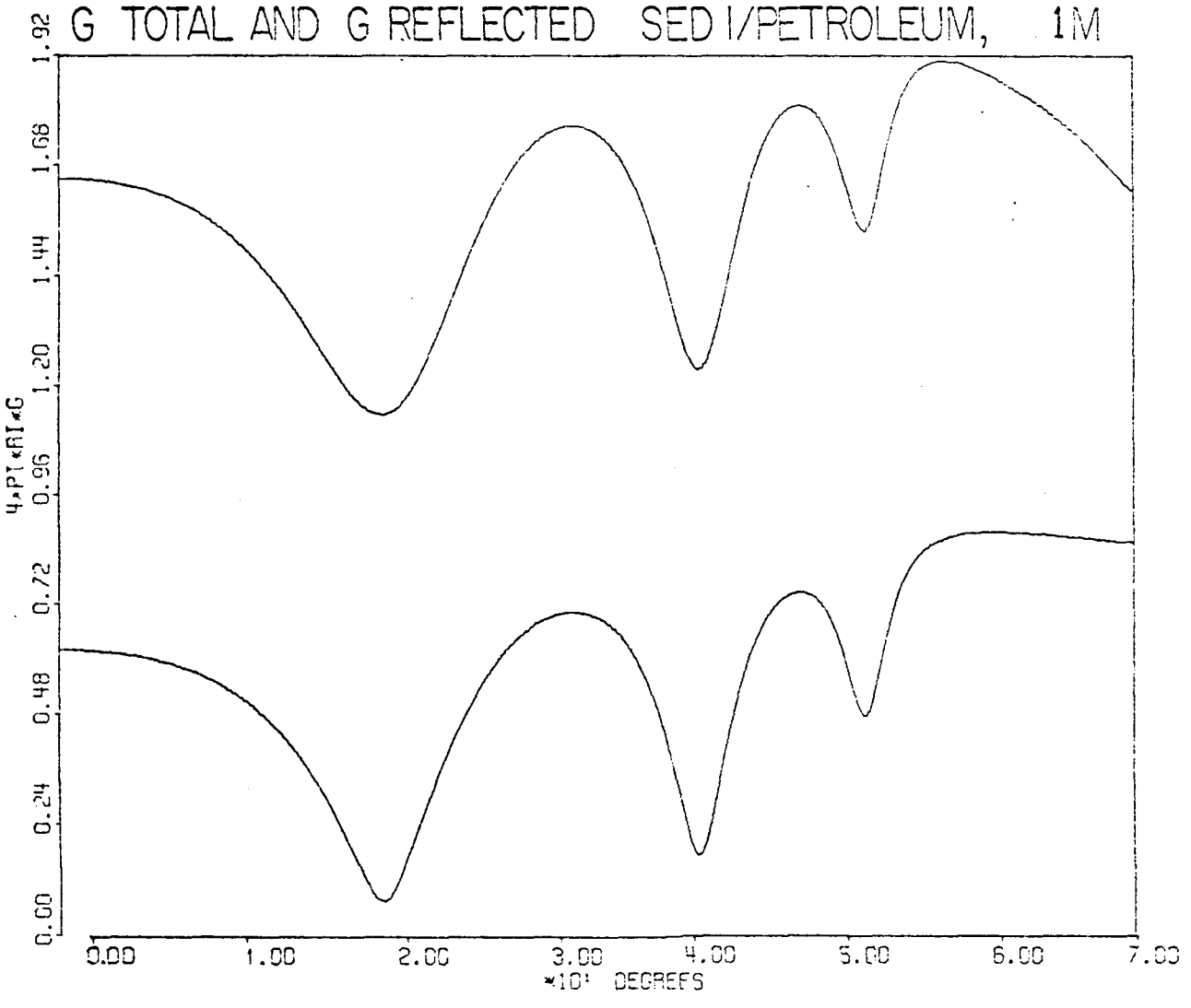

Figure 21b. Plotted is $4\pi R_I|G_b|\times 100\%$ vs. θ for the saddle-point approximation for G_b, where the subbottom consists of 1m of sediment #1 overlying a halfspace of petroleum.

REFERENCES

1. Mosberg, W., Yildiz, M., "Mean Square Response of Thermo-Viscoelastic Medium to Non-Stationary Random Excitation," accepted by Journal of Applied Mechanics, paper No. 5030.

2. Yildiz, M., "Spectral Representation of Wave Propagation in Thermo-Viscoelastic Medium," UNH-SG-158. Accepted for publication in Journal of Applied Mechanics, paper No. 5581 B.

3. Mindlin, R.D. and Tiersten, H.F., "Effect of Couple Stresses in Linear Elasticity," Archive for Rational Mechanics and Analysis Vol. 11, pp. 415-448 (1962).

4. Toupin, R.A., "Elastic Materials with Couple Stresses," Archive for Rational Mechanics and Analysis, Vol. 11, pp. 385-414 (1962).

5. Graff, K.F. and Pao, Y.H., "The Effects of Couple Stresses on the Propagation and Reflection of Plane Waves in an Elastic Halfspace," Journal of Sound and Vibration, Vol. 6, pp. 217-229 (1967).

6. Yildiz, A., "Light and Sound Radiations from Nonlinear Plasma-Fluctuations," Physical Review, Vol. 136, No. 2A, A393-394 (1964).

7. Yildiz, A., "Wave Propagation in an Elastic Field with Couple Stresses," Journal of Applied Mechanics, pp. 1146-1147 (December, 1972).

8. Cosserat, G. and Cosserat, F., "Theorie des Corps Deformable," pp. 953-1173 of O.D. Chwolson, Traite de Physique (transl. E. Davaux), second edition, Paris (1909).

9. Truesdell, C. and Toupin, R.A., "The Classical Field Theories," pp. 226-793 of Handbuch der Physik, Vol. III, I.S. Flugge, Ed. Springer (1960).

10. Aero, E.L. and Kuvshinskii, E.V., "Fundamental Equations of the Theory of Elastic Media with Rotationally Interacting Particles," Soviet Phys. Solid State Phys. 2, pp. 1272-1281 (1960).

11. Laval, M.J., "Elasticity of Crystals," C.R. Acad. Sci. (Paris) pp. 232 (1951).

12. Lax, M., "The Relation Between Microscopic and Macroscopic Theories of Elasticity," pp. 583-596, Proceedings of 1963 International Conference on Lattice Dynamics, Copenhagen, Pergammon Press (1965a).

13. Lax, M. and Nelson, D.F., "Linear and Nonlinear Electrodynamics in Elastic Anisotropic Dielectrics," Phys. Rev. B4, pp. 3694-3731 (1971).

14. Nelson, D.F., Lazay, R.D. and Lax, M., "Brillouin Scattering in Anisotropic Media; Calcite," Phys. Rev. B6, pp. 3109-3120 (1972).

15. Lax, M. and Nelson, D.F., "Crystal Electrodynamics," Atomic Structure and Properties of Solids," Vol. 52, Enrico Fermi Summer School, Varenna, Academic Press, pp. 48-118 (1973).

16. Toupin, R.A., "A Dynamical Theory of Elastic Dielectrics," Inter. J. Eng. Sci. 1, pp. 101-126 (1963). Also, "Theories of Elasticity with Couple Stress," Arch. for Rat'l. Mech. Anal. 17, pp. 85-112 (1964).

17. Laval, J., "The Atomic Theory of Elasticity Avoiding (the Assumption of) Central Forces," C.R. Acad. Sci. (Paris) 238, pp. 1773-1775 (1954).

18. Stewart, G., and Yildiz, M., "Acoustical Response in a Liquid Layer Overlying a Multilayered Thermo-Viscoelastic Halfspace," submitted for publication in Journal of Applied Mechanics.

19. Carrier, R. and Yildiz, M., "Measurements and Correlation Functions," UNH-SG-131.

20. Yildiz, M., "Some Aspects of Wave Propagation and the Effect of Boundaries and Excitation on the Electro-Acoustical Spectrum in the Isotropic Compressible Plasma," J. Electronics, Vol. 20, No. 2 (1966), 157-185.

21. Samaddar, S.N. and Yildiz, M., "Excitation of Coupled Electro Acoustical Waves by a Ring Source in a Compressible Plasma Cylinder," Can. J. Phys. 42 (1964), 638-656.

22. Magnuson, A.H., "Sound Propagation in a Liquid Overlying Viscoelastic Halfspace," Ph.D. Dissertation, Engineering Ph.D. Program, Theor. Appl. Mech., University of New Hampshire (Sept. 1972).

23. Sommerfeld, A., "Partial Differential Equations in Physics," Academic Press, New York (1967), 240-242.

24. Strick, E. and Ginsbarg, A.S., "Stonely Wave Velocities for a Fluid-Solid Interface," Bull. Seismol. Soc. Am. 46 (1956), 281-292.

25. Hamilton, E.L., "Elastic Properties of Marine Sediments," Journal of Geophysical Research, Vol. 76, No. 2, (Jan. 10, 1971) pp. 579-604.

26. Yildiz, A., "On the Science and Technology of Utilizing the Bottom Resources of the Continental Shelf," Technical Report to the National Sea Grant Office, 1970.

27. Zenneck, Ann. d. physik, Vol. 23, 1907.

28. Celikkol, B., and Vogel, P. see reference (3).

29. Thomson, W.T., "Transmission of Elastic Waves through a Stratified Solid Medium," Journal of Applied Physics, Vol. 21, pp. 89-93, February, 1950.

30. Haskell, N.A., :The Dispersion of Surface Waves on Multilayered Media," Bulletin of Seismological Society of America, Vol. 43, pp. 17-34, 1953.

31. Yildiz, M., "Spectral Representation of the Wave Propagation in Thermo-Viscoelastic Medium with the Couple Stresses," Submitted for publication in Journal of Applied Mechanics.

32. Breslau, L.R., "Classification of Sea Floor Sediments with a Shipborne Acousticsl System," Proc. Symp. Le Petrole et La Mer, Sec. I, No. 132; extensive discussion appears in L.R. Breslau, "Sound Reflection from the Sea Floor and its Geological Significance," Ph.D. Dissertation, Department of Geophysics and Geology, MIT (June 1964).

33. Hamilton, E.G., "Elastic Properties of Marine Sediments," Journal of Geophysical Research, Vol. 76, No. 2, pp. 579-604, January 10, 1971.

34. Hamilton, E.G., "Compressional-wave Attenuation in Marine Sediments," Geophysics, Vol. 37, No. 4, pp. 620-646, August 1972.

35. Press, Frank and Ewing, Maurice, "Propagation of Explosive Sound In A Liquid Layer Overlying a Semi-infinite Elastic Solid," Geophysics Vol. 15, pp. 426-446, 1950.

36. Yildiz, M., and Mawardi, O.K., J.A.S.A., Vol. 32, No. 12, 1685-1691, refer to Appendix A, Eqs. (A1 to A9) (December, 1960).

37. Celikkol, B., and Vogel, P.M., "A New Shear wave Velocity Measurement Technique in Ocean Bottom Soil Samples", Offshore Technology Conference, Houston, Texas, pp. 618-624. (1973).

38. Yildiz, A., "Effective Stresses in Subocean Soil," University of New Hampshire Sea Grant Report No. 119.

39. Celikkol, B., and Yildiz, M., "U.N.H. Damping Harmonic Oscillator Model of Porous Viscoelastic Soil Medium", University of New Hampshire Sea Grant No. (168) UNH-SG (168).

40. Carrier, R., and Yildiz, M., "Remote Measurement of Relative Q of Ocean Subbottom via Digital Signal Processing" U.N.H. -SG-158, August 1975.

41. Yildiz, M., Mechanical Engineering 882 lecture notes: Mathematical Methods in Engineering Science II, University of New Hampshire, Spring Semester, 1974.

42. Yildiz, M., Mechanical Engineering 824 lecture notes: Vibrations of Continuous Media, University of New Hampshire, Spring Semester, 1975.

43. Yildiz, M., Mechanical Engineering 922 lecture notes: Continuum Mechanics University of New Hampshire, Fall Semester, 1974.

44. Yildiz, M., Mechanical Engineering 890c lecture notes: Dynamics of Ocean Structures, University of New Hampshire, Fall Semester, 1974.

45. Yildiz, A., Mechanical Engineering 890 lecture notes: Random Vibration of Beams and Plates, University of New Hampshire, Spring Semester, 1975.

46. Yildiz, M., Mechanical Engineering 838 lecture notes: Theoretical Acoustics, University of New Hampshire, Spring Semester, 1975.

47. Yildiz, M., "Mean-Square-Response of a Viscoelastic Medium to Stationary Random Excitation," a report to the National Sea Grant Program of tthe National Oceanic and Atmospheric Administration, U.S. Department of Commerce, Report No. UNH-SG-125.

48. Yildiz, M., "Mean-Square-Response of Shear Waves of a Visco-elastic Medium to Nonstationary Random Excitation," a report to the National Sea Grant Program of the National Oceanic and Atmospheric Administration U.S. Department of Commerce, Report No. UNH-SG-129.

49. Yildiz, M., "Measurements and Correlation Functions," a report to The National Sea Grant Program of the National Oceanic and Atmospheric Administration, U.S. Department of Commerce, Report No. UNH-SG-131.

50. Yildiz, M., "Mean-Square Response of Waves of a Viscoelastic Medium to Nonstationary Random Excitation," a report to the National Sea Grant Program of teh National Oceanic and Atmospheric Administration U.S. Department of Commerce, Report No. UNH-SG-132.

51. Yildiz, M., "Wave Propagation in a Viscoelastic Field with Couple Stresses," a report to The National Sea Grant Program of the National Oceanic and Atmospheric Administration, U.S. Department of Commerce, Report No. UNH-SG-134.

52. Yildiz, M., "Nonstationary Random Inputs to Viscoelastic Compressional Wave Systems," a report to The National Sea Grant Program of the National Oceanic and Atmospheric Administration, U.S. Department of Commerce, Report No. UNH-SG-143.

53. Voigt, W., Theoretishce Studien uber die Elasticit atsuer haltnisse der Krystalle. Abh. Ges. Wiss. Gottingen 34 (1887).

54. Kolsky, H., "Stress Waves in Solids," Dover publications, (1953).

APPENDIX A

KRAMERS-KRONIG RELATIONS

Kramers-Kronig relations (5.12) have been proven in a most direct manner by De Groot and Mazur (1962). They are derived here, however, following the approach of Martin (1968), by a general technique valid for complex z. In particular, one seeks to express $G_{jm}(\vec{k};\omega)$ for complex z first in terms of $G''_{jm}(\vec{k};\omega')$ and then $G'_{jm}(\vec{k};\omega')$ in order to obtain, respectively relations (5.12a) and (5.12b).

Applying Cauchy's integral formula to the closed contour C' in the lower half of the complex z'-plane (see figure below) yields

$$G_{jm}(\vec{k};z) = \frac{-1}{2\pi i}\oint_{C'} \frac{G_{jm}(\vec{k};z')}{z' - z}\,dz' \quad , \quad 0 = \frac{-1}{2\pi i}\oint_{C'} \frac{G_{jm}(\vec{k};z')}{z' - z^*}\,dz' \quad , \tag{A.1}$$

since C' encloses z but does not enclose z^*. The minus sign takes into account that the contour C' is traversed in the negative (clockwise) sense, while z^* denotes the complex conjugate of z. Adding or subtracting equation (A.1), one obtains

$$G_{jm}(k;z) = \frac{-1}{2\pi i}\int_{C'} G_{jm}(k;z')\left[\frac{1}{z'-z} \pm \frac{1}{z'-z^*}\right]dz' \quad , \tag{A.2}$$

which may be expressed alternatively as

$$G_{jm}(\vec{k};z) = \frac{-1}{2\pi i}\int_{-R'}^{R'} G_{jm}(\vec{k};\omega')\left[\frac{1}{\omega'-z} \pm \frac{1}{\omega'-z^*}\right]d\omega' = \frac{-1}{2\pi i}\int_{\Gamma'} G_{jm}(\vec{k};z')\left[\frac{1}{z'-z} \pm \frac{1}{z'-z^*}\right]dz' \tag{A.3}$$

since the integral is to be evaluated along the closed path C' in the

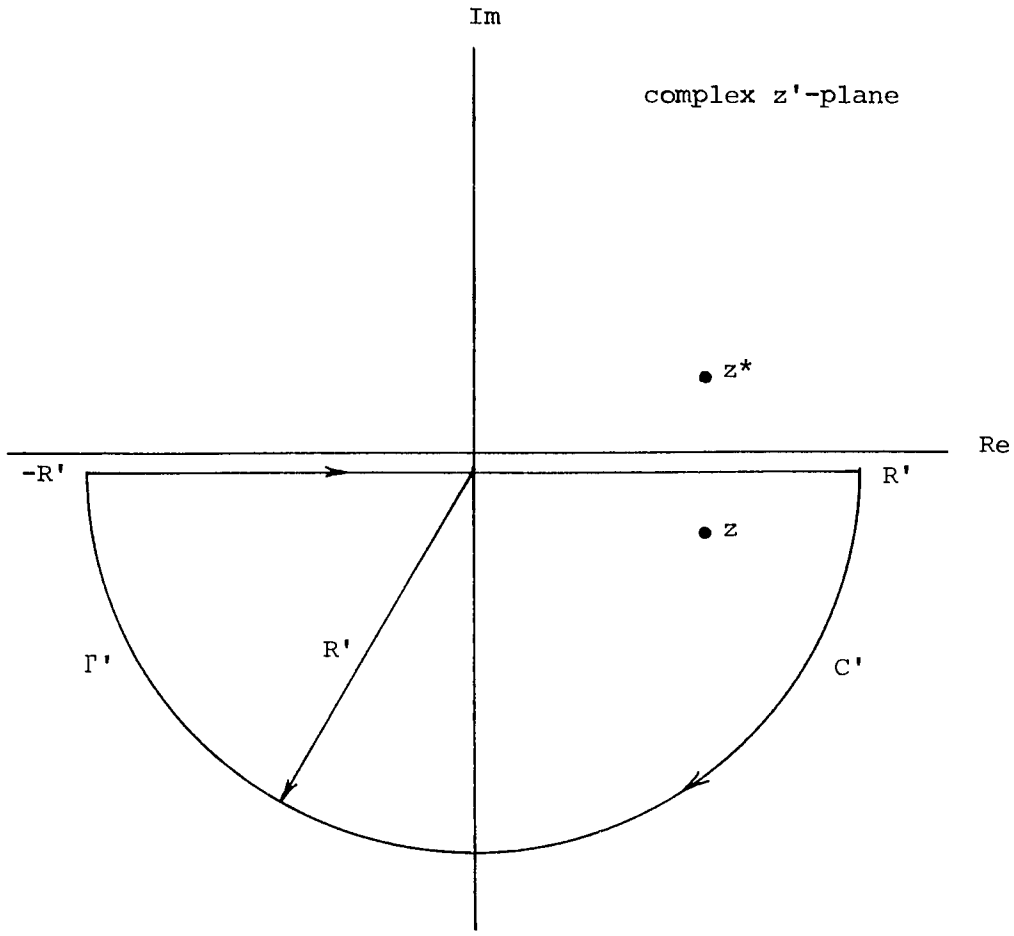

lower half of the z'-plane consisting of the real axis from $-R'$ to R' and the semicircle Γ' of radius R'. Taking the limit as $R' \to \infty$, equation (A.3) gives

$$G_{jm}(\vec{k};z) = \frac{-1}{2\pi i} \int_{-\infty}^{\infty} G_{jm}(\vec{k};\omega') \left[\frac{1}{\omega'-z} \pm \frac{1}{\omega'-z^*}\right] d\omega' \ . \qquad (A.4)$$

The integral over the semicircle Γ' does not contribute because the

integrand tends to zero as $R' \to \infty$. It follows from equation (A.4) that

$$G_{jm}(\vec{k};z) = -\int_{-\infty}^{\infty} G_{jm}(\vec{k};\omega')\,\mathrm{Re}\{\frac{1}{\omega'-z}\}\,\frac{d\omega'}{\pi i} = -\int_{-\infty}^{\infty} G_{jm}(\vec{k};\omega')\,\mathrm{Im}\{\frac{1}{\omega'-z}\}\,\frac{d\omega'}{\pi}\ , \tag{A.5}$$

depending upon whether the plus or minus is assumed.

If the real and imaginary parts of $G_{jm}(\vec{k};z)$ determined, respectively, from the first and second identities of equation (A.5) are added, one obtains

$$G_{jm}(\vec{k};z) = \mathrm{Re}\{G_{jm}(\vec{k};z)\} + i\ \mathrm{Im}\{G_{jm}(\vec{k};z)\}$$

$$= -\int_{-\infty}^{\infty} \mathrm{Im}\{G_{jm}(\vec{k};\omega')\}[\mathrm{Re}\{\frac{1}{\omega'-z}\} + i\ \mathrm{Im}\{\frac{1}{\omega'-z}\}]\,\frac{d\omega'}{\pi} = -\int_{-\infty}^{\infty} \frac{G''_{jm}(\vec{k};\omega')}{\omega' - z}\,\frac{d\omega'}{\pi}\ . \tag{A.6}$$

Clearly, if $z = \omega - i\varepsilon$ and $\varepsilon > 0$, the first of the Kramers-Kronig relations, equation (5.12a), is recovered since

$$G_{jm}(\vec{k};\omega) = G'_{jm}(\vec{k};\omega) + i\,G''_{jm}(\vec{k};\omega) = \lim_{\varepsilon\to 0} -\int_{-\infty}^{\infty} \frac{G''_{jm}(\vec{k};\omega')}{\omega'-(\omega-i\varepsilon)}\,\frac{d\omega'}{\pi}$$

$$= -P\int_{-\infty}^{\infty} \frac{G''_{jm}(\vec{k};\omega')}{\omega' - \omega}\,\frac{d\omega'}{\pi} + i\,G''_{jm}(\vec{k};\omega)\ , \tag{A.7}$$

because of the identity

$$\lim_{\varepsilon\to 0} \frac{1}{x \pm i\varepsilon} = P\,\frac{1}{x} \mp \pi i\delta(x)\ , \quad x = \omega' - \omega\ . \tag{A.8}$$

The second Kramers-Kronig relation, equation (5.12b), may be obtained in a similar manner. If the real and imaginary parts of $G_{jm}(\vec{k};z)$ determined, respectively, from the second and first identities of eqation (A.5) are added, one finds that

$$G_{jm}(\vec{k};z) = \mathrm{Re}\{G_{jm}(\vec{k};z)\} + i\ \mathrm{Im}\{G_{jm}(\vec{k};z)\}$$

$$= i \int_{-\infty}^{\infty} \mathrm{Re}\{G_{jm}(\vec{k};\omega')\}[\mathrm{Re}\{\frac{1}{\omega'-z}\} + i\ \mathrm{Im}\{\frac{1}{\omega'-z}\}]\ \frac{d\omega'}{\pi} = i \int_{-\infty}^{\infty} \frac{G'_{jm}(\vec{k};\omega')}{\omega' - z}\ \frac{d\omega'}{\pi}\ . \tag{A.9}$$

Applying identity (A.8) to the last equality in equation (A.9) then yields the second of the Kramers-Kronig relations as follows:

$$G_{jm}(\vec{k};\omega) = G'_{jm}(\vec{k};\omega) + i\ G''_{jm}(\vec{k};\omega)$$

$$= \lim_{\varepsilon\to 0} i \int_{-\infty}^{\infty} \frac{G'_{jm}(\vec{k};\omega')}{\omega'-(\omega-i\varepsilon)}\ \frac{d\omega'}{\pi} = G'_{jm}(\vec{k};\omega) + i\ P \int_{-\infty}^{\infty} \frac{G'_{jm}(\vec{k};\omega')}{\omega' - \omega}\ \frac{d\omega'}{\pi}\ . \tag{A.10}$$

APPENDIX B

AN ALTERNATIVE INTEGRAL REPRESENTATION FOR I_1^{ec}

The purpose of the development that follows is to illustrate in detail the process leading to the conversion of the integral expression for I_1^{ec} in equation (8.8a),

$$I_1^{ec} = \int_{-\infty}^{\infty} \frac{\sin[C_T(1+\ell^2k^2)^{1/2}k(t-t')]}{C_T(1+\ell^2k^2)^{1/2}} e^{-ik|\vec{x}-\vec{x}'|} dk \ , \qquad (B.1)$$

to the equivalent integral form for I_1^{ec} in equation (8.9) ,

$$I_1^{ec} = \frac{-2i}{C_T\ell} e^{-2a} \int_0^{\infty} e^{-4ay^2} \sinh[2^{1/2}b(y^2+1)^{1/2}]\cos[2^{1/2}by] \frac{dy}{(y^2+1)^{1/2}} \ . \qquad (B.2)$$

First of all, it should be noted that the integral for I_1^{ec} in equation (B.1) may be expressed equivalently as

$$I_1^{ec} = -2i \int_0^{\infty} \frac{\sin[C_T(1+\ell^2k^2)^{1/2}k(t-t')]}{C_T(1+\ell^2k^2)^{1/2}} \sin[k|\vec{x}-\vec{x}'|] dk \ , \qquad (B.3)$$

since only the even parts of the integrand contribute to the integral evaluated over the interval specified here. Employing the change of variables $\ell k + (1+\ell^2k^2)^{1/2} \to \zeta$, this form for I_1^{ec} gives

$$I_1^{ec} = \frac{-2i}{C_T\ell} \int_1^{\infty} \sin[b(\zeta-\zeta^{-1})]\sin[a(\zeta^2-\zeta^{-2})] \frac{d\zeta}{\zeta} \ , \qquad (B.4)$$

where

$$a = \frac{C_T(t-t')}{4\ell} \quad , \quad b = \frac{|\vec{x}-\vec{x}'|}{2\ell} \quad . \tag{B.4a}$$

For the purpose of evaluating I_1^{ec} , it is useful to express equation (B.4) as

$$I_1^{ec} = \frac{-2i}{C_T\ell} \{I_1^{ec^+} - I_1^{ec^-}\} \ , \tag{B.5}$$

where $I_1^{ec^+}$ and $I_1^{ec^-}$ denote the integrals

$$I_1^{ec^+} = \frac{1}{2i} \int_1^\infty \sin[b(\zeta-\zeta^{-1})] e^{ia(\zeta^2-\zeta^{-2})} \frac{d\zeta}{\zeta} \tag{B.5a}$$

and

$$I_1^{ec^-} = \frac{1}{2i} \int_1^\infty \sin[b(\zeta-\zeta^{-1})] e^{-ia(\zeta^2-\zeta^{-2})} \frac{d\zeta}{\zeta} \ . \tag{B.5b}$$

The real integrals $I_1^{ec^+}$ and $I_1^{ec^-}$ can be converted into complex integrals and subsequently treated as portions of these integrals by replacing ζ with the complex variable z . Applying Cauchy's theorem to the closed contours C and C' in the upper and lower halves of the complex z-plane (see figure below), where the integrals $I_1^{ec^+}$ and $I_1^{ec^-}$ are, respectively, well defined and exponentially decreasing, yields

$$\oint_C \sin[b(z-z^{-1})] e^{-ia(z^2-z^{-2})} \frac{dz}{z} = 0 \tag{B.6a}$$

and

$$\oint_{C'} \sin[b(z-z^{-1})] e^{-ia(z^2-z^{-2})} \frac{dz}{z} = 0 \ , \tag{B.6b}$$

since there are no singularities enclosed within these contours.

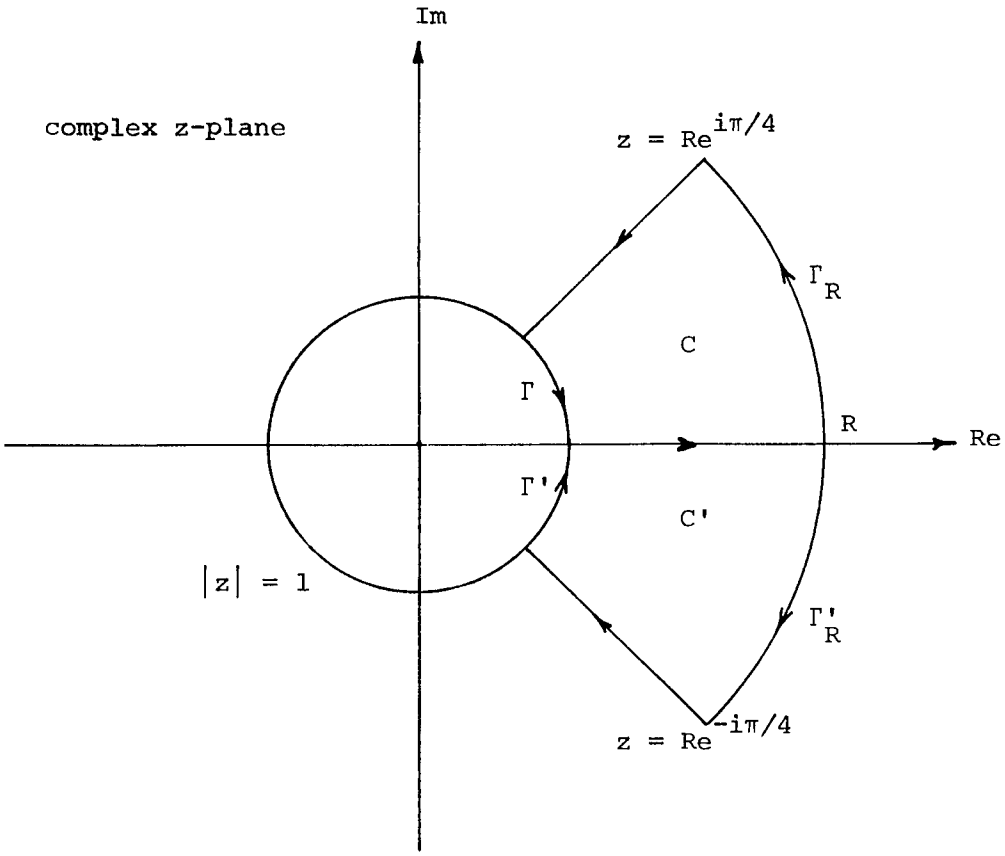

These integrals may be expressed alternatively in terms of the straight line segments and arcs which constitute the specified paths

of integration as

$$\int_1^R \sin[b(\zeta-\zeta^{-1})]e^{ia(\zeta^2-\zeta^{-2})}\,\frac{d\zeta}{\zeta}$$

$$+ i\int_0^{\pi/4} \sin[b(Re^{i\theta}-R^{-1}e^{-i\theta})]e^{ia(R^2e^{2i\theta}-R^{-2}e^{-2i\theta})}d\theta$$

$$+\int_R^1 \sin[b(re^{i\pi/4}-r^{-1}e^{-i\pi/4})]e^{ia(r^2e^{i\pi/2}-r^{-2}e^{-i\pi/2})}\,\frac{dr}{r}$$

$$+ i\int_{\pi/4}^0 \sin[2ibsin\theta]e^{-2asin2\theta}d\theta = 0 \ . \qquad \text{(B.7a)}$$

and

$$\int_1^R \sin[b(\zeta-\zeta^{-1})]e^{-ia(\zeta^2-\zeta^{-2})}\,\frac{d\zeta}{\zeta}$$

$$+ i\int_0^{-\pi/4} \sin[b(Re^{i\theta}-R^{-1}e^{-i\theta})]e^{-ia(R^2e^{2i\theta}-R^{-2}e^{-2i\theta})}d\theta$$

$$+\int_R^1 \sin[b(re^{-i\pi/4}-r^{-1}e^{i\pi/4})]e^{-ia(r^2e^{-i\pi/2}-r^{-2}e^{i\pi/2})}\,\frac{dr}{r}$$

$$+ i\int_{-\pi/4}^0 \sin[2ibsin\theta]e^{2asin2\theta}d\theta = 0 \ . \qquad \text{(B.7b)}$$

Taking the limit as $R \to \infty$, it follows from equation (B.7) that

$$\int_1^\infty \sin[b(\zeta-\zeta^{-1})]e^{ia(\zeta^2-\zeta^{-2})}\,\frac{d\zeta}{\zeta}$$

$$+\int_\infty^1 \sin[b(re^{i\pi/4}-r^{-1}e^{-i\pi/4})]e^{ia(r^2e^{i\pi/2}-r^{-2}e^{-i\pi/2})}\,\frac{dr}{r}$$

$$+ i\int_{\pi/4}^0 \sin[2ib\sin\theta]e^{-2a\sin 2\theta}d\theta = 0 \ . \qquad \text{(B.8a)}$$

and

$$\int_1^\infty \sin[b(\zeta-\zeta^{-1})]e^{-ia(\zeta^2-\zeta^{-2})}\,\frac{d\zeta}{\zeta}$$

$$+\int_\infty^1 \sin[b(re^{-\pi/4}-r^{-1}e^{i\pi/4})]e^{-ia(r^2e^{-i\pi/2}-r^{-2}e^{i\pi/2})}\,\frac{dr}{r}$$

$$+ i\int_{-\pi/4}^0 \sin[2ib\sin\theta]e^{2a\sin 2\theta}d\theta = 0 \ . \qquad \text{(B.8b)}$$

The integrals over the arcs Γ_R and Γ'_R both approach zero as $R \to \infty$, and thus do not contribute to their respective integrations.

Subtracting equation (B.8b) from equation (B.8a) gives

$$2i \int_1^\infty \sin[b(\zeta-\zeta^{-1})]\sin[a(\zeta^2-\zeta^{-2})]\ \frac{d\zeta}{\zeta}$$

$$= \int_1^\infty e^{-a(r^2+r^{-2})}\{\sin[\frac{b}{2^{1/2}}((r-r^{-1})+i(r+r^{-1}))]-\sin[\frac{b}{2^{1/2}}((r-r^{-1})-i(r+r^{-1}))]\}\ \frac{dr}{r}$$

$$= 2i \int_1^\infty e^{-a(r^2+r^{-2})}\sinh[\frac{b}{2^{1/2}}(r+r^{-1})]\cos[\frac{b}{2^{1/2}}(r-r^{-1})]\ \frac{dr}{r}\ . \qquad \text{(B.9)}$$

The change of variables $\theta \to -\theta$ indicates that the integrals over the arcs Γ and Γ' are identical to each other and cancel upon subtraction. Finally, employing the change of variables $1/2(r-r^{-1}) \to y$ and multiplying both sides of equation (b.9) by $-1/C_T\ell$ gives

$$I_1^{ec} = \frac{-2i}{C_T\ell} \int_1^\infty \sin[b(\zeta-\zeta^{-1})]\sin[a(\zeta^2-\zeta^{-2})]\ \frac{d\zeta}{\zeta}$$

$$= \frac{-2i}{C_T\ell}\, e^{-2a} \int_0^\infty e^{-4ay^2}\sinh[2^{1/2}b(y^2+1)^{1/2}]\cos[2^{1/2}by]\ \frac{dy}{(y^2+1)^{1/2}}\ .$$

(B.10)